
QA: QA

MDL-MGR-GS-000002 REV 02

August 2005

# Atmospheric Dispersal and Deposition of Tephra from a Potential Volcanic Eruption at Yucca Mountain, Nevada

**NOTICE OF OPEN CHANGE DOCUMENTS - THIS DOCUMENT IS IMPACTED BY THE LISTED CHANGE DOCUMENTS AND CANNOT BE USED WITHOUT THEM.**

---

**1) ACN-001, DATED 09/09/2005**
**2) ACN-002, DATED 03/06/2006**

Prepared for:
U.S. Department of Energy
Office of Civilian Radioactive Waste Management
Office of Repository Development
1551 Hillshire Drive
Las Vegas, Nevada 89134-6321

Prepared by:
Bechtel SAIC Company, LLC
1180 Town Center Drive
Las Vegas, Nevada 89144

Under Contract Number
DE-AC28-01RW12101

**DISCLAIMER**

This report was prepared as an account of work sponsored by an agency of the United States Government. Neither the United States Government nor any agency thereof, nor any of their employees, nor any of their contractors, subcontractors or their employees, makes any warranty, express or implied, or assumes any legal liability or responsibility for the accuracy, completeness, or any third party's use or the results of such use of any information, apparatus, product, or process disclosed, or represents that its use would not infringe privately owned rights. Reference herein to any specific commercial product, process, or service by trade name, trademark, manufacturer, or otherwise, does not necessarily constitute or imply its endorsement, recommendation, or favoring by the United States Government or any agency thereof or its contractors or subcontractors. The views and opinions of authors expressed herein do not necessarily state or reflect those of the United States Government or any agency thereof.

QA: QA

# Atmospheric Dispersal and Deposition of Tephra from a Potential Volcanic Eruption at Yucca Mountain, Nevada

**MDL-MGR-GS-000002 REV 02**

**August 2005**

BSC

# Model Signature Page/Change History

Complete only applicable items.



2. Type of Mathematical Model

☒ Process Model ☐ Abstraction Model ☐ System Model

Describe Intended Use of Model

The purpose of this model report is to provide documentation of a conceptual and mathematical model (Ashplume) for atmospheric dispersal and deposition of tephra from a potential volcanic eruption at Yucca Mountain, Nevada. This report also documents the ash (tephra) redistribution conceptual model.

3. Title

*Atmospheric Dispersal and Deposition of Tephra from a Potential Volcanic Eruption at Yucca Mountain, Nevada*

4. DI (including Rev. No.):

MDL-MGR-GS-000002 REV 02

| | Printed Name | Signature | Date |
|---|---|---|---|
| 5. Originator | G. Keating | | 8/15/05 |
| 6. Independent Technical Reviewer | R. Andrews | | 8/19/05 |
| 7. Checker | E. Gaffney | | 19 Aug 05 |
| 8. QER | K. McFall | | 8/19/05 |
| 9. Responsible Manager/Lead | G. Valentine | | 19 Aug 05 |
| 10. Responsible Manager | M. Cline | | 8/23/05 |

11. Remarks

Contributing authors to REV 02 include W.P. Imrie, C. Harrington, and J. Pelletier. Additional checkers include J. McCleary (Sections 6.3.2, 6.6, 6.7.2, 7.3.2, and Appendix I) and C. Hastings (Sections 2, 3, 4, and 5).

Change History

| 12. Revision No. | 13. Description of Change |
|---|---|
| 00 | Initial issue |
| 01 | Revised in response to recommendations of the Regulatory Integration Team Evaluation, and management approval of those recommendations. An alternative model for ash redistribution was also developed and is documented in this AMR. In addition, a different version of the NOAA wind speed and direction data set was used to produce REV 01 from the one used in REV 00. This different version was used based on issues identified in CR 3205. |
| 02 | Revised to incorporate an alternative waste particle size distribution and alternative conceptual model for magma-waste interaction in the repository drifts, eruptive conduit, and eruption plume (Appendix J). This revision closes CRs 4126, 4509, 4734, 5088, 5919, 6098, and 6137. Changes to text are indicated by change bars, except for Appendix I, which was revised to be consistent with software documentation for the ash redistribution model under development; and Appendix J, which is entirely new. Additional text added in Section 7 to address Ashplume model validation acceptance criteria. |
| | |
| | |
| | |

# CONTENTS

## CONTENTS (Continued)

Page

**CONTENTS (Continued)**

**Page**

INTENTIONALLY LEFT BLANK

## FIGURES

Page

## FIGURES (Continued)

Page

# TABLES

**Page**

## TABLES (Continued)

Page

## TABLES (Continued)

**Page**

INTENTIONALLY LEFT BLANK

## ACRONYMS AND ABBREVIATIONS

| | |
|---|---|
| BDCF | biosphere dose conversion factor |
| cm | centimeter |
| CDF | cumulative distribution function |
| DIRS | Document Input Reference System |
| DOE | U.S. Department of Energy |
| FEPs | features, events, and processes |
| g | gram |
| $g_c$ | gravitation acceleration constant |
| kg | kilogram |
| km | kilometer |
| m | meter |
| mm | millimeter |
| NRC | U.S. Nuclear Regulatory Commission |
| PDF | probability distribution function |
| RMEI | reasonably maximally exposed individual |
| s | second |
| TSPA | Total System Performance Assessment |
| TSPA-LA | Total System Performance Assessment for the License Application |
| TSPA-SR | Total System Performance Assessment for the Site Recommendation |
| TWP | technical work plan |
| YMRP | Yucca Mountain Review Plan |

INTENTIONALLY LEFT BLANK

# 1. PURPOSE

The purpose of this model report is to provide documentation of the conceptual and mathematical model (Ashplume) for atmospheric dispersal and subsequent deposition of ash on the land surface from a potential volcanic eruption at Yucca Mountain, Nevada. This report also documents the ash (tephra) redistribution conceptual model. Processes related to eruption and redistribution of tephra are described in the context of the entire igneous disruptive events conceptual model in *Characterize Framework for Igneous Activity* (BSC 2004 [DIRS 169989], Section 6.1.1). The Ashplume conceptual model accounts for incorporation and entrainment of waste fuel particles associated with a hypothetical volcanic eruption through the Yucca Mountain repository and downwind transport of contaminated tephra. The Ashplume mathematical model describes the conceptual model in mathematical terms to allow for prediction of radioactive waste/ash deposition on the ground surface given that the hypothetical eruptive event occurs. This model report also describes the conceptual model for tephra redistribution from a basaltic cinder cone within Fortymile Wash and on Fortymile Wash alluvial fan. Sensitivity analyses and model validation activities for the ash dispersal and redistribution models are also presented. Analyses documented in this model report update the previous documentation of the Ashplume mathematical model and its application to the Total System Performance Assessment (TSPA) for the License Application (TSPA-LA) igneous scenarios. This model report also documents the redistribution model product outputs based on analyses to support the conceptual model.

In this report, 'Ashplume' is used when referring to the atmospheric dispersal model and 'ASHPLUME' is used when referencing the code representing that model. Although the term "ash" means erupted material <2 mm in diameter and "tephra" is a general term for pyroclastic material (Fisher and Schmincke 1984 [DIRS 162806]), the terms "ash" and "tephra" are used interchangeably in this report to mean fragmental products of a volcanic eruption, rather than a specific size fraction. The terms "fuel" and "waste" are used interchangeably.

Two analysis and model reports provide direct inputs to this model report, namely the product output (DTN: LA0407DK831811.001 [DIRS 170768]) from *Characterize Eruptive Processes at Yucca Mountain, Nevada* (BSC 2004 [DIRS 169980]) and the product output (DTN: MO0504MWDNUMWP.001 [DIRS 173521]) from *Number of Waste Packages Hit by Igneous Intrusion* (BSC 2005 [DIRS 174066]).

This model report provides direct inputs to the TSPA, which uses the ASHPLUME software described and used in this model report. Thus, ASHPLUME software inputs are inputs to this model report for ASHPLUME runs in this model report. However, ASHPLUME software inputs are outputs of this model report for ASHPLUME runs by TSPA.

Revision 02 of this report has been prepared to document an alternative waste-particle size distribution and an alternative conceptual model for magma–waste interaction in the repository drifts, eruptive conduit, and eruption plume (Appendix J and referenced in Section 5). An alternative ash redistribution model was developed in REV 01 of this report (BSC 2004 [DIRS 170026]) and an update of that in-process model is included in Appendix I.

## 1.1 SCOPE OF WORK

The scope of this report is limited to descriptions of models for atmospheric dispersal of contaminated tephra during and after a violent Strombolian eruption of the type that could occur in the Yucca Mountain region (BSC 2004 [DIRS 169980], Section 6.3) and for redistribution of the contaminated tephra after the volcanic eruption. If such an eruption were to intersect the repository, the possibility exists for wastes to become entrained in the eruptive mixture and be transported via the same mechanisms as the ash plume. Although other eruption types that include nonviolent as well as violent phases exist, the violent Strombolian eruption has the greatest potential to erupt ash and waste particles high into the atmosphere, thus increasing the potential distance of dispersal (BSC 2004 [DIRS 169980], Section 6.1.3.2).

Figure 1-1 is a schematic representation of a possible future volcanic eruption at Yucca Mountain, showing transport of radioactive waste in an ash plume. In Figure 1-1, the scope of the Ashplume conceptual model includes only the eruptive ash plume, convective/dispersive transport of contaminated ash particles downwind, and deposition on the ground surface. The Ashplume mathematical model may be used to evaluate ash and waste concentration (areal density) at any one point or multiple points on the surface relative to the volcanic vent. The ash redistribution conceptual model is used to describe the erosion and subsequent deposition of contaminated ash. The north-south orientation and 18-km distance shown in Figure 1-1 are for illustration purposes only.

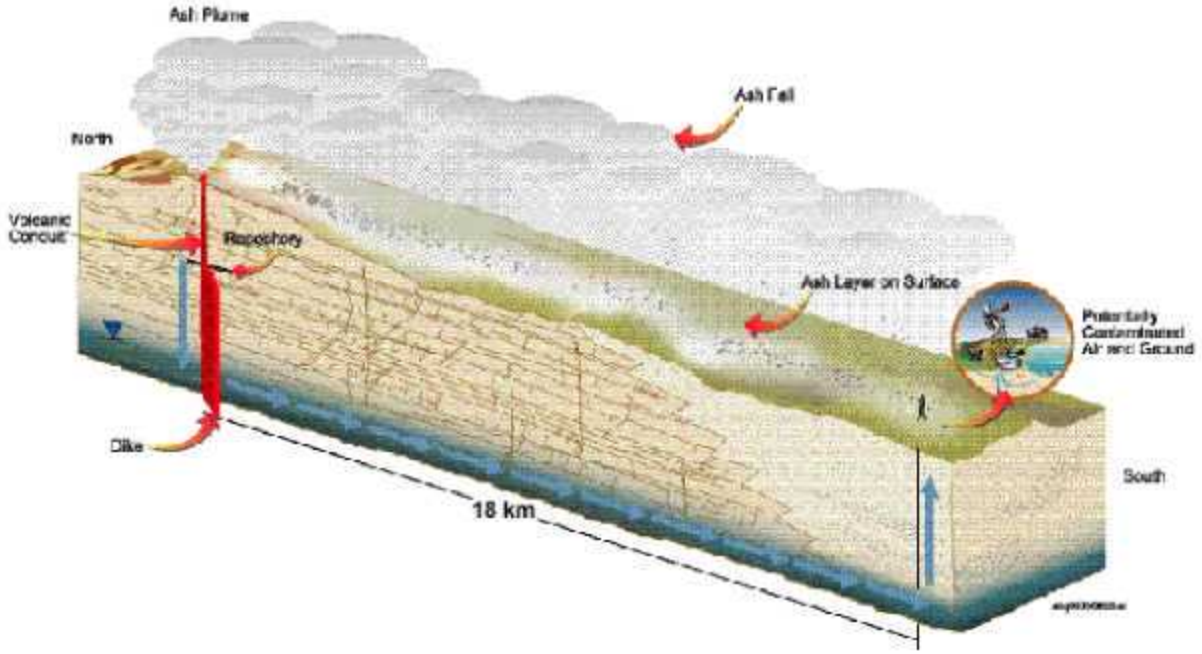


Source: Modified from CRWMS M&O (2000 [DIRS 153246], Figure 3.10-5).

NOTE: For illustration purposes only.

Figure 1-1. Schematic Representation of a Volcanic Eruption at Yucca Mountain, Showing Transport of Radioactive Waste in an Ash Plume

## 1.2 BACKGROUND

The following sections discuss both the ash dispersal model used for past Yucca Mountain TSPA analyses and the ash redistribution conceptual model and present the objectives of this report as defined by the *Technical Work Plan: Igneous Activity Assessment for Disruptive Events* (BSC 2005 [DIRS 174773]) for this activity.

### 1.2.1 Previous Use and Documentation

The *ASHPLUME Version 1.0–A Code for Contaminated Ash Dispersal and Deposition, Technical Description and User's Guide* (Jarzemba et al. 1997 [DIRS 100987]) implements the mathematical model of atmospheric dispersal and deposition of tephra of Suzuki (1983 [DIRS 100489]) for estimation of the areal density of tephra deposits on the surface of the Earth following a volcanic eruption. The code includes estimation of the areal density of spent fuel particles incorporated into tephra particles due to a volcanic event that intersects the repository.

For the Total System Performance Assessment for the Site Recommendation (TSPA-SR) (CRWMS M&O 2000 [DIRS 153246]), the original ASHPLUME V1.0 code (Jarzemba et al. 1997 [DIRS 100987]) was modified to incorporate eruptive parameters developed from natural analogue volcanoes that would be representative of any future volcanic event in the Yucca Mountain region. This modified version of the code, known as ASHPLUME 1.4LV-dll, was used as a component of the TSPA-SR model and was incorporated as a dynamically linked library directly within the TSPA-SR model. For current work, ASHPLUME_DLL_LA V.2.0 ([BSC 2003 [DIRS 166571]) is used for calculations within the TSPA-LA. As described below, ASHPLUME_DLL_LA V.2.0 is essentially the same as previous versions of the code but employs a modified set of input parameters that are based on those data analyzed within *Characterize Eruptive Processes at Yucca Mountain, Nevada*, REV 02 (BSC 2004 [DIRS 169980]).

The main difference between ASHPLUME 1.4LV (BSC 2002 [DIRS 161296]) and ASHPLUME_DLL_LA V.2.0 (BSC 2003 [DIRS 166571]) lies in the formulation of eruption column height. ASHPLUME 1.4LV uses an empirical relationship between volume and column height that was determined to be less accurate than the use of eruptive power to calculate mass discharge rate and, subsequently, column height (as is implemented in ASHPLUME_DLL_LA V.2.0). This new version of the code is more consistent with the state of practice among volcanologists. A form of ASHPLUME V.2.0 (CRWMS M&O 2001 [DIRS 152844]), compiled for use on the Windows NT 4.0 platform, was used for the model validation and sensitivity studies presented in Section 7; this form of the code differs insignificantly from ASHPLUME_DLL_LA V.2.0, which has been compiled to run on the Windows 2000 platform for TSPA. The change in the code from ASHPLUME 1.4LV (BSC 2002 [DIRS 161296]) to ASHPLUME_DLL_LA V.2.0 (BSC 2003 [DIRS 166571]) and ASHPLUME V.2.0 (CRWMS M&O 2001 [DIRS 152844]) produces slightly higher calculated column heights than does ASHPLUME 1.4LV. Therefore, a new set of wind data collected at Desert Rock (near Mercury, Nevada) (NOAA 2004 [DIRS 171035]) was used to calculate wind speed and direction up to a height of 13 km. This data set replaces the Nevada Test Site data (Quiring 1968 [DIRS 119317]) that were used for the TSPA-SR (CRWMS M&O 2000 [DIRS 153246]).

Parameterization for the atmospheric dispersal model used in all ASHPLUME versions was documented in *Igneous Consequence Modeling for the TSPA-SR* (BSC 2001 [DIRS 157876], Section 6.1.2). Tephra deposit thicknesses were simulated using ASHPLUME 1.4LV (BSC 2002 [DIRS 161296]) and ASHPLUME V.2.0 (CRWMS M&O 2001 [DIRS 152844]), and compared with actual tephra deposit thicknesses from the 1995 eruptive event at the Cerro Negro volcano in Nicaragua (CRWMS M&O 2000 [DIRS 152998]). The purpose of this model report is to consolidate and update documentation of the Ashplume conceptual and mathematical models, including parameterization and validation for ASHPLUME_DLL_LA V.2.0 (BSC 2003 [DIRS 166571]).

It should be noted that the ash redistribution conceptual model is new and was not used in the TSPA-SR; however, output from analyses supporting this model will be used in the TSPA-LA.

### 1.2.2 Technical Work Plan

This model report is governed by *Technical Work Plan: Igneous Activity Assessment for Disruptive Events* (BSC 2005 [DIRS 174773]). The technical work plan (TWP) specifies the activities to be carried out in consolidating and updating the documentation of the Ashplume conceptual and mathematical models.

The ASHPLUME code was not used to quantitatively assess the sensitivity of the erupted ash-waste distributions due to the conceptualization of the magma-waste form interaction. However, these effects are assessed in the assumptions and model conceptualization sections (Sections 5.1.2, 5.2.4, 6.3, and 6.5).

## 1.3 MODEL LIMITATIONS

### 1.3.1 Ashplume Model Limitations

A mathematical model is generally considered to be a mathematical description of a conceptual model that approximates the behavior of a system, process, or phenomenon with determinable limits of uncertainty. The Ashplume mathematical model is an approximation of the physical systems involved in the atmospheric dispersal and deposition of contaminated tephra (ash and waste particles) associated with a possible future volcanic eruption through the repository at Yucca Mountain. Limitations inherent in all mathematical representations of complex geologic processes include: (1) incomplete knowledge of details of a highly complex and heterogeneous natural process involving localized regions of the Earth's crust; (2) use of a mathematical representation that approximates, but does not specifically represent, every detail of the process; and (3) lack of comprehensive data describing every aspect of the complex, heterogeneous geologic natural process being represented. As a result of these limitations, the model provides predictive capability but does not provide an exact representation of the process.

The Ashplume model for Yucca Mountain is based on a model of Suzuki (1983 [DIRS 100489]) that Jarzemba et al. (1997 [DIRS 100987]) refined to represent violent Strombolian-type eruptions. Strombolian eruption involves ejection of magma into the atmosphere as a ballistic fountain of cm-sized scoria fragments from which μm- and mm-size ash is elutriated in a rising convective plume above the fountain. Whereas the fountain develops a cone of potentially

contaminated scoria around the vent orifice, the convective plume provides a source for distal transport of potentially contaminated ash downwind over a wide area. Fallout of ash from the plume forms a ground layer that generally thins with distance from the vent and is subject to redistribution by wind and water erosion. The Strombolian-type eruption is considered to be the most typical of the type of eruption possible in the Yucca Mountain region (BSC 2004 [DIRS 169980]). A Strombolian eruption includes violent phases as well as phases that are less violent, in which more effusive eruption processes dominate (BSC 2004 [DIRS 169980], Section 6.3.3). With increasing eruption violence, a larger fraction of the magma is fragmented to ash sizes, and a greater proportion of the magma contributes to the convective plume. The Ashplume model is limited to representation of the convective plume only and, thus, best models violent Strombolian eruptions. Accounting for overall mass on energy balance is not explicitly provided in the model results.

The Ashplume model solves diffusive transport (by atmospheric turbulence and wind) of particles distributed in a column (plume) of a height determined by the heat flux (power) of the column source. The duration of this transport for individual particles is the fallout time for particles governed by their terminal fall velocity (a function of their individual size, density, and shape factor) and their upward velocity in the plume. One limitation of the model is that Ashplume assumes a linear decrease in the plume's rise velocity from its initial rise velocity at the vent to zero at the top of the plume, but a buoyancy-driven velocity profile is not calculated.

Another limitation of the Ashplume model is its inability to accurately represent the transport of ash particles of mean diameter less than approximately 15 μm (Jarzemba et al. 1997 [DIRS 100987], Section 2.1). This cutoff in mean particle diameter is generally accepted to be the lower limit for the importance of gravitational settling. For particle sizes less than about 15 μm, atmospheric turbulence would tend to keep the particles aloft longer than would be predicted by the model. Because the typical mean diameter of ash particles after an eruption is generally much larger than 15 μm (see Section 6.5.2.4), the model described here is applicable to calculating the distribution of the majority of potential ash and radionuclide releases from a possible future eruption at Yucca Mountain (CRWMS M&O 2001 [DIRS 174768], p. 9). For the small number (approximately 10 percent) of model realizations in which the mean particle size is <30 μm, the effect of the model limitation is to overpredict the deposition of these fine particles in the Yucca Mountain region, leading to conservative predictions of ash and waste areal densities at the location of the reasonably maximally exposed individual (RMEI). A related limitation is that Ashplume does not consider ash particle aggregation within the plume or removal of particles from the plume by rainfall. These processes would tend to increase the deposition of particles from the plume, and could either increase or decrease the ash-waste deposition in the RMEI location. The model is limited to solid waste only and does not consider gaseous waste species.

The Ashplume mathematical model uses the simplification that wind speed is assumed to be constant throughout the atmospheric column. This assumption is discussed further in Section 5. This limitation is accommodated within the TSPA models by treating wind speed as an uncertain parameter. In addition, wind-speed data are taken from the upper altitudes reached by the ash plume where the majority of ash is dispersed from the eruptive column of a violent Strombolian eruption. The full range of wind speeds from near zero to the maximum winds observed at the higher altitudes is represented in the wind-speed distribution used in the TSPA-LA analyses.

This stochastic treatment of wind speed captures the uncertainty that exists in future wind speeds at all altitudes of the vertical eruptive column. Wind direction and wind speed are treated in a similar manner within the TSPA implementation of the dispersion model. The Ashplume mathematical model limits wind direction to a single value for a given realization of the model. However, in the TSPA, wind direction is also treated stochastically so that the distribution of wind direction and velocity, as a function of height, reflects the wind directions actually observed near the Yucca Mountain site.

The final limitation of the Ashplume model is its sensitivity to eruptive power and initial rise velocity, which are, in turn, functions of total erupted volume and duration. These parameters (power and initial rise velocity) are uncertain. ASHPLUME 1.4LV (BSC 2002 [DIRS 161296]) calculated these parameters from the theoretical relationship of conduit radius to magma ascent velocity given by Wilson and Head (1981 [DIRS 101034], p. 2,977), and, in that version, the initial rise velocity was termed the "eruption velocity at the vent." Because the actual eruption velocity at the vent in Strombolian eruptions is also a function of magma volatile content and the initial plume rise velocity is only weakly linked to eruption velocity, the previous relationship is not well-supported. ASHPLUME_DLL_LA V.2.0 (BSC 2003 [DIRS 166571]) must assume a conservative condition in which all the magma is fragmented and enters the convective plume (violent Strombolian) such that the initial plume rise velocity can be derived using a relationship between power, duration, and conduit diameter. This relationship is defined in Section 6.5.1, Equation 6-7, and the derivation of the initial rise velocity is discussed specifically in Section 6.5.2.10.

In spite of these limitations, the Ashplume model is considered to be appropriate, although conservative, for the analysis of the atmospheric transport and deposition of contaminated tephra in the eruption model case because the model includes those parameters that apply specifically to conditions of maximum entrainment of contaminated ash in an eruption column, dispersal of that ash downwind, and deposition of the ash at specified locations on the Earth's surface. The appropriateness of the model and the development of specific parameters are explained in detail in Section 6.

### 1.3.2 Ash Redistribution Model Limitations

Simple calculations, based on the conceptual model of tephra redistribution following a hypothetical eruption at Yucca Mountain, were completed to provide an abstraction of that conceptual model for use in the TSPA-LA. The ash redistribution conceptual model describes surficial processes that modify and distribute tephra that has been deposited from a hypothetical volcanic eruption at Yucca Mountain. This model is described in Sections 6.3.2 and 6.6.

Because of uncertainties, the limited amount of available data, and avoidance of mathematical complexity that does not provide value commensurate with the model purpose, limitations to the ash redistribution model are recognized. Among the limitations are:

- It is appropriate for erosion when climatic conditions are limited to those similar to the present climate or those included in *Future Climate Analysis* (BSC 2004 [DIRS 170002]).

- It emphasizes fluvial erosion and deposition, but does not specifically identify eolian deposition except as part of total deposition.

- Limited analogue tephra redistribution data do not provide sufficient quantification of the dilution (mixing) process within alluvial channels; therefore, this process is conservatively neglected for the initial abstraction for TSPA. The initial conditions for model outcomes producing tephra fallout predominantly in the Fortymile Wash watershed include post-eruptive transport of the more mobile ash and waste from Fortymile Wash to the RMEI location before stability is established on the surface of the Fortymile Wash alluvial fan.

- The redeposition of waste on the interchannel divides by sheet flooding is not represented by the model, but it is discussed conceptually as one of the processes operating on interchannel divides. The low frequency of these events, and the dilution (mixing) of waste that would occur in the redistributed material, support this simplification.

- The long-term geologic dynamics of fan interchannel divides and channel interactions are not represented.

The abstraction of the ash redistribution conceptual model (Section 6.7.2) is included in the TSPA model. However, it is now known that the simplified representation of redistribution and erosion in this model provides multiple accounting for waste mass, and the resulting degree of conservatism is more pronounced when primary ash layer is thin. For this reason, an alternative model (under development) is presented in Appendix I.

INTENTIONALLY LEFT BLANK

# 2. QUALITY ASSURANCE

This report documents a conceptual and mathematical model of atmospheric dispersal and subsequent deposition of contaminated tephra from a potential volcanic eruption at Yucca Mountain, and a conceptual model for subsequent redistribution of tephra by surficial processes. The report contributes to the analysis and modeling of a process that may disrupt natural and engineered barriers, which are classified in *Q-List* (BSC 2005 [DIRS 171190]) as "safety category" (SC) because of their importance to waste isolation, as defined in AP-2.22Q, *Classification Analyses and Maintenance of the Q-List*. Therefore, the results of this report are important to the demonstration of compliance with the postclosure performance objectives prescribed in 10 CFR 63.113 [DIRS 173273].

Development of this report revision and the supporting activities have been determined to be subject to the Yucca Mountain Project quality assurance program (BSC 2005 [DIRS 174773], Section 8.1). Approved quality assurance procedures identified in the TWP (BSC 2005 [DIRS 174773], Section 4) have been used to conduct and document the activities described in this report. The TWP also identifies the methods used to control the electronic management of data (BSC 2005 [DIRS 174773], Section 8.4). The revision of this report was performed with no variances to work described in the TWP (BSC 2005 [DIRS 174773]); it was developed in accordance with LP-SIII.10Q-BSC, *Models*.

INTENTIONALLY LEFT BLANK

# 3. USE OF SOFTWARE

## 3.1 SOFTWARE TRACKED BY CONFIGURATION MANAGEMENT

The sequence of versions showing the evolution of the ASHPLUME software is provided in Table 3-1. ASHPLUME_DLL_LA V.2.0 (BSC 2003 [DIRS 166571]) was used for the calculation of initial ash-fuel concentrations, which are described in Section 6.7 of this model report. ASHPLUME V.2.0 (CRWMS M&O 2001 ([DIRS 152844]) is the version used in this model report for the validation activities in Section 7. Both versions were obtained from Software Configuration Management and are appropriate for each application. Also, GoldSim V8.02 (BSC 2004 [DIRS 169844]) was used (Table 3-1) to estimate the mean concentrations of radioactive waste in the tephra sheet at 18 km from a hypothetical vent (Section 6.7.1 and Appendix E). These qualified codes were adequate for their intended uses as required by LP-SI.11Q-BSC, *Software Management*.

Table 3-1. Computer Software

| Software Title/ Version (V) | Software Tracking Number (STN) | Code Usage | Computer: Type, Platform, and Location |
|---|---|---|---|
| ASHPLUME V 2 0 (CRWMS M&O 2001 [DIRS 152844]) | 10022-2 0-00 | This version is used in validation studies as described in Section 7 3 1 of this report | PC, Windows NT 4 0 |
| ASHPLUME_DLL_LA V 2 0 (BSC 2003 [DIRS 166571]) | 11117-2 0-00 | This version is used for TSPA-LA calculations and calculation of initial ash/fuel areal concentrations for the ash redistribution conceptual model described in Section 6 7<br>Parameterization developed in this model report will directly feed this version of the software for TSPA-LA usage | PC, Windows 2000 |
| ASHPLUME 1 4LV (BSC 2002 [DIRS 161296]) | 10022-1 4LV-02 | This version is used, along with V 2 0, for comparison of calculated and measured ash deposition thickness for 1995 Cerro Negro eruption (see Section 7 3 1 1) | PC, Windows 2000 |
| GoldSim V8 02 (BSC 2004 [DIRS 169844]) | 10344-8 02-00 | In conjunction with ASHPLUME_DLL_LA V 2 0, this software was used for probabilistic simulations (Section 6 7 1 and Appendix E) | PC, Windows 2000 |

## 3.2 EXEMPT SOFTWARE

Commercial, off-the-shelf software used in support of this model report is listed in Table 3-2. This software is exempt from the requirements of LP-SI.11Q-BSC, *Software Management*. Formulas, inputs, and outputs are documented in the appropriate scientific notebooks.

Table 3-2. Exempt Software

| Software Name and Version (V) | Description | Computer and Platform Identification |
|---|---|---|
| Microsoft Excel, 2000 | The commercial software, Microsoft Excel 2000, was used for plotting graphs and statistical calculations. Only built-in standard functions in this software were used. No software routines or macros were used with this software to prepare this report. | PC, Windows 2000/NT |
| Microsoft Access, 2000 | The commercial software, Microsoft Access 2000, was used for unit conversions and data segregation. Only built-in standard query functions in this software were used. No software routines or macros were used with this software to prepare this report. | PC, Windows 2000 |
| OriginPro 7.5 | The commercial software, OriginPro 7.5, was used for data visualization and generation of basic statistics using built-in functions. No software routines or macros were used with this software to prepare this report. | PC, Windows 2000/XP |

# 4. INPUTS

## 4.1 DIRECT INPUT

This section discusses data, parameters, and inputs to the modeling activities that are documented in this report. External data used as direct input have been qualified as documented in Appendix A.

### 4.1.1 Data

Sources for data supporting the development of input parameters to the Ashplume model, and documented in this report, are listed in Table 4-1. These data are used to develop primary model inputs as described in Section 6.5.2. Ash physical characteristics required as inputs to the Ashplume model are developed in *Characterize Eruptive Processes at Yucca Mountain, Nevada* (BSC 2004 [DIRS 169980]). The report provides information about natural volcanic systems and the parameters that can be used to model their behavior and is appropriate for use as input to the ash dispersion model documented in this report.

The wind speed cumulative distribution functions (CDFs) and wind direction probability distribution functions (PDFs) appropriate for use in modeling a potential future volcanic eruption in the Yucca Mountain region are developed in this model report from data provided in *Upper Air Data: Desert Rock, Nevada, 1978-1995* (NOAA 2004 [DIRS 171035]). The development of the CDFs and PDFs from the raw climatological data is described in Sections 6.5.2.7 and 6.5.2.8.

The waste-particle-size distribution used as input to this model report is supported by documentation included in Appendix H. Air physical characteristics are taken from the *CRC Handbook of Chemistry and Physics, A Ready-Reference Book of Chemical and Physical Data* (Lide 1994 [DIRS 147834]).

Data sources providing input for the development of parameters used in the ash redistribution conceptual model documented in this report are identified in Table 4-2. These data provide the technical basis for the bounding model described in Section 6.7.2.

The qualification status of the input sources is provided in the Technical Data Management System and listed in the Document Input Reference System (DIRS) database. Data from external sources are used as direct input to the development of this model report. The data from these sources have been justified per requirements of LP-SIII.10Q-BSC, *Models*, and are considered to be qualified for intended use. These justifications are documented in Appendix A.

Table 4-1. Data Supporting the Development of Input Parameter Values for the Ashplume Model

| Data Description | Source | Section Where Discussed/Used |
|---|---|---|
| Eddy diffusivity | Suzuki 1983 [DIRS 100489] | Table 6-3, 6 5 2 1, 6 5 2 15 |
| Waste incorporation ratio | Jarzemba et al 1997 [DIRS 100987] | Table 6-3, 6 5 1(Eq 6-9), 6 5 2 6 |
| Column diffusion constant | Jarzemba et al 1997 [DIRS 100987] | Table 6-3, Table 8-2, 6 5 2 3 |
| Air physical characteristics (air viscosity) | Lide 1994 [DIRS 147834] | Table 6-3, 6 5 2 14, Table 8 2 |
| Air physical characteristics (air density) | Lide 1994 [DIRS 147834] | Table 6-3, 6 5 2 13, Table 8 2 |
| Wind speed | NOAA 2004 [DIRS 171035] | 6 5 2 7, 6 5 3 8, Tables 6-3, 8-2, 8-3, Appendix D |
| Wind direction | NOAA 2004 [DIRS 171035] | 6 5 2 8, 6 5 3 8, Tables 6-3, 8-2, 8-4, Figure 8-1, Appendix D |
| Specific heat capacity of magma | Drury 1987 [DIRS 156447] | 6 5 2 1 |
| Specific heat capacity of magma | Bacon 1977 [DIRS 165512] | 6 5 2 1 |
| Basaltic magma liquidus temperature | LA0407DK831811 001 [DIRS 170768] | 6 5 2 1 |
| Median number of waste packages calculated to be hit by a magmatic conduit | MO0504MWDNUMWP 001 [DIRS 173521] | 6 7 1 |
| Eruptive mass flux (maximum) | Detournay et al 2003 [DIRS 169660] | 6 5 1 (Eq 6-7b), 6 5 2 1 |
| Eruptive volume based upon the estimated eruption volumes of Quaternary volcanoes in the Yucca Mountain region | LA0407DK831811 001 [DIRS 170768] | 6 5 1 (Eq 6-7b), 6 5 2 1 |
| Duration of a single explosive phase constituting a violent Strombolian eruptive event | LA0407DK831811 001 [DIRS 170768] | Table 6-3, 6 5 2 2, Table 8-2 |
| Basaltic magma density | LA0407DK831811 001 [DIRS 170768] | 6 5 1 (Eq 6-7c), 6 5 2, 6 5 2 10, 6 5 2 11 |
| Conduit diameter (eruptive vent diameter) | LA0407DK831811 001 [DIRS 170768] | 6 5 1 (Eq 6-7c), 6 5 2, 6 5 2 10 |
| Clast characteristics (ash particle shape factor) | LA0407DK831811 001 [DIRS 170768] | Table 6-3, 6 5 2 12, Table 8-2 |
| Ash-particle density at minimum particle size | LA0407DK831811 001 [DIRS 170768] | Table 6-3, Table 8-2, 6 5 2 11 |
| Ash-particle density at maximum particle size | LA0407DK831811 001 [DIRS 170768] | Table 6-3, Table 8-2, 6 5 2 11 |
| Log ash-particle size at minimum ash density | LA0407DK831811 001 [DIRS 170768] | Table 6-3, Table 8-2, 6 5 2 11 |
| Log ash-particle size at maximum ash density | LA0407DK831811 001 [DIRS 170768] | Table 6-3, Table 8-2, 6 5 2 11 |
| Mean ash-particle diameter | LA0407DK831811 001 [DIRS 170768] | Tables 6-3, 8-2, 6 5 2 4, 6 7 2 2 |
| Ash particle diameter standard deviation | LA0407DK831811 001 [DIRS 170768] | Table 6-3, 6 5 2 5, Table 8-2 |
| Ash settled density | LA0407DK831811 001 [DIRS 170768] | 6 5 1 (Eq 6-7c), 6 5 2, 6 7 2 2 (Table 6-5) |
| Elevation of Yucca Mountain Crest | MO0103COV01031 001 [DIRS 155271] | Appendix D |

Table 4-2. Site-Specific Data Supporting the Ash Redistribution Conceptual Model

| Data Description | Source | Section Where Discussed/Used |
|---|---|---|
| $^{137}Cs$ values for soils on the Fortymile Wash alluvial fan, $^{137}Cs$ concentration in soil | DTN LA0308CH831811.002 [DIRS 164853] | Table 6-5, 6.7.2.3, 6.7.2.5 |
| $^{137}Cs$ values for soils in references profiles | DTN LA0302CH831811.002 [DIRS 162863] | 6.7.2.5.5 |
| Areal weights for landforms | DTN LA0507CH831611.001 [DIRS 174843] | 6.7.2.3, 6.7.2.4, Table 6-5, 6.7.2.5.1 |
| Estimated eolian erosion rate from $^{137}Cs$ studies | DTN LA0407DK831811.001 [DIRS 170768] | 6.6.4, 6.7.2.3, 6.7.2.5.2 |

### 4.1.2 Parameters and Parameter Uncertainty

The TSPA model, of which Ashplume is a component, uses Monte Carlo simulation as a method for mapping uncertainty in model parameters and future system states, expressed as probability distributions, into predictions of model output (BSC 2003 [DIRS 166296]). Large uncertainties exist in Ashplume model input parameters due to the uncertainty of future atmospheric conditions at the time of the hypothetical eruption and uncertainty in the characterization of the physical attributes of a future eruption. Ashplume model parameters that contain uncertainty and may significantly affect the results of TSPA calculations are developed in this model report as probability distributions for compatibility with the Monte Carlo methods used in the TSPA model.

Development of parameters used in the Ashplume model is documented in Section 6.5.2. Sampled parameters used in the ash redistribution conceptual model are documented in Section 6.7.2.

The eolian erosion rates developed in this report and used in the ash redistribution conceptual model are based on a 50-plus-year record of $^{137}Cs$ fallout (by-products of hydrogen bomb surface tests in the Pacific); therefore, considerable uncertainty is associated with the use of these rates for long-term (i.e., 10,000 years) erosion of the Fortymile Wash alluvial fan. Future climate variability may affect the rates of erosion. Although considerable uncertainty is associated with the long-term erosion rates, as long as future climate variations are relatively small, erosion rates are expected to remain within the uncertainty of current rates.

## 4.2 CRITERIA

The general requirements to be satisfied by the TSPA are stated in 10 CFR 63.114 [DIRS 173273]. Technical requirements to be satisfied by the TSPA are identified in the *Yucca Mountain Project Requirements Document* (Canori and Leitner 2003 [DIRS 166275]). The acceptance criteria that will be used by the Nuclear Regulatory Commission (NRC) to determine whether the technical requirements have been met are identified in the *Yucca Mountain Review Plan, Final Report* (YMRP) (NRC 2003 [DIRS 163274]). In cases where subsidiary criteria are listed in the YMRP for a given criterion, only the subsidiary criteria addressed by this scientific analysis are listed. Where a subcriterion includes several components, only some of those

components may be addressed. Details of how the criteria and key technical issues have been addressed in this report are provided in Appendix B.

### 4.2.1 Criteria for Ashplume Model

The *Yucca Mountain Review Plan, Final Report* (NUREG-1804; NRC 2003 [DIRS 163274]) associates the integrated subissue of airborne transport of radionuclides with the requirements listed in 10 CFR 63.114(a)-(c) and (e)-(g) [DIRS 173273]. NUREG-1804 (NRC 2003 [DIRS 163274], Section 2.2.1.3.10.3 lists the acceptance criteria that will be used by the NRC to evaluate the adequacy of information addressing volcanic disruption of waste packages. The YMRP (NRC 2003 [DIRS 163274], Section 2.2.1.3.11.3) describes the acceptance criteria that the NRC will use to evaluate the adequacy of information addressing the airborne transport of radionuclides in the license application. The YMRP (NRC 2003 [DIRS 163274], Section 2.2.1.3.13.3) describes the acceptance criteria that the NRC will use to evaluate the adequacy of information addressing redistribution of radionuclides in soil in the license application. Information addressing these acceptance criteria is presented in Appendix B.

## 4.3 CODES, STANDARDS, AND REGULATIONS

No other codes, standards or regulations other than those referenced in Section 4.2 apply to this model report.

# 5. ASSUMPTIONS

This section describes the assumptions applicable to the use of the Ashplume and ash redistribution models. Each assumption listed is followed by a rationale for use and its disposition in this report. Assumptions are grouped within this section according to whether they apply to the conceptual or mathematical model or to the model parameters. A summary of the described assumptions is provided in Table 5-1. Assumptions made in source documents are not discussed in this report.

Table 5-1. Summary of Key Assumptions

| Item # | Assumption | Summary Comment on Impact |
|---|---|---|
| **MODEL ASSUMPTIONS** | | |
| 5.1.1 | Volcanic eruption is violent Strombolian for entire duration | Enhances the potential for ash and waste dispersal by transport in convective plume |
| 5.1.2 | All waste particles smaller than a defined fraction of ash particles are transported by ash and dispersed | This is a conceptual assumption to ensure that waste and ash particles are appropriately paired, according to a particle size ratio, to provide reasonable waste transport to atmosphere. Sensitivity analysis indicates that impact of this assumption is small |
| 5.1.3 | Maximum potential exposure to the RMEI from ash redistribution is bounded by two model outcomes dependent on primary ash thickness at RMEI location | The two model outcomes (ash deposition at the RMEI location or ash deposition in the Fortymile Wash basin) are the basis for product outputs from the redistribution conceptual model for the TSPA. Other possible model outcomes (e.g., where tephra are deposited west of Yucca Mountain) would result in exposure to a RMEI less than that of the two outcomes considered |
| 5.1.4 | Future climate changes will have little impact on Fortymile Wash alluvial fan | If climate changes to a wetter conditions, the pluvial period is projected to have about 1 ½ to 2 times the current annual precipitation. However, the uncertainty in other ash redistribution model parameters is on the same order as the expected change in rainfall due to climate change. Therefore, this assumption is expected to have little effect on the model outcome |
| 5.1.5 | Fluvial transport and mixing of ash with sediment can be scaled from other analogue sites | Mixing of sediments while in transport down drainage channels is a fundamental sedimentary process and as such can be scaled from analogue data for drainage basins where the process has not yet been measured |
| 5.1.6 | The channels of the alluvial fan in area of the RMEI are stable for the regulatory period | Because the channels on the upper (northern) part of the fan are moderately incised, it is highly unlikely for the channels to be moved. Thus, when flow moves through these channels, material in the channels will be moved downstream to be replaced by other material as the flood wanes. Since the areal proportion of channels is expected to remain relatively constant, the actual location of these channels does not matter in the ash redistribution model |
| 5.1.7 | Initial redistributed tephra is undiluted | Data are insufficient for accurate prediction of mixing of ash and sediment. Therefore, no credit is taken for dilution. This assumption maximizes transport of ash in channels to RMEI area |
| 5.1.8 | Eolian erosion transports waste out of RMEI area without redeposition in RMEI area | The net loss of waste in the RMEI area is offset by the presence of a persistent layer of low contamination in the model. Therefore the effect of this assumption is thought to be small |

Table 5-1. Summary of Key Assumptions (Continued)

| Item # | Assumption | Summary Comment on Impact |
|---|---|---|
| **PARAMETER ASSUMPTIONS** | | |
| 5.2.1 | Wind data from Desert Rock station near Mercury, Nevada, acceptably approximates future wind conditions | Global climate model studies with available paleoclimate information support the assumption of little change to long-term average wind patterns. Postglacial qualitative trends include a lessening of frequency for northerly winds from the repository towards the RMEI |
| 5.2.2 | Wind speed and direction are constant during an eruptive event | Gives maximum distribution along centerline of wind direction, and toward the RMEI for corresponding wind conditions |
| 5.2.3 | Tephra dispersal is dictated by the wind speed and direction at the top of the eruption plume | Use of wind speed and direction corresponding with the top of plume results in high (conservative) dispersal of ash and waste |
| 5.2.4 | All waste intersected in eruptive conduits is dispersed as fine particulate of near fuel-form grain size | Appropriate analogue data from igneous extrusion through engineered systems are lacking. This assumption places a high (conservative) proportion of waste into the dispersed plume and uses a median particle size from laboratory tests that is consistent with a range that was reported as representing a high hot particle size fraction at 20 km from the Chernobyl Power Plant |
| 5.2.5 | Initial rise velocity of particles in plume is the minimum velocity necessary to supply eruptive thermal power to a convective plume | This assumption maximizes the dispersal of ash and waste in a high convective plume that is transported downwind |
| 5.2.6 | Net soil erosion for the regulatory period will be similar to that assessed from 50-year cesium tracer data unless major climatic changes occur during this time period | Produces realistic rate of erosion occurring over the last 50 years and should remain within the uncertainty of current rates unless large-scale climate changes that exceed expected changes (Asumption 5.1.4) occur in this time interval |

## 5.1 MODEL ASSUMPTIONS

### 5.1.1 Ashplume Representation of the Conceptual Model

**Assumption**–The Ashplume model assumes that volcanic eruptions in the Yucca Mountain region are violent Strombolian for the entire duration of the explosive phase. Erupted magma is presumed to be fragmented and dispersed in the convective plume for the entire duration of the eruption. This assumption is conservative in that it maximizes the potential for ash and waste dispersal during Strombolian activity. (Note that violent Strombolian does not reach the dispersive potential of more violent types of events that are not associated with the Yucca Mountain region, such as Vulcanian/Surtseyan [hydrovolcanic] eruptions or eruptive phases.) The validity of this assumption received support from the Igneous Consequences Peer Review Panel (Detournay et al. 2003 [DIRS 169660], Section 4.2).

**Rationale**–This assumption is considered to be conservative because normal Strombolian activity is dominated by short-duration bursts that throw relatively coarse fragments of melt out of the vent on ballistic trajectories, where most of the fragments are deposited immediately around the vent with only a very small fraction of finer particles rising higher and being dispersed by wind to form minor fallout sheets (BSC 2004 [DIRS 169980], Section 6.3.3.6.1).

In contrast, the Ashplume model represents the most violent type of Strombolian activity, in which the near-vent ballistic component is minimal and tephra dispersal in a wind-blown convective plume dominates, according to the conceptual model (Jarzemba et al. 1997 [DIRS 100987], p. 2-1). Clearly, this assumption maximizes the dispersal of contaminants for Strombolian activity. Uncertainties associated with the nature of violent Strombolian eruptive phases are their duration, eruption power (the heat flux carried by the tephra), and the volume of the erupted tephra (BSC 2004 [DIRS 169980], Section 6.3.3.4). These uncertainties are included in the model through the development of distribution functions for these parameters. The volume of the Lathrop Wells volcano is used to provide realistic bounds for these input parameters since it is the preferred analogue to a potential future volcanic eruption at Yucca Mountain (Section 6.5.2).

It is conservative to assume that an eruptive event can be modeled as being in the violent Strombolian phase during the entire period of eruption because typical eruptions include only a minor component, if any, of violent Strombolian activity. Most of a typical eruption is less energetic.

**Where Used**–This assumption is used in Section 6.3 to support the conceptual model for the volcanic eruption release.

### 5.1.2 Waste-Particle Incorporation with Ash

**Assumption**–The mathematical formulation of the Ashplume model makes the simplifying assumption that all waste particles with diameters less than a certain fraction of the diameter of ash particles, determined by the incorporation ratio (Section 6.5), are attached to ash particles for transport. The model also contains the assumption that any waste particles too large for incorporation are not transported downwind.

**Rationale**–There is no physical basis for this mathematical construct, but the assumption is consistent with the conceptualization that all waste material in canisters intersected by an eruptive conduit is incorporated into the magma (and, subsequently, into the eruption column). This mathematical formulation is required to transport an ash particle corrected for the density of the waste particle. It is reasonable to assume that small ash particles cannot host large waste particles for transport. A limiting factor must be introduced into the mathematical model to represent a reasonable waste/ash fraction. In this mathematical simplification, waste-particle size distributions and ash-particle size distributions are appropriately paired to ensure a reasonable fraction of waste is transported in the eruption.

This assumption is consistent with the conceptual model of ash-waste interaction. An alternative conceptual model of magma-waste interaction in the repository drifts, conduit, and eruptive plume is presented in Appendix J. This discussion includes an alternative value for the ASHPLUME input parameter, "waste incorporation ratio."

**Where Used**–This assumption is used in Section 6.5 in the development of the Ashplume mathematical model.

### 5.1.3 Tephra Sheet Distribution for Ash Redistribution Model

**Assumption**–The potential scenarios characterizing maximum potential exposure to the RMEI can be represented by two bounding model outcomes for tephra sheet distribution and orientation, and these outcomes can be distinguished by a criterion of minimum primary ash deposition as calculated by the Ashplume mathematical model.

**Rationale**–The possible orientation of tephra sheets from a basaltic volcanic eruption centered on Yucca Mountain suggests that the two model outcomes representing maximum potential exposure to the RMEI are: Outcome 1, in which the tephra sheet covers the location of the RMEI, and Outcome 2, in which the tephra sheet is located within the Fortymile Wash drainage basin upstream from the RMEI location. The properties of the Outcome 1 tephra sheet at the RMEI location are consistent with the waste concentrations and ash thickness calculated from ASHPLUME_DLL_LA V.2.0 (BSC 2003 [DIRS 166571]) and presented in Table 6-4 of Section 6.7.1. Properties of an Outcome 2 tephra sheet located in the Fortymile Wash drainage basin assume that available ash from the eruption, other than that forming the cinder cone, is deposited within the drainage basin and is available for redistribution primarily by fluvial processes. The two model outcomes are the basis for product outputs from the redistribution conceptual model for the TSPA. Other possible model outcomes (e.g., where tephra are deposited west of Yucca Mountain) would result in exposure to a RMEI less than that of the two outcomes outlined above.

The assumed criterion for distinction between model outcomes 1 and 2 is based on ash thickness at the RMEI location as first calculated by the Ashplume code within the TSPA GoldSim model. Outcome 1 is defined as including eruptive events where the calculated primary tephra thickness at the RMEI location is greater than or equal to the minimum mean ash particle size, 0.001 cm. All other events are defined as Outcome 2.

The two outcomes represent conditions that likely characterize maximum potential exposure to the RMEI in that ash deposited to the northeast is consistent with prevailing wind direction and is the most likely direction of any ash plume in a hypothetical eruption in the vicinity of Yucca Mountain including one located at Yucca Mountain. The deposition of ash to the south directly on the location of the RMEI would be the exceptional case as a northerly wind direction is uncommon (see Figure 6-1).

It is possible that the simplified bounding definition could classify as Outcome 1 some events in which an approximately westerly wind placed the primary tephra upstream of the RMEI location, but also provided sufficient thickness at the RMEI location to satisfy categorization as Outcome 1. This would result in omitting an upstream waste redistribution source to the RMEI location. The possibility of this sort of hybrid event is accounted for in the initial conditions for Outcome 1. Because of this potential shortcoming, the alternative ash redistribution model (see Appendix I) identifies an option for using wind direction sectors, rather than primary tephra thickness, to select initial conditions for ash redistribution.

**Where Used**–This assumption is used in Section 6.6.1 to support the ash redistribution conceptual model.

### 5.1.4 Future Climate

**Assumption**–The climate through much of the postclosure period will be similar to the present climate and, even with a projected increase in annual precipitation, will have relatively little impact on the Fortymile Wash alluvial fan.

**Rationale**–The probable future climate at Yucca Mountain is discussed in *Future Climate Analysis* (BSC 2004 [DIRS 170002]). If climate changes to wetter conditions, the pluvial period is projected to have about 1 and one-half to 2 times the current annual precipitation. The uncertainty in other ash redistribution model parameters is on the same order as the expected change in rainfall due to climate change. Therefore this additional uncertainty is not expected to make a significant difference in results of the TSPA-LA.

**Where Used**–Section 6.6.

### 5.1.5 Ash-Sediment Mixing during Fluvial Transport

**Assumption**–Fluvial transport and the mixing of basaltic ash with other sediment through the Fortymile Wash drainage system can be adequately described by scaling analogue data from other sites.

**Rationale**–Mixing of sediments while in transport down drainage channels is a fundamental sedimentary process and as such can be scaled from analogue data for drainage basins where the process has not yet been measured.

**Where Used**–Section 6.6.

### 5.1.6 Stability of Channels on the Upper Fortymile Wash Alluvial Fan

**Assumption**–The channels on the upper fan at the RMEI location are stable through the postclosure period.

**Rationale**–The upper fan of Fortymile Wash is close to being in equilibrium. The channels are slightly incised below the fan surface and, as such, sediment will pass through the channels during floods without modifying them. Thus, these channels are considered as stable features of the upper fan surface.

**Where Used**–Section 6.6.

### 5.1.7 Initial Redistributed Ash is Undiluted

**Assumption**–Initial redistributed tephra in Fortymile Wash and on its alluvial fan is assumed to be undiluted.

**Rationale**–This is an upper bound of the process. The lower bound would be a well-mixed sediment with no ash remaining incorporated. The lack of dilution data from younger analogue volcanoes precludes its use in TSPA so the default upper bound is used.

**Where Used**–Section 6.6.

### 5.1.8 No Eolian Transport of Waste to the RMEI

**Assumption**–Eolian erosion process is assumed to transport waste out of the RMEI area without redeposition in the RMEI area.

**Rationale**–The rate of deposition by eolian processes is not known. It is difficult to adequately measure and to model in a meaningful predictive manner. While this assumption results in a continual loss of contamination from the interchannel divide areas, the presence of a persistent low (1 percent) concentration of waste in these areas is designed, in part, to account for the continued remobilization of waste in the RMEI area.

**Where Used**–Section 6.6.

## 5.2 PARAMETER ASSUMPTIONS

### 5.2.1 Future Wind Speed and Direction

**Assumption**–Data characterizing variability in wind speed and wind direction under present climatic conditions in the Yucca Mountain region are provided in *Upper Air Data: Desert Rock, Nevada, 1978-1995* (NOAA 2004 [DIRS 171035]; and Appendix D, this document). These data are assumed to be acceptable approximations of variability in wind speed and direction for future wind conditions. Conceptually, this assumption corresponds to an assumption that climatic change will not significantly affect wind speed and direction. The magnitude of short-term variability in wind speed and direction, which is included in the data that characterize present wind conditions, is presumed to be significantly greater than long-term variability introduced by potential future climatic changes.

**Rationale**–Justification for future wind conditions in future climates is based on the observation that the magnitude of short-term variability in meteorological phenomena is great compared to changes in long-term averages. Emphasis for relatively brief volcanic events is appropriately placed on the short-term variability rather than on long-term averages in wind patterns.

Additional support for the reasonableness of this assumption comes from examination of published modeling studies of past climatic conditions that may be reasonable analogues for future climatic conditions at Yucca Mountain. Kutzbach et al. (1993 [DIRS 119269], p. 60) have modeled global climates at 3,000-year intervals during the last 18,000 years, using general circulation models with available paleoclimatic information used to define boundary conditions. Resolution of the model is extremely coarse (grid blocks are 4.4 degrees latitude by 7.5 degrees longitude (Kutzbach et al. 1993 [DIRS 119269], p. 60)), and results are not intended to be interpreted at local scales. However, model results (presented at a regional scale) provide qualitative information about modeled wind speeds and directions for the southwestern United States. Model results are provided for 18,000 years ago, at the end of the last major glaciation of northern North America, at 12,000, 9,000, and 6,000 years ago and also for present conditions. Climatic conditions at these times span the range of conditions that might reasonably occur during a future transition from the present climate to a glacial climate.

Modeled surface winds for the southwestern United States in winter and summer show a slightly stronger westerly component (away from the location of the RMEI south of the repository) 18,000 years ago than at present and are essentially unchanged from the present at 12,000, 9,000, and 6,000 years ago (Kutzbach et al. 1993 [DIRS 119269], Figures 4.6 and 4.8). Modeled winter (January) winds at the 500-millibar (mb) pressure isobars (about 5.5-km altitude) blow strongly from the west at all times and were somewhat stronger at 18,000 years ago than at present (Kutzbach et al. 1993 [DIRS 119269], Figure 4.14). Modeled summer (July) winds at 500 mb are weaker and less consistent than winter winds, blowing from the southwest and west at 18,000 and 12,000 years ago and at the present, and from the northwest 9,000 and 6,000 years ago (Kutzbach et al. 1993 [DIRS 119269], Figure 4.15).

The information relevant to the assumption discussed here is that significant changes in the Kutzbach et al. (1993 [DIRS 119269]) modeled wind speeds and directions in the southwestern United States are not dramatic during the modeled transition from glacial to interglacial climates. The largest changes, occurring during full glacial conditions 18,000 years ago, appear qualitatively to correspond to a decrease in the relative frequency of winds blowing toward the RMEI location south of Yucca Mountain. Therefore, these changes are reasonably and conservatively neglected, and variability in present wind conditions is assumed to characterize variability adequately in future conditions.

**Where Used**–This assumption is used to justify the distributions of future wind speed and direction that are recommended for use in the TSPA-LA analyses. The recommended wind direction and wind speed distribution functions are discussed in Section 6.5. Functionally, the assumption means that individual values of wind speed and direction can be sampled for time zero from distributions based on present data, and the same values can then be used for all time steps for each realization.

### 5.2.2 Wind Speed and Direction Remain Constant During an Eruptive Event

**Assumption**–Wind speed and direction are assumed to be constant during an eruptive event.

**Rationale**–This assumption prevents short-term variations in wind speed and direction from spreading the ash plume over a broader area and results in both a maximum quantity and maximum concentrations of waste at the centerline of the plume. This is a reasonable simplification, given the relatively short duration of violent eruptive events.

**Where Used**–Section 6.5.

### 5.2.3 Ashplume Utilization of Wind Speed and Direction

**Assumption**–The Ashplume model assumes that the wind speed and direction that dictate tephra dispersal are those that occur at the top of the plume.

**Rationale**–Wind speed and wind direction vary with altitude above the ground, and, thus, tephra dispersed from the plume at different altitudes follows trajectories governed by altitude-dependent wind vectors. The column diffusion constant ($\beta$) determines which locations in the column contribute the most tephra dispersal. This constant was presumed to be a log-uniform distribution from 0.01 to 0.5 (Jarzemba et al. 1997 [DIRS 100987], p. 4-1) without

justification (for the distribution type) other than it spans more than one order of magnitude. Because violent Strombolian eruptions typically form an anvil-shaped plume, most particles must rise to near the plume top before dispersal down wind. This suggests that large values of $\beta$ are common such that the distribution is likely uniform, as is implemented in this report. With a uniform distribution of beta between 0.01 and 0.5, the majority (about 80 percent) of violent Strombolian eruptions are modeled with $\beta$ greater or equal to 0.1, a level at and above which Suzuki (1983 [DIRS 100489], Figure 6) showed dominant dispersal from the upper half of the column. Hence, the wind speed and direction near the top of the plume are appropriate and maximize dispersal for modeled eruptions. This assumption is considered to be reasonable and consistent with the intended use of the Ashplume model.

**Where Used**–Section 6.5.

### 5.2.4 Waste-Particle Size

**Assumption**–For the purpose of estimating waste-particle diameters in the eruptive environment, all waste is assumed to be unaltered commercial spent fuel physically disaggregated to a size range that approximately relates to fuel form grain size.

**Rationale**–This assumption is considered reasonable for analyses of the 10,000-year postclosure performance period as specified in 10 CFR 63.311 [DIRS 173273].

Experimental evidence is lacking for processes, including fragmentation, from magmatic melt interaction with spent nuclear fuel in a volcanic eruption. The U.S. Department of Energy (DOE) performance assessments (Reamer 1999 [DIRS 119693], p. 82) have all assumed that the waste package fails upon contact with basaltic magma, therefore exposing the fuel form to the magma. *Characterize Eruptive Processes at Yucca Mountain, Nevada* (BSC 2004 [DIRS 169980], Section 6.3.3.5) discusses potential mechanisms of magmatic interaction with the waste packages and spent fuel form and observes that fuel form oxidation is a likely interaction process.

*Dike/Drift Interactions* (BSC 2004 [DIRS 170028], Section 6.4.8) considers that magmatic interaction with waste form could form molten and solid oxide solution complexes with some of the magmatic mineral constituents; however, chemically unchanged waste form is assumed due to lack of data on the mineral phases that could form. If chemical assimilation into the magmatic melt, rather than the assumption of physical disaggregation to fine particle size, were assumed for the Ashplume modeling purpose, the proportion of waste available for atmospheric dispersion would be smaller (less conservative) by an approximate factor of three. This would be the case since a major proportion of the waste, assimilated in the magma, would then allocate to cone and lava flow material rather than with the eruptive plume column ash. Glass waste form would be more readily expected to be assimilated with the magmatic melt; therefore, on account of both aspects, the assumption basis for treating all waste as fragmented particulate is conservative but reasonable.

If partly or wholly assimilated into the magma melt, the unaltered glass waste forms are likely to have particle diameters comparable to those of the ash particles, which are larger than the values used for spent fuel. Given the conceptualization that waste particles are transported by

combining with ash particles of larger sizes (see Assumption 5.1.2), the assumption to treat all waste as unaltered commercial spent fuel is also conservative but reasonable. The assumption that the waste form is unaltered prior to being disturbed in a volcanic event is reasonable for analyses of the 10,000-year postclosure performance period, given the relatively small number of waste packages expected to fail under nominal conditions during that period and the expected stability of the waste form within the undisturbed waste packages.

The assumed mechanism for disaggregation of spent fuel form to fine particulate, exposed after waste package failure, is based on oxidation of $UO_2$, the primary form of commercial pressurized water reactor fuel (DOE 2003 [DIRS 166027], p. 19). Oxidation rates and the accompanying morphological changes of nonirradiated and irradiated fuel form have been extensively studied (DOE 2003 [DIRS 166027], p. 19), though most reported work seems to be for temperatures below 400°C, presumably pertaining to spent fuel handling and storage. The chemistry of the uranium oxide system is complex because of the existence of hyperstoichiometric oxides (DOE 2003 [DIRS 166027], p. 20). At lower temperatures, the progressive oxidation of $UO_2$ to the higher valence states involves an incubation period; however, this trends to zero at 500°C (Dehaudt 2001 [DIRS 164019], p. 376). The same source reports that progression through oxidation states results in structural changes with initial densification (up to a O:U ratio of approximately 2.3) and subsequent specific volume increases (between O:U ratios of approximately 2.3 and 3.0) that lead to intergranular and intragranular decohesion of the fuel grains. At macro level, this has been seen to cause fragmentation to fuel form grain size and even to provide size distributions as small as 0.35 and 0.95 µm; however, no work has been found to provide an estimate of the overall size distribution from fuel exposed to the durations, temperatures and forces that are possible during an eruptive event. Sintered $UO_2$ does not readily break into single grains; rather transgranular fracture is common when grinding unirradiated $UO_2$. Also, because fission products tend to accumulate along grain boundaries during irradiation of the fuel (especially as gas bubbles and metal particles), the resulting loss of cohesion between grains allows spent fuel to break into individual grains more readily than does unirradiated $UO_2$.

Simulated accident events have been studied; however, resulting particulate size has not often been reported. Sandoval et al. (1983 [DIRS 156313], p. 46) report a mass median diameter of 210 micrometer for $UO_2$ particle and fume release after penetration by a high-energy device of a full size shipping cask containing depleted $UO_2$ fuel. However this shock circumstance of short duration may not adequately represent the oxidation state fragmentation mechanisms.

In reconstruction of the inhalation dose after the Chernobyl accident, the fractions of hot particles according to distance from the nuclear plant are reported (Mück et al. 2002 [DIRS 170378], Table 5) to be as shown in Table 5-2. This provides an analogue of distal size distributions of radionuclide outfall from an accidental thermal source, but not the total particle size distribution from that source.

Table 5-2. Fraction of Hot Particles by Size and Distance from Chernobyl Power Plant

| Distance from Chernobyl Nuclear Power Plant (km) | Fraction of Hot Particles with a Given Particle Size | | | |
|---|---|---|---|---|
| | 0 to 20 µm | 20 to 50 µm | 50 to 100 µm | 100 to 200 µm |
| 4 | – | 12.5% | 75% | 12.5% |
| 10 | – | 65% | 35% | – |
| 20 | 8% | 87% | 5% | – |
| 37 | 40% | 60% | – | – |
| 55 | 65% | 35% | – | – |

Source: Muck et al. 2000 [DIRS 170378]

While preparing spent $UO_2$ fuel (approved testing material (ATM) 103: ~30MW d/kg-U, Appendix H) for corrosion studies, Argonne National Laboratory made assessments of crushed and ground fuel particle size. The estimate of fuel particle size and relationship to natural grain size is provided in Appendix H. The majority (approximately 80 percent) of the size-reduced fuel was reported as being mostly single fuel grains, less than 45 µm and averaging 20 µm. A midsize range of 45 to 150 µm represented 11 percent of the ground fuel while 9 percent exceeded 150 µm. For the purpose of consideration to volcanic interaction with the repository, the Argonne National Laboratory author of Appendix H provides a professional judgment of suggested fuel particle size, based on that investigation, experience with observations of fuel, and cited sources. For unaltered fuel the suggested particle diameter range is 1 to 500 µm with a mean of 20 µm.

From the foregoing, and in the absence of data that more specifically represents interaction of magma with spent fuel, the Ashplume model assumes that fuel in the affected waste packages is available for entrainment in the ash plume as finely-divided particles with diameters in the range of 1 to 500 µm, with a mean of 20 µm.

An alternative waste particle size distribution has been developed based on available analogues and is presented in Appendix J.

**Where Used**–Section 6.5 to describe the waste-particle size distribution.

### 5.2.5 Initial Rise Velocity

**Assumption**–The initial rise velocity of tephra particles in the plume is assumed to be the minimum velocity required to provide the plume the modeled thermal power. The Ashplume model stipulates that the convective rise velocity of tephra particles linearly decreases from the initial rise velocity at the base of the convective plume to zero at the top of the plume. Because the upward velocity profile of buoyant plumes generally decreases with height to zero at their tops where neutral buoyancy is a complex relationship of plume and atmospheric density profiles and the rate of air entrainment and heating, this assumption represents the model-equivalent of the modeled plume's vertical velocity profile. In order for model-equivalence to give a reasonable numerical approximation, the initial rise velocity is constrained to values that are compatible with the plume height and, thus, eruptive power.

**Rationale**–Ashplume models a column (plume) instantaneously loaded with hot particles moving at some upward velocity. The height of the column determined by ASHPLUME is fixed by the power (heat flux) provided by erupting magma. The heat flux is directly proportional to the mass flux of magma from the vent, which, for continuity, is determined by the vent area, magma bulk density, and vent velocity. For any given vent area and mass flow rate, the density and velocity of the mixture are inversely related: minimum vent velocity occurs when the magma bulk density is at its maximum (gas-free) value and maximum vent velocity occurs when magma bulk density is at its minimum value. The eruption velocity may briefly exceed the sonic velocity of the mixture within or slightly above the eruptive vent, resulting in sub-atmospheric pressure in the jet; however, the pressure will quickly adjust to atmospheric conditions, which will determine the mixture density and, indirectly, its velocity. For the purposes of this study then, the minimum realistic magma bulk density arises when magma volatile components are expanded to atmospheric pressure. Realistic vent velocities fall between these two extremes. Before the magma and gas mixture enters the convective-thrust part of the plume, it rapidly decelerates by its interaction with the atmosphere and gravitational forces in a region known as the gas-thrust region (Section 6.3). Because the height of the gas-thrust region is generally less than 10 percent of the total eruptive column height, a convective plume model such as Ashplume that neglects this gas-thrust region is justified (Wilson et al. 1978 [DIRS 162859], p. 1,830). The Ashplume model must account for gas expansion and air entrainment as well as the deceleration of tephra in the gas-thrust region while maintaining continuity in order for the column height to eruptive power relationship to hold. Implicit in the convective plume model is that: (1) height is solely determined by the convection produced by the supplied thermal power and that (2) the contribution to the plume height by the momentum of gas-thrust region is negligible. This approximation stipulates that the velocity of tephra entering the plume must only be that required to deliver the required power. Thus, for eruptions involving gas expansion, the plume base area must be greater than the vent area by a factor equal to the amount of gas expansion. For plumes of circular cross section, the radius increases by the square root of the gas expansion. As an example, consider a mixture of gas and tephra issuing from a vent of 1-m radius for which the mixture expands by a factor of 200. The resulting plume would have a radius of approximately 14 m, and its initial velocity would be the minimum vent velocity. This assumption is considered reasonable and consistent with the intended use of the Ashplume model.

**Where Used**–Section 6.5.

### 5.2.6 Erosion Rate

**Assumption**–Net erosion during the regulatory period will be similar to that observed from field studies as assessed by 50-year $^{137}Cs$ tracer data.

**Rationale**–Field measurements of $^{137}Cs$ on interchannel divides result in erosion rates representative of the last 50 years only (the time since the deposition of $^{137}Cs$ began) and must be extrapolated for time periods greater than 50 years. In the absence of other local or analogue data and consistent with the assumption of relatively stable future climate (Section 5.1.4), the field-measured net erosion rate over 50 years is assumed to apply for longer time periods (i.e., tens to hundreds of years). Uncertainty in erosion rates is on the same order as the uncertainty in other ash redistribution model parameters, and therefore this additional uncertainty is not expected to make a significant difference in the results of the TSPA-LA.

**Where Used**–Section 6.7.

# 6. MODEL DISCUSSION

The potential consequences associated with the eruption model case require consideration of both the eruption and deposition of contaminated tephra and redistribution of that material after deposition. This section presents the objectives, technical bases, and applications of the two models that represent the eruption, deposition, and redistribution of volcanic ash. Section 6.1 presents the modeling objectives. Section 6.2 presents the applicable features, events, and processes addressed by the models. Section 6.3 provides the conceptual basis for the eruptive transport, deposition, and redistribution of waste-contaminated ash from a hypothetical volcanic eruption through a repository at Yucca Mountain. Section 6.4 discusses alternative conceptual models, and Section 6.5 presents the technical basis for application of the ash dispersal and deposition model. Sections 6.6 and 6.7 provide the technical basis for and application of the redistribution of waste-contaminated volcanic ash through sedimentary processes.

The Ashplume mathematical model is implemented for TSPA calculations by computer code ASHPLUME_DLL_LA V.2.0 (BSC 2003 [DIRS 166571]). The ASHPLUME_DLL_LA computer code is a component of the TSPA model of the nuclear waste repository at Yucca Mountain. The TSPA model is used to evaluate the performance of the geologic repository in protecting humans and the environment from the risk associated with exposure to spent nuclear fuel and high-level radioactive waste. Within the TSPA, the model of atmospheric dispersal and deposition of tephra implemented in the ASHPLUME code is used to predict the ground-level concentration or areal density ($g/cm^2$) of ash and waste after a violent Strombolian eruption that intersects the repository. The ash redistribution conceptual model describes the sedimentary processes acting on the tephra sheet after deposition. The concentration of waste-contaminated ash at the RMEI location (18 km south of the repository's southern boundary (40 CFR Part 197 [DIRS 173176])) resulting from sedimentary redistribution processes is calculated for different ash-fall deposition realizations. The waste concentration is then combined with biosphere dose conversion factors (BDCFs) to calculate a radiation dose to the RMEI. The model is discussed in Section 6.6.3 and is based on several site-specific investigations, including analogue studies of ash redistribution and erosional and depositional processes inferred from an analysis of $^{137}Cs$ data (BSC 2004 [DIRS 169980], Section 6.3.4).

## 6.1 MODELING OBJECTIVES

Two models have been developed to represent the dispersal, deposition, and redistribution processes for volcanic ash contaminated with radioactive waste from a hypothetical eruption through the repository at Yucca Mountain. The overall objectives of these two models are to:

- Represent the processes and the associated potential consequences related to deposition and redistribution of contaminated ash at and near the RMEI location.
- Provide representative abstractions of the models for inclusion in the TSPA model.

### 6.1.1 Objectives of the Ashplume Model

The Ashplume conceptual model provides the basis, supported by analogue descriptions, for the applicability of using the ASHPLUME code to model volcanic ash and waste dispersal during a

hypothetical future volcanic eruption through the repository. Development of the model uses the Eruptive Processes Conceptual Model (BSC 2004 [DIRS 169980], Section 6) and is based on comparison of the expected scenario characteristics with the physical processes modeled by Ashplume.

The Ashplume model implements the conceptual and mathematical model of Suzuki (1983 [DIRS 100489]) for estimation of the areal density of tephra (ash) deposits on the surface of the earth following a violent Strombolian-type volcanic eruption. The computer code, developed by Jarzemba et al. (1997 [DIRS 100987]) from the Suzuki mathematical model, includes estimation of the areal density on the Earth's surface of spent fuel particles incorporated into ash particles due to an eruption that intersects the repository at Yucca Mountain. Areal densities can be converted to deposit thickness by dividing the areal density by the value of settled (deposit) density (typically 1.0 g/cm$^3$ (BSC 2004 [DIRS 169980])).

ASHPLUME_DLL_LA V.2.0 (BSC 2003 [DIRS 166571]) includes a dynamically linked library module for use as a component of the TSPA GoldSim model to assess dose to the RMEI from exposure to contaminated ash from possible volcanic activity at the Yucca Mountain site. The results of the Ashplume model calculations (tephra and waste areal densities), modified by processes in the ash redistribution model, are used by the TSPA-LA model in conjunction with BDCFs to calculate dose to the RMEI. For compliance demonstration purposes for disruptive scenarios, the TSPA-LA assumes that the dose occurs to a hypothetical individual, the RMEI. ASHPLUME V.2.0 (CRWMS M&O 2001 [DIRS 152844]) also includes an executable module for stand-alone use, which is applied to making calculations shown in Section 7 of this report. The stand-alone version calls the dynamically linked library module for making the calculations and serves only to format user input parameters for the dynamically linked library. Thus, the following discussions in this report apply equally to both stand-alone and dynamically linked library implementations of ASHPLUME V.2.0.

### 6.1.2 Objectives of the Ash Redistribution Conceptual Model

The objective of the ash redistribution conceptual model is to describe the range of conditions that allow for the transport of waste-contaminated volcanic ash to the location of the RMEI by sedimentary processes. The consequences of a volcanic eruption include consideration of the potential increase in dose to the RMEI from the transport of radioactive-waste-contaminated ash through sedimentary processes. This potential consequence is described in greater detail as a specific disruptive events feature, event, and process (FEP) (FEP 1.2.04.07.0C) (BSC 2005 [DIRS 173981]). The ash redistribution conceptual model presents the basis for the ash redistribution abstraction, which is a component of the TSPA model. The ash redistribution conceptual model also addresses the conditions for the concentration of radionuclides (e.g., by the formation of placer deposits in the channel) resulting from the transport of waste-contaminated ash to the location of the RMEI.

## 6.2 FEATURES, EVENTS, AND PROCESSES INCLUDED IN THE MODEL

The development of a comprehensive list of FEPs potentially relevant to postclosure performance of the Yucca Mountain repository is an ongoing, iterative process based on site-specific information, design, and regulations. Table 6-1 provides a list of igneous-related

FEPs (DTN: MO0501SEPFEPLA.001 [DIRS 172601]) that are included in the TSPA-LA through the use of the results of the calculations described in this document. Details of the inclusion or exclusion of disruptive events FEPs are discussed in *Features, Events, and Processes: Disruptive Events* (BSC 2005 [DIRS 173981], Sections 6.2.1.7; 6.2.2.2; 6.2.2.3; 6.2.2.6; 6.2.2.7; 6.2.2.8).

For the igneous eruptive scenario, the TSPA-LA assumes that a hypothetical dike propagates upward, intersects the repository, provides a source for magma to enter the repository drifts, and magma, potentially with entrained waste, is transported to the surface via an eruptive conduit, released and dispersed in the atmosphere as contaminated tephra, and is redistributed by sedimentary processes. The FEPs listed in Table 6-1 are part of the conceptual basis for such a scenario. However, this report does not provide a direct basis for the inclusion in TSPA-LA of the FEPs listed in Table 6-1, with the exception of parameters developed to address ash redistribution. Rather, this report develops a basis for implementing the FEPs in TSPA-LA by helping to constrain the potential consequences of the listed FEPs. As such, a partial treatment of the included FEPs is provided herein, and the results of this model report and listed FEPs are considered to be implicitly included in the TSPA-LA.

Table 6-1. Included FEPs for This Model Report

| FEP Number | FEP Name | Relevant Section |
|---|---|---|
| 1.2.04.06.0A | Eruptive conduit to surface intersects repository | 6.3.1, 6.5.2 |
| 1.2.04.07.0A | Ashfall | 6.5, 6.7, 7.3.1 |
| 1.2.04.07.0C | Ash redistribution via soil and sediment transport | 6.3.2, 6.6, 6.7.2, 7.3.2, Appendix I |

Source: DTN: MO0501SEPFEPLA.001 [DIRS 172601]

## 6.3 BASIS OF CONCEPTUAL MODELS

### 6.3.1 Basis of Ashplume Conceptual Model

The basis for the conceptual model of a Strombolian eruption in the Yucca Mountain region is discussed in *Characterize Eruptive Processes at Yucca Mountain, Nevada* (BSC 2004 [DIRS 169980], Section 6.3), including details of volcanic eruption characteristics and supporting parameters, values, and distributions (BSC 2004 [DIRS 169980], Table 7-1). The following discussion develops the conceptual model using information from this source.

In the conceptual model for the atmospheric dispersal and deposition of contaminated tephra, the volcanic eruption is preceded by a basaltic dike rising through the Earth's crust and intersecting the proposed repository at Yucca Mountain (Figure 1-1). An eruptive conduit, or conduits, can form when a portion of the dike begins to widen and provides a preferential pathway to focus magma flow to the surface and results in an eruption. For modeling purposes, the eruption is assumed to be violent Strombolian in nature. If the conduit intersects one or more repository drifts, the waste packages located partially or entirely within the conduit provide no further protection to the waste, which will become fragmented and entrained within the rising magma (BSC 2004 [DIRS 170028]). This condition is inherent in the input parameter for the amount of waste erupted and is given a technical basis in *Number of Waste Packages Hit by Igneous Intrusion* (BSC 2005 [DIRS 174066]) for use in the TSPA-LA. The Ashplume model begins

with the thermal and mass characteristics of the erupted material entering the convective-thrust part of the eruption column (see below).

Existing data are limited regarding the expected state of the waste particles (e.g., grain size) resulting from a basaltic disruptive event and associated thermal, chemical, and physical processes (e.g., Codell 2003 [DIRS 165503]). The model assumes that fine-grained waste particles are entrained into a mixture of tephra and gas, rather than mixing directly into the magma prior to fragmentation (Section 5.2.4). As described in Section 6.5.1, the waste particle size distribution is paired with an appropriate ash size distribution and an incorporation ratio is used to account for the amount of waste fuel that is transported with the ash. For transport calculations, the paired ash and waste particles are modeled as density-corrected ash particles.

A Strombolian eruption is characterized by the eruption of a high-speed column of a gas-pyroclast-waste-particle mixture. The column consists of two regions. The lower region directly above the vent is called the gas-thrust region, and it behaves as a ballistic fountain of tephra moving under the influence of its eruption momentum. The upper region of the column is called the convective-thrust region, in which tephra rise by buoyant convective currents (Self and Walker 1994 [DIRS 162831]). Strombolian eruptions typically vary in eruptive intensity as measured by the degree of magma fragmentation and eruption column height (BSC 2004 [DIRS 169980], Sections 6.1.3.2 and 6.3.3). When the eruptive intensity reaches a point where a dominant portion of the tephra is carried into the convective-thrust region in a sustained eruption, the eruption is said to be in a violent Strombolian phase (BSC 2004 [DIRS 169980], Sections 6.1.3.2 and 6.3.3). Hence, a violent Strombolian eruption is one that is dominated by heating of entrained air, and the atmospheric transport of the fragmented magma and gas mixture approximates a thermally buoyant plume.

As the eruptive mixture rises in the plume of a violent Strombolian eruption, it entrains and heats air, which, in turn, reduces the bulk density of the mixture, and the plume becomes buoyant and continues to rise as a plume (BSC 2004 [DIRS 169980], Sections 6.3.3 and 6.4). The plume rises to an altitude of neutral buoyancy compared to the surrounding atmosphere, in which it then spreads laterally as an anvil-shaped cloud (the initial conditions for the ASHPLUME code calculations) and is transported down wind. Tephra particles fall out from the vertical eruption column and from the anvil cloud according to their settling velocities. Such eruptions produce a fallout sheet of varying thickness extending from the volcanic vent (e.g., Section 7.3.3, Figure 7-4). The thickness of the deposit depends on factors such as particle density, eruptive parameters, wind speed and direction, and distance from the vent (Suzuki 1983 [DIRS 100489]).

The Ashplume mathematical model is based on a two-dimensional diffusion model in which only horizontal turbulent diffusion is considered. The movement of air in the atmosphere is relatively random due to the many eddy currents that exist (Suzuki 1983 [DIRS 100489]). The movement of particles within the air mass is treated as random for the same reason. Particles diffuse in the atmosphere in both vertical and horizontal directions, but because the scale of horizontal turbulence is much greater than the scale of the vertical turbulence (Suzuki 1983 [DIRS 100489]), horizontal diffusion is the dominant factor in determining the width of a plume as it moves downwind. Therefore, the Ashplume model is based on a two-dimensional diffusion equation in which only horizontal turbulent diffusivity is considered.

Ashplume is designed to model violent Strombolian eruption behavior as a thermally buoyant plume, calculating the atmospheric dispersal of tephra and its deposition on the ground. Furthermore, Ashplume calculates the entrainment of waste in the erupted plume by an "incorporation ratio," which defines the minimum ash particle size needed to carry a given waste particle size in the plume (Section 6.5.1). By doing so, the fall of tephra carries fuel particles to where they are deposited on the ground, forming a contaminated fall deposit. The contaminated tephra fall has the potential to affect the food and water supplies of the RMEI by direct contamination or by later surface redistribution of tephra fall deposits, which could be carried to the RMEI location by a number of mechanisms (BSC 2004 [DIRS 169460], Section 6). The scope of this conceptual model begins with the intersection of waste by the magma and ends with the ash-waste mixture settling to the ground surface. The Ashplume conceptual and mathematical models are appropriate for estimating the ground-level concentration of waste fuel within the limitations discussed in Section 1.3. Outputs of the Ashplume model include prediction of ash-waste areal densities ($g/cm^2$) at prescribed points surrounding the volcanic vent. It is beyond the scope of this report to identify the mechanisms for human exposure due to the described eruptive model. Human exposure is addressed in *Biosphere Model Report* (BSC 2004 [DIRS 169460]).

The ground-surface concentration of waste, modified by redistribution processes and combined with BDCFs, will be used as input to the TSPA model to calculate the dose to the RMEI. The analysis documented in this model report improves and clarifies the previous documentation of the Ashplume model and its application to TSPA-LA igneous scenarios.

### 6.3.2 Basis of Ash Redistribution Model

The ash redistribution model is a conceptual model that considers two bounding outcomes (see Section 5.1.3) of ash atmospheric dispersion and settlement to the ground as calculated by Ashplume within the TSPA GoldSim model. Abstractions of numeric factors from the conceptual ash redistribution model are provided for use by the TSPA GoldSim code for the purpose of calculating initial ash layer thickness and ground surface concentration at the RMEI location, as well as for calculating changes in these parameters over the postclosure period.

If an eruption were to occur through the repository at Yucca Mountain, radioactive waste particulate could be ejected along with the volcanic ash as attached particles (see Section 6.3.1). Material that is ejected into the atmosphere from a volcanic eruption eventually falls to the ground surface and forms a feature known as a tephra sheet. The depositional process is described in *Characterize Eruptive Processes at Yucca Mountain Nevada* (BSC 2004 [DIRS 169980], Section 6.4 and Appendix C). The areal extent and thickness of the tephra sheet primarily depend on the volume of ash ejected, the eruptive power, and the wind speed. The tephra sheet generally decreases in thickness and grain size away from the vent (Section 7.3, Figures 7-1 and 7-2). After deposition, the ash and waste would be available for redistribution by normal sedimentary processes (erosion and deposition) by water and wind. The basis for the redistribution conceptual model process is also described in *Characterize Eruptive Processes at Yucca Mountain Nevada* (BSC 2004 [DIRS 169980], Section 6.3.4). For an eruption event, the TSPA GoldSim code executes the ASHPLUME code, while also sampling wind direction and velocity, to calculate ash deposition at the RMEI location. As can be seen from the wind rose data in Figure 6-1, and the topographical map of Figure 6-2, this sampling will include some

results in which little or no ash will deposit at or be redistributed to the RMEI location. For this reason, two bounding outcomes of ash atmospheric dispersion are defined (see Section 5.1.3) as a basis for the conceptual ash redistribution model in order to represent upper bound effects at the RMEI location.

Model Outcome 1 corresponds to cases in which the TSPA-sampled wind direction is toward the RMEI (near northerly wind direction), resulting in ash deposition at the RMEI area. Model Outcome 2 corresponds to cases where tephra is not deposited directly at the RMEI location and the Fortymile Wash watershed is used as the basis for the conceptual model. In this context and for the purposes of the TSPA, Outcome 1 is defined as including eruptions for which there is a non-negligible thickness of ash deposited at the RMEI location quantified as greater than or equal to the minimum ash particle size, 0.001 cm. Realizations in which the primary tephra thickness is less than 0.001 cm are then treated as examples of Outcome 2. Practically, Outcome 2 corresponds to predominant ash deposition within the Fortymile Wash watershed (consistent with prevailing southwesterly winds), which is then the source for potential downstream redistribution towards the RMEI location.

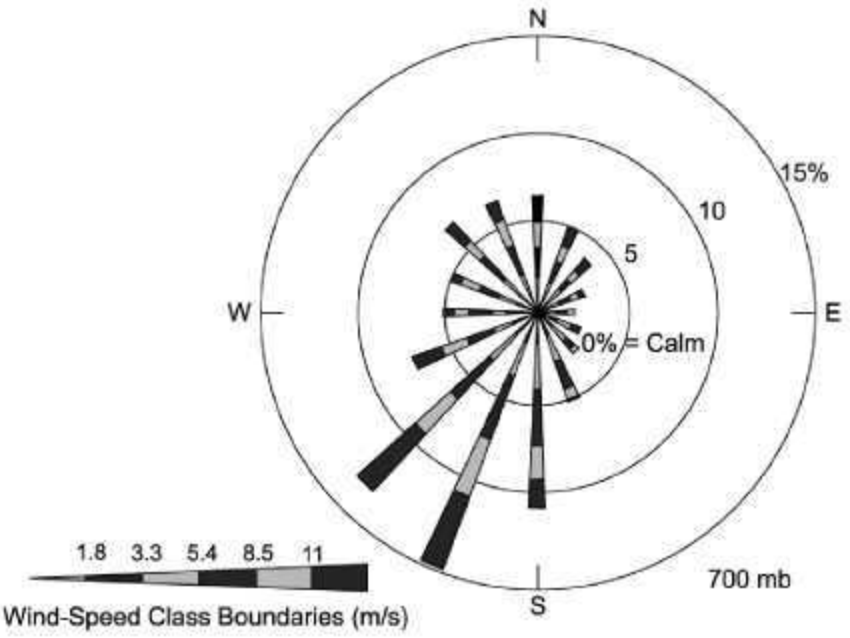


Source: CRWMS M&O (2000 [DIRS 151945], Figure 6.2-6 b).

NOTE: The diagram shows the frequency of occurrence for each direction from which the wind is blowing. The 700-mb windrose portrays data collected at approximately 2,000 m (6,560 ft) above the ground surface, from twice-daily upper-air rawinsonde ascents conducted by the National Weather Service at the Desert Rock Airport near Mercury. These data are used to represent regional near-surface wind patterns that can affect eolian features on the Fortymile Wash alluvial fan. Wind data collected closer to the ground surface are highly variable due to the effects of local topography (CRWMS M&O 2000 [DIRS 151945], Section 6.2.3.2).

Figure 6-1. Wind-Rose Plot for 700-mb Levels at Desert Rock Airport

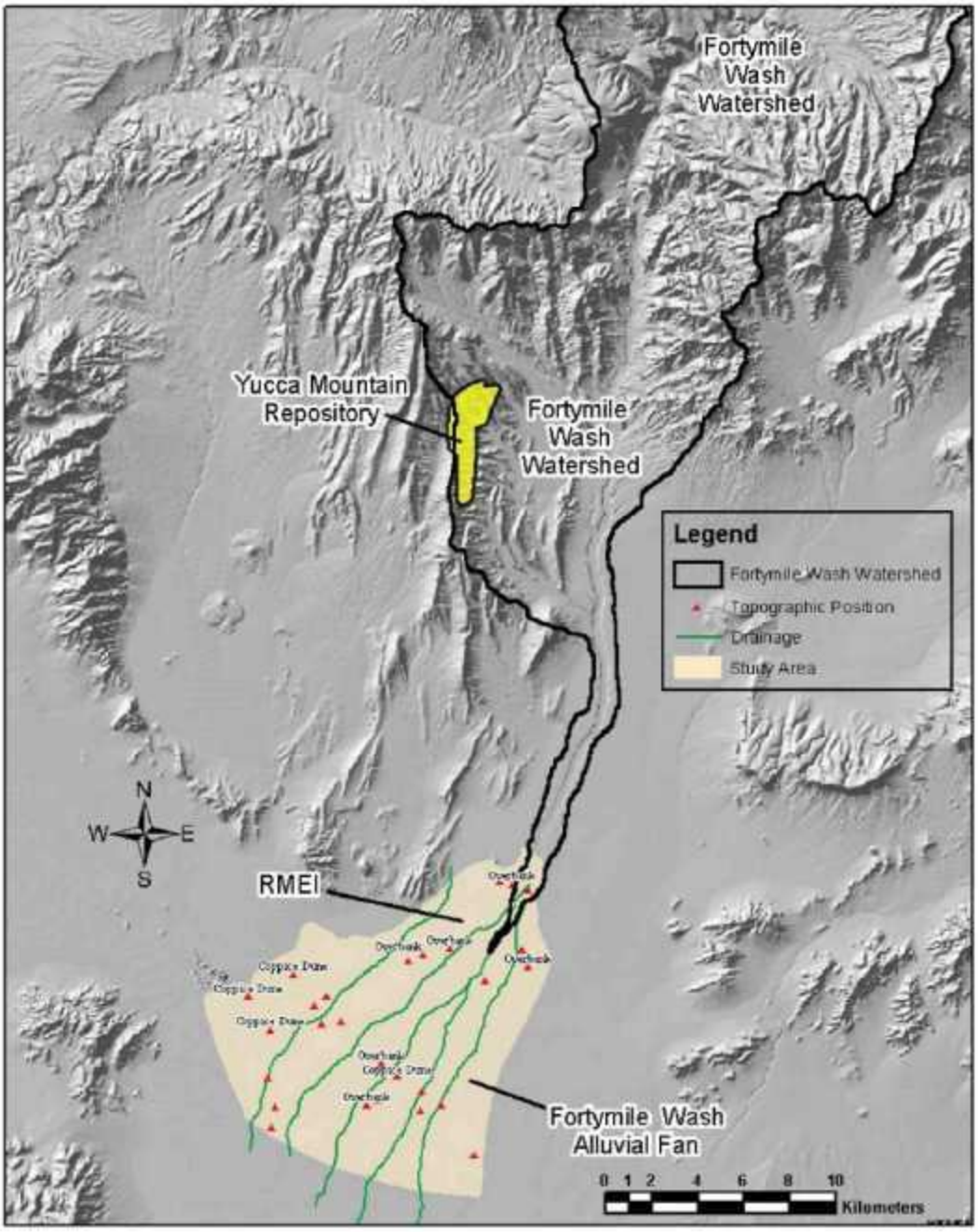


For illustration purposes only.

NOTE: The green-colored areas are distributary channels (18 percent of the total fan area), and the tan areas are interchannel divides (82 percent of the total fan area) (planimetered data measured from 1:100,000 topographic map, in DTN: LA0507CH831611.001 [DIRS 174843]). The triangles in the diagram are locations of overbank deposits and coppice dunes that form along the channels on the alluvial fan. Areal weights are calculated in Harrington (2004 [DIRS 171345], p. 77). The portion of the Fortymile Wash watershed upstream of the repository is approximately eight times the area downstream of the repository site.

Figure 6-2. Fortymile Wash Watershed

Tephra-sheet orientations that correspond with the approximate sector of winds from north easterly to southerly either eliminate ash from reaching the RMEI location or reduce the volume of ash available for redistribution to the RMEI location. It is therefore conservative to force such results to correspond with Outcome 2 if they do not satisfy the criterion of Outcome 1.

For Outcome 1, the initial condition of ground surface ash deposition (at the RMEI location) corresponds to the values calculated by Ashplume and executed by the TSPA GoldSim model. For Outcome 2, the initial conditions at the RMEI location include a transport of ash from the upstream Fortymile Wash basin. In this case the initial conditions are numerically expressed for TSPA, but based on assumption. Assumed initial conditions in Outcome 1 also account for the possibility of a hybrid outcome in which significant ash is deposited at both the RMEI location and in the near portions of Fortymile Wash.

For time steps after the initial condition, the conceptual ash redistribution model estimates the erosion, transport, and redeposition of contaminated ash. Based on local field data (BSC 2004 [DIRS 169980], Section 6.3.4), the model applies a set of parameters that captures the effects of erosion of the initial deposit, mixing and sorting during transport, and the eventual redeposition at the RMEI location (see Section 6.7.2). Since the RMEI location is on the upper part of the Fortymile Wash alluvial fan (Figure 6-2), the conceptual ash redistribution model parametrically differentiates between alluvial fan channels and interchannel divides.

The outputs of this model are treated as an abstraction for the TSPA-LA model for the purpose of combining with BDCFs to calculate the dose to the RMEI.

## 6.4 CONSIDERATION OF ALTERNATIVE CONCEPTUAL MODELS

The consideration of alternative conceptual models for each of the two models documented in this report is described in Sections 6.4.1 and 6.4.2. Note that the ash redistribution conceptual model is the first of its kind.

### 6.4.1 Consideration of Alternative Conceptual Models for Airborne Transport of Tephra

Several alternative conceptual models were considered to evaluate the violent Strombolian eruption and transport of the ash-waste mixture. The qualitative evaluations conducted are summarized in the following discussions.

#### 6.4.1.1 Gaussian-Plume Model

Methods used previously to estimate radionuclide dispersal by volcanism (Wescott et al. 1995 [DIRS 100476]) theorize that the ash cloud travels as a Gaussian plume, released at a stack height one half the volcanic column height. Application of the Gaussian-plume model presumes that a plume of contaminants travels in the same direction as the prevailing wind ($x$-direction) but may be somewhat depressed toward the Earth's surface due to gravitational settling. Contaminant concentration in the plume follows a Gaussian distribution in the dimensions perpendicular to the direction of travel ($y$- and $z$-directions).

The Gaussian-plume model does not accurately account for the effects of gravitational settling of volcanic particles with large diameters (i.e., centimeters). This shortcoming could lead to

predictions of a higher upper limit on the particle-size range for particles dispersed a significant distance downwind than would be the case in reality. The increased particle size would result in the distribution of a larger amount of waste farther downwind than would normally be expected after a basaltic eruption. Based on these factors, the Gaussian-plume alternative conceptual model is excluded from further evaluation because the model does not adequately portray a volcanic eruption column and is not conservative in the distribution of contaminated ash.

#### 6.4.1.2 PUFF

PUFF (Searcy et al. 1998 [DIRS 101015]) was evaluated conceptually based on descriptions in the scientific literature. The PUFF model was developed primarily to predict airborne distribution of ash plumes to aid aircraft navigation near volcanic eruptions. The PUFF conceptual model does not include incorporation of contaminated particles with the ash plume or calculate ground-level concentrations of ash resulting from settling. The PUFF model was excluded from further evaluation because of these limitations.

#### 6.4.1.3 Gas-Thrust Code

Another alternative conceptual model considered was the gas-thrust code that was proposed in the NRC's Igneous Activity Issue Resolution Status Report (Reamer 1999 [DIRS 119693], Section 4.2.2.3). Use of the code would require either the development of an atmospheric transport and deposition model to couple to the gas-thrust code or a code would have to be developed to retrofit the gas-thrust code to an existing atmospheric transport model. The ash-dispersion controlling constant (beta) within the ASHPLUME code has an analogous effect to the gas-thrust code. The parameter beta has the effect of generating a vertical distribution of particles above the volcano. The gas-thrust code is a variation on this concept and falls within the uncertainties associated with the input parameter values used in forming the beta distribution. The gas-thrust alternative conceptual model was excluded from further evaluation because the ASHPLUME code, without modification, uses input parameters that incorporate the vertical distribution of particles above a volcano.

#### 6.4.1.4 Alternative Igneous Source Term Model

The Alternative Igneous Source Term model was developed by Codell (2003 [DIRS 165503]) as an extension of Ashplume to investigate the processes of waste fragmentation and incorporation into the tephra. Despite an in-depth review of thermal, chemical, and physical processes of waste degradation in the presence of magma, no reliable means have been identified to predict the grain size of incorporated waste, and Codell concludes that one should assume that all waste from damaged waste packages is incorporated homogeneously into the magma-pyroclast medium as a fine-grained material. Codell's (2003 [DIRS 165503]) main improvement over Ashplume is the addition of a complex model for the mixing of ash and fuel particles. While Ashplume uses a fixed incorporation ratio to specify the mixing of fuel and ash by particle size, Codell's (2003 [DIRS 165503]) alternative model allows for a range of fuel concentrations on a given ash particle, following the rule that the fraction of mass of fuel incorporated into ash is proportional to the mass of the ash. To accomplish this, the alternative conceptual model bins the ash-particle-size distribution, develops symbolic "indicator particles" to represent the mass of ash in each bin, and then distributes the available mass of fuel to those indicator particles

according to a probability function. Therefore, Codell's (2003 [DIRS 165503]) particles range much more widely in density than those used in the current Ashplume model, which produces the possible existence of dense particles that would fall out of the column sooner than is predicted by the current model. However, Codell (2003 [DIRS 165503]) found that the difference in results between Ashplume and the alternative conceptual model was, on average, within a factor of two for fuel concentration and that Ashplume typically predicts higher concentrations, and is, therefore, more conservative. Codell (2003 [DIRS 165503]) concludes that given other, larger, uncertainties in modeling volcanism, Ashplume is credible.

In summary, this alternative model explores aspects of waste incorporation into the magma and ash beyond the scope of previous work. However, despite the detailed analysis of concepts of waste-magma mixing and a complex approach to the mixing of waste and ash particles, the resulting predictions of waste concentration on the ground are not significantly different from the current model and may, therefore, be excluded from consideration.

### 6.4.2 Consideration of Alternative Conceptual Model for Ash Redistribution

The ash redistribution conceptual model is based on observations and laboratory data from field work in Fortymile Wash, on the Fortymile Wash alluvial fan, and from drainages near the Lathrop Wells cone. Specifically, the ash redistribution conceptual model is based on erosion rate data, soil profile data, and surficial processes information collected in the Yucca Mountain area, including sample locations in Fortymile Wash and surrounding the Lathrop Wells cone. The documentation of this ash redistribution conceptual model is the first of its kind. The simplified representation of redistribution and erosion in this model is shown to result in conservatism due to multiple-accounting of waste mass. For this reason, an alternative numerical model is presented in Appendix I, and is being developed and is proposed for post TSPA-LA use.

### 6.4.3 Summary of Alternative Conceptual Models

Table 6-2 summarizes the alternative conceptual models considered for use to evaluate the volcanic direct release scenario and the screening status of the alternative models. Based on the screening of the alternative conceptual models considered, the Ashplume model was determined to be the most appropriate model for use in TSPA-LA calculations of atmospheric dispersal and deposition of tephra due to a volcanic eruption through the repository. The Ashplume model was specifically chosen because it incorporates both the ash dispersal and waste incorporation mechanisms required for the TSPA-LA analysis of ash-waste deposition, redistribution, and dose to man. The alternative conceptual models considered in Table 6-2 do not provide the full functionality required for the TSPA-LA analysis.

Development of the ash redistribution conceptual model is based on analogue data from sites at and near Yucca Mountain. The documentation of this model is the first of its kind; however an alternative conceptual model has been identified and is under development.

Table 6-2. Alternative Conceptual Models Considered for Airborne Transport of Tephra

| Alternative Conceptual Model | Key Assumptions | Screening Assessment and Basis |
|---|---|---|
| Gaussian Plume | Point source, Gaussian distribution of plume | Excluded—larger particles are not accurately accounted for in gravitational settling |
| PUFF | Convection and dispersion of ash from a volcanic eruption | Excluded—model still in development, waste-fuel interaction not included, surface concentrations not available |
| Gas-Thrust | Buoyancy of a vertical erupting column | Excluded—atmospheric transport not available, surface concentrations of waste and ash not available |
| Alternative Igneous Source Term | Ashplume plus probability model for size of waste particles mixing with a given ash particle | Excluded—results of alternative conceptual model not significantly different from those of Ashplume |

## 6.5 ASH DISPERSAL CONCEPTUAL MODEL DESCRIPTION

The model of atmospheric dispersal and deposition of tephra used in the TSPA-LA and implemented with the Ashplume mathematical model is based on a theoretical model for the dispersion of tephra developed by Suzuki (1983 [DIRS 100489]). Jarzemba et al. (1997 [DIRS 100987]) extended the mathematical model to include the incorporation of waste-fuel particles with tephra particles. This section presents the mathematical formulation of the Suzuki/Jarzemba dispersion model and discusses model inputs developed for use in the TSPA-LA.

### 6.5.1 Mathematical Description of the Base-Case Conceptual Model

The movement of air mass in the atmosphere is relatively random within the scale of eddy motions in wind currents (Suzuki 1983 [DIRS 100489]). Therefore, the dispersion of the ash-waste particles in the atmosphere is treated as random. Particles disperse in the atmosphere in both vertical and horizontal directions. However, the scale of horizontal turbulence is much greater than the scale of vertical turbulence (Suzuki 1983 [DIRS 100489]). Therefore, in the Suzuki (1983 [DIRS 100489]) development of the mathematical model, particle diffusion is considered to be two-dimensional in the horizontal x-y plane. Particle movement in the third (vertical) direction is accounted for by settling velocity in the Suzuki model.

The underlying two-dimensional partial differential equation relating the change in concentration, $\partial\xi$, at a point x-y (with x downwind) to wind velocity, u, and an eddy diffusivity constant, K, follows (Suzuki 1983 [DIRS 100489]):

$$\frac{\partial \xi}{\partial t} = -u\frac{\partial \xi}{\partial x} + \frac{\partial}{\partial x}\left(K\frac{\partial \xi}{\partial x}\right) + \frac{\partial}{\partial y}\left(K\frac{\partial \xi}{\partial y}\right) \qquad \text{(Eq. 6-1)}$$

By selecting an appropriate value for the diffusivity constant K, Equation 6-1 is appropriate for estimating the two-dimensional diffusion of particulate matter in the atmosphere downwind from a source of contamination. Because the x direction is assumed to be aligned with the wind, the y component of the convective term in Equation 6-1 is zero.

Suzuki (1983 [DIRS 100489]) developed the mathematical model shown in Equation 6-1 for application to atmospheric dispersal of tephra by applying source conditions and settling velocities suitable for explosive volcanic eruptions that are unlikely, but possible, in the Yucca Mountain region and termed violent Strombolian. Jarzemba et al. (1997 [DIRS 100987]) further developed the model to calculate the concentration of spent-fuel waste particles that become incorporated with ash particles in the case of a hypothetical volcanic eruption through the Yucca Mountain repository. A summary of the mathematical development in Suzuki (1983 [DIRS 100489]) and Jarzemba et al. (1997 [DIRS 100987]) of the ash-waste dispersal model follows.

To derive a solution to Equation 6-1 suitable for application to calculation of tephra dispersion in the atmosphere after a volcanic eruption, Suzuki (1983 [DIRS 100489]) used the following boundary and initial conditions.

- Erupted material (the source boundary) consists of a finite mass of volcanic ash particles contaminated with waste particles.
- The source of tephra particles is described by the distribution of the diameter of the released particles, and the distribution has a single mode.
- Combined ash-waste particles have a probability to diffuse out of the eruption column during upward travel in the column as well as during transport of the plume downwind.
- All particles fall at the terminal velocity and finally accumulate on the ground.

The solution to the mathematical model described in Equation 6-1 is provided by Suzuki (1983 [DIRS 100489]) and can be summarized by the following equation that describes the areal density of accumulated ash on the Earth's surface after an eruption:

$$X(x,y)=\int_{\rho=\rho_{min}}^{\rho_{max}}\int_{z=0}^{H}\frac{5Qp(z)f(\rho)}{8\pi C\left(t+t_s\right)^{5/2}}\exp\left[\frac{-5\left\{(x-ut)^2+y^2\right\}}{8C\left(t+t_s\right)^{5/2}}\right]dzd\rho \qquad \text{(Eq. 6-2)}$$

where

$X(x, y)$ = mass of ash per unit area accumulated at location $(x, y)$ in g/cm$^2$

$\rho$ = common logarithm of particle diameter $d$, where $d$ is in cm

$\rho_{min}$ = minimum value of $\rho$

$\rho_{max}$ = maximum value of $\rho$

$z$ = vertical distance of particle from ground surface in km

$H$ = height of eruption column above vent in km

$x$ = $x$ coordinate on the surface of the Earth oriented in the same direction as the prevailing wind in cm

$y$ = $y$ coordinate on the surface of the Earth, oriented perpendicular to the direction of the prevailing wind in cm

$Q$ = total quantity of erupted material in g

$p(z)$ = distribution function for particle diffusion out of the column within $\pm dz$ of height $z$

$f(\rho)$ = distribution function for log-diameter of particles within $\pm d\rho$ of $\rho$ normalized per unit mass

$C$ = constant relating eddy diffusivity and particle fall time in $cm^2/s^{5/2}$

$t$ = particle fall time in s

$t_s$ = particle diffusion time in eruption column in s

$u$ = wind speed in cm/s.

The probability density distribution function for particle diffusion out of the eruption column $p(z)$ is given by (Suzuki 1983 [DIRS 100489]):

$$p(z) = \frac{\beta W_0 Y e^{-Y}}{V_0 H \left\{1 - (1 + Y_0) e^{-Y_0}\right\}} \qquad \text{(Eq. 6-3)}$$

where

$Y = \dfrac{\beta W(z)}{V_0}$

$Y_0 = \dfrac{\beta W_0}{V_0}$

$\beta$ = a constant controlling diffusion of particles in the eruption column (dimensionless)

$W_0$ = initial particle rise velocity in cm/s, that represents initial rise velocity of the convective part of the plume.

$V_0$ = particle terminal velocity at mean sea level in cm/s

$W(z)$ = particle velocity as a function of height = $W_0\left(1 - \dfrac{z}{H}\right)$ in cm/s.

According to Jarzemba et al. (1997 [DIRS 100987]), the definitions of $Y$ and $Y_0$ differ from those found in Suzuki (1983 [DIRS 100489]), that is, $Y = \frac{\beta(W(z) - V_0)}{V_0}$ and $Y_0 = \frac{\beta(W_0 - V_0)}{V_0}$, for two reasons:

- The definitions in Suzuki (1983 [DIRS 100489]) lead to negative values of $p(z)$ at heights approaching the top of the column
- $p(z)$ (Equation 6-3) integrated over all column heights does not equal one using the definitions of $Y$ and $Y_0$ found in Suzuki (1983 [DIRS 100489]).

The particle terminal velocity at mean sea level is given by (Suzuki 1983 [DIRS 100489]):

$$V_0 = \frac{\psi_p g_c d^2}{9\eta_a F^{-0.32} + \sqrt{81\eta_a^2 F^{-0.64} + \frac{3}{2}\psi_p \psi_a g_c d^3 \sqrt{1.07 - F}}} \qquad \text{(Eq. 6-4)}$$

where

$\Psi_a$, $\Psi_p$ = density of air and of particles, respectively in g/cm$^3$

$g_c$ = gravitational acceleration constant = 980 cm/s$^2$

$\eta_a$ = dynamic viscosity of air in g/(cm·s)

$F$ = shape factor for particles—for an elliptically shaped particle with principal axes $a$, $b$, and $c$, $F = (b+c)/2a$, where $a$ is the longest axis

$d$ = mean particle diameter in cm.

The value for the gravitational accesleration constant, 980 cm/s$^2$, was programmed into the ASHPLUME code (CRWMS M&O 2001 [DIRS 174768], p. 38). Jarzemba et al. (1997 [DIRS 100987]) define particle density, $\Psi_p$ in g/cm$^3$, to be a function of the particle log-diameter, $\rho_a$ in cm, as follows:

$$\Psi_p = \begin{cases} \Psi_p^{high} & \text{for } \rho_a < \rho_a^{low} \\ \Psi_p^{low} - (\Psi_p^{high} - \Psi_p^{low})(\rho_a^{high} - \rho_a)/(\rho_a^{high} - \rho_a^{low}) & \text{for } \rho_a^{low} \le \rho_a \le \rho_a^{high} \\ \Psi_p^{low} & \text{for } \rho_a > \rho_a^{high} \end{cases} \qquad \text{(Eq. 6-5)}$$

where $\Psi_p^{high}$, $\Psi_p^{low}$, $\rho_a^{high}$, and $\rho_a^{low}$ are defined by user inputs.

The particle fall time (in s) is given by (Suzuki 1983 [DIRS 100489]):

$$t = 0.752 \times 10^{6} \left[ \frac{1 - e^{-0.0625z}}{V_0} \right]^{0.926} \quad \text{(Eq. 6-6)}$$

For a detailed derivation of Equations 6-2 through 6-6, the reader is referred to Suzuki (1983 [DIRS 100489]).

The height of the eruption column or plume, $H$, used in Equation 6-2, follows buoyant plume theory applied to volcanic eruptions by Wilson et al. (1978 [DIRS 162859]) and discussed in Jarzemba et al. (1997 [DIRS 100987]). In Ashplume, height in km is given as:

$$H = 0.0082 P^{0.25} \quad \text{(Eq. 6-7a)}$$

where the eruption column power, $P$, in watts, is determined by the eruption mass flux and heat content:

$$P = \dot{Q}\left(C_p \Delta T E\right) \quad \text{(Eq. 6-7b)}$$

The parameters in parentheses in Equation 6-7b represent the heat content and its efficiency in adding buoyancy; they are fixed by magma and tephra characteristics. The mass flux, $\dot{Q}$, can be evaluated by assuming a constant eruptive mass flux over the duration of the eruption, which is related to the erupted ash settled volume by Equation 6-7c. In that equation, the transformation, for purposes of power calculation, neglects the smaller mass and heat contribution from gas.

$$\dot{Q} = \frac{Q}{T_d} = \frac{V \psi_s}{T_d} = \psi_m W_0 \pi \left( \frac{d_c}{2} \right)^2 \quad \text{(Eq. 6-7c)}$$

where

- $C_p$ = heat capacity of magma (J/kgK)
- $\Delta T$ = temperature difference between magma and ambient (°C)
- $E$ = efficiency factor of heat usage (1.0 for Equation 6-7b)
- $Q$ = total mass of erupted material (kg)
- $V$ = ash erupted volume ($m^3$)
- $T_d$ = eruption duration (s)
- $\psi_s$ = ash settled density ($kg/m^3$)
- $\psi_m$ = bulk density of erupting magma and gas mixture ($kg/m^3$)
- $W_0$ = initial particle rise velocity (m/s)
- $d_c$ = effective conduit (vent) diameter (m).

Note that the units listed above are for Equations 6-7a through Equation 6-7c only. The Ashplume model input parameters of initial rise velocity, power, and duration are linked in Equations 6-7b and 6-7c and determine the plume height in Equation 6-7a; velocity also contributes to the probability density distribution function (Equation 6-3). Accordingly, the basis

for selecting these parameters is further discussed in Section 6.5.2. The value for the efficiency factor ($E$) is assumed to be 1.0 in this analysis, given the uncertainties in values for $C_\rho$ and $\Delta T$ (Keating 2005 [DIRS 173850], pp. 41 to 42). As already noted, the calculation neglects the mass and thermal content of gas in the plume. In the ASHPLUME code, the total mass of erupted material, $Q$, is calculated from input values for power, $P$, and eruption duration, $T_d$.

In the Suzuki mathematical model (Suzuki 1983 [DIRS 100489]), the volcanic ash mass is distributed log-normally with particle size:

$$f(\rho^a) = \frac{1}{\sqrt{2\pi}\sigma_d} \exp\left[-\frac{(\rho^a - \rho^a_{mean})^2}{2\sigma_d^2}\right] \quad \text{(Eq. 6-8)}$$

where

$f(\rho^a)$ = normalized (per unit mass) probability distribution for log diameter of ash
$\rho^a$ = log-diameter of ash particle size, with particle size in cm
$\rho^a_{mean}$ = mean of log-diameter of ash particle size, with particle size in cm
$\sigma_d$ = standard deviation of log particle size.

The TSPA analyses for Yucca Mountain require a prediction of spent fuel per unit area on the ground surface as a function of location relative to the volcanic vent (i.e., relative to the repository) after a hypothetical eruption through the repository. It is assumed (Section 5.1.2) that the transport mechanism for waste fuel particles is by attachment to ash particles larger than a certain relative size represented by an incorporation ratio.

The rationale for limiting the amount of fuel mass available for incorporation into a volcanic-ash particle of a given size is that for smaller volcanic-ash particles, an amount of fuel mass will be too large to be incorporated into these small particles. For example, it is unlikely that a 1-cm fuel particle could be incorporated into a 0.5-cm volcanic ash particle. Assuming a cutoff on the ratio of incorporable fuel diameter to volcanic ash diameter of 1:10 is equivalent to assuming an incorporation ratio ($\rho_c$) of 1. Mathematically, the incorporation ratio is defined as (Jarzemba et al. 1997 [DIRS 100987]):

$$\rho_c = \log_{10}\left[\frac{d^a_{min}}{d^f}\right] \quad \text{(Eq. 6-9)}$$

where

$d^a_{min}$ = minimum ash particle size needed for incorporation, in cm
$d^f$ = fuel particle size in cm.

Setting the incorporation ratio, $\rho_c$ equal to 0.3, is roughly equivalent to allowing all fuel mass of size less than or equal to one-half of the volcanic-ash particle size to be available for incorporation.

Fuel mass is defined by Jarzemba et al. (1997 [DIRS 100987]) as following a log-triangular distribution function of the log-diameter of fuel particles (specifically, a log-triangular distribution for fuel mass within $\pm d\phi^f$ of $\phi^f$ normalized per unit mass). The log-triangular distribution is defined in Equation 6-10. It should be noted that an error in the Jarzemba et al. (1997 [DIRS 100987]) presentation of the fuel particle size log-triangular distribution has been corrected here in Equation 6-10 by reversing the sign on the coefficient $k_2$.

$$\begin{aligned} m(\phi^f) &= k_1(\phi^f - \phi^f_{min}) && \text{for } \phi^f_{min} < \phi^f \le \phi^f_{mode} \\ &= k_1(\phi^f_{mode} - \phi^f_{min}) - k_2(\phi^f - \phi^f_{mode}) && \text{for } \phi^f_{mode} < \phi^f \le \phi^f_{max} \\ &= 0 && \text{otherwise} \end{aligned} \qquad \text{(Eq. 6-10)}$$

where

$m(\phi^f)$ = log-triangular distribution of fuel particle size
$\phi^f$ = log-diameter of fuel particle size, with particle size in cm

$$k_1 = \frac{2}{(\phi^f_{max} - \phi^f_{min})(\phi^f_{mode} - \phi^f_{min})}$$

$$k_2 = \frac{2}{(\phi^f_{max} - \phi^f_{min})(\phi^f_{max} - \phi^f_{mode})}$$

$\phi^f_{min}$ = minimum log-diameter of fuel particle size, with particle size in cm
$\phi^f_{max}$ = maximum log-diameter of fuel particle size, with particle size in cm
$\phi^f_{mode}$ = mode log-diameter of fuel particle size, with particle size in cm.

Jarzemba et al. (1997 [DIRS 100987]) determined the fuel fraction (ratio of fuel mass to ash mass) as a function of $\phi^a$ by considering that all fuel particles of size smaller than $(\phi^a - \rho_c)$ have the ability to be incorporated simultaneously into volcanic-ash particles of size $\phi^a$ or larger. The fuel fraction as a function of $\phi^a$ is determined by summing all the incremental contributions of fuel mass to the volcanic ash mass from fuel sizes smaller than $(\phi^a - \rho_c)$. An expression for the fuel fraction is given as

$$FF(\phi^a) = \frac{U}{Q} \bullet \int_{\rho=-\infty}^{\rho-\phi^a} \frac{m(\rho - \rho_c)}{1 - F(\rho)} d\rho \qquad \text{(Eq. 6-11)}$$

where

$Q$ = the total mass of ash ejected in the event in g
$U$ = total mass of fuel ejected in the event in g
$m$ = probability density function of fuel particle size
$F(\phi^a)$ = cumulative distribution of $f(\phi^a)$.

Equation 6-11 assumes the resulting contaminated particles follow the same size distribution as the original volcanic ash particles. This assumption seems reasonable because the total mass of volcanic ash erupted will be much greater than the total mass of fuel available for incorporation. Introduction of a relatively small amount of fuel mass into the ash mass is unlikely to alter the size distribution of the ash. The mathematical and computational models do, however, adjust the density of ash particles to account for the incorporation of fuel. The particle density used in the calculation of the terminal velocity of a particle is adjusted as a combined particle in the dispersion calculation. The combined-particle density is adjusted by a statement in the ASHPLUME code: ashden = ashden × [1 + fuel fraction]. In this statement, "ashden" represents the ash particle density and "fuel fraction" represents the mass fraction of fuel in the combined particle. The integrand of Equation 6-2 is multiplied by $FF(\rho^e)$ and then recalculated to find the spent fuel density at the $(x, y)$ location.

### 6.5.2 Core Model Inputs

The values for input parameters to Ashplume are developed from observed, or primary, data from analogue volcanoes. This development is based on the approach outlined in *Characterize Eruptive Processes at Yucca Mountain, Nevada* (BSC 2004 [DIRS 169980], Section 6.3.3.4), but it has been altered to meet the needs of this model abstraction. While field measurements provide ranges for the values of individual eruption parameters, field measurements do not provide integrated or mathematically self-consistent sets of eruption parameters such as those that are required as input for Ashplume. Therefore, the input parameters required in the model abstraction are developed from observed (field) measurements by applying mathematical relationships (Section 6.5.1). The resulting set of self-consistent eruption input parameters may differ slightly from the field measurements but honors the ranges of important parameters (e.g., erupted volume) observed at analogue volcanoes.

Self-consistent relationships among eruptive duration, eruptive volume, and vent radius are used in Equation 6-7c to derive values for initial rise velocity and mass flux (see Section 5.2.5 for further discussion). Mass flux is in turn used to derive eruptive power (a primary model input) in Equation 6-7b. Finally, eruptive height, calculated from power, is used to define the atmospheric height bin from which wind speed and direction are sampled. While values for mass flux (or power) and initial eruptive velocity could be chosen from published values, the model is kept self-consistent by the use of appropriate ranges in primary data for the Yucca Mountain region (e.g., eruptive volume, eruptive duration, and vent radius) developed in *Characterize Eruptive Processes at Yucca Mountain, Nevada* (BSC 2004 [DIRS 169980], Section 6.3.3). In addition, the relationships among the primary data provide upper and lower bounds on the distributions for derived input parameters (Keating 2005 [DIRS 173850]); for instance, the minimum mass flux is derived from the minimum erupted volume and the maximum eruption duration. These values, combined with reasonable material properties data (ash settled density, magma density, magma specific heat, and temperature difference), provide a firm link between the model performance and primary data. The ash settled density, which is the bulk density of the ash that settles on the ground after an eruption, is provided in DTN: LA0407DK831811.001 [DIRS 170768] as 1.0 g/cm$^3$. Magma density is also provided in DTN: LA0407DK831811.001 [DIRS 170768]. Note that while eruptive volume is not a direct input parameter for ASHPLUME V.2.0 (CRWMS M&O 2001 [DIRS 152844]), it is used in the modeling process as one of the primary means to constrain the realism of the combinations of input parameters that define each modeled eruption

(Sections 6.5.2.2, 8.2). Once the primary input parameter values have been developed (e.g., eruptive power and duration), they are used within the ASHPLUME code at run time to calculate values for column height (from power) and total mass of ash (from power and duration), among others, for use in transport calculations. Because these values are calculated using equivalent mathematical relationships, the results of the model are consistent with the primary data used to develop the input parameter values.

Because of the model simplification in which the observed data (e.g., volume and duration) are treated as independent variables, the result is a broader range in derived parameters (e.g., power) than would be seen in natural analogues. For example, eruption volume and duration have some general correlation in the natural world, and the range in possible eruptive power is therefore more restricted than is calculated by assuming the two variables are independent. The conservatism introduced by this simplification is mitigated by restricting the set of input parameters for each model realization such that the overall erupted volume is realistic (Section 8.2). The end result is that each model realization is considered reasonable and the simplification does not adversely affect the model results.

For the ASHPLUME_DLL_LA V.2.0 computer code (BSC 2003 [DIRS 166571]) to calculate the concentration of ash and waste fuel on the ground surface according to Equation 6-2, parameter values must be provided for all of the unknown coefficients in the governing Equations 6-2 to 6-11 (Section 6.5.1). ASHPLUME_DLL_LA V.2.0 allows parameters that are distributions to be sampled outside of the ASHPLUME code (within the TSPA-LA GoldSim model). GoldSim then passes the sampled point values for each parameter into the ASHPLUME_DLL_LA V.2.0 code. Each realization simulates only one volcanic event at a time, and the single volcanic event in each realization represents the entire output of the volcano as one violent Strombolian eruption. The following sections discuss each of the parameters given in Table 6-3 in more detail and provide the technical basis for the parameter values and distributions.

**Table 6-3. Inputs for the Ashplume Model**

| Coefficient (Equation Number) | Input Description | Point Value or Distribution | Data Source |
|---|---|---|---|
| *x and y* (Eq 6-2) | Determined by wind direction | Wind direction is a distribution | Based on location of the RMEI |
| $\psi_p^{high}$ (Eq 6-5) | Ash particle density at minimum particle size | Point value | DTN LA0407DK831811.001 [DIRS 170768] |
| $\psi_p^{low}$ (Eq 6-) | Ash particle density at maximum particle size | Point value | DTN LA0407DK831811.001 [DIRS 170768] |
| $\sigma_s^{high}$ (Eq 6-5) | Log ash particle size at minimum ash density | Point value | DTN LA0407DK831811.001 [DIRS 170768] |
| $\sigma_s^{low}$ (Eq 6-5) | Log ash particle size at maximum ash density | Point value | DTN LA0407DK831811.001 [DIRS 170768] |
| *F* (Eq 6-4) | Ash particle shape factor | Point value | DTN LA0407DK831811.001 [DIRS 170768] |
| $\psi_a$ (Eq 6-4) | Air density | Point value | Lide 1994 [DIRS 147834] |
| $\eta_a$ (Eq 6-4) | Air viscosity | Point value | Lide 1994 [DIRS 147834] |

Table 6-3. Inputs for the Ashplume Model (Continued)

| Coefficient (Equation Number) | Input Description | Point Value or Distribution | Data Source |
|---|---|---|---|
| $C$ (Eq. 6-2) | Eddy diffusivity constant | Point value | Calculated from information in Suzuki 1983 [DIRS 100489] |
| $d_{max}$ | Maximum particle diameter for transport | Point value | Jarzemba et al. (1997 [DIRS 100987]) |
| $d_{min}$ (Eq. 6-10) | Minimum waste particle size | Point value | Appendix H |
| $d_{mode}$ (Eq. 6-10) | Mode waste particle size | Point value | Appendix H, Section 6.5.2.16 |
| $d_{max}$ (Eq. 6-10) | Maximum waste particle size | Point value | Appendix H |
| $H_{mo}$ | Minimum height of eruption column | Point value | Minimum practical value (Section 6.5.3.3) |
| *Ash Cutoff* | Threshold limit on ash accumulation | Point value | Minimum practical value (Section 6.5.3.4) |
| $\beta$ (Eq. 6-3) | Column diffusion constant | Distribution | Jarzemba et al. 1997 [DIRS 100987] |
| $d$ (Eq. 6-4) | Mean ash particle diameter | Distribution | DTN: LA0407DK831811.001 [DIRS 170768] |
| $\sigma_d$ (Eq. 6-8) | Ash particle diameter standard deviation | Distribution | DTN: LA0407DK831811.001 [DIRS 170768] |
| $\rho_c$ (Eq. 6-9) | Waste incorporation ratio | Point value | Jarzemba et al. 1997 [DIRS 100987] |
| $U$ (Eq. 6-11) | Mass of waste to incorporate | Distribution determined by TSPA model | N/A |
| *Wind Direction* | Wind direction | Distribution | NOAA 2004 [DIRS 171035] |
| $u$ (Eq. 6-2) | Wind speed | Distribution | NOAA 2004 [DIRS 171035] |
| $W_o$ (Eq. 6-3) | Initial rise velocity | Distribution | See Section 6.5.2.10 |
| $P$ (Eqs. 7a and 6-7b) | Eruptive power | Distribution | See Section 6.5.2.1 |
| $T_d$ | Eruption duration | Distribution | DTN: LA0407DK831811.001 [DIRS 170768] |

### 6.5.2.1 Eruptive Power, *P*

Type: log-uniform distribution
Value: $6.17 \times 10^{8}$-$5 \times 10^{12}$
Units: watts

The range of eruptive power is a function of settled volumes and eruption duration as shown in Equations 6-7b and 6-7c. The heat capacity ($Cp$) used for magma is 1,000 J/(kg·K) derived as a rounded value from Bacon (1977 [DIRS 165512], Figures 1 and 2) and Drury (1987 [DIRS 156447], Table 2). The difference in temperature between magma and ambient is approximated at 1,000 K (lowest liquidus magma temperature is 1,046°C (DTN: LA0407DK831811.001 [DIRS 170768]), ambient is about 25°C at repository depth; temperature difference is rounded to 1,000°C or 1,000 K). The range for the event eruptive volume to be expected in the Yucca Mountain region is defined in DTN: LA0407DK831811.001 [DIRS 170768] as 0.004 $km^3$ to 0.08 $km^3$. The range of eruption duration is discussed below in Section 6.5.2.2. By converting the lowest volume to mass, using

the settled density (1.0 g/cm$^3$; see Section 6.5.2), and dividing this mass by the longest duration to get eruptive mass flux, the lower limit of eruptive power is set by Equation 6-7b. In contrast, the upper limit of power is set to the value using the maximum mass flux recommendations of the Igneous Consequences Review Panel (Detournay et al. 2003 [DIRS 169660], p. 18). The mass and thermal energy of gas in the plume are neglected. This range in power is consistent with and slightly more conservative than the distribution for eruptive power developed in Jarzemba (1997 [DIRS 100460], Table 2).

#### 6.5.2.2 Eruption Duration, $T_d$

Type: log-uniform distribution
Value calculated in TSPA (see Section 8.2)
Units seconds

The range of eruption durations and rationale for using this range of values is discussed in *Characterize Eruptive Processes at Yucca Mountain, Nevada* (BSC 2004 [DIRS 169980], Table 7-1; and DTN: LA0407DK831811.001 [DIRS 170768]). The range of values provided in that document spans 0.5 hour to 75 days ($1.8 \times 10^3$ to $6.48 \times 10^6$ seconds) for the duration of a single explosive phase constituting a violent Strombolian eruption, as observed at analogue volcanoes.

Eruption duration is used for two purposes, one during the development of input parameter values, and one within the ASHPLUME code during computation. The range in eruption duration provided in BSC (2004 [DIRS 170768]) is used to develop the upper and lower bounds for the distribution for mass flux and hence eruptive power, P, using Equations 6-7b and 6-7c (Section 6.5.2). For example, minimum mass flux is a function of minimum volume and maximum duration, while maximum mass flux is derived from maximum volume and minimum duration. Eruption duration is also used within ASHPLUME to calculate the total mass erupted, Q, for each realization. The actual limits on the range of eruption duration used in each TSPA model realization are established at run-time, determined by Equations 8-1a and 8-1b (Section 8.2) such that the total volume of the eruption remains within the bounds provided in DTN: LA0407DK831811.001 [DIRS 170768]. The primary considerations used to verify the realism of each TSPA model realization (Section 8.2) are eruptive power and eruptive volume, two parameters that well characterize the magnitude of violent Strombolian eruptions (BSC 2004 [DIRS 169980], Section 6.3.3.4). While the range of duration developed in a TSPA model realization for a given sampled value of power (Equations 8-1a, 8-1b) may range from about 0.22 hours to four years, the limits of total eruptive volume (0.004 km$^3$ to 0.08 km$^3$ (DTN: LA0407DK831811.001 [DIRS 170768])) are honored. These end members of the possible range of eruptive duration remain within the range of the duration for the formation of an entire volcano (DTN: LA0407DK831811.001 [DIRS 170768]).

### 6.5.2.3 Column Diffusion Constant, $\beta$

Type: uniform distribution
Value: 0.01-0.5
Units: N/A

The column diffusion constant ($\beta$) is set at a uniform distribution with a minimum value of 0.01 and a maximum value of 0.5.

The column diffusion constant was discussed by Suzuki (1983 [DIRS 100489], pp. 104 to 107). This parameter affects the distribution of particles vertically in the ash column and helps determine where particles exit the column. The erupted ash cloud is assumed (by Suzuki) to spread axially a distance of half the height. Ashplume takes a beta value and determines the vertical profile of particle sizes in the erupted column that will then be transported down wind. Suzuki discussed beta values of 0.01, 0.1, and 0.5. The larger beta becomes, the more the particle distribution becomes skewed towards the top of the column. Therefore, a value of 0.5 generates a column particle distribution that contains very few particles in the lower 70 percent of the column, whereas a beta value of 0.01 gives an upwardly decreasing distribution that contains the most particles lower in the column. The beta parameter, in effect, is related to the buoyancy of particles in the eruptive column and determines how high most particles will travel before exiting the column. Suzuki (1983 [DIRS 100489]) suggests that beta values of 0.5 or greater are possible but are not very likely to occur. Jarzemba et al. (1997 [DIRS 100987], p. 4-1) uses a log-uniform distribution for beta that has a minimum value of 0.01 and a maximum value of 0.5. This range of values spans more than an order of magnitude and encompasses the range that is valid for the Ashplume model. However, in order to simulate the anvil cloud associated with a violent Strombolian eruption properly, samples from the range in beta should be focused toward the upper end of the range; therefore, a uniform (rather than log-uniform) distribution is recommended.

### 6.5.2.4 Mean Ash Particle Diameter, *d*

Type: log-triangular distribution
Value: 0.001-0.01-0.1
Units: cm

The ash particle diameter is defined within the Ashplume model by two parameters: the mean ash particle diameter and the ash particle diameter standard deviation. The mean ash particle diameter for the volcanic eruption is defined in DTN: LA0407DK831811.001 [DIRS 170768], as a log triangular distribution with a minimum value of 0.001 cm, a mode value of 0.01 cm, and a maximum value 0.1 cm. The rationale for using this range of mean ash particle diameter is discussed in *Characterize Eruptive Processes at Yucca Mountain, Nevada* (BSC 2004 [DIRS 169980] Sections 6.3.3 and 7.1). The lower end of the distribution is intended to capture the respirable fraction between 0.001 cm and 0.01 cm (BSC 2004 [DIRS 169980] Section 6.3.3). For comparison, Jarzemba (1997 [DIRS 100460], p. 137) gives a log-triangular distribution with a minimum of 0.01 cm, a median of 0.1 cm, and a maximum of 10 cm. Although this upper range would account for the larger lapilli sizes and smaller blocks and bombs, these particles would fall on or near the cone and would not contribute much or any mass to the downwind

tephra deposit, as is demonstrated by measurements of historic violent Strombolian eruptions (BSC 2004 [DIRS 169980], Table 6-6).

#### 6.5.2.5 Ash Particle Diameter Standard Deviation, $\sigma_d$

Type: uniform distribution
Value: 1.3-1.9
Units: log (cm)

The ash particle diameter standard deviation is discussed in *Characterize Eruptive Processes at Yucca Mountain, Nevada* (BSC 2004 [DIRS 169980], Section 6.3.3.6.1) and is derived from analogue data. The referenced report (BSC 2004 [DIRS 169980], Table 7-1; and DTN: LA0407DK831811.001 [DIRS 170768]) suggests a uniform distribution from 1 phi to 3 phi units (phi units are defined to be the negative logarithm in base 2 of the particle diameter in millimeters). This range is equivalent to −1.9 to −1.3 log (cm), which are the units required by ASHPLUME_DLL_LA V.2.0 (BSC 2003 [DIRS 166571]). The ASHPLUME code requires that values for this parameter be positive, so the absolute value of the size range is used, 1.3 log (cm) to 1.9 log (cm).

#### 6.5.2.6 Waste Incorporation Ratio, $\rho_c$

Type: point value
Value: 0.3
Units: N/A

The incorporation ratio describes the ratio of ash/waste particle sizes that can be combined for transport. An incorporation ratio of 0.3 was used by Jarzemba et al. (1997 [DIRS 100987], Table 5-1) and is used here (see Section 6.5.1 for additional discussion). An incorporation ratio of 0.3 corresponds to a maximum incorporated waste particle size equal to half the diameter of the ash particle (i.e., any waste particles larger than half the ash particle diameter cannot be incorporated into the ash).

The waste mass is distributed among the ash mass based on relative particle sizes. The waste mass is not divided equally among the ash particles. Incorporation of waste particles requires ash particles of a certain size or larger. Thus, larger ash particles will carry more waste mass, and smaller ash particles will carry less or maybe even no waste mass.

#### 6.5.2.7 Wind Speed, $u$

Type: empirical distribution
Value: Tables D-10 through D-22 (Appendix D)
Units: cm/s

*Upper Air Data: Desert Rock, Nevada, 1978-1995* (NOAA 2004 [DIRS 171035]) provides wind speed data for the Desert Rock area for a 16-year period from 1978 to 1993 (see Appendix D). After converting height data to height above Yucca Mountain, data were grouped into 1-km increments from 0 km up to 13 km. The wind speed data for each height interval were then used to calculate CDFs with bins set to 100 cm/s intervals. Appendix D contains a detailed

description of the steps required to develop the wind speed CDFs. Although Quiring (1968 [DIRS 119317]) provides wind speed data for the Yucca Mountain region for a seven-year period from 1957 to 1964, those data do not extend to sufficiently high altitudes to address fully the range of potential column heights that Ashplume considers; thus, the data from Desert Rock are more appropriate.

#### 6.5.2.8 Wind Direction, Determines *x* and *y*

Type: empirical distribution
Value: Tables D-23 through D-35 (Appendix D)
Units: Ashplume degrees

*Upper Air Data: Desert Rock, Nevada, 1978-1995* (NOAA 2004 [DIRS 171035]) provides wind direction data for the Desert Rock area for a 16-year period from 1978 to 1993. After converting Desert Rock height data to height above Yucca Mountain, data were grouped into 1-km increments from 0 km up to 13 km. The wind direction data for each height interval were then used to calculate PDFs and associated wind-rose diagrams, with bins set to 30-degree intervals. Appendix D contains a detailed description of the steps required to develop the wind direction PDFs. Although Quiring (1968 [DIRS 119317]) provides wind speed data for the Yucca Mountain region for a seven-year period from 1957 to 1964, those data do not extend to sufficiently high altitudes to address fully the range of potential column heights that Ashplume considers; thus, the data from Desert Rock are more appropriate.

#### 6.5.2.9 Mass of Waste Available for Incorporation, U

Value: distribution will be passed to Ashplume; determined by the TSPA-LA model
Units: grams

The mass of waste available for incorporation with ash particles is an input for the ASHPLUME V.2.0 code (CRWMS M&O 2001 [DIRS 152844]). However, this parameter is not developed within this model report. The waste mass depends upon factors such as waste inventory and the number of waste packages disturbed in a volcanic eruption (BSC 2005 [DIRS 174066]). These factors are defined elsewhere in the TSPA-LA model, and the resulting waste mass available is passed to ASHPLUME_DLL_LA V.2.0 (BSC 2003 [DIRS 166571]) at run time.

#### 6.5.2.10 Initial Rise Velocity, $W_o$

Type: log-uniform distribution
Value: $1.0\text{-}1.2 \times 10^4$
Units: cm/s

Termed "the eruption velocity at the vent" for previous versions of ASHPLUME software, the initial rise velocity is assumed to be the minimum velocity required to provide the modeled power to the plume as described in Section 5.2.5. This velocity is a function of vent velocity. Although vent velocities are shown to be a function of magma volatile content in *Characterize Eruptive Processes at Yucca Mountain, Nevada* (BSC 2004 [DIRS 169980]), those velocities do not reflect the deceleration of the tephra particles that occurs before their entry into the plume,

which must be assumed for application of the Ashplume model. Hence, this distribution must be calculated by Equations 6-7a through 6-7c, using maximum magma bulk density. This calculated distribution is solely a function of eruption power and conduit diameter: the former being a distribution specified in Section 6.5.2.1, and the latter enumerated in DTN: LA0407DK831811.001 [DIRS 170768] as ranging from 5 to 150 m. As stated in Section 5.2.5, the importance of the initial rise velocity is to deliver the thermal mass (power) to the eruption column, and the velocity of the material entering the plume must only be that required to deliver the necessary power. Neglecting the gas-thrust part of the eruption column and given that the heat flux is directly proportional to the mass flux of magma to the vent, the simplest approach to developing the minimum initial rise velocity is to consider the minimum velocity of magma at the vent. This minimum value can be derived from the minimum mass flux and maximum radius; the maximum is derived from maximum mass flux and minimum radius. Given the ranges in these values (Keating 2005 [DIRS 173850], p. 41) and a magma density of 2.6 g/cm$^3$ (DTN: LA0407DK831811.001 [DIRS 170768]), the range in $W_0$ is 0.001 cm/s to 12,000 cm/s. Wilson and Head (1981 [DIRS 101034], p. 2,977) report that the minimum practical value for rise speed of basalt in a 0.22-m-radius conduit is 0.12 m/s (12 cm/s); for a conduit in the range of tens of meters in radius (and for the same mass flux), this velocity could drop by an order of magnitude. The minimum value for $W_0$ has, therefore, been increased to 1.0 cm/s to provide a realistic lower bound while providing appropriate velocity values that successfully deliver the thermal mass to the eruption column. This increase in $W_0$ implies that, for minimum mass flux, the maximum effective vent radius is about 27 m, which is within the range of analogous conduit radii (DTN: LA0407DK831811.001 [DIRS 170768]).

### 6.5.2.11 Ash Particle Density, $\Psi_p$

Type: point values
Values: Table 8-2
Units: g/cm$^3$

The ash particle density used in Equation 6-4 is defined in Equation 6-5. The ash particle density is defined to be a function of particle diameter in *Characterize Eruptive Processes at Yucca Mountain, Nevada* (BSC 2004 [DIRS 169980], Section 6.3.3.6.2). The ASHPLUME_DLL_LA V.2.0 (BSC 2003 [DIRS 166571]) code requires inputs for the densities of large and small ash particles. *Characterize Eruptive Processes at Yucca Mountain, Nevada* defines the densities of ash particles as a function of the magma density. This model report uses a magma density of 2.6 g/cm$^3$, which is within the range of magma densities reported in DTN: LA0407DK831811.001 [DIRS 170768]. DTN: LA0407DK831811.001 [DIRS 170768] defines the density of a 0.001-cm ash particle to be 80 percent of the magma density (2.08 g/cm$^3$), whereas a 1.0-cm ash particle has a density of 40 percent of the magma density (1.04 g/cm$^3$) as a result of the typically greater volume of voids (vesicles) in larger pyroclasts. ASHPLUME requires two sets of values to be entered related to the ash particle density, ash particle density at minimum and maximum particle size (described above) and log ash particle size at minimum and maximum ash density. The particle diameters for input to parameters $\rho_a^{high}$ and $\rho_a^{low}$ must be entered as log values, that is, as log (cm).

### 6.5.2.12 Ash Particle Shape Factor, *F*

Type: point value
Value: 0.5
Units: N/A

The ash-particle shape factor is a parameter that is used to describe the shape of the ash particles being transported in the model. The shape factor is used in determining the settling velocity according to Equation 6-4. The shape factor (F) is defined as F = (b + c)/2a, where a, b, and c are the length of the longest, middle, and shortest axes of the particles. DTN: LA0407DK831811.001 [DIRS 170768] provides a particle shape factor of 0.5. This parameter applies to the ash and does not apply to the waste. The waste is incorporated into ash particles in order to be transported downwind, and the Ashplume model treats all particles (ash and ash-waste combined) as having the same shape factor.

### 6.5.2.13 Air Density, $\Psi a$

Type: point value
Value: 0.001117
Units: $g/cm^3$

The air density is used in calculating the particle-settling velocity in Equation 6-4. Because the density is nearly constant within the altitude range of interest, air density was selected as a point value (constant). The density was selected at an altitude of 1,000 m above mean sea level and at ambient temperature of 25°C. The value of 0.001117 $g/cm^3$ was taken from *CRC Handbook of Chemistry and Physics, A Ready-Reference Book of Chemical and Physical Data* (Lide 1994 [DIRS 147834]).

### 6.5.2.14 Air Dynamic Viscosity, $\eta_a$

Type: point value
Value: 0.0001758
Units: g/(cm·s)

The air viscosity is used in calculating the particle-settling velocity in Equation 6-4. Because the viscosity is nearly constant within the altitude range of interest, air viscosity was selected as a point value (constant). The viscosity was selected at an altitude of 1,000 m above mean sea level and at ambient temperature of 25°C. The value of 0.0001758 g/cm-s was taken from *CRC Handbook of Chemistry and Physics, A Ready-Reference Book of Chemical and Physical Data* (Lide 1994 [DIRS 147834]).

#### 6.5.2.15 Eddy Diffusivity Constant, *C*

Type: point value
Value: 400
Units: $cm^2/s^{5/2}$

The constant (C) controlling eddy diffusivity relative to particle fall time was modeled by Suzuki (1983 [DIRS 100489], p. 99). The eddy diffusivity (K) of the particles is expressed by Suzuki as a function of the particle fall time, K = Ct3/2, where t is the particle fall time. This relationship is based on turbulent particle diffusion and the simplification that the particle diffusion time equals the particle fall time (i.e., time to settle to the ground in seconds). The above relationship is obtained from Suzuki (1983 [DIRS 100489], p. 99) because eddy turbulent diffusion occurs over large-scale eddies and can, thus, be related to the particle fall times. The apparent eddy diffusivity (AL) of particles in the atmosphere is related to the scale of diffusion (L) according to Suzuki (1983 [DIRS 100489], p. 99) by AL = 0.08073C2/5L6/5 with AL given in $cm^2/s$ and L in cm. Suzuki (1983 [DIRS 100489], Figure 6-3) shows a linear relationship between log(AL) and log(L) in the atmosphere; the correlation between L and AL is defined as AL = 0.887L6/5. Combining these equations yields a constant value for C of 400 $cm^2/s^{5/2}$, which is the value selected in this model report.

#### 6.5.2.16 Waste Particle Size (Minimum, Mode, Maximum)

Type: point values
Values: 0.0001 minimum, 0.0016 mode, 0.05 maximum
Units: cm

Waste fuel mass is treated as a log-triangular distribution with particle size in the Ashplume model (Equation 6-10). The minimum, mode, and maximum values defining the distribution are fixed values in the TSPA analyses and are provided to the ASHPLUME_DLL_LA V.2.0 (BSC 2003 [DIRS 166571]) code in units of cm. The values are converted to log (cm) within the code. Assumptions providing the minimum (0.0001), mean (0.002), and maximum (0.05) particle diameter in centimeters are discussed in Section 5.2.4. Because ASHPLUME requires a mode value for the log-triangular distribution, the mean value, 0.002 cm, (Section 5.2.4) was converted to a mode value of 0.0016 cm according to $\mu = (a + b + c)/3$ where $\mu$ is the log of the mean value, a is the log of the minimum value, b, is the log of the mode value, and c is the log of the maximum value (Evans et al. 1993 [DIRS 112115]).

### 6.5.3 Other Model Inputs

Ashplume requires several other input parameters to control code operation that are not directly related to the mathematical model described in this section. These parameters are computational grid locations, maximum particle diameter for transport, minimum height of eruption column considered in transport, and threshold limit on ash accumulation. These additional model inputs are discussed in the following sections.

#### 6.5.3.1 Grid Location and Spacing for the *X* and *Y* Axes, $X_{min}$, $X_{max}$, $Y_{min}$, $Y_{max}$, $N_x$, $N_y$

Any grid (receptor) location can be specified for calculation of ash and fuel concentrations in the ASHPLUME_DLL_LA V.2.0 (BSC 2003 [DIRS 166571]) code. The only limitation is that the volcanic vent location (0, 0) cannot be specified. The grid locations are defined by specifying a minimum and maximum X and Y location and the number of desired grid locations between the minimum and maximum. These parameters are shown in Table 8-2 in Section 8 for the TSPA-LA model feeds. As an example, to calculate the ash and fuel concentrations at a single point corresponding to the RMEI located approximately 18 km due south of the repository, the minimum and maximum X locations would be specified as 0.0 each, and the minimum and maximum Y locations would be specified as 0.0 and −18 km each, respectively. The number of X and Y locations would be specified as 1 and 2, respectively. In the ASHPLUME coordinate system, the point (0, 0) corresponds to the volcanic vent, 0 degrees is due east, 90 degrees is due north, 180 degrees is due west, and −90 degrees is due south. The appropriate coordinate transformations are made within the ASHPLUME_DLL_LA V.2.0 (BSC 2003 [DIRS 166571]) code to be consistent with Equation 6-2.

#### 6.5.3.2 Maximum Particle Diameter for Transport, $d_{max}$

The maximum particle diameter that can be transported down wind is specified as 10 cm in this model report. This parameter is a simple check within the code to limit the maximum size of particles that are considered for transport in the model. *Characterize Eruptive Processes at Yucca Mountain, Nevada* (BSC 2004 [DIRS 169980], Section 6.3.3.6.1) describes the range in tephra particle sizes observed at Tolbachik and Cerro Negro volcanoes, which are analogues for a volcano that could possibly form in the Yucca Mountain region. Mean tephra particle sizes from these volcanoes range from 0.19 to 0.37 mm. Thus, these data support the hypothesis that grain sizes greater than about 1 cm are not transported a significant distance down wind but, rather, fall ballistically near the cone. Therefore, the use of a 10-cm tephra-size cutoff for transport provides reasonable mathematical efficiency without biasing the model results.

#### 6.5.3.3 Minimum Height of Eruption Column, $H_{min}$

This parameter allows the definition of a lower threshold height below which particle transport is not calculated within the code. It represents the lower limit of the inner integral of Equation 6-2. A value of 1 m is chosen because this is essentially zero, considering the heights of eruption that are simulated from Equation 6-7b. A value identically equal to zero is not numerically possible in the ASHPLUME_DLL_LA V.2.0 (BSC 2003 [DIRS 166571]).

#### 6.5.3.4 Threshold Limit on Ash Accumulation, *Ash Cutoff*

The value of $10^{-10}$ (g/cm$^2$) selected in this model report defines the lower limit for the calculation of ash accumulation; below this value, the ash-concentration value is set to zero in the ASHPLUME_DLL_LA V.2.0 (BSC 2003 [DIRS 166571]) code. This limit is reasonable because any values lower than this will have a negligible effect on model results. This limit is intended to speed code calculations for large grids by eliminating calculations that result in concentrations below this value.

### 6.5.4 Summary of the Computational Model

The Ashplume mathematical model is implemented as a computer code using the standard FORTRAN 77 language. The integrations defined in the mathematical model are solved using standard numerical integration techniques. For use in the TSPA-LA, the ASHPLUME_DLL_LA V.2.0 (BSC 2003 [DIRS 166571]) code is implemented directly within the GoldSim software as a dynamically linked library. All model inputs are entered in GoldSim templates and passed directly to the ASHPLUME DLL. Table 8-2 in Section 8 provides a summary of all inputs required by GoldSim and relates Ashplume input parameters to the corresponding GoldSim variable names.

Model results are primarily produced within the TSPA-LA model (GoldSim). The model results presented in this report include the calculation of mean fuel concentration at the RMEI location in Section 6.7.2 and the validation activity in Section 7. The ASHPLUME_DLL_LA V.2.0 (BSC 2003 [DIRS 166571]) code is required as a component of the TSPA model of the nuclear waste repository at Yucca Mountain. Within the TSPA-LA, the atmospheric dispersal and deposition of tephra model implemented in the ASHPLUME code is used to predict the ground-level concentration of ash and waste after a violent Strombolian eruption that intersects the repository. The waste concentration is then modified by processes in the ash redistribution model and then combined with BDCFs in the TSPA model to calculate an annual dose to the RMEI. Ashplume model results are produced at run time within the TSPA-LA model. The Ashplume model inputs discussed in this section, and summarized in Section 8, are provided as inputs to the TSPA-LA model as GoldSim variables. These variables are passed to the ASHPLUME_DLL_LA V.2.0 (BSC 2003 [DIRS 166571]) module at run time, and ASHPLUME calculates ash and fuel deposition in $g/cm^2$. The ash and fuel deposition values are passed back to the GoldSim model. Limited base-case model results are provided in the calculation of mean fuel concentration at the RMEI location (Section 6.7.1) via 100 realizations of distributed parameter values (except wind direction, which was held constant).

## 6.6 ASH REDISTRIBUTION CONCEPTUAL MODEL DESCRIPTION

### 6.6.1 Outline

The ash redistribution conceptual model describes the sedimentary processes that occur when contaminated volcanic ash is deposited at, or redistributed to, the location of the RMEI from a hypothetical volcanic eruption through the repository. The conceptual model represents the sedimentary processes affecting the Fortymile Wash alluvial fan, and specifically the effects on the RMEI area at the head of the Fortymile Wash alluvial fan (Figure 6-2). The basis for the ash redistribution conceptual model is provided in Section 6.3.2.

The model applies a set of parameters that captures the effects of erosion of the initial deposit, mixing and sorting during transport, and the eventual redeposition at the RMEI location (Section 6.7.2). The model captures the effects of sedimentary processes leading to redistribution of contaminated ash at the location of the RMEI. The outputs of this conceptual model are treated as an abstraction for the TSPA-LA model.

### 6.6.2 Initial Conditions

As described in Section 6.3.2, the conceptual ash redistribution model is based on two bounding conditions, model Outcome 1 and Outcome 2, that are defined by the criterion of minimum ash deposition at the RMEI area (Figure 6-3). If the specified criterion is met, the tephra-sheet axis is assumed to be sufficiently aligned with the RMEI area that it represents a maximal primary ash outfall at the RMEI location. This corresponds with Outcome 1, and the criterion used to define such a case is that the primary tephra thickness at the RMEI area is greater than or equal to the minimum ash particle size, 0.001 cm. All realizations in which the primary tephra thickness is less than 0.001 cm are treated as examples of Outcome 2, in which the primary ash outfall is assumed to be entirely within the Fortymile Wash basin and therefore a source for potential downstream redistribution toward the RMEI location. In the case of Outcome 2, the conceptual ash redistribution model provides TSPA with numerical representation of primary ash transported from the Fortymile Wash basin to the channels and interchannel divides at the RMEI area.

### 6.6.3 Tephra Redistribution and Dilution

The regional trend toward homogeneity of sediment loads with distance from the primary eruptive deposit is fundamental to the conceptual model for ash redistribution (Section 6.3.2). If ash were ejected into the atmosphere from a hypothetical eruption at Yucca Mountain, deposition would likely occur on the flanks of Yucca Mountain and onto adjacent stream channels, washes, or alluvial fans (Figure 6-2) (BSC 2004 [DIRS 169980], Section 6.3.4). As suggested by sedimentary processes at analogue volcanoes, normal sedimentary processes would begin redistributing the ash and waste shortly after such an eruption. Redistribution by fluvial and eolian processes would lead to dilution of the sediment load. Dilution is defined here as mixing with non-ash-containing sediment, thus reducing the quantity of ash per unit volume of sediment.

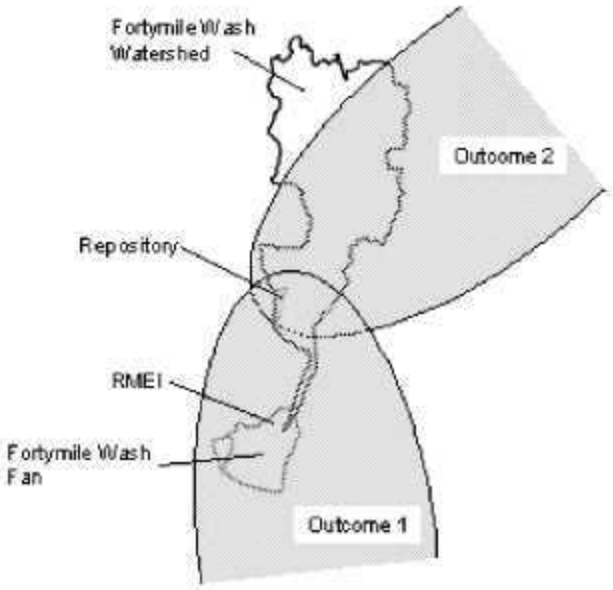


NOTES: For illustration purposes only.

Outcome 1 results in maximum primary tephra deposition at the RMEI area. Outcome 2 results in no significant tephra deposition at the RMEI location but instead significant tephra deposition in the Fortymile Wash watershed, available for transport to the RMEI area by sedimentary processes.

Figure 6-3. Schematic Illustration of Possible Eruption Model Outcomes for an Eruption Vent within the Repository Footprint

The conditions for tephra fall and redistribution include the two main geomorphic features present at the RMEI location, interchannel divide areas and distributary channels. These features are characteristic of alluvial fans that develop in semi-arid and arid climates. Given the strong eolian action in the northern Amargosa Valley, where the RMEI is located, it is highly unlikely that tephra would remain unmodified or undiluted for more than a few decades. Alluvial action (e.g., extreme flood events) could also transport and dilute material.

Shortly after deposition of a tephra sheet, normal sedimentary processes (Folk 1980 [DIRS 164773], Chapter 2) would begin redistributing the ash. Wind and water would begin eroding, transporting, sorting, mixing, and depositing the unconsolidated ash and waste in greater or lesser concentrations, depending on the mixing processes. If ash-waste deposition were to occur at the RMEI location, exposure from the radionuclides contained within the redistributed deposits would occur. On this basis, surface redistribution of contaminated tephra deposits is evaluated here for inclusion in the TSPA.

The transport of tephra occurs both by wind and water action; however, while water in a flooding event can transport large amounts and much larger sizes of material in a short period of time, wind is a major source of transport (Bull 1991 [DIRS 102040], pp. 105 to 106), as evidenced by the presence of dunes and large sand ramps in the Yucca Mountain region. Transport of tephra by water begins with hillslope erosion processes and continues as sediment moves into

drainages, then is transported as bedloads in the drainages that coalesce into larger and larger drainage channels. At junctions of all scales within drainage systems, water and sediment from different channels begin a process of mixing that ultimately leads to a homogeneous sediment containing elements derived from all drainages in the basin (Folk 1980 [DIRS 164773], Chapter 2). Mixing of sediments occurs in all environments where sediment is transported by water or wind, including intermittent as well as perennial stream systems. The mixing in stream channels occurs at higher rates with larger clast sizes in larger drainages and on steeper slopes than in smaller drainages and on lower-gradient landscape surfaces, such as the Fortymile Wash alluvial fan with a longitudinal gradient of one-half degree. Mixing also occurs from wind action by transporting sediment across the landscape. Wind is the major erosional agent on the upper part of the interchannel divides on the Fortymile Wash fan but also is effective in bringing sand onto and transporting sand across the fan where it forms coppice dunes around vegetation on the fan surface. However, during high-intensity storms (summer monsoon-type thunderstorms), the larger, regional drainage channels that would form and flow across newly deposited tephra sheets would exhibit the same processes as those observed in other streams. Therefore, after small transport distances, even the channels on newly deposited tephra sheets would have well-mixed sediment loads.

In small channels developed on tephra sheets northwest of the Lathrop Wells cone, tephra moves downslope as small debris flows with dimensions typically tens of centimeters wide and tens of meters long. Tephra moves downslope through progressive generations of these small debris flows until it reaches a channel at the base of the slope. The channel may then merge with larger channels. Depending upon initial tephra thickness, each step in the process results in some dilution of the tephra with other material (Harrington 2003 [DIRS 164775], pp. 14 to 16).

In the region around Yucca Mountain, sediments in drainage channels are mainly volcaniclastic materials, derived from the dominantly silicic Southern Nevada Volcanic field, and eolian quartz sand and silt. Where basaltic tephra from the Lathrop Wells cone has been transported into a drainage channel containing tuff and quartz clasts, the tephra component is progressively diluted during transport relative to the total sediment volume. In addition, tephra may be diluted prior to fluvial mobilization due to the infiltration of eolian sand and silt.

The sedimentary depositional system at the Lathrop Wells volcanic cone near Yucca Mountain (Harrington 2003 [DIRS 164775], pp. 14 to 16) was studied to assess the significance of dilution (mixing) in the ash redistribution conceptual model. The dilution rates (Section 7.3.2) analyzed for the drainages around the Lathrop Wells cone were not included in the abstraction of the ash redistribution conceptual model because the drainage system at Lathrop Wells is very small relative to the Fortymile Wash drainage. In addition, the ash was deposited approximately 77,000 years ago, and the drainage system at the Lathrop Wells cone is most likely nearing equilibrium. Although dilution rates at the Lathrop Wells cone are not necessarily representative of the rates that may be expected from sedimentary processes affecting a young tephra sheet, those rates do demonstrate that the process of dilution can be significant.

### 6.6.4 Rates of Eolian Erosion on the Interchannel Divides of the Fortymile Wash Alluvial Fan

To understand potential tephra redistribution, it is important to constrain the current rates of surficial processes along the main Fortymile Wash drainage. Fortymile Wash is a major drainage area along the base of the eastern slope of Yucca Mountain. It has an 800-$km^2$ drainage basin that includes the entire eastern slope of Yucca Mountain and the Fortymile Wash alluvial fan. In the upper or northern half of the fan, the channels are well defined (Figure 6-2). The drainage pattern is a distributary system where channels are widely spaced, but sizable interchannel areas occur between all pairs of channels. These interchannel divide tracts are more prominent on the upper fan. On the lower fan (not shown in Figure 6-2), they are neither as topographically prominent nor as wide. Estimates of surficial process rates in the Fortymile Wash are based on $^{137}Cs$ concentrations in the sediments. Eolian erosion on the interchannel divides is estimated to occur at the rate of 0.02 cm/yr to 0.04 cm/yr (DTN: LA0407DK831811.001 [DIRS 170768]), based on interpretation of the $^{137}Cs$ data, representing the last 50 years, and mapping on the interchannel divides.

### 6.6.5 Equilibrium on the Fortymile Wash Alluvial Fan

It must be noted, however, that sediment likely moves off the surface slowly. As sand particles are loosened from the underlying sediment, they likely form coppice dunes anchored to vegetation on the sediment surface. Thus, over time, the net effect on the upper fan interchannel divides is probably a very small net loss, which could be easily replaced by the creation of $A_y$ horizons from incoming dust and sand blown onto the surface. With time, and assuming no large (500 year to 1,000 year) floods occur, the surfaces of the divides are in near equilibrium with the present climate and will change little over this extended period.

### 6.6.6 Model Outcome 1: Primary Tephra Deposition at the RMEI Location

If an eruption through the repository were to occur while the wind was blowing toward the south, the eruption would result in tephra deposition at the RMEI location (Figure 6-3). The deposit would initially blanket both distributary channels and interchannel divide surfaces, which stand several tens of centimeters to a maximum of about 1 m above the channel fill.

In the case where tephra is deposited directly at the RMEI location, the following factors will determine the evolution of that deposit with time. Such a deposit is most likely to be thin (2 cm or less, based on the model abstraction presented in Section 6.7.1) and fine grained, consisting of ash-sized particles (less than or equal to 2 mm). Tephra deposited on interchannel divide surfaces may be subject to the following processes:

- Removal and redistribution by wind
- In-situ dilution by eolian sand and silt
- Mechanical and chemical infiltration into the underlying soil profile (see results of the $^{137}Cs$ study in BSC 2004 [DIRS 169980], Section 6.3.4.2).

Extreme (e.g., plus 500 years) flood events could also dilute and transport material that was originally deposited on interchannel divide surfaces into runoff channels. For tephra deposited directly onto distributary channel bottoms, the above processes are relevant, as well as the additional dilution and redistribution of tephra by occasional flash floods.

### 6.6.7 Model Outcome 2: Primary Tephra Deposition Upstream in Fortymile Wash

Outcome 2 represents an eruption through the repository accompanied by west or southwest winds that disperse and deposit tephra to the east of the repository in the Fortymile Wash drainage basin and upstream of the RMEI location. Figure 6-4 illustrates the conceptual model for redistribution of tephra toward the RMEI. Such redistribution would be dominated by fluvial transport down Fortymile Wash and can best be illustrated by considering the time evolution of tephra concentration on the surface at locations (stations) along the wash. Station A is at the point where Fortymile Wash is closest to the repository, while Stations B and C are progressively downstream, and Station D roughly corresponds to the location of a RMEI at the depositional mouth (alluvial fan) of the wash where it drains into the Amargosa Valley. The plots on the right side of Figure 6-4 conceptually show the relative concentration of tephra on the surface of the wash, averaged across the wash, as a function of time after the initial eruptive deposition of the tephra. These plots are qualitative and do not represent particular data from the Yucca Mountain region or other sites. Note that Figure 6-4 represents both individual flood events and the longer time-averaged behavior of the system.

Immediately after an eruption, the surface concentration of tephra at Station A will be unity, representing the presence of an undisturbed tephra deposit blanketing the wash. With time, this concentration will be reduced as sediment is transported in from upstream sources. Initially, this process will result in upstream-derived sediments being mixed with, or deposited on the surface of, the primary tephra deposit. Eventually, the primary tephra deposit will be locally incised to its base, exposing underlying sediments, and, ultimately, the primary deposit may be completely incised across the entire width of the wash so that no primary deposit remains. At that time, it is likely that tephra will continue to be transported into the wash from the flanks and hillslopes immediately adjacent to the wash (e.g., Yucca Mountain itself), especially where slopes are greater than about 10 percent and tephra can be swept off the slope and into the adjacent drainage channel by short, intense thunderstorms.

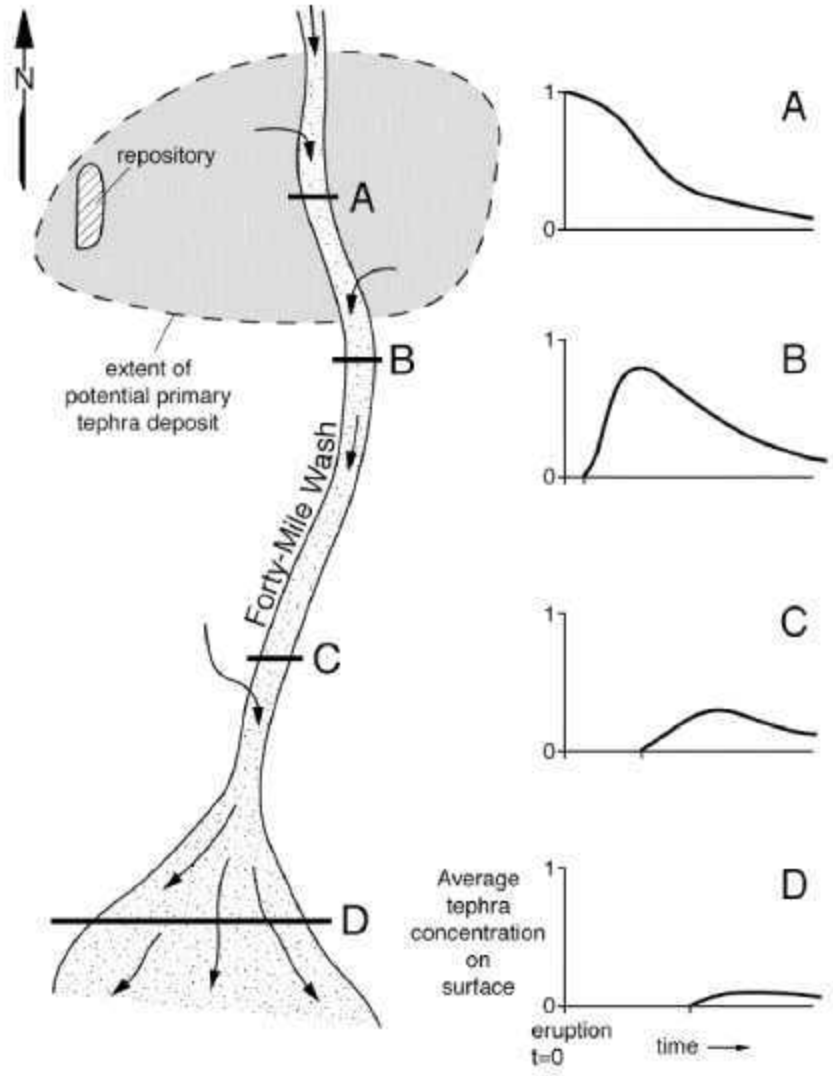


NOTE: For illustration purposes only.

Figure 6-4. Illustration of Conceptual Model for Redistribution of Tephra Toward a RMEI for Outcome 2

Slopes that are less steep are likely to be incised first and ash would be removed at a much lower rate, as is observed throughout the Sunset Crater ash depositional area (Harrington 2004 [DIRS 171345], p. 77). Therefore, the average concentration of tephra at Station A will gradually decline, rather than immediately going to a value of zero, after an initial phase of cutting through the primary deposit.

Station B is not blanketed by the primary tephra deposit, so there will be a period of time between the eruption and the first arrival of tephra via sedimentary processes. The tephra concentration at Station B will increase relatively rapidly as the upstream tephra deposit is incised and that material moves downstream. However, *on average*, the tephra concentration will peak at some value less than unity because of dilution of the tephra by other sediments from sources upstream of the tephra deposit and by sediment washed directly off the slopes above the wash near Station B, and by mixing with pre-existing sediments on the floor of the wash. The

concentration at Station B will gradually decline but will continue to be fed by tephra washing in from upstream environs (e.g., around Station A).

Stations C and D will experience successively longer lag times between the eruption and first arrival of tephra via the sediment transport system. In addition, the peak concentration at each station will be successively lower due to dilution as described above. The general effect is that of a downstream-propagating tephra "wave" that is progressively diluted, damped, and dispersed. Station D will experience the longest lag time before contaminated tephra arrives, and the lowest peak concentration, but the longest period during which contaminated tephra is being fed to the location.

The processes of sediment transport in a setting such as Fortymile Wash are complex and sporadic and are difficult to model. For example, introduction of hillslope material directly into the tributary washes and/or main wash might occur during relatively localized, intense thunderstorms, but these are not likely to result in transport far downstream in the wash (see more detailed discussion in *Characterize Eruptive Processes at Yucca Mountain Nevada* (BSC 2004 [DIRS 169980], Section 6.3.4)). Major flood events (e.g., 100-year storms) can mobilize hill-slope material into the wash and additionally transport material downwash many kilometers. The effects, both during individual storm events and integrated over long times and many events, would be dominated by:

- Dilution of tephra by the arrival of upstream-sourced sediments
- Dilution of tephra by material washed from the wash flanks directly into the wash
- Mixing with pre-existing sediments along the bed of the wash.

Also, note that the conceptual plots in Figure 6-4 represent *average* surface concentration of tephra across the wash – in reality, there may be small sub-channels with very high tephra concentrations while other parts of the wash remain free of tephra. In the alluvial fan area of Fortymile Wash (e.g., Station D), tephra variations across the wash might be especially pronounced as the wash branches into distributary channels separated by higher-standing interchannel divides that might only receive new sediment during extreme (e.g., +500 years) flood events (the distinction between distributary channels and interchannel divides becomes important in determining dose to the RMEI). Vertically, in the uppermost deposits in a channel after an eruption, there might also be tephra-rich layers and tephra-poor layers, reflecting a variety of sediment transport and local depositional mechanisms. In practice, it is not possible to predict such details nor is it necessary to model this level of detail because the average behavior is appropriate for the purposes of the analysis.

Rainstorms at Yucca Mountain can be classed into two types: local, infrequent storms and regional storms that cover very broad areas on scales larger than entire drainage basins (Coe et al. 1997 [DIRS 104691], p. 15). Typically, regional storms have longer durations with periods of heavy rains during part or most of the storms. These storms occur more commonly in winter, although they can occur at any time of the year.

It is the intense, very localized thunderstorm that would be the likely initiator of movement of the tephra particles from the ridge-top drainage heads into the parallel channels. Undercutting of slopes could cause sloughing of masses of tephra and result in the addition of disaggregated

tephra to the drainage systems. In most localized thunderstorms, water infiltrates into the underlying soil quite rapidly and does not carry its bedload long distances. At Yucca Mountain, these storms seldom feed abundant material into Fortymile Wash (Coe et al. 1997 [DIRS 104691], pp. 24 to 26). To get abundant material into the wash and to transport it a long distance requires the much broader, longer-period regional rainstorms.

It is, therefore, the broad, regional storms that are responsible for moving most, and possibly all, of the sediment through the lower part of Fortymile Wash below Yucca Mountain. The material being moved and mixed is not only the sediment from the east flanks of Yucca Mountain, but includes the entirety of the sediment that is derived from the drainage basin of Fortymile Wash, including the terraces along the length of the wash.

If overall climate in the Yucca Mountain region were to change to wetter weather patterns, there would be a major change in the dominant storm type and resulting impacts on the landscape. During wetter conditions associated with future glacial transition climates (see *Future Climate Analysis* (BSC 2004 [DIRS 170002]), long-duration regional storms would become more frequent, and summer monsoon storms would become less frequent, or perhaps disappear. Regardless of the details of such storms, mixing of contaminated sediment would still occur as the material moves down Fortymile Wash alluvial fan and beyond. Most predictions for increased rainfall in this area project one-and-one-half to two times the modern rate of 190 mm/yr. to 270 mm/yr. (BSC 2004 [DIRS 170002]).

### 6.6.8 Wind Data

A wind-rose diagram of regional wind patterns in Jackass Flats and on the Fortymile Wash fan is shown in Figure 6-1. Prevailing winds are predominantly from the southwest and move material toward the northeast. Frequently, strong winds blow across the fan, pick up the sand and smaller size fractions, and remove them from the fan and from the Fortymile Wash drainage.

Although the effects of wind erosion can be inferred from the $^{137}Cs$ data (BSC 2004 [DIRS 169980], Table 6-8), there is also evidence of eolian deposition on some surfaces. The presence of coppice dunes along the edges of the interchannel divide areas indicates that vegetation traps some of the eroded materials before the eolian materials can be carried off the divide area. Supporting data for wind transport and deposition of material throughout the Yucca Mountain area include the presence of stratified eolian horizons of fine sand and silt marked by the presence of gas bubble vesicles ($A_v$ horizons). The presence of Big Dune in close proximity to the Fortymile Wash fan, from which material is being removed and deposited almost continuously, clearly demonstrates that this is an area where eolian processes play an important role in landscape modification.

## 6.7 MODEL RESULTS AND ABSTRACTIONS

This section provides results and abstractions on ash dispersal, deposition, and redistribution for use in the TSPA-LA model. Section 6.7.1 presents Ashplume results required to implement selected conditions of the redistribution abstraction in which representative amounts of ash and waste deposited at the RMEI location are required for initial conditions. To establish the initial conditions, 100 simulations of a single eruption were conducted with the wind fixed southward.

The resulting mean concentrations of radioactive waste in the tephra sheet were calculated at the location of the RMEI, about 18 km south of the repository (Section 6.7.1). Section 6.7.2 presents the overall redistribution abstraction, which uses the Ashplume results presented in Section 6.7.1.

### 6.7.1 Waste-Form Concentrations in Ash from an Ash Plume 18 km from a Vent

This section describes the results of calculations using the ASHPLUME_DLL_LA V.2.0 code (BSC 2003 [DIRS 166571]) to estimate the mean concentrations of radioactive waste at a point 18 km south from a hypothetical vent along the midline of a tephra sheet. For the purposes of this calculation, 100 simulations of a single eruption were conducted using sampled values for all distributed ASHPLUME inputs except wind direction, which was held fixed so that the mid-line of the plume would be the same in each realization. Distributions for the sampled inputs are as described below. Results are presented in Table 6-4 in terms of concentration of ash and waste form per unit area ($g/cm^2$) of ash for each of the 100 realizations. The mean waste concentration, termed the Mean Primary Waste Concentration, incorporates effects of uncertainty in the ASHPLUME inputs and, is the value to be used by the TSPA-LA for certain realizations, time periods, and geomorphic surfaces in the model for redistribution described in Section 6.7.2.

Parameter values used in this calculation were chosen using the base-case values and ranges of values presented in Section 6.5.2. For those values with a distribution ($\beta$, $d$, $\sigma_d$, $W_0$, $P$, $T_a$, and $u$), 100 realizations were generated randomly from these distributions by implementing the ASHPLUME code within GoldSim. ASHPLUME_DLL_LA V.2.0 (BSC 2003 [DIRS 166571]) and GoldSim V 8.02 (BSC 2004 [DIRS 169844]) were used to implement this calculation. Wind direction was held fixed (due south towards the RMEI) for each of the 1-km altitude bins in the wind data (Output DTN: MO0408SPADRWSD.002). The validity of each realization (combination of randomly chosen parameter values) was ensured by following the methodology outlined in Section 8.2, which requires that the values of the sampled parameters remain within established ranges. The 100 realizations of distributed input values are provided in Appendix E.

The value for the total fuel mass available for entrainment in this 100-run exercise was chosen based on the mass of fuel in commercial spent nuclear fuel waste, which is expected to comprise about 90 percent of the waste in the repository (CRWMS M&O 2001 [DIRS 153938], p. 49). A total of 63,000 metric tonnes of heavy metals commercial spent nuclear fuel is expected to be emplaced in 7,860 waste packages (CRWMS M&O 2001 [DIRS 153938]). The total mass of waste available for entrainment ($4.01 \times 10^7$ g) was calculated based on a median value of five waste packages calculated to be damaged if a hypothetical eruptive conduit were to intersect the repository (BSC 2005 [DIRS 174066]; DTN: MO0504MWDNUMWP.001 [DIRS 173521]).

The results of this Monte Carlo analysis are presented in Table 6-4, including the geometric mean of the concentration of the fuel form calculated for the RMEI at a location 18 km south of the repository (the location of the RMEI for these analyses). The areal ash concentrations reported in Table 6-4 can be interpreted as ash thicknesses based on a value for ash settled density of 1.0 $g/cm^3$ (DTN: LA0407DK831811.001 [DIRS 170768]). This set of 100 realizations was rerun for REV 01 of this report due to the following changes:

- the version of GoldSim used for REV 00 runs had been superseded.

- $\sigma_d$ range changed from −1.9, −1.3 to +1.3 to +1.9
- Sequence numbers 8 and 9 in Table 8-2 have been reversed; that is, sequence number 8 is "ash particle density at maximum particle size" (1.04) and sequence number 9 is "ash particle density at minimum particle size" (2.08).
- The wind speed and direction data were revised.

The parameter values were changed as a result of errors found in the previous implementation. This set of parameters is consistent with those reported in Table 8-2 and those used in TSPA-LA.

**Table 6-4. Calculated Concentration of Ash and Waste in the Midline of a Volcanic Plume at a Location 18 km South of the Repository**

| Realization Number | Ash Concentration ($g/cm^2$) | Log Ash Concentration Log ($g/cm^2$) | Waste Concentration ($g/cm^2$) | Log Waste Concentration Log ($g/cm^2$) |
|---|---|---|---|---|
| 1 | 0 8295 | -0 0812 | 4 58E-06 | -5 3392 |
| 2 | 14 1120 | 1 1496 | 2 15E-05 | -4 6681 |
| 3 | 15 5240 | 1 1910 | 2 09E-05 | -4 6807 |
| 4 | 3 9393 | 0 5954 | 1 89E-05 | -4 7225 |
| 5 | 1 9151 | 0 2822 | 4 10E-06 | -5 3871 |
| 6 | 0 2256 | -0 6466 | 2 47E-06 | -5 6080 |
| 7 | 1 6457 | 0 2164 | 8 09E-06 | -5 0923 |
| 8 | 0 2022 | -0 6942 | 1 34E-06 | -5 8725 |
| 9 | 0 6565 | -0 1828 | 2 27E-06 | -5 6434 |
| 10 | 1 2757 | 0 1057 | 1 87E-06 | -5 7284 |
| 11 | 3 4480 | 0 5376 | 1 58E-06 | -5 8019 |
| 12 | 13 0700 | 1 1163 | 1 10E-05 | -4 9577 |
| 13 | 4 8394 | 0 6848 | 4 45E-06 | -5 3516 |
| 14 | 0 4601 | -0 3372 | 5 20E-06 | -5 2843 |
| 15 | 0 2396 | -0 6205 | 4 27E-07 | -6 3698 |
| 16 | 3 1807 | 0 5025 | 1 46E-05 | -4 8355 |
| 17 | 19 2360 | 1 2841 | 1 62E-05 | -4 7915 |
| 18 | 0 3520 | -0 4534 | 2 30E-06 | -5 6391 |
| 19 | 3 6054 | 0 5570 | 2 08E-06 | -5 6812 |
| 20 | 10 0200 | 1 0009 | 2 15E-05 | -4 6668 |
| 21 | 4 6591 | 0 6683 | 7 98E-06 | -5 0981 |
| 22 | 1 8903 | 0 2765 | 8 76E-06 | -5 0575 |
| 23 | 1 1967 | 0 0780 | 4 99E-06 | -5 3021 |
| 24 | 1 0053 | 0 0023 | 4 94E-06 | -5 3059 |
| 25 | 4 2214 | 0 6255 | 1 60E-05 | -4 7947 |
| 26 | 1 4585 | 0 1639 | 1 80E-06 | -5 7450 |
| 27 | 3 5631 | 0 5518 | 1 13E-05 | -4 9460 |
| 28 | 1 9372 | 0 2872 | 5 74E-06 | -5 2407 |

Table 6-4. Calculated Concentration of Ash and Waste in the Midline of a Volcanic Plume at a Location 18 km South of the Repository (Continued)

| Realization Number | Ash Concentration ($g/cm^2$) | Log Ash Concentration Log ($g/cm^2$) | Waste Concentration ($g/cm^2$) | Log Waste Concentration Log ($g/cm^2$) |
|---|---|---|---|---|
| 29 | 1 6432 | 0 2157 | 5 54E-06 | -5 2565 |
| 30 | 0 3628 | -0 4404 | 2 61E-06 | -5 5840 |
| 31 | 2 6091 | 0 4165 | 1 56E-05 | -4 8065 |
| 32 | 2 7975 | 0 4468 | 5 11E-06 | -5 2914 |
| 33 | 54 7780 | 1 7386 | 3 78E-05 | -4 4222 |
| 34 | 5 9887 | 0 7773 | 3 99E-06 | -5 3989 |
| 35 | 1 1886 | 0 0750 | 7 29E-06 | -5 1371 |
| 36 | 5 6287 | 0 7504 | 4 16E-06 | -5 3805 |
| 37 | 1 1673 | 0 0672 | 7 07E-07 | -6 1505 |
| 38 | 0 9830 | -0 0074 | 1 26E-05 | -4 9004 |
| 39 | 7 6290 | 0 8825 | 7 75E-06 | -5 1105 |
| 40 | 0 2549 | -0 5936 | 1 05E-06 | -5 9773 |
| 41 | 1 6752 | 0 2241 | 1 86E-06 | -5 7298 |
| 42 | 0 5012 | -0 3000 | 4 52E-06 | -5 3445 |
| 43 | 1 5501 | 0 1904 | 9 50E-06 | -5 0221 |
| 44 | 0 7844 | -0 1055 | 1 74E-06 | -5 7604 |
| 45 | 1 0445 | 0 0189 | 2 15E-06 | -5 6678 |
| 46 | 17 6450 | 1 2466 | 1 15E-05 | -4 9378 |
| 47 | 0 4742 | -0 3241 | 3 57E-07 | -6 4468 |
| 48 | 0 5477 | -0 2615 | 4 98E-07 | -6 3026 |
| 49 | 0 6642 | -0 1777 | 2 55E-06 | -5 5929 |
| 50 | 6 8837 | 0 8378 | 1 03E-05 | -4 9886 |
| 51 | 5 3238 | 0 7262 | 3 25E-06 | -5 4885 |
| 52 | 1 6343 | 0 2133 | 3 21E-06 | -5 4934 |
| 53 | 0 9331 | -0 0301 | 7 34E-06 | -5 1345 |
| 54 | 0 1181 | -0 9279 | 1 79E-07 | -6 7470 |
| 55 | 0 2576 | -0 5890 | 4 23E-07 | -6 3734 |
| 56 | 1 4787 | 0 1699 | 6 31E-06 | -5 2002 |
| 57 | 0 4137 | -0 3833 | 2 07E-06 | -5 6843 |
| 58 | 0 3862 | -0 4132 | 1 84E-06 | -5 7341 |
| 59 | 1 3546 | 0 1318 | 1 91E-06 | -5 7179 |
| 60 | 1 2762 | 0 1059 | 2 63E-06 | -5 5808 |
| 61 | 0 2162 | -0 6652 | 2 12E-06 | -5 6746 |
| 62 | 6 3530 | 0 8030 | 1 24E-05 | -4 9065 |
| 63 | 2 9069 | 0 4634 | 4 65E-06 | -5 3326 |
| 64 | 0 5417 | -0 2663 | 1 12E-06 | -5 9519 |
| 65 | 0 3347 | -0 4754 | 8 41E-07 | -6 0751 |
| 66 | 4 0544 | 0 6079 | 2 18E-05 | -4 6619 |
| 67 | 9 6663 | 0 9853 | 4 57E-06 | -5 3400 |
| 68 | 14 2640 | 1 1542 | 1 54E-05 | -4 8113 |

Table 6-4. Calculated Concentration of Ash and Waste in the Midline of a Volcanic Plume at a Location 18 km South of the Repository (Continued)

| Realization Number | Ash Concentration ($g/cm^2$) | Log Ash Concentration Log ($g/cm^2$) | Waste Concentration ($g/cm^2$) | Log Waste Concentration Log ($g/cm^2$) |
|---|---|---|---|---|
| 69 | 14 0560 | 1 1479 | 2 32E-05 | -4 6353 |
| 70 | 0 6735 | -0 1716 | 2 64E-06 | -5 5780 |
| 71 | 0 5081 | -0 2940 | 1 38E-06 | -5 8606 |
| 72 | 0 2639 | -0 5785 | 3 78E-07 | -6 4227 |
| 73 | 18 7750 | 1 2736 | 1 92E-05 | -4 7162 |
| 74 | 18 5570 | 1 2685 | 1 44E-05 | -4 8425 |
| 75 | 0 4519 | -0 3450 | 2 71E-06 | -5 5674 |
| 76 | 0 6969 | -0 1569 | 5 46E-07 | -6 2630 |
| 77 | 1 9662 | 0 2936 | 1 86E-06 | -5 7302 |
| 78 | 12 7860 | 1 1067 | 5 89E-06 | -5 2298 |
| 79 | 21 8310 | 1 3391 | 2 23E-05 | -4 6513 |
| 80 | 0 0719 | -1 1433 | 2 16E-07 | -6 6664 |
| 81 | 1 3540 | 0 1316 | 1 01E-05 | -4 9946 |
| 82 | 7 8789 | 0 8965 | 6 00E-06 | -5 2222 |
| 83 | 16 9640 | 1 2295 | 1 77E-05 | -4 7532 |
| 84 | 0 9268 | -0 0330 | 9 66E-06 | -5 0149 |
| 85 | 18 3640 | 1 2640 | 3 08E-05 | -4 5110 |
| 86 | 1 2716 | 0 1044 | 1 44E-06 | -5 8402 |
| 87 | 2 6627 | 0 4253 | 1 04E-05 | -4 9817 |
| 88 | 1 6779 | 0 2248 | 5 76E-06 | -5 2393 |
| 89 | 4 0114 | 0 6033 | 2 05E-06 | -5 6885 |
| 90 | 5 2712 | 0 7219 | 1 38E-05 | -4 8597 |
| 91 | 2 2160 | 0 3456 | 1 54E-05 | -4 8129 |
| 92 | 2 3157 | 0 3647 | 2 26E-05 | -4 6458 |
| 93 | 4 9456 | 0 6942 | 3 64E-06 | -5 4394 |
| 94 | 5 2503 | 0 7202 | 1 04E-05 | -4 9825 |
| 95 | 0 6850 | -0 1643 | 2 47E-07 | -6 6079 |
| 96 | 0 7750 | -0 1107 | 4 03E-06 | -5 3942 |
| 97 | 0 7421 | -0 1295 | 7 25E-06 | -5 1394 |
| 98 | 0 2479 | -0 6058 | 1 85E-06 | -5 7334 |
| 99 | 5 6625 | 0 7530 | 4 36E-06 | -5 3610 |
| 100 | 0 5271 | -0 2781 | 1 07E-06 | -5 9712 |
| **Mean of logs** | | **0.2705** | | **-5.3809** |
| **Geometric Mean Concentration** | **Ash Concentration** | | **WASTE: (Mean Primary Waste Concentration)** | |
| | **1.8641 $g/cm^2$** | | **4.1605E-06 $g/cm^2$** | |
| **Standard Deviation** | **7.3831 $g/cm^2$** | | **7.47E-06 $g/cm^2$** | |

Source Output DTN LA0408GK831811 001

### 6.7.2 Ash Redistribution Model Abstraction

#### 6.7.2.1 Model Description

The ash redistribution model describes the range of conditions that allows for the transport of contaminated ash to the RMEI location by sedimentary processes. The model implicitly includes both alluvial and eolian transport processes as well as sediment transport mechanisms that could concentrate radionuclides, such as placer deposition along the channel, at the RMEI location.

If a volcano were to intersect the repository, the eruption would most likely result in waste-contaminated tephra being dispersed in the northeasterly direction as determined by the prevailing wind during a future eruption (Section 5.2.1), but primary deposition of contaminated waste at the RMEI location could also occur (Figure 6-1). Tephra that originally did not fall at the RMEI location could be redistributed to the RMEI location by sedimentary processes.

#### 6.7.2.2 Formulation

Field studies of tephra dilution in drainages around the Lathrop Wells cone and of surficial erosion/deposition rates based on $^{137}Cs$, along with general considerations of the sediment transport systems around Yucca Mountain, suggest a simple model for TSPA. This model and its output parameters for use in TSPA are summarized in Table 6-5 in terms of the two tephra fall/redistribution outcomes described in Section 6.6.1, as well as the two main geomorphic features at the RMEI location (interchannel divides and distributary channels). In Outcome 1, the primary tephra sheet is deposited at the location of the RMEI. In Outcome 2 the tephra sheet is deposited within the Fortymile Wash drainage basin (consistent with prevailing southwestern winds) at some distance upstream from the RMEI location. For the purposes of TSPA, the distinction between Outcomes 1 and 2 should be made on the basis of the presence of non-negligible thickness of ash at the RMEI location. Non-negligible ash thickness should be defined as greater than or equal to the smallest mean ash particle diameter of 0.001 cm. This thickness, or greater, of ash constitutes ash fall at the RMEI location (Outcome 1); less than 0.001 cm constitutes Outcome 2. Model Outcomes 1 and 2 represent the maximum availability of waste-contaminated ash at the RMEI location. Other tephra-sheet orientations either eliminate ash from reaching the RMEI location, or reduce the available volume of ash to be redistributed to the RMEI location.

#### 6.7.2.3 Interchannel-Divide Areas

The interchannel divides are the broad, nearly flat surfaces of the fan that separate active channels. Interchannel divides comprise 82 percent of the Fortymile Wash alluvial fan (DTN: LA0507CH931611.001 [DIRS 174843]).

**Outcome 1**–For igneous eruptive events that produce an initial ash fall at the RMEI location (Table 6-5), the initial tephra thickness is provided by TSPA Ashplume results. An ash and soil removal factor ranging from 0.02 cm/yr to 0.04 cm/yr (DTN: LA0407DK831811.001 [DIRS 170768]) is applied so that removal of 10 cm tephra or soil by erosion would occur in 250 to 500 years.

Table 6-5. Ash Redistribution Model Abstraction for the TSPA-LA Model

| | Interchannel Divide | Distributary Channels |
|---|---|---|
| **Areal Weight** | **0.82** | **0.18** |
| Outcome 1<br>Primary tephra (ash fall) in the vicinity of the RMEI location | **Initial condition**<br>Ash-layer (tephra) thickness calculated by ASHPLUME in the TSPA model<br>Initial waste areal concentration calculated in TSPA for the ash layer at the location of the RMEI<br><br>**Ash removal**<br>At a rate uniformly distributed between 0.02 to 0.04 cm/yr<br><br>**Residual conditions**<br>9-cm contaminated soil layer beneath initial ash. Volumetric concentration of the waste (see NOTES below) in this layer decreases linearly from the initial value calculated in the ash to 1/100th of that value at 9 cm. This layer is removed at the same rate as the initial ash layer, consistent with $^{137}Cs$ observations. The linear volumetric concentration decrease is conservative with respect to the exponential decrease observed for $^{137}Cs$<br>Below the 9-cm layer is an additional 1 to 2 cm (uniform distribution) layer with 1/100th of the initial volumetric concentration. Assumed to remain indefinitely<br>Represents infiltration from initial ash layer before removal | **Initial condition**<br>Initial ash-layer thickness: uniform distribution from 1 to 15 cm, or the initial ash layer thickness calculated for the divide areas in the TSPA model, whichever is greater<br>Initial waste concentration: Mean Primary Waste Concentration (see Table 6-4 and NOTES below) except for realizations in which the ash thickness calculated in the TSPA is greater than the thickness sampled from the 1 to 15 cm uniform distribution, in those cases, use the waste volumetric concentration calculated in TSPA for the ash layer at the location of the RMEI<br><br>**Ash removal**<br>Volumetric concentration of waste in the ash layer decreases linearly from its initial volumetric concentration to 1/100th of its initial volumetric concentration within a time period uniformly distributed between 100 and 1,000 years. This decrease in volumetric concentration represents dilution during removal and replacement of the initial sediment<br><br>**Residual conditions**<br>After removal of the initial volumetric concentration, a layer with the same initial thickness but with 1/100th of the initial volumetric concentration is assumed to remain indefinitely<br>This residual layer represents lower levels of contamination that may be brought down the wash or exposed from underlying soil |

Table 6-5. Ash Redistribution Model Abstraction for the TSPA-LA Model (Continued)

| | Interchannel Divide | Distributary Channels |
|---|---|---|
| **Areal Weight** | **0.82** | **0.18** |
| Outcome 2<br>No primary tephra fall on or near the RMEI location. Primary tephra deposition in upper Fortymile Wash drainage basin | Possible contamination by eolian processes or major flood events is approximated by a 1 to 2 cm (uniform distribution) layer. 1/100th of the initial Mean Primary Waste Concentration (see Table 6-4) is assumed to remain indefinitely | **Initial condition**<br>Initial ash-layer thickness: uniform distribution from 1 to 15 cm<br>Initial waste concentration: Mean Primary Waste Concentration (see Table 6-4)<br><br>**Ash removal**<br>Volumetric concentration of waste in the ash layer decreases linearly from its initial volumetric concentration to 1/100th of its initial volumetric concentration within a time period uniformly distributed between 100 and 1,000 years. This decrease in volumetric concentration represents dilution during removal and replacement of the initial sediment<br>**Residual conditions**<br>After removal of the initial volumetric concentration, a layer with the same initial thickness but with 1/100th of the initial volumetric concentration is assumed to remain indefinitely<br>This residual layer represents lower levels of contamination that may be brought down the wash or exposed from underlying soil |

Source: Output DTN: LA0408CH831811.001

NOTES: 1. The uniform distribution of erosion rate of 0.02 cm/yr to 0.04 cm/yr (DTN: LA0407DK831811.001 [DIRS 170768]) is based on current climate conditions. Although there is considerable uncertainty associated with long-term (10,000 yr) erosion rates, the range provided is considered reasonable for the parts of the regulatory time frame when conditions are essentially as they are today. Major changes in precipitation, or storm type may result in significant changes in erosion rates on these alluvial surfaces.

2. Areal weights are developed in DTN: LA0507CH931611.001 [DIRS 174843].

3. Volumetric waste concentrations specified in this table should be derived from the Mean Primary Waste Concentration calculated at 18 km, at the midpoint of the plume, as reported in Table 6-4, and from the mean ash layer thickness at the same location, which is also based on the results in Table 6-4. A value of 1.0 g/cm$^3$ should be used for ash settled density (DTN: LA0407DK831811.001 [DIRS 170768]). For example, ash areal concentration (g/cm$^2$) divided by ash settled density (g/cm$^3$) equals ash thickness (cm); waste areal concentration (g/cm$^2$) divided by ash (or deposit) thickness (cm) equals waste volumetric concentration (g/cm$^3$). The resulting volumetric concentration should then be applied to the layer thicknesses (e.g., 1 to 15 cm uniformly distributed or 1 cm to 2 cm uniformly distributed) in this table.

The technical basis for the ash removal rate distribution is a $^{137}$Cs study and interpretation of this data yields an estimate of erosion of 1 cm to 2 cm of the upper soil horizon in interchannel divide areas over a 50-year period. The uniform distribution of erosion rates of 0.02 cm/yr to 0.04 cm/yr is based on current climate conditions (Section 5.1.4).

The concentration of waste in ash is represented by a contaminated soil layer 9-cm thick (Figure 6-5), in which radionuclide concentration within the layer decreases linearly from the value initially in the ash to 1 percent of that value at 9-cm depth (Table 6-5). The linear concentration decrease is conservative with respect to the exponential decrease observed in $^{137}$Cs studies (BSC 2004 [DIRS 169980], Section 6.3.4.2; DTN: LA0308CH831811.002

[DIRS 164853]; Anspaugh et al. 1975 [DIRS 151548]). An examination of the cesium concentrations in a reference soil profile demonstrates that cesium is concentrated in the upper 3 cm, and $^{137}Cs$ concentration decreases exponentially with depth in the soil profile. The concentration of $^{137}Cs$ decreases an order of magnitude from the upper 3 cm to the next interval sampled at 3 cm to 6 cm. At 6 to 9 cm, concentration is reduced by two orders of magnitude relative to the concentration in the upper 3 cm (BSC 2004 [DIRS 169980], Section 6.3.4.2; DTN: LA0308CH831811.002 [DIRS 164853]). The 9-cm thick layer is removed at the same rate as the initial ash layer, consistent with $^{137}Cs$ observations (BSC 2004 [DIRS 169980], Section 6.3.4.2; DTN: LA0308CH831811.002 [DIRS 164853]).

In the model abstraction, a persistent layer of subsurface contamination following removal of the 9-cm layer is represented by a layer 1-cm to 2-cm thick (uniform distribution) with 1 percent of the initial concentration (Table 6-5). This layer, which is assumed to remain indefinitely, accounts for the effects of infiltration of waste from the initial ash layer before removal as well as the potential low-level influx of waste-contaminated eolian dust over time. The field data indicate that the assumption of the presence of a persistent contaminated soil layer below the 9-cm soil layer is conservative. Field investigations show that carbonate layers are widespread at depths of about 9 cm. $^{137}Cs$ has not been found in samples collected below this depth on the fan (Harrington 2003 [DIRS 164775], pp. 28 to 53). For thin surface layers, the model provides a reasonable approximation for the inhalation pathway to the RMEI. Inhalation pathways are dominated by exposure to contaminated materials from thin surface layers of several millimeters. However, this model abstraction may cause significant overestimation of dose from ingestion and external exposure pathways.

**Outcome 2**–Tephra falls upstream of the location of the RMEI in the Fortymile Wash drainage and is then available for redistribution by eolian or fluvial processes (Table 6-5). Contaminated ash may be present on interchannel divides, as a result of wind transport or infrequent flood events that fill channels and spill onto the interchannel divides

This process is represented by a layer 1-cm to 2-cm thick (uniform distribution) containing residual contamination at 1 percent of the initial waste concentration (Table 6-5). The TSPA model assumes the same constant residual contamination model as in Outcome 1. However, instead of using probabilistic Ashplume output from TSPA, the model conservatively uses the Mean Waste Concentration (Table 6-4) calculated at 18 km south of the repository with wind direction fixed southward (Section 6.7.1). The residual concentration remains indefinitely at 1 percent of the Mean Primary Waste Concentration. The resulting volumetric concentration is applied to the sampled layer thicknesses.

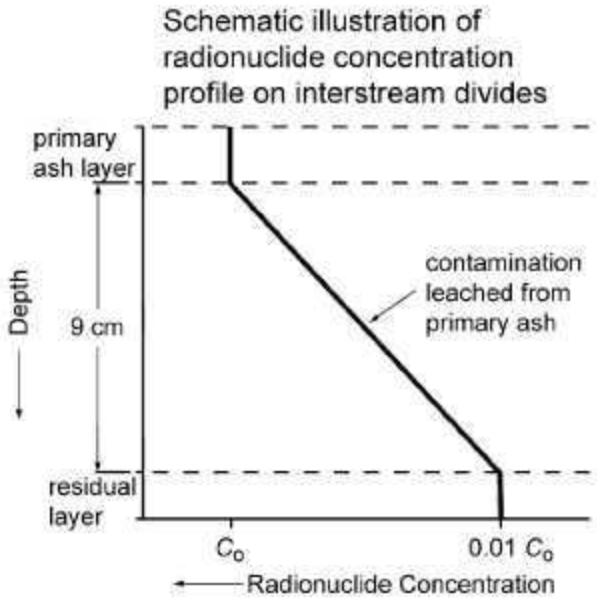


Source: BSC 2004 [DIRS 169980], Section 6.3.4.2.

NOTE: For illustration purposes only.

Figure 6-5. Schematic of Decrease in Radionuclide Concentration in Soil

### 6.7.2.4 Distributary Channels

Distributary channels are the parts of an alluvial fan that act as active drainages during runoff events. Distributary channels compose 18 percent of the Fortymile Wash alluvial fan (DTN: LA0507CH931611.001 [DIRS 174843]).

**Outcome 1**–Processes are likely to be more complex in the distributary channels because tephra can be washed in from upstream areas during storm events. Redistributed sediment is in transient storage, and redistributed tephra thicknesses are variable with time within distributary channels. Although dilution (mixing) is likely to occur, it is conservatively assumed that the initial washed-in tephra is not mixed but is deposited in channels at the RMEI location in layers ranging from 1-cm to 15-cm thick. The upper value for this range was chosen on the basis of channel depths; sediment greater than 15-cm thick would likely overtop the channel margins in this area of the alluvial fan.

The initial conditions in the distributary channels account for the rapid transport of contaminated ash in channels near the RMEI location in the first few years after the eruption. In addition, the initial conditions account for the possibility of a hybrid model outcome in which significant ash is deposited at both the RMEI location and in the near portions of Fortymile Wash and rapid transport within the wash results in enhanced thicknesses of ash in the distributary channels at the RMEI location. The initial thickness is determined as the greater of two values:

- A 1-cm to 15-cm thick layer sampled from a uniform distribution
- The initial ash layer thickness calculated for the interchannel divide areas.

For these two possibilities, the concentration of waste in the ash is defined as, respectively:

- The geometric mean of the concentration calculated by ASHPLUME at 18 km (Table 6-4)
- The concentration calculated for ash fall on the interchannel divides.

The volumetric concentration of waste in the ash layer is assumed to decrease linearly from its initial concentration to 1 percent of its initial concentration within a time period uniformly distributed between 100 and 1,000 years. This decrease in volumetric concentration represents dilution during removal and replacement of the initial sediment by fluvial processes (Table 6-5). The ash redistribution model abstraction includes an implicit equivalence between waste volumetric concentration and areal concentration in this case, since waste dilution (in situ mixing) in channel sediments results from removal of waste from the RMEI area, rather than simple dilution by vertical migration. After removal of the initial concentration, a layer with the same initial thickness but with 1 percent of the initial concentration of waste is assumed to remain indefinitely (Section 6.7.2, Table 6-5).

**Outcome 2**–Initial conditions assume a 1- to 15-cm thick ash layer in the stream channels as a result of rapid erosion and transport from upstream slopes (but no primary ash fall at the RMEI location). The upper value for this range was chosen on the basis of channel depths; sediment greater than 15-cm thick would likely overtop the channel margins in this area of the alluvial fan. The concentration of waste in the ash layer decreases linearly from its initial concentration (the Mean Primary Waste Concentration on Table 6-4) to 1 percent of its initial concentration within a time period uniformly distributed between 100 years and 1,000 years (Section 6.7.2). This decrease in concentration represents dilution (mixing) during removal and replacement of the initial sediment by fluvial processes. The scenario assumes dilution occurs in a linear fashion until the tephra volume concentration reaches 1 percent of the initial concentration, after which there is no further decline in concentration. In other words, after dilution of the initial concentration, a layer with the same initial thickness, but with 1 percent of the initial waste concentration, is assumed to remain indefinitely. This residual layer represents lower levels of contamination that may be brought down the wash or exposed from underlying soil (Section 6.7.2, Table 6-5).

### 6.7.2.5 Model Parameters

Input parameters to TSPA for the ash redistribution model are based on geomorphological field studies in the Yucca Mountain region (DTN: LA0407DK831811.001 [DIRS 170768]). The $^{137}Cs$ profiles are used as a proxy for all radionuclides because no other radionuclide data are available for the Fortymile Wash fan. For the purpose of the alternative ash redistribution model (Appendix I), datasets from the Nevada Test Site and the Chernobyl accident have been used for corroboration of the field $^{137}Cs$ data.

#### 6.7.2.5.1 Areal Weights for Channels and Interchannel Divides

Type: point values
Value: 0.18, 0.82
Units: N/A

The relative area factors (areal weights) for distributary channels and interchannel divides are used in TSPA-LA to combine the processes occurring on the two different landforms within the ash redistribution model (Table 6-5). The relative area covered by distributary channels on the upper portion of the Fortymile Wash alluvial fan is 0.18, while the relative area covered by interchannel divides is 0.82 (DTN: LA0507CH931611.001 [DIRS 174843]). These values were developed by the use of a planimeter (Figure 6-2).

#### 6.7.2.5.2 Ash erosion Rate from Interchannel Divide Areas

Type: uniform distribution
Value: 0.02-0.04
Units: cm/yr

The ash erosion rate is defined as the range (0.02 cm/yr to 0.04 cm/yr) for the removal of ash from interchannel divide areas in the Yucca Mountain region. The ash erosion rate is based on $^{137}Cs$ concentrations in samples collected from the Yucca Mountain region (BSC 2004 [DIRS 169980], Section 6.3.4). This rate is consistent with regional and statewide erosion for cultivated and non-cultivated farmland (BSC 2004 [DIRS 169980], Section 6.3.4.2.5).

#### 6.7.2.5.3 Residual Concentration Factor for Waste In soil

Type: point value
Value: 0.01
Units: N/A

The concentration of waste in the ash layer decreases linearly from its initial concentration to 1 percent of its initial concentration within a time period uniformly distributed between 100 years and 1,000 years. This decrease in concentration represents dilution during removal and replacement of the initial sediment. The assumed decrease in waste concentration in ash is consistent with the decrease in $^{137}Cs$ concentrations in soil from the surface to depths of about 9 cm. $^{137}Cs$ concentrations decrease rapidly with depth and reach non-detectable levels at 9 cm or less (BSC 2004 [DIRS 169980], Section 6.3.4.2; DTN: LA0308CH831811.002 [DIRS 164853]). No $^{137}Cs$ has been detected below about 9 cm apparently because of the occurrence of a carbonate-rich layer that impedes infiltration of $^{137}Cs$. Based on the apparent analogy between waste concentration in ash-laden sediments and $^{137}Cs$ concentration in soil, the use of a residual waste concentration in ash is reasonable and perhaps conservative.

#### 6.7.2.5.4 Time for Ash Dilution in Channels

Type: uniform distribution
Value: 100 to 1,000
Units: years

The concentration of waste in the ash layer decreases linearly from its initial concentration to 1 percent of its initial concentration within a time period uniformly distributed between 100 and 1,000 years. This decrease in concentration represents dilution (mixing) during removal and replacement of the initial sediment, as discussed in Folk (1980 [DIRS 164773]). The range in this parameter is intended to provide order-of-magnitude bounds on uncertainty in the process of soil removal and sediment transport in the Fortymile Wash fan area.

#### 6.7.2.5.5 Thickness of Residual Contaminated Soil Layer

Type: point value
Value: 9
Units: cm

The concentration of waste in ash is represented by a contaminated soil layer 9-cm thick (Figure 6-5), based on the maximum depth of $^{137}Cs$ observed in alluvial soils in the Yucca Mountain region (BSC 2004 [DIRS 169980], Section 6.3.4.2; DTN: LA0308CH831811.002 [DIRS 164853]). The results of analyses of soil samples from reference soil profiles on stable alluvial fan surfaces indicated that at or below 9 cm the concentration of $^{137}Cs$ was generally below detection limit (DTN: LA0302CH831811.002 [DIRS 162863]). Based on these results, it was concluded that 9 cm was the maximum thickness of the residual contaminated soil layer, and subsequent sampling of younger alluvial fan surfaces was limited to the 0-9 cm layer (BSC 2004 [DIRS 169980], Section 6.3.4.2.3).

#### 6.7.2.5.6 Distribution of Contamination within Soil Layer

Type: linear decrease
Value: 1.0, 0.01
Units: N/A

The concentration of waste in ash in the 9-cm thick contaminated soil layer (Figure 6-5), decreases linearly from the value initially in the ash to 1 percent of that value at 9 cm (Table 6-5). The linear concentration decrease is conservative with respect to the exponential decrease observed in $^{137}Cs$ studies (BSC 2004 [DIRS 169980], Section 6.3.4.2; DTN: LA0308CH831811.002 [DIRS 164853]; Anspaugh et al. 1975 [DIRS 151548]). An examination of the cesium concentrations in a reference soil profile indicates that cesium is concentrated in the upper 3 cm, and $^{137}Cs$ concentration decreases exponentially with depth in the soil profile. The concentration of $^{137}Cs$ decreases an order of magnitude from the upper 3 cm to the next interval sampled at 3 cm to 6 cm. At 6 to 9 cm, concentration is reduced by two orders of magnitude relative to the concentration in the upper 3 cm (BSC 2004 [DIRS 169980], Section 6.3.4.2; DTN: LA0308CH831811.002 [DIRS 164853]).

INTENTIONALLY LEFT BLANK

# 7. MODEL VALIDATION

Validation, or confidence building, is a means to ensure that the system behavior simulated by models is sufficiently consistent with observed behavior to give confidence in model outcomes.

Model validation guidelines, presented in LP-2.29Q-BSC, are based on three levels of model importance and are commensurate with each level. These levels of model importance were based on the TSPA system sensitivity analyses and conclusions presented in *Risk Information to Support Prioritization of Performance Assessment Models* (BSC 2003 [DIRS 168796]), referred to herein as the *Prioritization Report*. The *Prioritization Report* stated that, with regard to the atmospheric transport of erupted radionuclides, the only parameters that bear significantly on the estimate of the mean annual dose to the RMEI, are wind speed and direction (BSC 2003 [DIRS 168796], Sections 3.3.13 and 5.1.10). Accordingly, LP-2.29Q-BSC (Table 1) indicates that, in the area of transport of radionuclides after an igneous eruption, adequate confidence can be gained with regard to the Ashplume component in TSPA-LA (which addresses windspeed and direction) through a Level II model validation of the Ashplume model. Appendix C of REV 04 of the *Technical Work Plan: Igneous Activity Assessment for Disruptive Events* (BSC 2003 [DIRS 166289]) described the planned validation of the Ashplume model and the ash redistribution conceptual model, which was originally presented in REV 00 of this report. Additional validation discussion has been added to Section 7 of this revision of the model report, per REV 08 of the TWP (BSC 2005 [DIRS 174773], Section 2.6.3.1).

Although LP-SIII.10Q-BSC, *Models*, does not require post-development model validation for a conceptual model, the ash redistribution conceptual model has been given the same level of importance as the Ashplume mathematical model because the ash redistribution conceptual model and its representation in the TSPA may impact dose. Appendix C of REV 04 of the *Technical Work Plan: Igneous Activity Assessment for Disruptive Events* (BSC 2003 [DIRS 166289]) described the planned process for validating the ash redistribution conceptual model.

## 7.1 VALIDATION PROCEDURES

Procedure LP-2.29Q-BSC, Attachment 3 requires a single post-development model validation method for Level II importance models; the validation methods are described in LP-SIII.10Q-BSC, *Models* (Section 5.3.2c). Although LP-2.29Q-BSC, Attachment 3 calls for Level II validation of the ash dispersal model, sufficient validation activity was performed for the Ashplume model to meet Level III standards. Specifically, two post-development model validation methods were completed for the Ashplume model. Two methods of post-development model validation (independent technical review and ash dilution study) were completed for the ash redistribution conceptual model. Table 7-1 summarizes the validation activities carried out to satisfy the validation criteria, defined in LP-SIII.10Q-BSC (Section 5.3.2), for the Ashplume and ash redistribution models and specifies the location in this model report in which each activity is discussed.

Table 7-1. Confidence-Building and Post-Model Development Validation Activities

| LP-SIII.10Q-BSC Validation Approaches | Location of Discussion in this Model Report |
|---|---|
| **Confidence-Building Activities Related to Model Development** | |
| Selection of input parameters and/or data, and a discussion of how the selection process builds confidence in the model (confidence building during model development (5 3 2(b)(1))) | Input parameters were selected to represent conditions expected for a volcanic eruption specific to the Yucca Mountain region and to include the range of values representing uncertainty in future eruption parameters, atmospheric conditions, and erosion/dilution rates Model input discussion is in Sections 6 5 and 6 6 |
| | Model assumptions and simplifications are discussed in Section 5 |
| | A special calculation has been completed to demonstrate that the model is mass conservative (DOE 2003 [DIRS 166506]) |
| Description of calibration activities, and/or initial/boundary condition runs, and/or run convergences, and a discussion of how the activity or activities build confidence in the model Include a discussion of impacts of any run non-convergences (confidence building during model development (5 3 2(b)(2)) | A sensitivity analysis was performed in which model simulations were carried out to span the entire range of all parameters represented by distributions, outputs were checked for consistency See Section 7 2 |
| Discussion of the impacts of uncertainties to model results (confidence building during model development (5 3 2(b)(3))) | Parameter uncertainties, including wind speed and direction, are discussed in Sections 4, 6 5, 6 6, and 7 2<br>The representation of important model parameters with distributions of values to be used in the TSPA-LA Monte Carlo approach ensures that the range of possible outcomes is fully represented Discussion of selection of the parameter distributions is in Section 6 5 Parametric uncertainties are discussed in Sections 7 3 1 4 and 7 3 2 2 |
| **Post-Development Model Validation Activities** | |
| Corroboration of model results with data acquired from the laboratory, field experiments, analogue studies or other relevant observations, not previously used to develop or calibrate the model (post-development model corroboration (5 3 2(c)(1))) | Calculations were performed to compare Ashplume model results to data collected for three volcanoes representative of volcanic ash deposits in the Yucca Mountain region (Cerro Negro, Lathrop Wells, and Cinder Cone)<br>The comparisons are documented in Section 7 3 1 A corroborative ash dilution study was completed on the Lathrop Wells cone for the ash redistribution conceptual model and is discussed in Section 7 3 2 1 |
| Technical review, planned in the applicable TWP, by reviewers independent of the development, checking, and interdisciplinary review of the model documentation (post-development model validation (5 3 2(c)(5))) | An independent review was performed by Dr Frank Spera of the University of California to assess the applicability of the Ashplume model The independent technical review is documented in Section 7 4 (see Appendix F for text of the technical review) |
| Technical review, planned in the applicable TWP, by reviewers independent of the development, checking, and interdisciplinary review of the model documentation (post-development model validation (5 3 2(c)(5))) | An independent review was performed by Dr David Buesch and Dr Dennis O'Leary, U S Geological Survey, to assess the applicability of the ash redistribution conceptual model The independent technical review is documented in Section 7 4 (see Appendix G for text of the technical review) |

## 7.2 SENSITIVITY ANALYSIS

A sensitivity analysis was performed to test the Ashplume model over the entire range of model input parameter values to be used in the TSPA analysis. This sensitivity analysis both ensured that the model operated as expected over the parameter ranges selected and identified limits to model validity due to any numerical constraints. In addition, the sensitivity analysis identified the model parameters to which the calculated waste concentration is most sensitive, and are thus

important in the TSPA dose calculations. The uncertainty in these parameters is represented in the TSPA analysis by a distribution of values covering the ranges developed in the input selection process (BSC 2003 [DIRS 166289]).

The sensitivity analysis was performed by varying the following input parameters: eruptive power, mean particle diameter, particle diameter standard deviation, column diffusion constant (beta), initial rise velocity, wind speed, wind direction, eruption duration, waste incorporation ratio, waste particle size distribution, and waste available for transport. These parameters were represented in the input set as distributions of parameters (Table C-12). During a TSPA-LA simulation, these parameters might take on any value within the distribution of values defined in Section 6.5. The input parameter values used in the sensitivity runs were selected from the tables shown in Appendix C. The model was run over the full range of values for each parameter shown in the tables.

The results of each ASHPLUME V.2.0 (CRWMS M&O 2001 [DIRS 152844]) run for a given parameter were plotted and evaluated for sensitivity to change in value. The plots shown in Appendix C (Figure C-1 to Figure C-11) exhibit expected trends that are in accordance with increasing parameter values. No significant discontinuities in results were detected, which indicates numerical convergence in all simulations (Keating 2005 [DIRS 173850], pp. 96 to 107). The analysis indicates that the Ashplume model results are most sensitive to eruptive power, wind speed, wind direction, and eruption duration; the variations in these parameters over their respective ranges results in two or three order-of-magnitude changes in ash thickness. The model is much less sensitive to variations in beta, mean particle diameter, particle diameter standard deviation, initial rise velocity, and waste incorporation ratio; variations in these parameters over their respective ranges results in variations of ash thickness by less than a factor of three.

An additional sensitivity analysis considered the effect of variations in mass of waste available for transport (Table C-10, Figure C-10). Three scenarios were considered, based on numbers of waste packages calculated to be intersected (hit) during the development of a volcanic conduit through the repository (BSC 2005 [DIRS 174066]): median (5 waste packages), 95th percentile (40 waste packages), and all waste packages in a drift (120 waste packages). The resulting trend in calculated waste concentration at the RMEI follows a linear increase: the 95th percentile number of waste packages hit produces an eight-fold increase and the evaluation of the entire drift produces a 24-fold increase in waste concentration compared to the base case.

The final sensitivity analysis was performed (Table C-11, Figure C-11) to assess the effect of the alternative waste particle size distribution developed in Appendix J. This alternative size distribution provides an enhanced technical basis over that presented in Section 5.2.4. The alternative waste particle size distribution provides a 14 percent decrease in waste concentration at the RMEI compared to the base case distribution (base-case inputs presented in Table 8-2).

As described in *FY 01 Supplemental Science and Performance Analyses, Volume 1: Scientific Bases and Analyses* (BSC 2001 [DIRS 155950], Section 14.3.3.4), the DOE completed analyses to evaluate the effects of uncertainties in waste-particle size on dose. This parameter is associated with the volcanic eruption scenario (BSC 2001 [DIRS 157876], Section 6.1 and Table 4). Waste-particle diameter was varied over a range of values (BSC 2001 [DIRS 155950],

Section 14.3.3.4) sufficient to address uncertainties in the distribution. The sensitivity analysis showed that performance is relatively insensitive to uncertainty in waste-particle size within the range considered in the analysis (BSC 2001 [DIRS 154659], Section 3.3.1.2.2). The sensitivity of performance to uncertainties in waste-particle size distribution is well understood and was sufficiently documented in the *FY01 Supplemental Science and Performance Analyses, Volume 2: Performance Analyses* (BSC 2001 [DIRS 154659], Section 3.3.1.2.2).

## 7.3 NATURAL ANALOGUE STUDIES FOR ASHPLUME AND THE ASH REDISTRIBUTION CONCEPTUAL MODEL

### 7.3.1 Ashplume

Natural analogue studies addressed the adequacy and accuracy of the Ashplume model by comparing model results to observed tephra fall thickness distributions at Cerro Negro volcano, Nicaragua; Lathrop Wells volcano, Nevada; and Cinder Cone, California.

**Validation Criteria**

Based on a review of relevant published tephra dispersal modeling studies (Keating 2005 [DIRS 174988], pp. 62-66, and 76), the Ashplume studies used in natural analogue comparisons of computed vs. measured tephra thickness below will be deemed sufficiently accurate for the model's intended use if:

I. The error in match between computed and measured tephra thickness at specific locations is within a factor of 2 (e.g., Glaze and Self 1991 [DIRS 110277], pp. 1,238 to 1,240), or

II. The correlation coefficient ($R^2$) is greater than or equal to 0.9 and the slope of the regression line is within 30 percent of unity (B statistic = 0.7 to 1.3), or

III. There is a reasonable match between the computed and observed pattern of the tephra deposit, in terms of two-dimensional profile or three-dimensional tephra sheet pattern. A reasonable match will be one in which there is consistency in tephra thicknesses and dispersal patterns, based on visual inspection.

Criterion I compares computed vs. measured tephra thicknesses at each observation point independently. Criterion II is more stringent than criterion I (which could result in regression slopes $\leq 2$), and it includes the general goodness-of-fit of the modeled thickness to *all* measured points (via the correlation coefficient). Criterion III provides a means to evaluate the overall goodness-of-fit of the modeled pattern of the tephra blanket compared to interpretations of field data (e.g., an isopach map). If the validation exercise is successful in meeting these accuracy acceptance criteria while using reasonable input parameter values, the scientific basis for the model is deemed to be adequate. Reasonable input parameter values are those which are either derived from field observations native to the case study at hand or input parameter values generalized from worldwide studies (e.g., Section 6.5.2).

**A Note on Matching Observed Tephra Thickness**–Tephra-dispersal models, such as ASHPLUME and others based on Suzuki's (1983 [DIRS 100489]) mathematical model, simplify

the eruption column as a vertical line source, rather than explicitly modeling eruption column physics. As a result, the computed tephra concentrations are valid only for distances sufficiently far from the source that the tephra dispersal processes can be described by advection-dispersion and particle settling processes (Pfeiffer et al. 2005 [DIRS 174826], pp. 273 and 274). In practice, this means that, in model validation comparisons of computed vs. observed tephra thicknesses, greater weight should be given to matching distal data. For example, modeling studies that fitted proximal data in order to reconstruct tephra distributions resulted in extreme underestimation of total erupted mass (Pfeiffer et al. 2005 [DIRS 174826], pp. 291 and 292). In the modeling studies of analogue cases in the following sections, fits to the distal data have been emphasized in the evaluation of the performance of the model relative to accuracy criteria.

#### 7.3.1.1 Cerro Negro

The Cerro Negro volcano is one of a number of active basaltic volcanoes within an active volcanic chain in Nicaragua. Cerro Negro is located on the Caribbean tectonic plate, and the volcanic activity expressed within this long volcanic chain, which continues from southern Mexico to Costa Rica, is directly related to subduction of the Pacific tectonic plate under the Caribbean tectonic plate. Volcanism at Cerro Negro has a 150-year history with at least 22 documented eruptions. Its last eruption (1995) produced a tephra volume (0.004 $km^3$) (Hill et al. 1998 [DIRS 151040]) similar to, but less than, that of the Lathrop Wells cone (> 0.04 $km^3$) (BSC 2004 [DIRS 169980], Section 6.3.3.4). The 1995 Cerro Negro eruption may be analogous to the type of eruption that could occur in the Yucca Mountain region. However, Cerro Negro's relatively long history, shape, and magma production rate suggest that it may represent a young composite volcano rather than a simple, long-lived cinder cone (McKnight and Williams 1997 [DIRS 162827]).

The measured eruption parameters published by Hill et al. (1998 [DIRS 151040]) for their study using a model similar to Ashplume were used to develop input parameters for the ASHPLUME code (versions 1.4 and 2.0). Because these field measurements were assumed to accurately represent the actual 1995 eruption of Cerro Negro (CRWMS M&O 2000 [DIRS 152998]), these parameters were not varied in ASHPLUME to attempt to match the field data. Because of the uncertainties associated with the atmospheric and eruption conditions of the Cerro Negro event, comparison of ash fall thicknesses between the observed distribution and the Ashplume result is qualitative. However, this comparison provides confidence that the Ashplume model can give a reasonable representation of ash deposition for the type of a possible future eruption at Yucca Mountain.

As shown in Figure 7-1 the Ashplume calculations compare well with the observed data for distances from the volcanic vent greater than 10 km. For distances less than 10 km, the Ashplume results give ash thickness values greater than the observed data. The lobe on the northern side of the measured ash thickness data is interpreted to be a result of a variation in wind direction and/or speed that occurred during the eruption. This variation probably accounts for some of the discrepancy because Ashplume assumes a constant wind speed and direction for a given simulation. In addition, comparison of results using ASHPLUME 1.4LV (BSC 2003 [DIRS 161296]) and ASHPLUME V.2.0 (CRWMS M&O 2001 [DIRS 152844] show the overall consistency between the two versions (Figure 7-1) in terms of ash thickness and dispersal patterns. This study meets the qualitative accuracy requirement (#III) above.

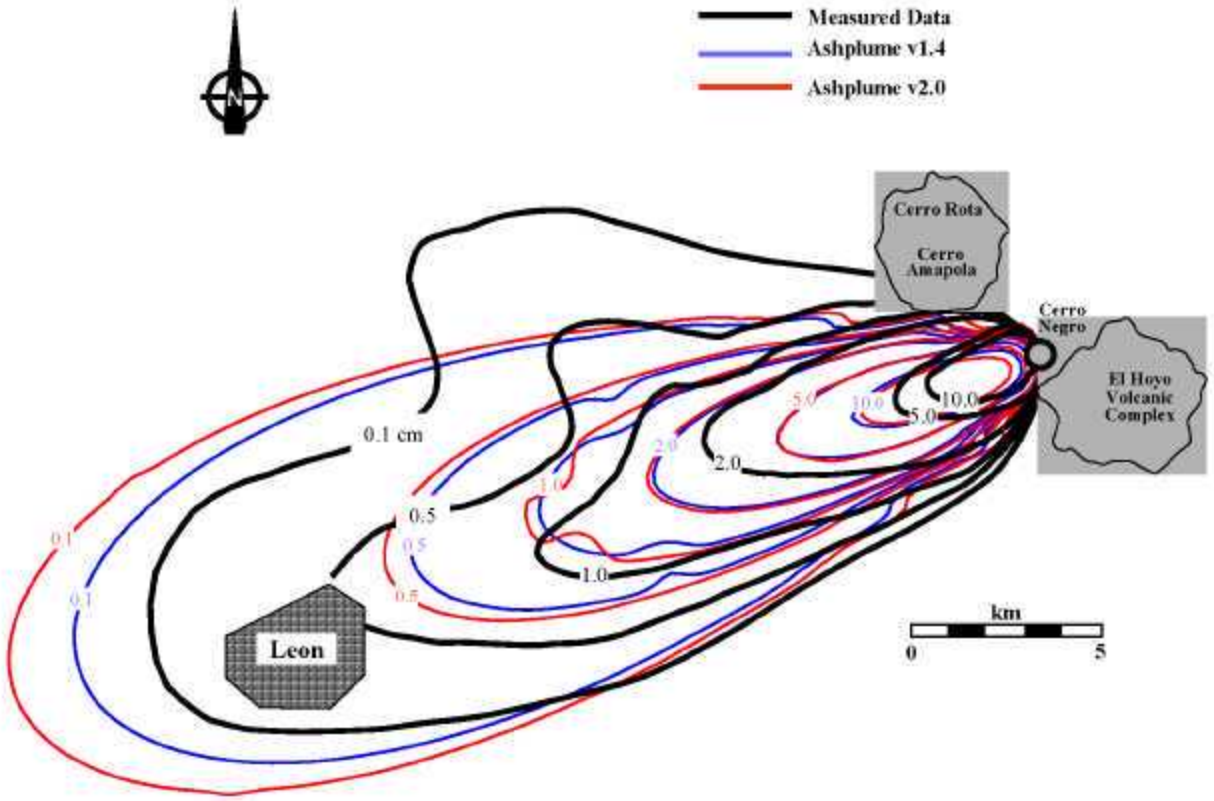


Source: CRWMS M&O (2000 [DIRS 152998], Figure 6).

Figure 7-1 Comparison of Calculated and Measured Ash Deposition Thickness (cm) for 1995 Cerro Negro Eruption: Isopachs of Model Results from ASHPLUME 1.4LV and V.2.0 Compared to Observed (Measured) Ash Thickness

### 7.3.1.2 Lathrop Wells

At 77,000-years old (Heizler et al. 1999 [DIRS 107255], p. 803), the Lathrop Wells Cone, Nevada, is the youngest basaltic volcano in the Yucca Mountain region. It is the southern-most surface expression of the Plio-Pleistocene Crater Flat Volcanic Zone (CFVZ) (Crowe and Perry 1990 [DIRS 100973], p. 328) and is located approximately 18 km south of Yucca Mountain. Characteristics of the volcanism comprising the CFVZ are documented in Perry et al. (1998 [DIRS 144335], Chapters 2 and 4). Eruptive history of the Lathrop Wells cone and volume estimates of the cone, lava flows, and eruptive tephra are provided in *Characterize Eruptive Processes at Yucca Mountain, Nevada* (BSC 2004 [DIRS 169980], Appendix C). The volume of tephra was estimated from field sample points, which located ash fall deposits that are now shallowly buried beneath younger colluvium and eolian deposits. Due to deeper burial or non-deposition of the tephra, data points to the south of the cone are largely absent, and this results in an apparent tephra fall pattern directed northward from the vent area. Additionally, there are no data for ash deposits less than 1-cm thick, which limits the identification of the northward extent of the ash fall. The tephra distribution presented in *Characterize Eruptive Processes at Yucca Mountain, Nevada* (BSC 2004 [DIRS 169980]) is, therefore, a minimum distribution.

For the Lathrop Wells cone simulation, all parameters were set to base-case values (Table 8-2); those parameters with distributed ranges in Table 8-2 were set to midrange values, except ash particle size standard deviation, for which a representative value was used from CRWMS M&O (2001 [DIRS 174768], Table 2). Several calculations were performed using wind speed sampled from the full range that will be used for the TSPA-LA and results were compared to the Lathrop Wells cone data (Figure 7-2). The figure also shows the results of a simulation using wind speeds of 800 cm/s (Model 4), which most closely matches the Lathrop Wells cone tephra data. The simulations showed that observed Lathrop Wells data fall within the range of results produced by ASHPLUME V.2.0 (CRWMS M&O 2001 [DIRS 152844]) using wind speeds within the range provided to TSPA-LA (Section 8.2).

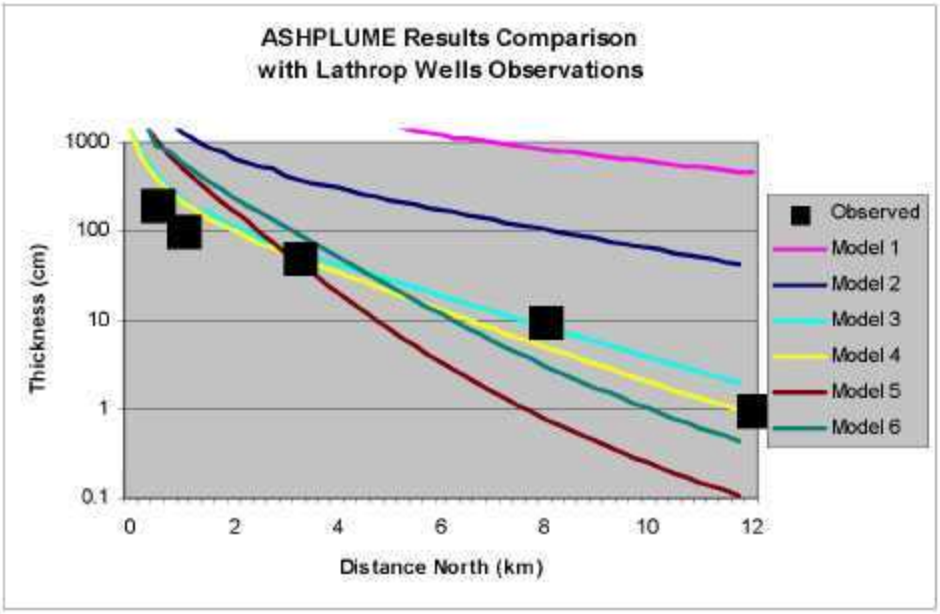


Source: Keating 2005 [DIRS 173850].

NOTE: Observed data are from an isopach map in Krier and Harrington (2003 [DIRS 164023], p. 153), measured north from the vent (tabulated in Krier 2004 [DIRS 173810], p. 11). The 300-cm thickness observed value is not shown for clarity (falls close to 200-cm point). Models are realizations for a wind blowing to the north. Parameters held constant for these comparisons are $\beta = 0.3$, $d = 0.0572$ cm, $\sigma_d = 0.2518$, $\rho_c = 0.3$, and $U = 0$. The following list shows the varied parameters in each model with V calculated from P and $T_d$ by Equations 6-7a through 6-7c for a conduit diameter of 10 m (Models 1 and 2) and 4.5 m (Models 3 to 6).

Model 1: $P = 5.0 \times 10^{12}$ W, $V = 0.08$ km$^3$, $Td = 0.2$ d, $W_0 = 24.5$ m/s, $u = 1{,}000$ cm/s
Model 2: $P = 5.0 \times 10^{11}$ W, $V = 0.04$ km$^3$, $Td = 1.0$ d, $W_0 = 12.1$ m/s, $u = 1{,}000$ cm/s
Model 3: $P = 5.0 \times 10^{10}$ W, $V = 0.004$ km$^3$, $Td = 1.0$ d, $W_0 = 1.2$ m/s, $u = 1{,}000$ cm/s
Model 4: $P = 5.0 \times 10^{10}$ W, $V = 0.004$ km$^3$, $Td = 1.0$ d, $W_0 = 1.2$ m/s, $u = 800$ cm/s
Model 5: $P = 6.2 \times 10^{8}$ W, $V = 0.004$ km$^3$, $Td = 75.0$ d, $W_0 = 0.01$ m/s, $u = 1{,}000$ cm/s
Model 6: $P = 6.2 \times 10^{8}$ W, $V = 0.004$ km$^3$, $Td = 75.0$ d, $W_0 = 0.01$ m/s, $u = 1{,}400$ cm/s.

Figure 7-2. Comparison of Ashplume Results to Lathrop Wells Ash-Thickness Observations

For the purposes of model validation, tephra thicknesses computed by the ASHPLUME model were compared to distances from vent to isopachs along the centerline of the plume developed from field measurements, reported by Krier and Harrington (2003 [DIRS 164023], p. 153) (Figure 7-3). Model fits to the medial and distal data are generally good (within a factor of 4

to 5 proximally and within 10 percent medially and distally. The overall pattern of the centerline profile of the deposit was reproduced by the better model fits (Figure 7-2). The correlation figure (Figure 7-3) illustrates this good fit for small tephra thicknesses and larger overpredictions for higher thicknesses (proximal deposits). Models 3 and 4 provide the best fits overall.

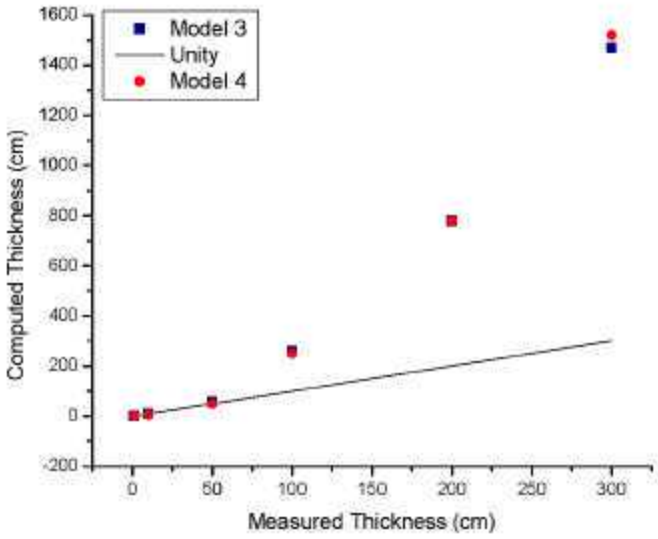


Source: Developed DTN: LA0508GK831811.002.

NOTE: Measured data are from an isopach map in Krier and Harrington (2003 [DIRS 164023], p. 153). Black line represents perfect correlation. The best model runs (3 and 4) matched the distal deposits well but overestimate proximal deposits (computed thicknesses above 300 cm).

Figure 7-3. Results of Lathrop Wells Validation Runs, Plotted as Measured vs. Computed Tephra Thickness

The statistics of the correlations provide a means to assess the adequacy of the validation exercise. Linear regressions were performed on the data in Figure 7-3 using built-in functions of OriginPro V7.5. Linear regressions that include model values for all six points (Table 7-2) show the effects of the overpredictions for larger ash thicknesses (proximal areas). Models 3 and 4 produce linear regression slopes of about 5. These regression slopes approach unity (1.2 and 1.03) when only the medial and distal data (3 km to 12 km) are considered, indicating that the model did a good job of matching the observed deposits in distal areas. These statistics compare well to the acceptance criteria developed from published tephra modeling studies, including model predictions within a factor of 2 of observed values and regression slopes within 30 percent of unity. Computed proximal deposits ($\leq$1 km) fit less well to the measured values, but the ASHPLUME model does not calculate the dispersal of tephra associated with the construction of the cinder cone, which is generally emplaced by ballistic trajectories. Because of this aspect of the model, model fits of medial and distal deposit thicknesses are deemed to be more important in the validation exercise.

Table 7-2. Lathrop Wells Model Validation Statistics: Correlation of Modeled vs. Observed Tephra Thickness

| ASHPLUME Run Number | Linear Regression Slope (all data) | Correlation Coefficient, R (all data) | Linear Regression Slope (3-12 km) | Correlation Coefficient, R (3-12 km) |
|---|---|---|---|---|
| 3 | 4 9 | 0 98 | 1 2 | 0 999 |
| 4 | 5 0 | 0 98 | 1 03 | 0 997 |

Source Developed DTN LA0508GK831811 002

Based on the model validation acceptance criteria described in Section 7.3.1, the goodness-of-fit of computed vs. measured tephra thickness demonstrated by this validation exercise indicate that the model is sufficiently accurate and adequate for its intended use.

### 7.3.1.3 Cinder Cone

Basaltic ash thickness data from Cinder Cone, a 277-m-high Holocene cone in Lassen Volcanic National Park, California, is provided in Heiken (1978 [DIRS 162817]). Cone and tephra-sheet volume (0.038 $km^3$ and 0.032 $km^3$, respectively), composition, monogenetic behavior, and eruptive sequence make Cinder Cone a good analogue for a future eruption in the Yucca Mountain region. Several ASHPLUME V.2.0 (CRWMS M&O 2001 [DIRS 152844]) simulations were carried out to compare ASHPLUME results (predictions) to observed ash-thickness data. For the Cinder Cone simulation (Figure 7-4), all parameters were set to base-case values (Table 8-2); those parameters with distributed ranges in Table 8-2 were set to midrange values, except for mean ash particle size and ash particle size standard deviation (see Note to Figure 7-4). These parameters were set to match specific ash particle size data at Cinder Cone (Heiken 1978 [DIRS 162817]). Several calculations were performed using wind speeds sampled from the full range used for the TSPA-LA and results were compared to the Cinder Cone data. Figure 7-4 shows the results of the simulation in terms of profiles along the centerline of the tephra deposit. The 2,000-cm/s (Model 2) wind speed provides a good fit to the proximal and distal data. The simulations show that observed Cinder Cone data fall well within the range of results produced by Ashplume using values from the TSPA-LA range of wind speeds.

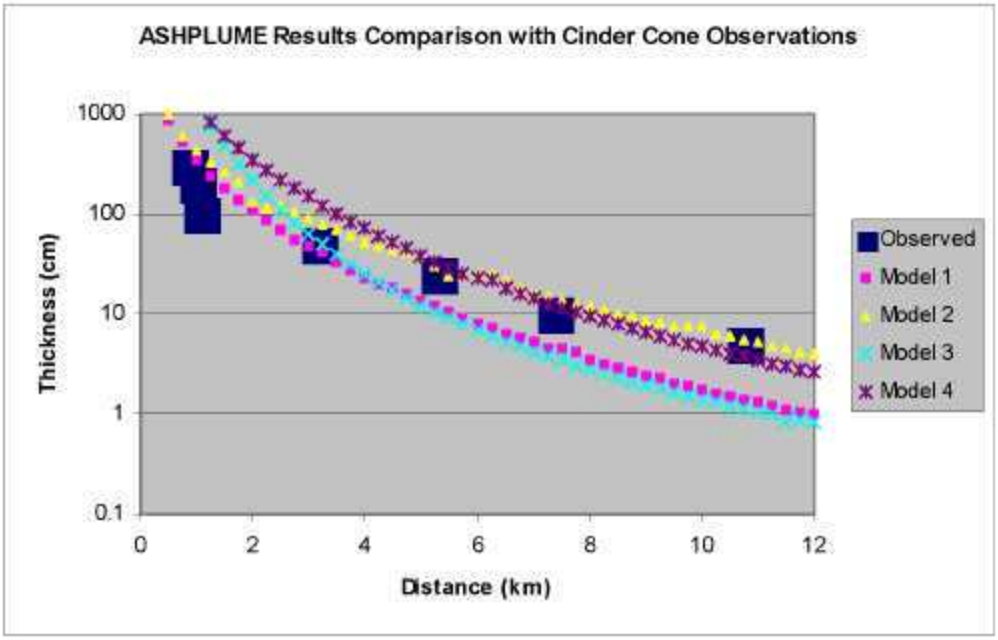


Source: Keating (2005 [DIRS 173850]).

NOTE: Observed data are from Heiken (1978 [DIRS 162817], Figure 3). Models are realizations for a wind blowing to the east. Parameters held constant for these comparisons are $\beta$ = 0.3, $d$ = 0.193 cm, $\sigma_d$ = –0.78, $\rho_s$ = 0.3, and $U$ = 0. The following list shows the varied parameters in each model with $V$ calculated from $P$ and $T_d$ by Equations 6-7a – 6-7c for a conduit diameter of 5.0 m (Models 1 and 2) and 8 m (Models 3 and 4).

Model 1: P = 5.0 x $10^{10}$ W, V = 0.004 $km^3$, Td = 1.0 d, $W_0$ = 24.5 m/s, u = 1,000 cm/s
Model 2: P = 5.0 x $10^{10}$ W, V = 0.004 $km^3$, Td = 1.0 d, $W_0$ = 1.2 m/s, u = 2,000 cm/s
Model 3: P = 7.5 x $10^{10}$ W, V = 0.065 $km^3$, Td = 10.0 d, $W_0$ = 0.5 m/s, u = 200 cm/s
Model 4: P = 6.8 x $10^{10}$ W, V = 0.018 $km^3$, Td = 3.0 d, $W_0$ = 0.5 m/s, u = 800 cm/s.

Figure 7-4. Comparison of Ashplume Results to Cinder Cone Ash Thickness Observations

For the purposes of model validation, tephra thickness predictions from the ASHPLUME model were compared to observed data at specific points (distances from vent to isopachs along the centerline of the plume in Heiken (1978 [DIRS 162817], Figure 3) (Figure 7-5). Model fits to the medial and distal data are generally good (within a factor of 2 proximally and within 10 percent medially and distally. The overall pattern of the centerline profile of the deposit was reproduced by the better model fits (Figure 7-4). The correlation figure (Figure 7-5) illustrates this good fit for small tephra thicknesses and larger overpredictions for higher thicknesses (proximal deposits). Models 1 and 2 provide the best fits overall.

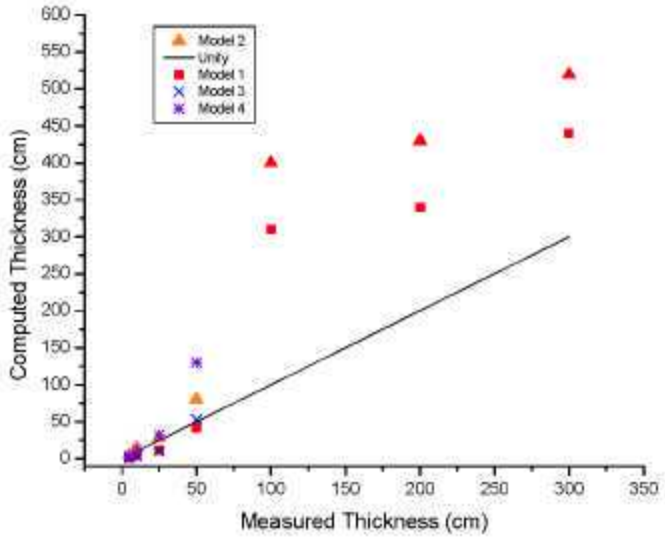


Source: Developed DTN: LA0508GK831811.002.

NOTE: Measured thickness points are taken from distances from vent to isopachs in Heiken et al. (1978 [DIRS 162817], Figure 3). Note that proximal (large computed thickness) points for Models 3 and 4 are not shown, as the computed thicknesses were above 1,000 cm. Black line represents perfect correlation. The best model runs (1 and 2) matched the distal deposits well but overestimate proximal deposits (computed thicknesses above 300 cm).

Figure 7-5. Results of Cinder Cone Validation Runs, Plotted as Measured versus Computed Tephra Thickness

The statistics of the correlations provide a means to assess the adequacy of the validation exercise. Linear regressions were performed on the data in Figure 7-5 using built-in functions of OriginPro V7.5. Linear regressions including model values for all seven points (Table 7-3) show the effects of the overpredictions for larger ash thicknesses (proximal areas). Models 1 and 2 produce linear regression slopes of 1.6 to 1.9. These regression slopes approach unity (0.9, Model 1) when only the medial and distal data (3-10 km) are considered, indicating that the model did a good job of matching the observed deposits in distal areas. These statistics compare well to the acceptance criteria developed from published tephra modeling studies, including model predictions within a factor of 2 of observed values and regression slopes within 30 percent of unity. Computed proximal deposits ($\leq$1 km) fit less well to the measured values, but the ASHPLUME model does not calculate the dispersal of tephra associated with the construction of the cinder cone, which is generally emplaced by ballistic trajectories. Because of this aspect of the model, model fits of medial and distal deposit thicknesses are deemed to be more important in the validation exercise.

Table 7-3. Cinder Cone Model Validation Statistics: Correlation of Modeled versus Observed Tephra Thickness

| ASHPLUME Run Number | Linear Regression Slope (all data) | Correlation Coefficient, R (all data) | Linear Regression Slope (3-10 km) | Correlation Coefficient, R (3-10 km) |
|---|---|---|---|---|
| 1 | 1 6 | 0 94 | 0 91 | 0 98 |
| 2 | 1 9 | 0 92 | 1 6 | 0 99 |
| 3 | 6 9 | 0 95 | 1 2 | 0 96 |
| 4 | 5 4 | 0 94 | 2 8 | 0 97 |

Source Developed DTN LA0508GK831811 002

Based on the model validation acceptance criteria described in Section 7.3.1, the goodness-of-fit of computed versus measured tephra thickness demonstrated by this validation exercise indicate that the model is sufficiently accurate and adequate for its intended use.

The Lathrop Wells and Cinder Cone simulations of tephra thicknesses provide additional confidence that the Ashplume model and model parameters selected for use in the TSPA-LA can produce ash thickness results that cover the range of values expected for volcanoes in the Yucca Mountain region.

#### 7.3.1.4 Uncertainty

The Ashplume model has been validated by comparisons to tephra deposits at three analogue volcanoes and by extensive sensitivity analyses on individual parameters (Sections 7.2, 7.3.1 and Appendix C). The results of the validation studies indicate that the model can successfully reproduce the pattern and thickness of tephra deposits when the model input parameters are derived from available site-specific eruption information supplemented by generalized "base-case" parameter values (Table 8-2) derived from the volcanological literature and field studies. Sensitivity studies indicate that the model results are relatively insensitive to variation in most parameters, the exceptions being wind speed and direction, eruption power, and eruption duration. These four parameters were reasonably well constrained for each of the analogue studies: in the case of Cerro Negro, field observations constrained all four; in the case of Cinder Cone and Lathrop Wells, the tephra deposits were reproduced within the accuracy criteria by specifying reasonable "base-case" parameter values for these four parameters.

### 7.3.2 Ash Redistribution

#### 7.3.2.1 Dilution

The sedimentary processes affecting the tephra sheet at the Lathrop Wells volcanic cone were studied (Harrington 2003 [DIRS 164775], pp. 14 to 16) to determine the extent of tephra dilution and to validate the significance of the process. The observations demonstrate that dilution is an important feature of the ash redistribution conceptual model. The significance of the dilution is demonstrated by the estimate of ash dilution rates. This estimate of dilution rates is used in support of the conceptual model of ash redistribution presented in Section 6.7.2 and to provide confidence in the alternative mathematical model (under development) for ash redistribution presented in Appendix I.

Redistribution of volcanic ash initiates in small channels developed on tephra sheets northwest of the Lathrop Wells cone. The tephra moves downslope as small debris flows with dimensions typically tens of centimeters wide and tens of meters long. Tephra moves through progressive generations of these small debris flows until it reaches a channel at the base of the slope. The channel may then merge with larger channels. Depending upon initial tephra thickness, each step in the process results in some dilution of the tephra with other material (Harrington 2003 [DIRS 164775], pp. 14 to 16).

There are two principal drainage systems that transport ash from the Lathrop Wells cone (Figure 7-6):

- The western drainage system transports material from the exposed tephra sheet on the northwest side of Lathrop Wells cone to the west and south into the Amargosa Valley.
- The eastern drainage system heads near the northern limit of the exposed tephra sheet and transports material around the eastern side of the Lathrop Wells cone.

The two drainage systems on the Lathrop Wells tephra sheet were sampled at depths of approximately 0.5 m to evaluate dilution rates by determining the ratio of tephra to non-tephra components. The stream sediment samples were split in the laboratory, analyzed by microscope, and separated by a magnet to obtain the percentages of basaltic ash components relative to their transport distance from the tephra sheet (Table 7-4).

Mixing occurs along the eastward drainage around the Lathrop Wells volcanic cone according to the trend evident in the table of basaltic ash content in the total sediment (Table 7-4). The data in Table 7-4 indicate that the concentration of basaltic ash is reduced by more than 50 percent within 1-km distance from the head of the tephra-sheet drainage and shows substantial dilution in the first 1,400 m. The channel on the west side has less than 40 percent basaltic ash after 1.9 km of transport. These data are illustrative of the effects of dilution during tephra redistribution in channels but also have uncertainties due to (1) the small number of samples, and (2) the fact that tephra redistribution processes around the Lathrop Wells cone have matured since the eruption approximately 77,000 years ago (Heizler et al. 1999 [DIRS 107255], p. 803). Dilution rates may have been substantially different shortly after the eruption. Also, differences in catchment area, bedrock types, vegetation, elevation, and precipitation may limit the direct analogy with a potential redistribution processes following an eruption at Yucca Mountain.

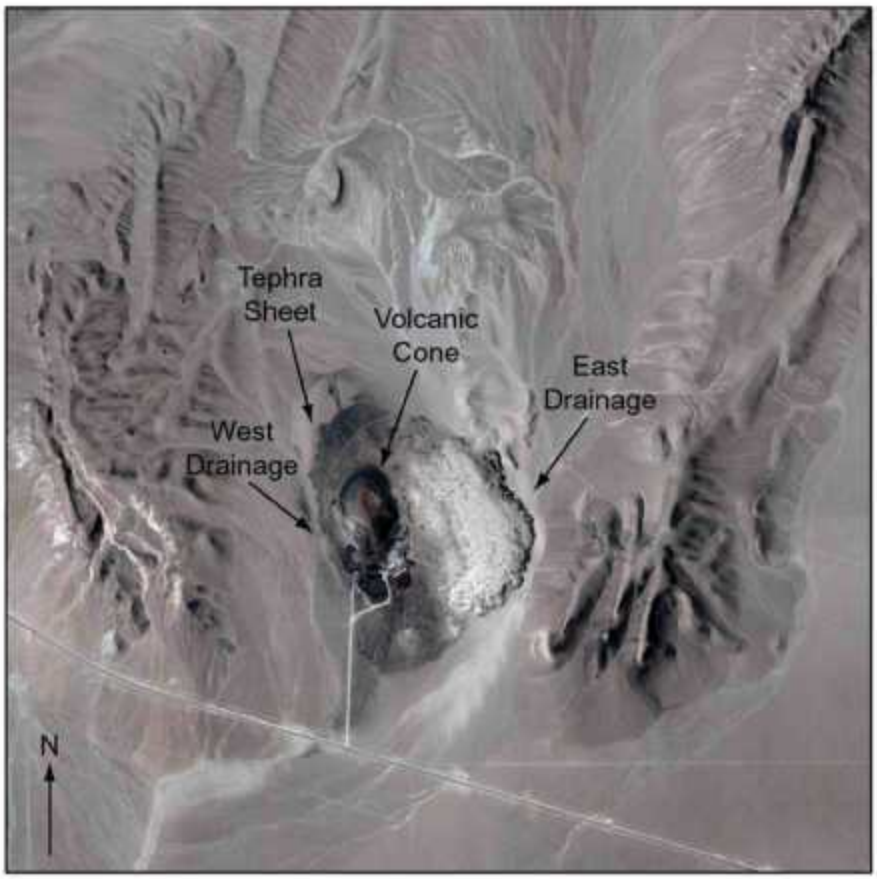


For illustration purposes only.

Photo source: EG&G Mission, August 28, 1994, Photo frame 140, Elevation 32,000 ft.

NOTE: The Lathrop Wells basaltic cone is shown in the center of the photo with a tephra sheet draping the hill to the north. Two sets of samples were collected: one beyond the tephra sheet and in the east drainage system around the cone; the second set follows the drainage channel that lies west of the cone. The Amargosa Valley is south of the photo.

Figure 7-6. Aerial Photograph Showing Lathrop Wells Drainage System

Table 7-4. Ash Weight Percentages in Samples of Drainage Channels Near Lathrop Wells Cone

| Sample Number | Basaltic Ash (wt. %) | Distance from Head of Channel (m) |
|---|---|---|
| **Lathrop Wells Cone, West Side** | | |
| LWASH1-07/11/02-1 | 98.7 | 0 |
| LWASH1-07/11/02-3 | 92.3 | ~100 |
| LWASH1-07/11/02-5 | 35.0 | ~200 |
| LWASH1-07/12/02-3 | 50.8 | ~900 |
| LWASH1-07/12/02-5 | 39.6 | ~1,900 |

Table 7-4. Ash Weight Percentages in Samples of Drainage Channels Near Lathrop Wells Cone (Continued)

| Sample Number | Basaltic Ash (wt. %) | Distance from Head of Channel (m) |
|---|---|---|
| **Lathrop Wells Cone, East Side** | | |
| LWASH2-08/1/02-1 | 54 9 | 0 |
| LWASH2-08/1/02-3 | 59 4 | ~300 |
| LWASH2-08/1/02-6 | 10 1 | ~1,400 |
| LWASH2-08/1/02-8 | 0 8 | ~2,200 |

DTN LA0405CH831811 001 [DIRS 169998]

NOTE Sample locations are shown in BSC 2004 [DIRS 169980], Figure 6-10

### 7.3.2.2 Uncertainty

Uncertainties in the ash redistribution conceptual model include the effects of future climate change on erosion rates, depth of migration of radionuclides within the soil profile, and dilution processes during fluvial redistribution. These uncertainties have been discussed in Sections 5 and 6.7.2, and model limitations related to these uncertainties have been discussed in Section 1.3. The parametric uncertainties have been propagated by the use of parameter value distributions for use in Monte Carlo sampling in TSPA-LA. The validation of the model by independent technical reviews considered these uncertainties, and the evaluations of the reviewers supported the use of parameter distributions and conservative values for uncertain parameters (e.g., the persistent presence in the soil of 1 percent of the initial waste concentration).

## 7.4 INDEPENDENT TECHNICAL REVIEW

Independent technical reviews were conducted for both the Ashplume model and the ash redistribution conceptual model as part of the validation activities. Summaries of these reviews are presented in Sections 7.4.1 and 7.4.2, respectively.

**Acceptance Criteria**

The following criteria were evaluated by the independent technical reviewers during their evaluation of the ash redistribution model (BSC 2003 [DIRS 166289], Appendix C).

1. Is the conceptual model reasonable and appropriate for its intended use?
2. For given inputs, are the outputs of the model reasonable?
3. Are limitations of field and analytical data addressed with respect to the conceptual model described?
4. Are there other approaches that may enhance the confidence in use of this model?
5. Are there other alternative models that should be considered?

### 7.4.1 Ashplume Mathematical Model

Consistent with the guidance in AP-SIII.10Q, *Models*, for validation of mathematical models, an independent technical review was conducted to assess the application of Ashplume for representing potential future volcanic events at Yucca Mountain. The review was conducted by Dr. Frank Spera, Professor of Geology at the University of California, Santa Barbara, from March 24, 2003, to April 10, 2003. Revision 00, Draft B of this model report was made available to Dr. Spera for his review (see Appendix F) along with other requested material. Dr. Spera was also a member of the Peer Review Panel that addressed the approach used by the Yucca Mountain Project to evaluate igneous consequences from a potential igneous event intersecting a repository at Yucca Mountain, Nevada (Detournay et al. 2003 [DIRS 169660]). Dr. Spera was requested to consider whether the mathematical model is appropriate for representing the conceptual model (i.e., is Ashplume appropriate for its intended use), which is to represent the atmospheric dispersal of waste-contaminated tephra from a potential volcanic eruption at Yucca Mountain.

Dr. Spera observed that the fundamental factors governing the fallout distribution of volcanic tephra include the height of the steady-state volcanic column, a function of eruptive mass flow rate, total eruptive volume, and the wind speeds and direction affecting the tephra being ejected into the atmosphere at different levels above the volcanic vent. He concluded that, if available, additional analogues should be considered. Since his review, work to characterize the Lathrop Wells tephra sheets has been completed and documented in the revision to the scientific analysis report, *Characterize Eruptive Processes at Yucca Mountain, Nevada* (BSC 2004 [DIRS 169980]). In addition, analogue studies of physical volcanology have been completed and documented in *Characterize Eruptive Processes at Yucca Mountain, Nevada* (BSC 2004 [DIRS 169980]) for Cinder Cone. These studies provide additional bases for validation of Ashplume in this model report.

Dr. Spera also recommended that the Ashplume model be compared to other similar mathematical models. He specifically recommended ASHFALL for this purpose. This comparison has not been performed because the ASHFALL code has not been made available by the developer.

Finally, Dr. Spera recommended that greater mass discharge rates and corresponding higher plume heights be considered when Ashplume is implemented. In response to this recommendation, new wind information (NOAA 2004 [DIRS 171035]) has been implemented in this model report to better represent eruption mechanics, including consideration of greater eruptive power and mass discharge rate, and consideration of the behavior of an ash plume at greater altitudes (up to 13 km).

Based on information available and a full understanding of its limitations, Dr. Spera concluded that the outputs of Ashplume provide reasonable representations of products that could result from a volcanic eruption at Yucca Mountain. In response to Dr. Spera's discussion of strengths and weaknesses of the Ashplume model, additional validation studies have been performed and parametric uncertainties have been characterized and propagated to the TSPA-LA.

### 7.4.2 Ash Redistribution Conceptual Model

At the time of the model development, REV 04 of the TWP (BSC 2003 [DIRS 166289]) identified an independent technical review of the ash redistribution model to be completed as a post-development validation activity to build confidence in the model. The ash redistribution model is presently a conceptual model, and only simple mathematical abstractions were completed (see Table 6-5) for input to the TSPA model; nevertheless, this model has been assigned a "moderate" (Level II) level of importance based on guidance in LP2.29Q-BSC (Table 1) and the rationale described in the TWP (BSC 2003 [DIRS 166289], Appendix C). The independent technical review was conducted to assess the ash redistribution conceptual model and its abstraction for representing the deposition of tephra in the vicinity of the RMEI following a potential future volcanic event at Yucca Mountain. Two technical reviewers with expertise in sedimentary processes and Quaternary geology, Dr. David Buesch and Dr. Dennis O'Leary of the U.S. Geological Survey, reviewed the ash redistribution conceptual model between October 31, 2003 and November 19, 2003. Drs. Buesch and O'Leary, both familiar with the Yucca Mountain Project, were requested to evaluate whether the conceptual model and its abstraction are appropriate for their intended use in the TSPA. In other words, do the model and its abstraction represent the sedimentary processes that would affect contaminated ash deposited in Fortymile Wash (the two model outcomes for the deposition of volcanic ash resulting in maximum potential exposure to the RMEI being upstream or at the location of the RMEI) from a hypothetical volcanic eruption at Yucca Mountain? Revision 00, Draft H, of this model report was made available to Drs. Buesch and O'Leary for their review (see Appendix G). While the whole document was made available, the two reviewers were requested to concentrate on Sections 1.0, 4.0, 5.0, 6.6, 6.7, 7.0, and 8.0 of the draft report.

The reviewers concluded that the conceptual model is reasonably representative of the past sedimentary processes in the Fortymile Wash drainage basin and that the model also represents expected future sedimentary processes. They further conclude that the model abstractions (outputs) were logical and representative of the conceptual model. Both reviewers stated that the database is limited and the conceptual model is preliminary in its development. It can be inferred from the reviews that the conceptual model, as described, and its abstraction are sufficient to bound the range of uncertainty in the deposition of the tephra sheet and the post-ash-deposition sedimentary processes. Additional confirmatory studies are recommended that will provide additional confidence in the sedimentary processes that are occurring in the Fortymile Wash drainage basin and the application of localized processes to the larger scale of Fortymile Wash.

The reviewers also concluded that the limitations of the model were addressed in the model discussions; however, the reviewers differed on the level at which they were addressed. Dr. Buesch believed that the discussions of data and model limitations should be strengthened, while Dr. O'Leary believed that the data and model limitations were adequately addressed. The authors of the text clearly recognize the limitations of both the data and model and have addressed these in the text, where appropriate.

Both reviewers recommended that the description of the conceptual model be improved to better describe the model. The authors have edited the text to better present the conceptual model. The reviewers recommended further development of the conceptual model and the consideration of

other conceptual models. It is the belief of Dr. Buesch that a new conceptual model may ultimately emerge from consideration of alternative models and further analyses of the Fortymile Wash drainage basin and analogue dilution studies of recent ash deposits. The authors agree that, at a minimum, a more sophisticated model is a likely outcome of additional confirmatory activities because additional parameters will most likely be integrated into the model, but the authors contend that the basic conceptual model will remain the same.

The independent technical reviewers identified a number of issues (italics) that are addressed in the following paragraphs.

*Is it appropriate to extrapolate the local-scale studies of surface erosion (based on cesium-137 profiles) and ash dilution (based on drainages immediately adjacent to the Lathrop Wells volcano) to the larger scale processes that would accompany redistribution of tephra in the Fortymile Wash drainage?*

Surface erosion rates for interchannel divides are based on data obtained directly in the area of the RMEI and, therefore, should directly apply given current climate and tectonic conditions. A technical basis for how these erosion rates might differ after changes occur in climate and tectonic processes (e.g., subsidence of Amargosa Valley) is lacking. Ash dilution studies around the Lathrop Wells cone are an indicator of ash dilution but are limited in their application due to the size of the Lathrop Wells drainage compared to the Fortymile Wash drainage (scaling) and the age of the tephra sheet (approximately 77,000 years). The dilution factors measured there today might not accurately reflect those in the decades immediately following an eruption, which is key to the TSPA. Therefore, the model that is used for redistribution of tephra down the Fortymile Wash system by the TSPA assumes that the tephra is not diluted by other sedimentary material–rather, it is emplaced as a 1- to 15-cm package of pure tephra (contaminated by radioactive waste) at the RMEI location.

*The model for infiltration of radioactive contamination into soils beneath a primary tephra deposit is based (both in absolute value and in its trend with depth) on measured concentrations of cesium-137. Is cesium-137 an appropriate analog for all significant radionuclides that might be present in tephra erupted through the repository?*

This question relates both to the short half-life of $^{137}Cs$, compared to spent nuclear fuel radionuclides, as well as its mobility in the subsurface. Several published reports corroborate the $^{137}Cs$ data as representative of the infiltration of radionuclides into surficial soils (see Appendix I, Section I9.1).

*An eruption through the Yucca Mountain repository is most likely to produce a fallout deposit that extends into Jackass Flats and possibly into the Calico Hills areas that drain into Topopah Wash (rather than Fortymile Wash). Could this be an additional source of material to the RMEI location?*

The model proposed in this report is valid regardless of the fluvial pathway of redistributed tephra to the RMEI location. The two redistribution model outcomes encompass the conditions in which the maximum concentration of waste would be delivered to the RMEI location; all other conditions and pathways would deliver lower concentrations.

*Data on surface wind speeds, which are available in other Project reports, might be useful in discussing eolian processes, as would more detailed information on the mobilization of tephra off slopes of different steepness and bedrock types.*

It is agreed that such studies would be an approach to test the model parameters described in this report.

*For Ashplume calculations, assumptions are made about the nature of incorporation of SNF into ash-tephra particles. Are these same assumptions made in the development of the ash redistribution model?*

Yes, these same assumptions are made in the development of the ash redistribution conceptual model.

*More information on how ash dilution data from the Lathrop Wells volcano can be extended into the Fortymile Wash transport system, based on data from analog sites such as Sunset Crater, need to be provided.*

It is agreed that data from such analogue sites would enhance confidence in the technical basis but are not planned for the conceptual ash redistribution model, but that the validation discussion provided in the preceding sections support the adequacy and defensibility of the model in the absence of such additional information.

Many of the questions summarized above resulting from the independent technical reviews of the ash redistribution conceptual model have been addressed in the development of the alternative ash redistribution model described in Appendix I. The alternative conceptual model incorporates quantitative representations of the processes involved in tephra redistribution in the Fortymile Wash watershed and in the soils at the RMEI location. Parametric uncertainties will be characterized in detail and propagated to the TSPA.

INTENTIONALLY LEFT BLANK

# 8. CONCLUSIONS

The objectives of this model report are the following:

- Update documentation of the Ashplume conceptual and mathematical models, including parameterization and validation for the ASHPLUME V.2.0 code (CRWMS M&O 2001 [DIRS 152844]) and the ASHPLUME_DLL_LA V.2.0 code (BSC 2003 [DIRS 166571]) as implemented in the TSPA-LA.
- Document a conceptual model for tephra redistribution after a hypothetical volcanic eruption through a repository at Yucca Mountain.
- Present results of a model of ash and waste form concentrations at a point 18 km downwind of a hypothetical volcanic vent, used to develop a Mean Primary Waste Concentration value for use in the tephra redistribution model.
- Provide representative wind speed and direction data for the Yucca Mountain region at altitudes up to 13 km.
- Address the criteria of Section 4.2 as shown in Appendix B.

## 8.1 SUMMARY OF MODELING ACTIVITY

The Ashplume conceptual model accounts for incorporation and entrainment of waste particles in an eruption plume and atmospheric transport of the contaminated tephra. The Ashplume mathematical model describes the conceptual model in mathematical terms to allow for prediction of radioactive waste-ash deposition on the ground surface in case the hypothetical eruptive event occurs. A key activity in the development of these models is the identification of realistic and representative values for the input parameters. The Ashplume mathematical model is implemented by the ASHPLUME_DLL_LA V.2.0 (BSC 2003 [DIRS 166571]) computer code, which is a required component of the TSPA-LA model of the nuclear waste repository at Yucca Mountain. Within the TSPA, the model for atmospheric dispersal and deposition of tephra, implemented in the ASHPLUME code, is used to predict the ground-level concentration (areal density) of ash and waste after a violent Strombolian eruption that intersects the repository. The waste concentration is modified by processes in the ash redistribution model and then combined with BDCFs in the TSPA-LA model to calculate an annual dose to the RMEI. Other uses of Ashplume have not been evaluated in this report.

The conceptual model for tephra redistribution from a basaltic cone addresses the sedimentary processes that occur after eruption and deposition of the tephra sheet. In this case, the volcanic eruption occurs through a repository at Yucca Mountain. The erosional processes that occur within Fortymile Wash are representative processes that could redistribute material from a tephra sheet upgradient from the RMEI location. The conceptual model describes the erosional and depositional processes that are expected to occur on two landforms (interchannel divides and distributary channels) that may be locally covered by the tephra sheet. Supported by the results of site-specific and natural-analogue ash dilution and $^{137}Cs$ studies, the ash redistribution model develops parameters that will be implemented in the TSPA-LA. The TSPA redistribution model

considers tephra thicknesses, tephra-soil removal rates, and long-term residual contamination after erosion of the tephra sheet within the context of these two geomorphic landforms (Section 6.7.2).

## 8.2 MODEL REPORT OUTPUTS

The output from this model report consists of four components, which are summarized in Table 8-1. First, a set of input parameter values (points and ranges of values) for ASHPLUME_DLL_LA V.2.0 (BSC 2003 [DIRS 166571]) are summarized in Table 8-2 for use in the TSPA modeling. Second, a set of summary data characterizing wind speed and direction in the Yucca Mountain region for heights above the surface of Yucca Mountain up to 13 km are presented in Tables 8-3 and 8-4, respectively. (The full set of wind speed and wind direction data are given in Appendix D.) Third, output from the Ashplume model providing the Mean Primary Waste Concentration, a mean concentration of waste 18 km downwind of a hypothetical eruption through the repository, is presented in Table 6-4. Fourth, the ash redistribution model abstraction is presented in Table 6-5. These outputs are described in detail in the following paragraphs.

Table 8-1. Output Data

| Data Description | Data Tracking Number | Location of Output DTNs in this Report |
|---|---|---|
| Parameter values to be used as input for the ASHPLUME_DLL_LA V 2 0 model for TSPA | LA0408GK831811 002 | Table 8-2 |
| Desert Rock wind speed and wind direction data analyses for years 1978 – 1995 | MO0408SPADRWSD 002 | Section 6 7 1, Tables 8-3 and 8-4, Figure 8-1, Table D-1, Tables D-10 through D-45, Figures D-3 through D-15 |
| Mean Primary Waste Concentration (calculation of waste-form concentrations in ash from an ash plume at 18 km from a vent) | LA0408GK831811 001 | Table 6-4 |
| Ash redistribution model abstraction for the TSPA-LA model | LA0408CH831811 001 | Table 6-5 |

Two additional DTNs (MO0505WPSD1STR.001 and MO0506SPACHERN.000) were developed in the alternative waste particle size analysis described in Appendix J, Table J-7 and Section J2.3. The DTN: MO0506SPACHERN.000 presents the results of the evaluations of Chernobyl data. The information compiled in DTN: MO0506WPSDISTR.001 contributes to the assessment of the uncertainty of the outputs presented above. An additional developed DTN (LA0508GK831811.002) documents the Ashplume model validation statistics for the Cinder Cone and Lathrop Wells Volcano case studies (Section 7.3.1).

Table 8-2 lists the parameterization and other code inputs required to run the ASHPLUME_DLL_LA V.2.0 code (BSC 2003 [DIRS 166571]) within the TSPA-LA model, which is implemented within the GoldSim modeling system. GoldSim requires a vector of Ashplume inputs for each realization of the model. Some of the Ashplume parameters required in GoldSim are represented as point values and do not change from one realization to the next. Some input parameters are represented by distributions that are sampled by GoldSim. The

sampled values are then passed to Ashplume for each realization. Following are instructions for sampling the distributed parameter values and building an input file for each realization:

1. Sample distributions for the parameters $\beta$, $d$, $\sigma_d$, $W_0$, and $P$.

2. Calculate limits for the total eruption duration ($T_{d\_min}$, $T_{d\_max}$, in seconds) using Equations 6-7b and 6-7c such that the range of allowable total eruption volume (0.004 -0.08 km$^3$) is respected (using $P$ in watts):

$$T_{d\_min} = \frac{V_{min\ \ s}}{\dot{Q}} = \frac{V_{min\ \ s}}{P/(C_p \Delta T)} = \frac{(0.004\ \text{km}^3)\left(10^{18}\ \frac{\text{W}\cdot\text{s}}{\text{km}^3}\right)}{P\ (\text{W})} \qquad \text{(Eq. 8-1a)}$$

$$T_{d\_max} = \frac{V_{max\ \ s}}{\dot{Q}} = \frac{V_{max\ \ s}}{P/(C_p \Delta T)} = \frac{(0.08\ \text{km}^3)\left(10^{18}\ \frac{\text{W}\cdot\text{s}}{\text{km}^3}\right)}{P\ (\text{W})} \qquad \text{(Eq. 8-1b)}$$

3. Sample $T_d$ from the range (log-uniform) bounded by $T_{d\_min}$, $T_{d\_max}$.

4. Calculate eruption column height by Equation 6-7a: $H = 0.0082(P^{0.25})$, with $H$ in km and $P$ in watts.

5. Use eruption column height to sample the appropriate altitude bin in the cumulative distribution functions for wind direction (*udir*) and wind speed ($u$); if the column height is exactly equal to an altitude bin boundary (e.g., 8.00 km), sample the next higher bin (e.g., 8 to 9 km).

Two outputs are contained in the output vector from Ashplume after a single realization within the GoldSim model: (1) $x_{ash}$, the ash deposition in g/cm$^2$, and (2) $x_{fuel}$, the fuel deposition in g/cm$^2$.

All output feeds from this model report to the TSPA-LA model are identified in Tables 6-2 and 8-2 and in Appendix D, Tables D-10 through D-35. Table 8-2 indicates the relative position within the input vector required by Ashplume (i.e., the sequence number), the variable name used within GoldSim, a brief description of the parameter, the units of the parameter, the value(s) for the parameter, and the distribution type. Two parameters–wind speed and wind direction–are identified in Table 8-2 as having distribution type "empirical." For the empirical-distribution type, the TSPA-LA model requires a tabular listing of the CDF or PDF of the parameter.

In this report, wind speed and wind direction data tables were formulated (Output DTN: MO0408SPADRWSD.002) to be used as input to the TSPA-LA model. These data have also been modified further to fit the specific form and function of the model. The tabular listings for the wind speed CDFs at incremental distances above Yucca Mountain are given in Tables D-10 through D-22. Table 8-3 (also included as Table D-9) gives a summary of wind speed in relation to height above Yucca Mountain. The tabular listings for wind direction PDF for incremental distances above Yucca Mountain are given in Tables D-23 through D-35, and corresponding wind rose diagrams are given in Figures D-3 through D-15. Tables 8-3 and

8-4 and Figure 8-1 below are representative samples of the more complete listings found in Appendix D.

Section 6.7.2 (Table 6-5) summarizes the ash redistribution conceptual model to be implemented in the TSPA-LA. The general results of an ash dilution study are assessed in conjunction with results of a $^{137}Cs$ study to aid in establishing a technical basis for erosion rates. The $^{137}Cs$ studies are also directly used in the redistribution model to help define parameters related to erosion and removal rates of the tephra sheet and to abstract predicted concentrations of diluted, redeposited sediments. A separate set of ASHPLUME_DLL_LA V.2.0 (BSC 2003 [DIRS 166571]) calculations are developed to define the Mean Primary Waste Concentration (Table 6-4) for those realizations in which there is no ash fall realized at the RMEI location during a particular TSPA realization.

The Mean Primary Waste Concentration analyses were calculated using ASHPLUME_DLL_LA V.2.0 (BSC 2003 [DIRS 166571]) (Table 6-4, Appendix E). The uncertainty in parameter values was incorporated by using a Monte Carlo method involving 100 realizations of distributed input parameters (beta, particle size, standard deviation of particle size, initial eruption velocity, power, duration of eruption event, and wind speed). Individual realizations were screened for validity by following the methodology given in Steps 1 through 5, in this section, to ensure that the values of the sampled parameters were within established ranges. Based on this modeling, the mean concentration of waste form at a point 18 km directly downwind from a volcanic vent is $4.16 \times 10^{-6}$ g/cm$^2$ with a standard deviation of $7.47 \times 10^{-6}$ g/cm$^2$.

Table 8-2. Input Parameter Values for the ASHPLUME_DLL_LA V.2.0 Model for TSPA

| Seq. No.[A] | ASHPLUME Parameter | Description | Units | Value | Distribution Type |
|---|---|---|---|---|---|
| 1 | iscrn | Run type (0 = no screen output) | none | 0 | point value |
| 2 | $X_{min}$ | Minimum X grid location | km | 0 | point value |
| 3 | $X_{max}$ | Maximum X grid location | km | 0 | point value |
| 4 | $Y_{min}$ | Minimum Y grid location | km | 0 | point value |
| 5 | $Y_{max}$ | Maximum Y grid location | km | –18 | point value |
| 6 | $N_x$ | Number of X grid locations | none | 1 | point value |
| 7 | $N_y$ | Number of Y grid locations | none | 2 | point value |
| 8 | $\psi_\rho^{low}$ | Ash particle density at maximum particle size | g/cm$^3$ | 1.04 | point value |
| 9 | $\psi_\rho^{high}$ | Ash particle density at minimum particle size | g/cm$^3$ | 2.08 | point value |
| 10 | $\rho_a^{low}$ | Log ash particle size at maximum ash density | log (cm) | –3 | point value |
| 11 | $\rho_a^{high}$ | Log ash particle size at minimum ash density | log (cm) | 0 | point value |

Table 8-2. Input Parameter Values for the ASHPLUME_DLL_LA V.2.0 Model for TSPA (Continued)

| Seq. No.* | ASHPLUME Parameter | Description | Units | Value | Distribution Type |
|---|---|---|---|---|---|
| 12 | $F$ | Ash particle shape factor | none | 0.5 | point value |
| 13 | $\Psi_a$ | Air density | g/cm$^3$ | 0.001117 | point value |
| 14 | $\eta_a$ | Air viscosity | g/cm/s | 0.0001758 | point value |
| 15 | $C$ | Eddy diffusivity constant | cm$^2$/s$^{5/2}$ | 400.0 | point value |
| 16 | $d_{max}$ | Maximum particle diameter for transport | cm | 10 | point value |
| 17 | $\delta_{min}$ | Minimum waste particle size | cm | 0.0001 | point value |
| 18 | $\delta_{mode}$ | Mode waste particle size | cm | 0.0016 | point value |
| 19 | $\delta_{max}$ | Maximum waste particle size | cm | 0.05 | point value |
| 20 | $H_{min}$ | Minimum height of eruption column | km | 0.001 | point value |
| 21 | Ash Cutoff | Threshold limit on ash accumulation | g/cm$^2$ | $1 \times 10^{-10}$ | point value |
| 22 | $\beta$ | Column diffusion constant (Beta) | none | 0.01 – 0.5 | uniform |
| 23 | $d$ | Mean ash particle diameter | cm | 0.001 – 0.01 – 0.1 | log triangular |
| 24 | $\sigma_d$ | Ash particle diameter standard deviation | log (cm) | (1.3) – (1.9) | uniform |
| 25 | $\rho_c$ | Waste incorporation ratio | none | 0.3 | point value |
| 26 | $U$ | Mass of waste to incorporate | g | Calculated within the TSPA model | N/A |
| 27 | Wind Direction | Wind Direction | degrees | DTN: MO0408SPADRWSD.002 | empirical |
| 28 | U | Wind Speed | cm/s | DTN: MO0408SPADRWSD.002 | empirical |
| 29 | $W_0$ | Initial rise velocity | cm/s | $1.0 \times 10^0$ – $1.2 \times 10^4$ | log-uniform |
| 30 | $P$ | Eruptive power | W | $6.17 \times 10^8$ – $5 \times 10^{12}$ | log-uniform |
| 31 | $T_d$ | Eruption duration | s | See Equations 8-1a and 8-1b | log-uniform |

Source: Output DTN: LA0408GK831811.002

NOTE: *Seq. No. = GoldSim sequence number

Table 8-3. Wind Speed in Relation to Height Above Yucca Mountain

| Height above YM (km) | Minimum Wind Speed (cm/s) | Maximum Wind Speed (cm/s) | Average Wind Speed (cm/s) |
|---|---|---|---|
| 0 to 1 | 0 | 4,670 | 668 |
| 1 to 2 | 0 | 4,480 | 617 |
| 2 to 3 | 0 | 5,000 | 1,007 |
| 3 to 4 | 0 | 6,400 | 1,215 |
| 4 to 5 | 0 | 10,500 | 1,486 |
| 5 to 6 | 0 | 14,100 | 1,695 |
| 6 to 7 | 0 | 10,300 | 1,949 |
| 7 to 8 | 0 | 11,000 | 2,160 |

Table 8-3. Wind Speed in Relation to Height above Yucca Mountain (Continued)

| Height above YM (km) | Minimum Wind Speed (cm/s) | Maximum Wind Speed (cm/s) | Average Wind Speed (cm/s) |
|---|---|---|---|
| 8 to 9 | 0 | 8,700 | 2,294 |
| 9 to 10 | 0 | 8,640 | 2,416 |
| 10 to 11 | 0 | 8,900 | 2,437 |
| 11 to 12 | 0 | 9,900 | 2,311 |
| 12 to 13 | 0 | 7,300 | 2,064 |

Source NOAA 2004 [DIRS 171035] Output DTN MO0408SPADRWSD 002

NOTE This table is also given as Table D-9 in Appendix D of this report The data listed in this table are representative of the wind-speed data listed in the attachment

Table 8-4. Wind Direction PDF at 3 to 4 km Above Yucca Mountain

| Compass Degrees | Ashplume Degrees | Count | PDF |
|---|---|---|---|
| 165 to 195 | 90 (North) | 5788 | 0 818 |
| 195 to 225 | 60 | 9821 | 0 1388 |
| 225 to 255 | 30 | 12019 | 0 1699 |
| 255 to 285 | 0 (East) | 11030 | 0 1559 |
| 285 to 315 | –30 | 10186 | 0 1440 |
| 315 to 345 | –60 | 7486 | 0 1058 |
| 345 to 15 | –90 (South) | 4402 | 0 0622 |
| 15 to 45 | –120 | 2497 | 0 0353 |
| 45 to 75 | –150 | 1639 | 0 0232 |
| 75 to 105 | 180 (West) | 1407 | 0 0199 |
| 105 to 135 | 150 | 1743 | 0 0246 |
| 135 to 165 | 120 | 2730 | 0 0386 |
| Total | | 33,093 | 1 0000 |

Source NOAA 2004 [DIRS 171035] Output DTN MO0408SPADRWSD 002

NOTE This table is also given as Table D-26 in Appendix D The data listed in this table are representative of the wind-direction data listed in the attachment to this report

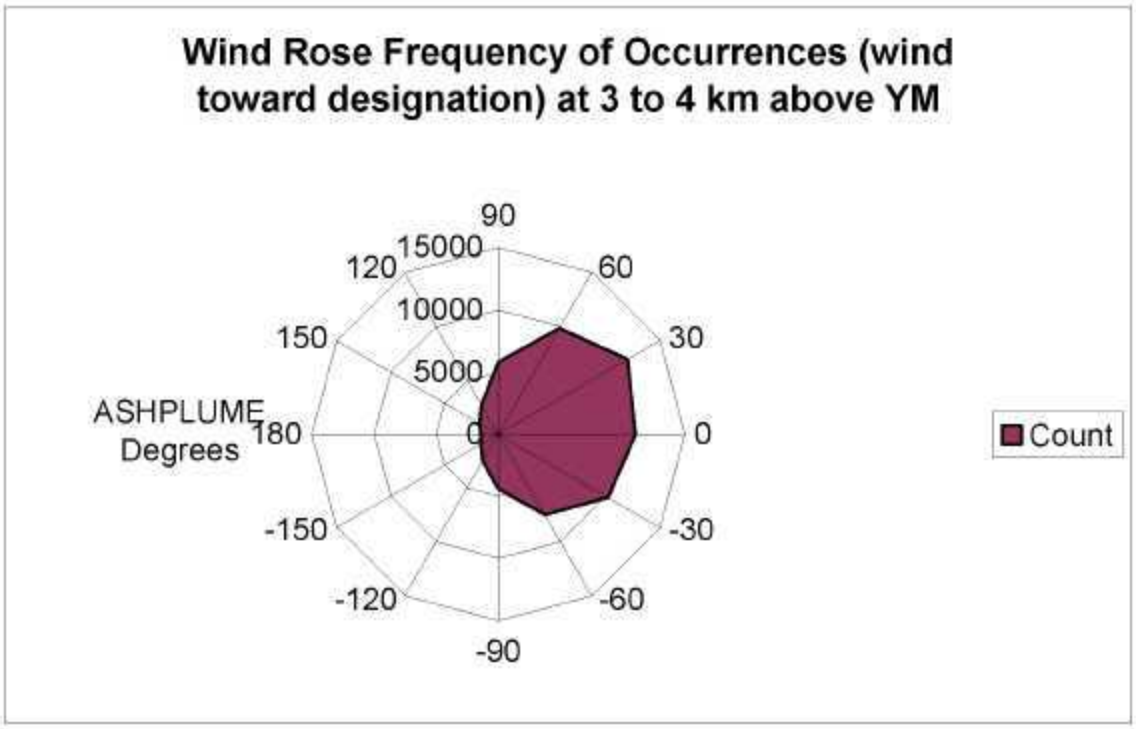


Source: NOAA 2004 [DIRS 171035]. Output DTN: MO0408SPADRWSD.002.

NOTE: This figure is also given as Figure D-6 in Appendix D. The wind rose frequency of occurrences shown in this figure is a representation of the wind-direction data listed in Table 8-4 above (see also Table D-26 in Appendix D).

Figure 8-1. Wind-Rose Frequency of Occurrences at 3 to 4 km Above Yucca Mountain

## 8.3 OUTPUT UNCERTAINTY

The TSPA-LA model uses Monte Carlo simulation as a method for mapping uncertainty in model parameters and future system states, expressed as probability distributions, into predictions of model output (BSC 2003 [DIRS 166296]). Epistemic uncertainties exist in Ashplume model input parameters due to the uncertainty in underlying data or imperfect knowledge of other required inputs (model for volcanic eruption). Sensitivity analyses (Section 7.2) illustrate the strong effect on the model results due to uncertainty in the input parameters eruptive power, eruptive duration, wind speed, and wind direction. Ashplume model parameters that contain uncertainty and that may significantly affect the outcome of TSPA-LA calculations are expressed as probability distributions to be compatible with the Monte Carlo method used in the TSPA-LA model. Table 8-2 shows all ASHPLUME input parameters and indicates those that are represented by probability distributions and those that use fixed values.

The ash redistribution conceptual model abstraction (Table 6-5) for the TSPA-LA has considerable uncertainty due to the limited database and use of $^{137}Cs$ as a proxy for representing long-lived radionuclides; however, the mathematical implementation of the conceptual model and the output parameter values are considered to be sufficiently conservative to bound any uncertainty. A key factor in the conceptual model for contaminated ash redistribution is dilution. It was observed (Section 7.3) that mixing with non-ash material is significant and that any

contaminated ash reaching the location of the RMEI will be significantly diluted by mixing with pre-existing, uncontaminated rock material. Although dilution is a significant factor, there are insufficient data available to include it in the output parameter values provided as input for the TSPA-LA.

These parameter uncertainties, represented by the parameter distributions developed and documented in this model report, are propagated throughout the TSPA-LA model and reflected in the annual dose calculated by the TSPA-LA model to the RMEI.

This revision of the report provides additional assessment of the uncertainty of outputs presented above. An alternative waste particle size distribution is presented in Appendix J, along with a alternative conceptual model for magma partitioning. These analyses are based on additional literature surveys and applying geologic realism to the portion of waste that might be entrained in the tephra sheet. The results of these analyses and the sensitivity analyses included in Appendix C suggest that the alternative waste particle size and magma partitioning conceptual model would each decrease the waste concentration calculated at the RMEI location. The alternative waste particle size distribution alone could provide a 14 percent decrease in waste concentration at the RMEI compared to the base case distribution (Table 8-2). The alternative conceptual model regarding magma partitioning concludes that only about one-third of the waste would likely be entrained in the tepha sheet, with the remaining waste being incorporated in relatively resistant geologic features (scoria cones and lava flows) that would be relatively stable on the landscape. The current TSPA-LA model assumes that all the waste is deposited in the tephra sheet. These assessments indicate that the values in Table 8-2 that are used by TSPA-LA are conservative with regard to the impacts on the dose to the RMEI during the 10,000-year postclosure period.

This revision of the report presents a description of the alternative ash redistribution model (Appendix I), a mathematical model that provides several improvements over the base-case model described in Section 6. The development of a mathematical model of radionuclide migration in soils (and the use of more realistic initial conditions) corrects the mass-balance error due to the partitioning of initial surface waste concentration over the thickness of the soil profile. In addition, the landscape model of the mixing of waste-contaminated tephra with sediment during fluvial transport provides more realistic estimates of waste concentration in channels at the RMEI location. While quantitative comparisons of the current and alternative models have not yet been completed, it is expected that the waste dilution (sediment mixing) processes incorporated into the alternative model will provide a reduction in waste concentration at the RMEI location.

# 9. INPUTS AND REFERENCES

## 9.1 DOCUMENTS CITED

The following is a list of the references cited in this document. Column 2 represents the unique six-digit numerical identifier (the Document Input Reference System [DIRS] number), which is placed in the text following the reference callout (e.g., BSC 2003 [DIRS 168796]). The purpose of these numbers is to assist the reader in locating a specific reference in the DIRS database.


Anspaugh, L.R.; Shinn, J.H.; Phelps, P.L.; and Kennedy, N.C. 1975. "Resuspension and Redistribution of Plutonium in Soils." *Health Physics, 29,* (4), 571-582. New York, New York: Pergamon Press. TIC: 248619. 151548

Anspaugh, L.R.; Simon, S.L.; Gordeev, K.I.; Likhtarev, I.A.; Maxwell, R.M.; and Shinkarev, S.M. 2002. "Movement of Radionuclides in Terrestrial Ecosystems by Physical Processes." *Health Physics, 82,* (5), 669-679. Baltimore, Maryland: Lippincott Williams & Wilkins. TIC: 256136. 169793

Bacon, C.R. 1977. "High Temperature Heat Content and Heat Capacity of Silicate Glasses: Experimental Determination and a Model for Calculation." *American Journal of Science, 277,* 109-135. New Haven, Connecticut: Yale University, Kline Geology Laboratory. TIC: 255125. 165512

Best, M.G. 1982. *Igneous and Metamorphic Petrology.* New York, New York: W.H. Freeman and Company. TIC: 247662. 147740

BSC (Bechtel SAIC Company) 2001. *FY 01 Supplemental Science and Performance Analyses, Volume 1: Scientific Bases and Analyses.* TDR-MGR-MD-000007 REV 00 ICN 01. Las Vegas, Nevada: Bechtel SAIC Company. ACC: MOL.20010801.0404; MOL.20010712.0062; MOL.20010815.0001. 155950

BSC 2001. *Igneous Consequence Modeling for the TSPA-SR.* ANL-WIS-MD-000017 REV 00 ICN 02. Las Vegas, Nevada: Bechtel SAIC Company. ACC: MOL.20011107.0005. 157876

BSC 2001. *Performance Analyses.* Volume 2 of *FY01 Supplemental Science and Performance Analyses.* TDR-MGR-PA-000001 REV 00. Las Vegas, Nevada: Bechtel SAIC Company. ACC: MOL.20010724.0110. 154659

BSC 2003. *Risk Information to Support Prioritization of Performance Assessment Models.* TDR-WIS-PA-000009 REV 01 ICN 01 [Errata 001]. Las Vegas, Nevada: Bechtel SAIC Company. ACC: MOL.20021017.0045; DOC.20031014.0003. 168796

BSC 2003. *Technical Work Plan: Igneous Activity Assessment for Disruptive Events.* TWP-WIS-MD-000007 REV 04. Las Vegas, Nevada: Bechtel SAIC Company. ACC: DOC.20031125.0006. 166289

BSC 2003. *Total System Performance Assessment-License Application Methods and Approach.* TDR-WIS-PA-000006 REV 00 ICN 01. Las Vegas, Nevada: Bechtel SAIC Company. ACC: DOC.20031215.0001. 166296

BSC 2004. *Agricultural and Environmental Input Parameters for the Biosphere Model.* ANL-MGR-MD-000006 REV 02. Las Vegas, Nevada: Bechtel SAIC Company. ACC: DOC.20040915.0007. 169673

BSC 2004. *Atmospheric Dispersal and Deposition of Tephra from a Potential Volcanic Eruption at Yucca Mountain, Nevada.* MDL-MGR-GS-000002 REV 01. Las Vegas, Nevada: Bechtel SAIC Company. ACC: DOC.20041025.0003; DOC.20050606.0004. 170026

BSC 2004. *Biosphere Model Report.* MDL-MGR-MD-000001 REV 01. Las Vegas, Nevada: Bechtel SAIC Company. ACC: DOC.20041108.0005. 169460

BSC 2004. *Characterize Eruptive Processes at Yucca Mountain, Nevada.* ANL-MGR-GS-000002 REV 02. Las Vegas, Nevada: Bechtel SAIC Company. ACC: DOC.20041004.0006. 169980

BSC 2004. *Characterize Framework for Igneous Activity at Yucca Mountain, Nevada.* ANL-MGR-GS-000001 REV 02. Las Vegas, Nevada: Bechtel SAIC Company. ACC: DOC.20041015.0002. 169989

BSC 2004. *D&E / PA/C IED Subsurface Facilities.* 800-IED-WIS0-00103-000-00A. Las Vegas, Nevada: Bechtel SAIC Company. ACC: ENG.20040309.0028. 168370

BSC 2004. *Dike/Drift Interactions.* MDL-MGR-GS-000005 REV 01. Las Vegas, Nevada: Bechtel SAIC Company. ACC: DOC.20041124.0002. 170028

BSC 2004. *Future Climate Analysis.* ANL-NBS-GS-000008 REV 01. Las Vegas, Nevada: Bechtel SAIC Company. ACC: DOC.20040908.0005. 170002

BSC 2005. *Characteristics of the Receptor for the Biosphere Model.* ANL-MGR-MD-000005 REV 04. Las Vegas, Nevada: Bechtel SAIC Company. ACC: DOC.20050405.0005. 172827

BSC 2005. *Features, Events, and Processes: Disruptive Events.* ANL-WIS-MD-000005 REV 03. Las Vegas, Nevada: Bechtel SAIC Company. 173981

BSC 2005. *IED Waste Package Configuration [Sheet 1 of 1].* 800-IED-WIS0-00601-000-00A. Las Vegas, Nevada: Bechtel SAIC Company. ACC: ENG.20050406.0005. 173501

BSC 2005. *Number of Waste Packages Hit by Igneous Intrusion.* ANL-MGR-GS-000003 REV 02. Las Vegas, Nevada: Bechtel SAIC Company. 174066

BSC 2005. *Q-List.* 000-30R-MGR0-00500-000-001. Las Vegas, Nevada: Bechtel SAIC Company. ACC: ENG.20050217.0010. 171190

BSC 2005. *Technical Work Plan for: Igneous Activity Assessment for Disruptive Events.* TWP-WIS-MD-000007 REV 08. Las Vegas, Nevada: Bechtel SAIC Company. ACC: DOC.20050815.0001. 174773

BSC 2005. *Waste Package Damage Due to Interaction with Magma.* CAL-WIS-MD-000013 REV 00A. Las Vegas, Nevada: Bechtel SAIC Company. ACC: DOC.20050706.0006. 173802

Bull, W.B. 1991. *Geomorphic Responses to Climate Change.* New York, New York: Oxford University Press. TIC: 223847. 102040

Canori, G.F. and Leitner, M.M. 2003. *Project Requirements Document.* TER-MGR-MD-000001 REV 02. Las Vegas, Nevada: Bechtel SAIC Company. ACC: DOC.20031222.0006. 166275

Carslaw, H.S. and Jaeger, J.C. 1959. *Conduction of Heat in Solids.* 2nd Edition. Oxford, Great Britain: Oxford University Press. TIC: 206085. 100968

Codell, R. 2003. "Alternative Igneous Source Term Model for the Yucca Mountain Repository." *Proceedings of the 10th International High-Level Radioactive Waste Management Conference (IHLRWM), March 30-April 2, 2003, Las Vegas, Nevada.* Pages 405-412. La Grange Park, Illinois: American Nuclear Society. TIC: 254559. 165503

Coe, J.A.; Glancy, P.A.; and Whitney, J.W. 1997. "Volumetric Analysis and Hydrologic Characterization of a Modern Debris Flow Near Yucca Mountain, Nevada." *Geomorphology, 20,* (1-2), 11-28. Amsterdam, The Netherlands: Elsevier. TIC: 241945. 104691

Crowe, B.M. and Perry, F.V. 1990. "Volcanic Probability Calculations for the Yucca Mountain Site: Estimation of Volcanic Rates." *Proceedings of the Topical Meeting on Nuclear Waste Isolation in the Unsaturated Zone, FOCUS '89, September 17-21, 1989, Las Vegas, Nevada.* Pages 326-334. La Grange Park, Illinois: American Nuclear Society. TIC: 212738. 100973

CRWMS M&O 1996. *Probabilistic Volcanic Hazard Analysis for Yucca Mountain, Nevada.* BA0000000-01717-2200-00082 REV 0. Las Vegas, Nevada: CRWMS M&O. ACC: MOL.19971201.0221. 100116

CRWMS M&O 2000. *Comparison of ASHPLUME Model Results to Representative Tephra Fall Deposits.* CAL-WIS-MD-000011 REV 00. Las Vegas, Nevada: CRWMS M&O. ACC: MOL.20001204.0032. 152998

CRWMS M&O 2000. *Total System Performance Assessment for the Site Recommendation.* TDR-WIS-PA-000001 REV 00 ICN 01. Las Vegas, Nevada: CRWMS M&O. ACC: MOL.20001220.0045. 153246

CRWMS M&O 2000. *Yucca Mountain Site Description.* TDR-CRW-GS-000001 REV 01 ICN 01. Las Vegas, Nevada: CRWMS M&O. ACC: MOL.20001003.0111. 151945

CRWMS M&O 2001. *ASHPLUME, V2.0, User's Manual.* Software Document Number: 10022-UM-2.0-00. Las Vegas, Nevada: CRWMS M&O. ACC: MOL.20011119.0008. 174768

CRWMS M&O 2001. *Miscellaneous Waste-Form FEPs.* ANL-WIS-MD-000009 REV 00 ICN 01. Las Vegas, Nevada: CRWMS M&O. ACC: MOL.20010216.0006. 153938

Dehaudt, P. 2001. "Physical and Chemical State of the Nuclear Spent Fuel After Irradiation." Section 5.2 of *Synthesis on the Long Term Behavior of the Spent Nuclear Fuel.* Poinssot, C., ed. CEA-R-5958(E). Volume I. Paris, France: Commissariat à l'Énergie Atomique. TIC: 253976. 164019

Detournay, E.; Mastin, L.G.; Pearson, J.R.A.; Rubin, A.M.; and Spera, F.J. 2003. *Final Report of the Igneous Consequences Peer Review Panel, with Appendices.* Las Vegas, Nevada: Bechtel SAIC Company. ACC: MOL.20031014.0097; MOL.20030730.0163. 169660

DOE (U.S. Department of Energy) 2003. *Review of Oxidation Rates of DOE Spent Nuclear Fuel Part 2. Nonmetallic Fuel.* DOE/SNF/REP-068, Rev. 0. Idaho Falls, Idaho: U.S. Department of Energy, Idaho Operations Office. ACC: DOC.20030905.0009. 166027

DOE 2003. *Validation Test Report for: ASHPLUME_DLL_LA Version 2.0.* 11117-VTR-2.0-00. Las Vegas, Nevada: U.S. Department of Energy, Office of Repository Development. ACC: MOL.20031212.0443. 166506

Drury, M.J. 1987. "Thermal Diffusivity of Some Crystalline Rocks." *Geothermics, 16,* (2), 105-115. New York, New York: Pergamon Press. TIC: 251764. 156447

Einziger, R.E.; Thomas, L.E.; Buchanan, H.C.; and Stout, R.B. 1992. "Oxidation of Spent Fuel in Air at 175 to 195°C." *Journal of Nuclear Materials, 190,* 53-60. Amsterdam, The Netherlands: North-Holland Publishing Company. TIC: 238511. 101607

EPRI (Electric Power Research Institute) 2004. *Potential Igneous Processes Relevant to the Yucca Mountain Repository: Extrusive-Release Scenario.* EPRI TR-1008169. Palo Alto, California: Electric Power Research Institute. TIC: 256654. 171915

Evans, M.; Hastings, N.; and Peacock, B. 1993. *Statistical Distributions.* 2nd Edition. New York, New York: John Wiley & Sons. TIC: 246114. 112115

Fisher, R.V. and Schmincke, H.-U. 1984. *Pyroclastic Rocks.* New York, New York: Springer-Verlag. TIC: 223562. 162806

Folk, R.L. 1980. *Petrology of Sedimentary Rocks.* Austin, Texas: Hemphill Publishing Company. TIC: 254754. 164773

Freeman, T.G. 1991. "Calculating Catchment Area with Divergent Flow Based on a Regular Grid." *Computers & Geosciences, 17,* (3), 413-422. New York, New York: Pergamon Press. TIC: 257286. 174195

Gale, H.J.; Humphreys, D.L.O.; and Fisher, E.M.R. 1964. "Weathering of Caesium-137 in Soil." *Nature, 201,* (491), 257-261. London, England: Macmillan Magazines. TIC: 256310. 169807

Gilbert, R.O. and Eberhardt, L.L. 1976. "Statistical Analysis of 'A Site' Data and Interlaboratory Comparisons for the Nevada Applied Ecology Group." *Studies of Environmental Plutonium and Other Transuranics in Desert Ecosystems, Nevada Applied Ecology Group Progress Report (Workshop Session - May, 1975).* White, M.G. and Dunaway, P.B., eds. NVO-159. Pages 117-154. Las Vegas, Nevada: U.S. Energy Research and Development Administration, Nevada Operations Office. TIC: 201475. 169808

Glaze, L.S. and Self, S. 1991. "Ashfall Dispersal for the 16 September 1986, Eruption of Lascar, Chile, Calculated by a Turbulent Diffusion Model." *Geophysical Research Letters, 18,* (7), 1237-1240. Washington, D.C.: American Geophysical Union. TIC: 245739. 110277

Guenther, R.J.; Blahnik, D.E.; Campbell, T.K.; Jenquin, U.P.; Mendel, J.E.; Thomas, L.E.; and Thornhill, C.K. 1991. *Characterization of Spent Fuel Approved Testing Material - ATM-105.* PNL-5109-105. Richland, Washington: Pacific Northwest Laboratory. TIC: 203785. 127061

Guenther, R.J.; Blahnik, D.E.; Jenquin, U.P.; Mendel, J.E.; Thomas, L.E.; and Thornhill, C.K. 1991. *Characterization of Spent Fuel Approved Testing Material–ATM-104.* PNL-5109-104. Richland, Washington: Pacific Northwest Laboratory. TIC: 203846. 109207

Harrington, C. 2003. Ash and Soil Redistribution Studies. Scientific Notebook SN-LANL-SCI-285-V1. ACC: MOL.20030411.0312. 164775

Harrington, C. 2004. Ash and Soil Redistribution Studies [partial submittal]. Scientific Notebook SN-LANL-SCI-285-V1. Pages 71-79. ACC: MOL.20040116.0145; MOL.20040817.0271. 171345

Harrington, C. 2004. Ash and Soil Redistribution Studies. Scientific Notebook SN-LANL-SCI-285-V1 [partial submittal]. Pages 82-94. ACC: MOL.20040817.0271; MOL.20040929.0089. 171907

Harrison, R.M. 1993. "Atmospheric Pathways." Chapter 3 of *Radioecology after Chernobyl, Biogeochemical Pathways of Artificial Radionuclides.* Warner, F. and Harrison, R.M., eds. SCOPE 50. New York, New York: John Wiley & Sons. TIC: 257252. 173851

Hawkes, H.E. 1976. "The Downstream Dilution of Stream Sediment Anomalies." *Journal of Geochemical Exploration, 6,* 345-358. Amsterdam, The Netherlands: Elsevier. TIC: 257351. 174136

Heiken, G. 1978. "Characteristics of Tephra from Cinder Cone, Lassen Volcanic National Park, California." *Bulletin of Volcanology, 41-2,* 119-130. New York, New York: Springer-Verlag. TIC: 235508. 162817

Heizler, M.T.; Perry, F.V.; Crowe, B.M.; Peters, L.; and Appelt, R. 1999. "The Age of Lathrop Wells Volcanic Center: An $^{40}Ar/^{39}Ar$ Dating Investigation." *Journal of Geophysical Research, 104,* (B1), 767-804. Washington, D.C.: American Geophysical Union. TIC: 243399. 107255

Helgen, S.O. and Moore, J.N. 1996. "Natural Background Determination and Impact Quantification in Trace Metal-Contaminated River Sediments." *Environmental Science & Technology, 30,* (1), 129-135. Easton, Pennsylvania: American Chemical Society. TIC: 257357. 174138

Hill, B.E.; Connor, C.B.; Jarzemba, M.S.; La Femina, P.C.; Navarro, M.; and Strauch, W. 1998. "1995 Eruptions of Cerro Negro Volcano, Nicaragua, and Risk Assessment for Future Eruptions." *Geological Society of America Bulletin, 110,* (10), 1231-1241. Boulder, Colorado: Geological Society of America. TIC: 245102. 151040

Jarzemba, M.S. 1997. "Stochastic Radionuclide Distributions After a Basaltic Eruption for Performance Assessments of Yucca Mountain." *Nuclear Technology, 118,* 132-141. Hinsdale, Illinois: American Nuclear Society. TIC: 237944. 100460

Jarzemba, M.S.; LaPlante, P.A.; and Poor, K.J. 1997. *ASHPLUME Version 1.0—A Code for Contaminated Ash Dispersal and Deposition, Technical Description and User's Guide.* CNWRA 97-004, Rev. 1. San Antonio, Texas: Center for Nuclear Waste Regulatory Analyses. ACC: MOL.20010727.0162. 100987

Jones, K.H. 1998. "A Comparison of Algorithms Used to Compute Hill Slope as a Property of the DEM." *Computers & Geosciences, 24,* (4), 315-323. New York, New York: Pergamon. TIC: 257285. 174197

Keating, G. 2005. Magnetic Separation of Surficial Materials for Disruptive Events Field Investigations [final closure]. Scientific Notebook SN-LANL-SCI-292-V1. Pages 1-149. ACC: MOL.20050321.0177. 173850

Keating, G. 2005. Volcanological Investigations. Scientific Notebook: SN-LANL-SCI-311-V1 [partial submittal]. Pages TOC - 5, 8-59 and 62-82. ACC: MOL.20050622.0222; MOL.20050810.0012; MOL.20050808.0238. 174988

Krier, D. 2004. Ash Redistribution, Lava Morphology, and Igneous Processes Studies (Volume 2) [partial submittal]. Scientific Notebook SN-LANL-SCI-286-V2. Pages TOC-33 and 35-56. ACC: MOL.20041220.0168. 173810

Krier, D. and Harrington, C.D. 2003. Ash Redistribution, Lava Morphology, and Igneous Processes Studies. Scientific Notebook SN-LANL-SCI-286-V1. ACC: MOL.20030701.0109. 164023

Kutzbach, J.E.; Guetter, P.J.; Behling, P.J.; and Selin, R. 1993. "Simulated Climatic Changes: Results of the COHMAP Climate-Model Experiments." Chapter 4 of *Global Climates Since the Last Glacial Maximum.* Wright, H., Jr.; Kutzbach, J.; Webb, T., III; Ruddiman, W.; Street-Perrott, F., Bartlein, P., eds. Minneapolis, Minnesota: University of Minnesota Press. TIC: 234248. 119269

Lide, D.R., ed. 1994. *CRC Handbook of Chemistry and Physics, A Ready-Reference Book of Chemical and Physical Data.* 75th Edition. Boca Raton, Florida: CRC Press. TIC: 102972. 147834

Likhtarev, I.A.; Kovgan, L.N.; Jacob, P.; and Anspaugh, L.R. 2002. "Chernobyl Accident: Retrospective and Prospective Estimates of External Dose of the Population of Ukraine." *Health Physics, 82,* (3), 290-303. Baltimore, Maryland: Lippincott Williams & Wilkins. TIC: 256138. 169810

Luhr, J.F. and Simkin, T., eds. 1993. *Paricutin, The Volcano Born in a Mexican Cornfield.* Phoenix, Arizona: Geoscience Press. TIC: 247017. 144310

Machette, M.N. 1985. "Calcic Soils of the Southwestern United States." *Soils and Quaternary Geology of the Southwestern United States.* Weide, D.L. and Faber, M.L., eds. Special Paper 203. Pages 1-21. Boulder, Colorado: Geological Society of America. TIC: 239387. 104660

McEachern, R.J. and Taylor, P. 1997. *A Review of the Oxidation of Uranium Dioxide at Temperatures Below 400°C.* AECL-11335. Pinawa, Manitoba, Canada: Atomic Energy of Canada Limited. TIC: 232575. 101726

McKnight, S.B. and Williams, S.W. 1997. "Old Cinder Cone or Young Composite Volcano?: The Nature of Cerro Negro, Nicaragua." *Geology, 25,* (4), 339-342. Boulder, Colorado: Geological Society of America. TIC: 254104. 162827

Mück, K.; Pröhl, G.; Likhtarev, I.; Kovgan, L.; Golikov, V.; and Zeger, J. 2002. "Reconstruction of the Inhalation Dose in the 30-km Zone After the Chernobyl Accident." *Health Physics, 82,* (2), 157-172. Philadelphia, Pennsylvania: Lippincott Williams & Wilkins. TIC: 256234. 170378

NEA (Nuclear Energy Agency) 2002. *Chernobyl, Assessment of Radiological and Health Impacts.* Paris, France: Organization for Economic Co-Operation and Development, Nuclear Energy Agency. TIC: 257424. 174224

NOAA (National Oceanic and Atmospheric Administration) 2004. *Upper Air Data for Desert Rock, Nevada Years 1978-2003. NCDC (National Climatic Data Center) Digital Upper Air Files TD 6201 and 6301 (Includes Compact Disk and Special Instruction Sheet with Listing of Files).* Asheville, North Carolina: National Oceanic and Atmospheric Administration. ACC: MOL.20040817.0103. 171035

NRC (U.S. Nuclear Regulatory Commission) 1998. *Issue Resolution Status Report Key Technical Issue: Igneous Activity.* Rev. 0. Washington, D.C.: U.S. Nuclear Regulatory Commission. ACC: MOL.19980514.0576. 100297

NRC 1999. "Issue Resolution Status Report Key Technical Issue: Igneous Activity." Rev. 2. Washington, D.C.: U.S. Nuclear Regulatory Commission. Accessed September 18, 2000. TIC: 247987. http://www.nrc.gov/NMSS/DWM/ia-rev2.htm 151592

NRC 2002. *Integrated Issue Resolution Status Report.* NUREG-1762. Washington, D.C.: U.S. Nuclear Regulatory Commission, Office of Nuclear Material Safety and Safeguards. TIC: 253064. 159538

NRC 2003. *Yucca Mountain Review Plan, Final Report.* NUREG-1804, Rev. 2. Washington, D.C.: U.S. Nuclear Regulatory Commission, Office of Nuclear Material Safety and Safeguards. TIC: 254568. 163274

Pareschi, M.T.; Santacroce, R.; Sulpizio, R.; and Zanchetta, G. 2002. "Volcaniclastic Debris Flows in the Clanio Valley (Campania, Italy): Insights for the Assessment of Hazard Potential." *Geomorphology, 43,* 219-231. New ork, New York: Elsevier. TIC: 256431. 171394

Pelletier, J.D. 2004. "Persistent Drainage Migration in a Numerical Landscape Evolution Model." *Geophysical Research Letters, 31,* (L20501), 1-4. Washington, D.C.: American Geophysical Union. TIC: 257363. 174135

Perry, F.V.; Crowe, B.M.; Valentine, G.A.; and Bowker, L.M., eds. 1998. *Volcanism Studies: Final Report for the Yucca Mountain Project.* LA-3478. Los Alamos, New Mexico: Los Alamos National Laboratory. TIC: 247225. 144335

Pfeiffer, T.; Costa, A.; and Macedonio, G. 2005. "A Model for the Numerical Simulation of Tephra Fall Deposits." *Journal of Volcanology and Geothermal Research, 140,* 273-294. New York, New York: Elsevier. TIC: 257591. 174826

Press, W.H.; Teukolsky, S.A.; Vetterling, W.T.; and Flannery, B.P. 2002. *Numerical Recipes in C, the Art Scientific Computing.* 2nd Edition. New York, New York: Cambridge University Press. TIC: 257274. 174134

Quiring, R.F. 1968. *Climatological Data Nevada Test Site and Nuclear Rocket Development Station.* ESSA Research Laboratories Technical Memorandum - ARL 7. Las Vegas, Nevada: U.S. Department of Commerce, Environmental Science Services Administration Research Laboratories. ACC: NNA.19870406.0047. 119317

Reamer, C.W. 1999. "Issue Resolution Status Report (Key Technical Issue: Igneous Activity, Revision 2)." Letter from C.W. Reamer (NRC) to Dr. S. Brocoum (DOE/YMSCO), July 16, 1999, with enclosure. ACC: MOL.19990810.0639. 119693

Romney, E.M.; Mork, H.M.; and Larson, K.H. 1970. "Persistence of Plutonium in Soil, Plants, and Small Mammals." *Health Physics, 19,* (4), 487-491. New York, New York: Pergamon Press. TIC: 256308. 169811

Rose, W.I., Jr.; Bonis, S.; Stoiber, R.E.; Keller, M.; and Bickford, T. 1973. "Studies of Volcanic Ash from Two Recent Central American Eruptions." *Bulletin Volcanologique, XXXVII-3,* 338-364. New York, New York: Springer-Verlag. TIC: 246073. 116087

Sagar, B., ed. 1997. *NRC High-Level Radioactive Waste Program Annual Progress Report: Fiscal Year 1996.* NUREG/CR-6513, No. 1. Washington, D.C.: U.S. Nuclear Regulatory Commission. ACC: MOL.19970715.0066. 145235

Sandoval, R.P.; Weber, J.P.; Levine, H.S.; Romig, A.D.; Johnson, J.D.; Luna, R.E.; Newton, G.J.; Wong, B.A.; Marshall, R.W., Jr.; Alvarez, J.L.; and Gelbard, F. 1983. *An Assessment of the Safety of Spent Fuel Transportation in Urban Environs.* SAND82-2365. Albuquerque, New Mexico: Sandia National Laboratories. ACC: NNA.19870406.0489. 156313

Schlueter, J.R. 2003. "Igneous Activity Agreement 2.09, Additional Information Needed." Letter from J.R. Schlueter (NRC) to J.D. Ziegler (DOE/ORD), March 25, 2003, 0331036684, with enclosure. ACC: MOL.20031009.0249. 165740

Searcy, C.; Dean, K.; and Stringer, W. 1998. "PUFF: A High-Resolution Volcanic Ash Tracking Model." *Journal of Volcanology and Geothermal Research, 80,* 1-16. Amsterdam, The Netherlands: Elsevier. TIC: 238696. 101015

Self, S. and Walker, G.P.L. 1994. "Ash Clouds: Characteristics of Eruption Columns." *Volcanic Ash and Aviation Safety: Proceedings of the First International Symposium on Volcanic Ash and Aviation Safety held in Seattle, Washington in July 1991.* Casadevall, T.J., ed. U.S. Geological Survey Bulletin 2047. Pages 65-74. Washington, D.C.: U.S. Government Printing Office. TIC: 254494. 162831

Suzuki, T. 1983. "A Theoretical Model for Dispersion of Tephra." *Arc Volcanism: Physics and Tectonics, Proceedings of a 1981 IAVCEI Symposium, August-September, 1981, Tokyo and Hakone*. Shimozuru, D. and Yokoyama, I., eds. Pages 95-113. Tokyo, Japan: Terra Scientific Publishing Company. TIC: 238307. 100489

Ushakov, S.V.; Burakov, B.E.; Shabalev, S.I.; and Anderson, E.B. 1997. "Interaction of $UO_2$ and Zircaloy During the Chernobyl Accident." *Scientific Basis for Nuclear Waste Management XX, Materials Research Society Symposium Held December 2-6, 1996, Boston, Massachusetts, U.S.A.* Gray, W.J. and Triay, I.R., eds. *465*, 1313-1318. Pittsburgh, Pennsylvania: Materials Research Society. TIC: 238884. 174141

Wescott, R.G.; Lee, M.P.; Eisenberg, N.A.; McCartin, T.J.; and Baca, R.G., eds. 1995. *NRC Iterative Performance Assessment Phase 2, Development of Capabilities for Review of a Performance Assessment for a High-Level Waste Repository*. NUREG-1464. Washington, D.C.: U.S. Nuclear Regulatory Commission. ACC: MOL.19960710.0075. 100476

Wilson, L. and Head, J.W., III 1981. "Ascent and Eruption of Basaltic Magma on the Earth and Moon." *Journal of Geophysical Research, 86*, (B4), 2971-3001. Washington, D.C.: American Geophysical Union. TIC: 225185. 101034

Wilson, L.; Sparks, R.S.J.; Huang, T.C.; and Watkins, N.D. 1978. "The Control of Volcanic Column Heights by Eruption Energetics and Dynamics." *Journal of Geophysical Research, 83*, (B4), 1829–1836. Washington, D.C.: American Geophysical Union. TIC: 254493. 162859

## 9.2 CODES, STANDARDS, REGULATIONS, AND PROCEDURES

10 CFR 63. 2005 Energy: Disposal of High-Level Radioactive Wastes in a Geologic Repository at Yucca Mountain, Nevada. ACC: MOL.20050405.0118. 173273

40 CFR 197. 2004 Protection of Environment: Public Health and Environmental Radiation Protection Standards for Yucca Mountain, Nevada: ACC: MOL.20050324.0101. 173176

AP-2.12Q, Rev. 0, ICN 4. *Peer Review*. Washington, D.C.: U.S. Department of Energy, Office of Civilian Radioactive Waste Management. ACC: MOL.20020619.0084.

AP-2.22Q, Rev. 1, ICN 1. *Classification Analyses and Maintenance of the Q-List.* Washington, D.C.: U.S. Department of Energy, Office of Civilian Radioactive Waste Management. ACC: DOC.20040714.0002.

LP-SI.11Q-BSC, Rev. 0, ICN 1. *Software Management.* Washington, D.C.: U.S. Department of Energy, Office of Civilian Radioactive Waste Management. ACC: DOC.20041005.0008.

LP-SIII.2Q-BSC, REV 0 ICN 0. *Qualification of Unqualified Data.* Washington, D.C.: U.S. Department of Energy, Office of Civilian Radioactive Waste Management. ACC: DOC.20050119.0003.

AP-SIII.10Q, REV 2 ICN 0. *Models.* Washington, D.C.: U.S. Department of Energy, Office of Civilian Radioactive Waste Management. ACC: DOC.2003029.0003.

AP-SV.1Q, Rev. 1, ICN 2. *Control of the Electronic Management of Information.* Washington, D.C.: U.S. Department of Energy, Office of Civilian Radioactive Waste Management. ACC: DOC.20050119.0004.

LP-SIII.10Q-BSC, Rev. 0, ICN 1. *Models.* Washington, D.C.: U.S. Department of Energy, Office of Civilian Radioactive Waste Management. ACC: DOC.20050623.0001.

## 9.3 SOFTWARE

BSC 2002. *Software Code: ASHPLUME.* 1.4LV. PC, Windows 2000/NT/98. 10022-1.4LV-02. 161296

BSC 2003. *Software Code: ASHPLUME_DLL_L4.* V2.0. PC, Windows 2000. 11117-2.0-00. 166571

BSC 2004. *Software Code: GoldSim.* V 8.02. PC, Windows 2000. 10344-8.02-00. 169844

CRWMS M&O 2001. *Software Code: ASHPLUME.* V2.0. PC. 10022-2.0-00. 152844

## 9.4 SOURCE DATA, LISTED BY DATA TRACKING NUMBER

LA0302CH831811.002. Ash Redistribution, Lava Morphology, and Igneous Process Studies SITP-02-DE-001, REV 00A. Submittal date: 02/18/2003. 162863

LA0305DK831811.002. Characterize Eruptive Processes at Yucca Mountain Nevada. Submittal date: 05/14/2003. 164678

LA0308CH831811.002. Interpretation of 137-Cesium Profile Values for Samples from the Fortymile Wash Alluvial Fan. Submittal date: 08/20/2003. 164853

LA0405CH831811.001. Basaltic Ash Weight Percentages of Drainage Channel Samples Near Lathrop Wells Cone. Submittal date: 04/05/2004. 169998

LA0407DK831811.001. Physical Parameters of Basaltic Magma and Eruption Phenomena. Submittal date: 07/15/2004. 170768

LA0507CH831611.001. Interchannel Divides and Channel Areas on the Upper Fortymile Wash Alluvial Fan. Submittal date: 07/18/2005. 174843

MO0103COV01031.000. Coverage: BORES3Q. Submittal date: 03/22/2001. 155271

MO0501SEPFEPLA.001. LA FEP List and Screening. Submittal date: 01/17/2005. 172601

MO0504MWDNUMWP.001. Number of Waste Packages Hit by Igneous Intrusion. Submittal date: 04/22/2005. 173521

## 9.5 DEVELOPED DATA, LISTED BY DATA TRACKING NUMBER

LA0408GK831811.001. Calculation of Waste-Form Concentrations in Ash from an Ash Plume at 18 km from a Vent. Submittal date: 08/19/2004.

LA0408GK831811.002. Input Parameter Values for the ASHPLUME V2.0DLL Model for TSPA-LA. Submittal date: 08/19/2004.

LA0408CH831811.001. Ash Redistribution Model Abstraction for TSPA-LA. Submittal date: 08/19/2004.

MO0408SPADRWSD.002. Desert Rock Wind Speed and Wind Direction Analyses for Years 1978-1995. Submittal date: 08/17/04.

LA0508GK831811.002. Ashplume Model Validation Statistics for Lathrop Wells Volcano and Cinder Cone Case Studies. Submittal date: 08/122005.

MO0505WPSDISTR.001. Alternative Analysis of Waste Particle Size, Partitioning of Magma/Waste into Eruptive Products, and Waste Incorporation Ratio. Submittal date: 05/23/05.

MO0506SPACHERN.000. Analysis of Chernobyl Hot Particle Data to Assess Source-Term Maximum Particle Size. Submittal date: 06/16/2005.

# APPENDIX A

# QUALIFICATION OF EXTERNAL SOURCES

# APPENDIX A
# QUALIFICATION OF EXTERNAL SOURCES

External sources have provided unqualified data that have been used as direct input to this document. The inputs from these sources are qualified for intended use within the document using the criteria found in LP-SIII.10Q-BSC, *Models*. These criteria represent a subset of the methods and attributes required for qualification of data per LP-SIII.2Q-BSC, *Qualification of Unqualified Data*. The following information is provided for each source: The full reference citation, a description of the data that were used from the source, and the extent to which the data demonstrate the properties of interest. In addition one or more of the following criteria is also addressed:

- Reliability of data source
- Qualifications of personnel or organizations generating the data
- Prior uses of the data
- Availability of corroborating data.

The criteria described above meet the requirements of LP-SIII.10Q-BSC and are provided as justification that the data that have been used from these sources are considered to be qualified for intended use.

## A1. JARZEMBA, M.S.; LAPLANTE, P.A.; AND POOR, K.J. 1997

**Reference**–Jarzemba, M.S.; LaPlante, P.A.; and Poor, K.J. 1997. *ASHPLUME Version 1.0—A Code for Contaminated Ash Dispersal and Deposition, Technical Description and User's Guide*. CNWRA 97-004, Rev. 1. San Antonio, Texas: Center for Nuclear Waste Regulatory Analyses. ACC: MOL.20010727.0162 [DIRS 100987].

**Description of Use**–Jarzemba et al. (1997 [DIRS 100987]) are the source of two parameters required by the ASHPLUME computer code. The two parameters and their reference location in Jarzemba are as follows:

- Column Diffusion Constant, $\beta$ (p. 4-6, Table 5-1)
- Waste Incorporation Ratio, $\rho_c$ (Section 2.2, Eq. 2-7)

The specific range of values for the column diffusion constant is discussed as in Section 6.5.2.3. The column diffusion constant ($\beta$) is set at a uniform distribution with a minimum value of 0.01 and a maximum value of 0.5. The column diffusion constant was discussed earlier by Suzuki (1983 [DIRS 100489], pp. 104 to 107). This parameter affects the distribution of particles vertically in the ash column and helps determine where particles exit the column. Jarzemba et al. (1997 [DIRS 100987], p. 4-1) uses a log-uniform distribution for beta that has a minimum value of 0.01 and a maximum value of 0.5. This range of values spans more than an order of magnitude and encompasses the range that is valid for the ASHPLUME model. However, to simulate the anvil cloud associated with a violent Strombolian eruption properly, samples from the range in beta should be focused toward the upper end of the range; therefore, a uniform (rather than log-uniform) distribution is recommended.

The specific value for the mass incorporation ratio ($\rho_c = 0.3$) is discussed as in Section 6.5.2.6. The incorporation ratio describes the ratio of ash-waste particle sizes that can be combined for transport. An incorporation ratio of 0.3 corresponds to a maximum incorporated waste particle size equal to half the diameter of the ash particle (i.e., any waste particles larger than half the ash particle diameter cannot be incorporated into the ash).

**Extent to which the Data Demonstrate the Properties of Interest**–Studies have been underway by the Yucca Mountain Project, as well as by the Center for Nuclear Waste Regulatory Analysis at the Southwest Research Institute, which provides technical support for the Yucca Mountain Project. The computer code, ASHPLUME, was developed by Jarzemba at Southwest Research Institute, under contract to the NRC. The code is used to model volcanic ash and waste dispersal during a hypothetical future volcanic eruption through the repository. The two parameters are provided in the documentation for the ASHPLUME code, *ASHPLUME Version 1.0—A Code for Contaminated Ash Dispersal and Deposition, Technical Description and User's Guide*, Jarzemba et al. (1997 [DIRS 100987]).

**Qualifications of Personnel or Organizations Generating the Data and Prior Use of the Data**–The source document (Jarzemba et al. 1997 [DIRS 100987]) is the technical description and user's guide for ASHPLUME, Version 1.0. ASHPLUME Version 1.0, a code for contaminated ash dispersal and deposition, was prepared for the NRC under contract to the Center for Nuclear Waste Regulatory Analyses, San Antonio, Texas. The Center for Nuclear Waste Regulatory Analyses at Southwest Research Institute is a federally funded research and development center created to support the NRC. The principal author of the code was Dr. Mark S. Jarzemba.

**Qualifications of M.S. Jarzemba**:

Education:

B.S. 1988, Engineering Physics, Ohio State University
M.S. 1991, Nuclear Engineering, Ohio State University
Ph.D. 1993, Nuclear Engineering, Ohio State University

Dr. Jarzemba has over 15 years of research and professional experience. His background includes nuclear instrumentation and shielding, radon gas-phase transport modeling, environmental/dose pathway analyses and criticality analyses. At the time of publication, Dr. Jarzemba was a research scientist with Southwest Research Institute. Dr. Jarzemba is the author and co-author of numerous books and publications.

Based on the foregoing discussion, the data cited from Jarzemba et al. (1997 [DIRS 100987]), can be accepted as qualified for use in this report.

### A2. SUZUKI, T. 1983

**Reference**–Suzuki, T. 1983. "A Theoretical Model for Dispersion of Tephra." *Arc Volcanism: Physics and Tectonics, Proceedings of a 1981 IAVCEI Symposium, August-September, 1981, Tokyo and Hakone.* Shimozuru, D. and Yokoyama, I., eds.

Pages 95-113. Tokyo, Japan: Terra Scientific Publishing Company. TIC: 238307. [DIRS 100489]

**Description of Use**–Suzuki (1983 [DIRS 100489], p. 99) is the source for eddy diffusivity (400 $cm^2/s^{5/2}$) discussed in Section 6.5.1 and the value is listed in Table 6-3 of this model report. Suzuki developed the mathematical model that underlies the ASHPLUME code, which is used in development of this model report. The underlying two-dimensional partial differential equation relates the change in concentration, $\xi$, at a point x-y (with x downwind) to wind velocity, $u$, and an eddy diffusivity constant, $C$.

**Extent to which the Data Demonstrate the Properties of Interest**–The Ashplume model for Yucca Mountain is based on a mathematical model of Suzuki (1983 [DIRS 100489]) that Jarzemba et al. (1997 [DIRS 100987]) refined to represent violent Strombolian-type eruptions. The code is used to model volcanic ash and waste dispersal during a hypothetical future volcanic eruption through the repository. The eddy diffusivity constant was developed as part of that mathematical model.

**Prior Use of the Data**–The above-listed reference document provides the basis for ASHPLUME, Version 1.0, a code for contaminated ash dispersal and deposition, prepared by the Center for Nuclear Waste Regulatory Analyses at Southwest Research Institute, San Antonia Texas, under contract to the NRC. The code was developed for use in evaluation of potential igneous events at Yucca Mountain. The specific value for eddy diffusivity, 400 $cm^2/s^{5/2}$, was used as an input value to the code as documented in Tables 5-1 and 5-2 of Jarzemba et al. (1997 [DIRS 100987]). The resultant graph, Figure 5-1b, is identical to the results recorded by Suzuki (1983 [DIRS 100489], Figure 6c).

Based on the foregoing discussion, the data cited from Suzuki [DIRS 100489], can be accepted as qualified for use in this AMR.

**A3. BACON, C.R. 1977; DRURY, M.J. 1987; BEST, M.G. 1982**

**References**–Bacon, C.R. 1977. "High Temperature Heat Content and Heat Capacity of Silicate Glasses: Experimental Determination and a Model for Calculation." *American Journal of Science, 277,* 109-135. New Haven, Connecticut: Yale University, Kline Geology Laboratory. TIC: 255125. [DIRS 165512]

Drury, M.J. 1987. "Thermal Diffusivity of Some Crystalline Rocks." *Geothermics, 16,* (2), 105-115. New York, New York: Pergamon Press. TIC: 251764. [DIRS 156447]

Best, M.G. 1982. *Igneous and Metamorphic Petrology.* New York, New York: W.H. Freeman and Company. TIC: 247662. [DIRS 147740]

**Description of Use**–Bacon (1977 [DIRS 165512]) and Drury (1987 [DIRS 156447]), are used as the basis for the value (1,000 J/(kg-K)) selected for the heat capacity of magma. The value is rounded from data presented in Figures 1 and 2 in the Bacon article, and from Table 2 in the Drury reference. Heat capacity is one of the variables in the calculation of eruptive power, which is a direct feed to TSPA-LA.

**Extent to which the Data Demonstrate the Properties of Interest**–The Bacon (1977 [DIRS 165512]) reference documents the results of experimental work to determine the thermodynamic properties of silicate melts. The property of interest, heat capacity, is plotted for different compositions of silicate glasses at different temperatures. Bacon's compositions one through three bracket the magma compositions (discussed in *Characterize Eruptive Processes at Yucca Mountain, Nevada* (BSC 2004 [DIRS 169980])) assumed for this model report. Drury (1987 [DIRS 156447]) also reports thermodynamic data from experimental work on igneous materials of different compositions, including the heat capacity for basalt.

**Corroborative Data and Prior Use**–The values and ranges for heat capacity for melts of basaltic compositions from these two articles are corroborative. For compositions close to those proposed for this model report, the Bacon reference shows experimental heat capacities ranging from 800 to 1,100 J/(kg-K). In Drury (1987 [DIRS 156447]), a value of 1,010 J/(kg-K) is listed for the basaltic composition. A value of 1,000 J/(kg-K) for specific heat is also reported in *Characterize Eruptive Processes at Yucca Mountain, Nevada* (BSC 2004 [DIRS 169980], Table 6-5), where the property is also used to calculate mass discharge rate. The source that is used as a basis for the latter value is Best (1982 [DIRS 147740], p. 301). This reference book presents a range of specific heat of 800 to 1,300 J/kg. The similarity of reported values in the three references, combined with the prior use of the specific values in other igneous studies for Yucca Mountain provide the necessary justification that this value is qualified for the intended use.

# APPENDIX B

# YUCCA MOUNTAIN REVIEW PLAN (NUREG-1804)
# ACCEPTANCE CRITERIA

# APPENDIX B
# YUCCA MOUNTAIN REVIEW PLAN (NUREG-1804) ACCEPTANCE CRITERIA

## B1. BACKGROUND

Early in 1995, the NRC recognized the need to refocus its prelicensing repository program on resolving issues most significant to repository performance. In 1996, the NRC identified 10 key technical issues (Sagar 1997 [DIRS 145235]) intended to reflect the topics that the NRC considered most important to repository performance. Nine of the issues were technical, and the tenth concerned the development of the dose standard for a repository at Yucca Mountain (see 40 CFR Part 197 [DIRS 173176]). The technical issues included igneous activity, and the status of resolution of each issue and associated open items were described by the NRC in a series of Issue Resolution Status Reports (e.g., Reamer 1999 [DIRS 119693]). In 2002, the NRC consolidated the subissues into a series of integrated subissues and replaced the series of nine issue resolution status reports with an Integrated Issue Resolution Status Report (NRC 2002 [DIRS 159538]). The Integrated Issue Resolution Status Report was based on the realization that the issue resolution process was "mature enough to develop a single Integrated Issue Resolution Status Report that would clearly and consistently reflect the interrelationships among the various key technical issue subissues and the overall resolution status" (NRC 2002 [DIRS 159538], pp. xviii and xix). The Integrated Issue Resolution Status Report and periodic letters from the NRC (e.g., Schlueter 2003 [DIRS 165740]) provide information about the resolution status of the integrated subissues that are described in the Yucca Mountain Review Plan, NUREG-1804 (NRC 2003 [DIRS 163274]).

## B2. IGNEOUS ACTIVITY KEY TECHNICAL ISSUE

The key technical issue for igneous activity was defined by the NRC staff as "predicting the consequence and probability of igneous activity affecting the repository in relationship to the overall system performance objective" (NRC 1998 [DIRS 100297], p. 3). Hence, the NRC defined two subissues for the igneous activity key technical issue: probability and consequences (NRC 1998 [DIRS 100297], p. 3). The probability subissue addresses the likelihood that future igneous activity would disrupt a repository at Yucca Mountain. The DOE estimated the probability of future disruption of a repository at Yucca Mountain in the *Probabilistic Volcanic Hazard Analysis for Yucca Mountain, Nevada* (CRWMS M&O 1996 [DIRS 100116]). For the TSPA-LA, an analysis based on the *Probabilistic Volcanic Hazard Analysis for Yucca Mountain, Nevada* results and consideration of the repository LA design were both updated and documented in the scientific analysis report, *Characterize Framework for Igneous Activity at Yucca Mountain, Nevada* (BSC 2004 [DIRS 169989]).

The consequences subissue examined the effects of igneous activity on various engineered and natural components of the repository system. The consequences subissue comprises four integrated subissues: mechanical disruption of engineered barriers (NRC 2003 [DIRS 163274] Section 2.2.1.3.2); volcanic disruption of waste packages ((NRC 2003 [DIRS 163274] Section 2.3.1.3.10); airborne transport of radionuclides (NRC 2003 [DIRS 163274] Section 2.3.1.3.11); and redistribution of radionuclides in soil (NRC 2003 [DIRS 163274] Section 2.3.1.3.13). This model report addresses the integrated subissues of airborne transport of

radionuclides and redistribution of radionuclides in soil (NRC 2003 [DIRS 163274] Section 2.3.1.3.11). Mechanical disruption of engineered barriers and volcanic disruption of waste packages are addressed in *Dike/Drift Interactions* (BSC 2004 [DIRS 170028]), and *Number of Waste Packages Hit by Igneous Intrusion* (BSC 2005 [DIRS 174066]).

For the TSPA-SR, the DOE defined two igneous scenarios to evaluate the effects of igneous activity on the repository and its contents (BSC 2001 [DIRS 157876]):

- A direct-release scenario featuring penetration of the repository by an ascending basaltic dike followed by eruption of contaminated ash at the surface
- An indirect release or igneous-intrusion, groundwater-release scenario featuring penetration of the repository by an ascending basaltic dike and no surface eruption.

In the latter scenario, release of radionuclides would be through the groundwater pathway. Both igneous scenarios are being carried forward for TSPA-LA.

For the TSPA-LA, the direct-release model has been described, and documentation is provided in this model report. For the indirect-release scenario, the potential effects of the repository on the propagation of a basaltic dike, the environmental conditions accompanying intersection of the repository by an ascending dike, and analyses of effects of intrusive igneous activity on repository structures and components are documented in the model report *Dike/Drift Interactions* (BSC 2004 [DIRS 170028]).

In addition, this model report describes the ash redistribution conceptual model and documents the development and validation of this model (Sections 6.6.2 and 7). This conceptual model is potentially important to the TSPA-LA because reworking of contaminated tephra deposits could increase the concentration of radioactive waste material at the RMEI location and, thereby, potentially increase the dose to the RMEI.

## B3. YUCCA MOUNTAIN REVIEW PLAN ACCEPTANCE CRITERIA

The Yucca Mountain Review Plan (NUREG-1804, NRC 2003 [DIRS 163274]) associates the integrated subissue of airborne transport of radionuclides with the requirements listed in 10 CFR 63.114(a)-(c) and (e)-(g) [DIRS 173273]). NUREG-1804 (NRC 2003 [DIRS 163274], Sections 2.2.1.3.11 and 2.2.1.3.13) describes the acceptance criteria that the NRC will use to evaluate the adequacy of information addressing the airborne transport of radionuclides and redistribution of radionuclides in soil in the license application. The application acceptance criteria may also be addressed in other analysis model reports. The acceptance criteria will be considered fully addressed when this report is considered in conjunction with those reports. The following discussion provides a summary of how the information in this model report addresses those criteria that are associated with the development and use of the ASHPLUME model.

## B4. NUREG-1804, REV 2, SECTION 2.2.1.3.10.3: VOLCANIC DISRUPTION OF WASTE PACKAGES

**Acceptance Criterion 1: System Description and Model Integration Are Adequate**

*(2) Models used to assess volcanic disruption of waste packages are consistent with physical processes generally interpreted from igneous features in the Yucca Mountain region and/or observed in activity igneous systems.*

This model report provides information about the basis for the ASHPLUME conceptual model (Suzuki 1983 [DIRS 100489]) in Section 6.3.1. Section 6.3.1 also describes the consistency of the conceptual model with physical phenomena associated with violent Strombolian eruptions and the development and propagation of an ash cloud downwind of the eruption site followed by deposition of tephra deposits on the ground surface. Base-case model inputs and uncertainties and their consistency with igneous features either observed in the Yucca Mountain region or with features observed at analogue igneous systems are described in Section 6.5.2. The bases for the selection of an appropriate distribution for each uncertain parameter are described in this report (Section 6.5.2). Model inputs that are developed and documented in other analyses or models are appropriately identified, described, and cross-referenced.

Alternative models considered are described in Section 6.4.1.

*(3) Models account for changes in igneous processes that may occur from interaction with engineered repository systems.*

The ASHPLUME model does not account for changes in igneous processes that might result from interactions between processes and components of the engineered barrier system. Such interactions are described in other analyses or model reports, as appropriate (e.g., *Dike/Drift Interactions* (BSC 2004 [DIRS 170028]) and *Number of Waste Packages Hit by Igneous Intrusion* (BSC 2005 [DIRS 174066]).

**Acceptance Criterion 2: Data Are Sufficient For Model Justification**

*(1) Parameter values used in the license application to evaluate volcanic disruption of waste packages are sufficient and adequately justified. Adequate descriptions of how the data were used, interpreted, and appropriately synthesized into the parameters are provided.*

Uses of the parameter values are generally described as part of the mathematical description of the base-case model in Section 6.5.1. The development of all model inputs used for the atmospheric dispersal model is discussed in Section 6.5.2. Subsections describe the individual model input parameters and provide detailed technical bases supporting the use of the numerical value or range for each parameter. Model report outputs for the TSPA-LA are described in Section 8.2.

*(2) Data used to model processes affecting volcanic disruption of waste packages are derived from appropriate techniques. These techniques may include site-specific field measurements, natural analog investigations, and laboratory experiments.*

The parameter values used as inputs for ASHPLUME V.2.0 dll are described in the model report in Section 4.1, and model outputs are described in Section 8.2. Modeling objectives, the characteristics of the base-case model, consideration of alternative conceptual models, and the basis for the selection of ASHPLUME for modeling airborne transport of radionuclides are discussed in Sections 6.1, 6.3, and 6.4, respectively. The formulation of the mathematical model is described in Section 6.5.1, and the base-case model inputs and their appropriateness are described in Section 6.5.2.

This model report describes the conceptual model, formulation of the mathematical model, identification of parameters, selection of appropriate parameter values or distributions, and discusses the consideration of alternative models. All of these considerations are included in the basis for selection of the ASHPLUME model as appropriate for analyzing the airborne transport of radionuclides for the license application. The alternative models considered are described in Section 6.4.1, and a summary of alternative conceptual models is provided in Section 6.4.3. Section 7.3 of the report discusses validation of the model and shows how the validation exercises have shown the efficacy of the ASHPLUME model to represent observed variations in tephra deposit thicknesses at analogue sites. The validation work also shows that the model is internally consistent and produces numerical convergence in simulations. These lines of evidence demonstrate that the ASHPLUME model is appropriate to analyze the airborne transport of radionuclides.

*(3) Sufficient data are available to integrate features, events, and processes, relevant to volcanic disruption of waste packages into process-level models, including determination of appropriate interrelationships and parameter correlations.*

FEPs related to the development and use of the ASHPLUME model are discussed in Section 6.2. Table 6-1 includes descriptions of the specific data elements associated with the FEPs associated with the ASHPLUME model and summarizes how objectives for the integration of FEPs are addressed by the development of the model.

**Acceptance Criterion 3: Data Uncertainty Is Characterized and Propagated Through the Model Abstraction**

*(1) Models use parameter values, assumed ranges, probability distributions, and bounding assumptions that are technically defensible, and reasonably account for uncertainties and variabilities, and do not result in an under-representation of the risk estimate.*

The development of the individual mathematical formulations for the model is described in the model report (Section 6.5.1) as are the inputs to the model and assumptions needed to use the ASHPLUME model for analysis (Section 6.5.2). Uncertainties associated with changes in igneous processes are included in

ASHPLUME analyses through the use of parameter distributions (Section 6.5.2). The bases for the selection of an appropriate distribution for each uncertain parameter are described in the report (Section 6.5.2). The reasonableness of values and distributions for parameters and their suitability for use are described in Section 6.5.2. Assumptions associated with the appropriateness of the ASHPLUME model are described in Section 5.1, and assumptions associated with specific model parameters are described in Section 5.2. The appropriateness of the base-case model is described in Section 6.3.1, and the consideration of alternative models is documented in Section 6.4.1. The screening of an alternative basis for the selection of ASHPLUME is also documented in Section 6.4.1 (see Table 6-2). Input parameter uncertainty is addressed in Section 4.1.2.

(2) *Parameter uncertainty accounts quantitatively for the uncertainty in parameter values observed in site data and the available literature (i.e., data precision), and the uncertainty in abstracting parameter values to process-level models (i.e., data accuracy).*

Data precision is addressed in the mathematical description of the base case conceptual model (Section 6.5.1) and in the development of the input parameters (Section 6.5.2 and subsections). Data accuracy is addressed by evaluating uncertainties introduced by model abstraction. These uncertainties are explicitly addressed by the results of the model validation exercise (Sections 7.1, 7.2, and 7.3), which shows how well the ASHPLUME model outputs conform to evaluation criteria, including sensitivity of outputs to variations in input parameters (Section 7.2), comparison of model ash thicknesses with observed thicknesses at analogue sites (Section 7.3), and conservation of mass (DOE 2003 [DIRS 166506]) (Section 7.3).

Uncertainties associated with changes in igneous processes are included in ASHPLUME analyses through the use of parameter distributions (Section 6.5.2). The bases for the selection of an appropriate distribution for each uncertain parameter are described in the report (Section 6.5.2). Parameter uncertainty is addressed in Section 4.1.2.

**Acceptance Criterion 4: Model Uncertainty Is Characterized and Propagated Through the Model Abstraction**

(1) *Alternative modeling approaches to volcanic disruption of the waste package are considered and are consistent with available data and current scientific understandings, and the results and limitations are appropriately considered in the abstraction.*

The alternative models that were considered for modeling airborne transport of radionuclides are described in Section 6.4.1, including the screening of an alternative basis for the selection of ASHPLUME (see Table 6-2). The consistency of the ASHPLUME model with data and current scientific understanding is described in Sections 6.3.1 and 6.5.1. Sections 7.1 through 7.3 discuss validation of the model and show how the validation exercises have demonstrated the efficacy of the ASHPLUME

model to represent observed variations in tephra deposit thicknesses at analogue sites. The validation work shows that the model is internally consistent and produces numerical convergence in simulations. Limitations of the ASHPLUME model are discussed in Section 1.3.

*(2) Uncertainties in abstracted models are adequately defined and documented, and effects of these uncertainties are assessed in the total system performance.*

Uncertainties associated with ASHPLUME model outputs are described in Section 8.3, and input parameters and parameter uncertainties are described in Section 4.1.2. Section 7.2 describes the sensitivity analyses that were done to evaluate the response of the ASHPLUME model over the entire range of model input parameter values. The results show that the model is sensitive to variations in eruptive power, wind speed, wind direction, and eruption duration. TSPA sensitivity to parameter variations is beyond the scope of this report.

*(3) Consideration of conceptual model uncertainty is consistent with available site characterization data, laboratory experiments, field measurements, natural analog information and process-level modeling studies; and the treatment of conceptual model uncertainty does not result in an under-representation of the risk estimate.*

The basis of the ASHPLUME conceptual model is described in Section 6.3.1, and the mathematical description of the base-case conceptual model is provided in Section 6.5.1. Uncertainties in the model outputs are described in Section 8.3, and conservatisms included to assure that model outputs to the TSPA do not result in an under representation of risk are described as part of the conceptual model (Section 6.5.2 and subsections).

The alternative models that were considered for modeling airborne transport of radionuclides are described in Section 6.4.1 and are summarized in Section 6.4.3. The screening of an alternative basis for the selection of ASHPLUME is also documented in Section 6.4.1 (see Table 6-2). The consistency of the ASHPLUME model with data and current scientific understanding is described in Sections 6.3.1 and 6.5.1. Sections 7.1 through 7.3 discuss validation of the model and show how the validation exercises have demonstrated the efficacy of the ASHPLUME model to represent observed variations in tephra deposit thicknesses at analogue sites. The validation work shows that the model is internally consistent and produces numerical convergence in simulations. Limitations of the ASHPLUME model are discussed in Section 1.3.

**Acceptance Criterion 5: Model Abstraction Output is Supported by Objective Comparisons**

*(1) Models implemented in the volcanic disruption of waste packages abstraction provide results consistent with output from detailed process-level models and/or empirical observations (laboratory and field testings and/or natural analogs).*

Section 6.2 lists the specific FEPs that are included in the ASHPLUME model. Section 6.3.1 provides a detailed description of the basis for the ASHPLUME conceptual model and the appropriateness of that model for the analysis of airborne transport of radionuclides. Section 6.5.1 provides a detailed description of the mathematical formulation of the base-case conceptual model and the consistency of that formulation with natural processes. Sections 7.1 through 7.3 of the model report discuss validation of the model and show how the validation exercises have shown the efficacy of the ASHPLUME model to represent observed variations in tephra deposit thicknesses at analogue sites. The validation work also shows that the model is internally consistent and produces numerical convergence in simulations.

*(2) Inconsistencies between abstracted models and comparative data are documented, explained, and quantified. The resulting uncertainty is accounted for in the model results.*

The model outputs are described in Section 8.2 and model output uncertainties are described in Section 8.3. Sections 7.1 through 7.3 discuss validation of the model and show how the validation exercises have shown the efficacy of the ASHPLUME model to represent observed variations in tephra deposit thicknesses at analogue sites (Section 7.3). The validation work also shows that the model is internally consistent and produces numerical convergence in simulations.

## B5. NUREG 1804, REV 2, SECTION 2.2.1.3.11.3: INTEGRATED SUBISSUE: AIRBORNE TRANSPORT OF RADIONUCLIDES

**Acceptance Criterion 1: System Description and Model Integration Are Adequate**

*(1) Total system performance assessment adequately incorporates important design features, physical phenomena, and couplings, and uses consistent and appropriate assumptions throughout the airborne transport of radionuclides abstraction process.*

This model report documents the use of the ASHPLUME code to model the airborne transport of radionuclides. This report provides information about the development of the ASHPLUME conceptual model by Suzuki (1983 [DIRS 100489]) (Section 6.3) and describes the consistency of the conceptual model with physical phenomena associated with violent Strombolian eruptions and the development and propagation of an ash cloud downwind of the eruption site followed by deposition of tephra deposits on the ground surface (Section 6.3). This report also documents the consistency between the conceptual model and the ASHPLUME mathematical model used in the TSPA (Section 6.5). A mathematical description of the base case conceptual model is described in Section 6.5.1. The inputs to the model are described in Section 6.5.2.

Model assumptions needed to use the ASHPLUME model are described in Section 5.1, and parameter assumptions are described in Section 5.2. The TSPA code, GoldSim, includes the ASHPLUME code (ASHPLUME V.2.0 dll) as a dynamic link library. Inclusion of ASHPLUME as a DLL ensures that physical phenomena and couplings important to the analysis of airborne transport of radionuclides are consistently and appropriately treated in performance assessment.

(2) *Models used to assess airborne transport of radionuclides are consistent with physical processes generally interpreted from igneous features in the Yucca Mountain region and/or observed at active igneous systems.*

This model report provides information about the basis for the ASHPLUME conceptual model (Suzuki 1983 [DIRS 100489]) in Section 6.3.1. Section 6.3.1 also describes the consistency of the conceptual model with physical phenomena associated with violent Strombolian eruptions and the development and propagation of an ash cloud downwind of the eruption site followed by deposition of tephra deposits on the ground surface. Base-case model inputs and uncertainties and their consistency with igneous features either observed in the Yucca Mountain region or with features observed at analogue igneous systems are described in Section 6.5.2. The bases for the selection of an appropriate distribution for each uncertain parameter are described in this report (Section 6.5.2). Model inputs that are developed and documented in other analyses or models are appropriately identified, described, and cross-referenced.

Alternative models considered are described in Section 6.4.1.

(3) *Models account for changes in igneous processes that may occur from interactions with engineered repository systems.*

The ASHPLUME model does not account for changes in igneous processes that might result from interactions between processes and components of the engineered barrier system. Such interactions are described in other analyses or model reports, as appropriate (e.g., *Dike/Drift Interactions* (BSC 2004 [DIRS 170028]) and *Number of Waste Packages Hit by Igneous Intrusion* (BSC 2005 [DIRS 174066]).

(4) *Guidance in NUREG-1297 and NUREG-1298 (Altman et al. 1988; Altman et al. 1988), or in other acceptable approaches for peer review and data qualification is followed.*

Quality assurance considerations for modeling activities associated with development of the ASHPLUME V.2.0 software (CRWMS M&O 2001 [DIRS 152844]) are described in Section 2. Data, parameters, and other model inputs are described in Section 4.1.

NUREG-1297 describes the generic technical position with respect to the use of peer reviews on high-level waste repository programs. The independent peer review of the ASHPLUME model is described in Section 7.4.1. Additional documentation is provided in Appendix F. The review was done in accordance with the Project procedure, *Peer Review* (AP-2.12Q). NUREG-1298 describes the generic technical

position with respect to qualification of existing data. External sources have provided unqualified data that have been used as direct input to this document. The inputs from these sources are qualified for intended use within the document using the criteria found in LP-SIII.10Q, *Models*. These criteria represent a subset of the methods and attributes required for qualification of data per LP-SIII.2Q-BSC, *Qualification of Unqualified Data*. These methods and attributes are based on those that are presented in NUREG-1298, which are meant to provide "the level of confidence in the data ... commensurate with their intended use.

**Acceptance Criterion 2: Data Are Sufficient for Model Justification**

*(1) Parameter values used in the license application to evaluate airborne transport of radionuclides are sufficient and adequately justified. Adequate descriptions of how the data were used, interpreted, and appropriately synthesized into the parameters are provided.*

Uses of the parameter values are generally described as part of the mathematical description of the base-case model in Section 6.5.1. The development of all model inputs used for the atmospheric dispersal model is discussed in Section 6.5.2. Subsections describe the individual model input parameters and provide detailed technical bases supporting the use of the numerical value or range for each parameter. Model report outputs for the TSPA-LA are described in Section 8.2.

*(2) Data used to model processes affecting airborne transport of radionuclides are derived from appropriate techniques. These techniques may include site-specific field measurements, natural analog investigations, and laboratory experiments.*

The parameter values used as inputs for ASHPLUME V.2.0 dll are described in the model report in Section 4.1, and model outputs are described in Section 8.2. Modeling objectives, the characteristics of the base-case model, consideration of alternative conceptual models, and the basis for the selection of ASHPLUME for modeling airborne transport of radionuclides are discussed in Sections 6.1, 6.3, and 6.4, respectively. The formulation of the mathematical model is described in Section 6.5.1, and the base-case model inputs and their appropriateness are described in Section 6.5.2.

This model report describes the conceptual model, formulation of the mathematical model, identification of parameters, selection of appropriate parameter values or distributions, and discusses the consideration of alternative models. All of these considerations are included in the basis for selection of the ASHPLUME model as appropriate for analyzing the airborne transport of radionuclides for the license application. The alternative models considered are described in Section 6.4.1, and a summary of alternative conceptual models is provided in Section 6.4.3. Section 7.3 of the report discusses validation of the model and shows how the validation exercises have shown the efficacy of the ASHPLUME model to represent observed variations in tephra deposit thicknesses at analogue sites. The validation work also shows that the model is internally consistent and produces numerical convergence in simulations.

These lines of evidence demonstrate that the ASHPLUME model is appropriate to analyze the airborne transport of radionuclides.

*(3) Sufficient data are available to integrate features, events, and processes, relevant to airborne transport of radionuclides into process-level models, including site-specific determination of appropriate interrelationships and parameter correlations.*

FEPs related to the development and use of the ASHPLUME model are discussed in Section 6.2. Table 6-1 includes descriptions of the specific data elements associated with the FEPs associated with the ASHPLUME model and summarizes how objectives for the integration of FEPs are addressed by the development of the model.

**Acceptance Criterion 3: Data Uncertainty is Characterized and Propagated Through the Model Abstraction**

*(1) Models use parameter values, assumed ranges, probability distributions, and bounding assumptions that are technically defensible, reasonably account for uncertainties and variabilities, and do not result in an under-representation of the risk estimate.*

The development of the individual mathematical formulations for the model is described in the model report (Section 6.5.1) as are the inputs to the model and assumptions needed to use the ASHPLUME model for analysis (Section 6.5.2). Uncertainties associated with changes in igneous processes are included in ASHPLUME analyses through the use of parameter distributions (Section 6.5.2). The bases for the selection of an appropriate distribution for each uncertain parameter are described in the report (Section 6.5.2). The reasonableness of values and distributions for parameters and their suitability for use are described in Section 6.5.2. Assumptions associated with the appropriateness of the ASHPLUME model are described in Section 5.1, and assumptions associated with specific model parameters are described in Section 5.2. The appropriateness of the base-case model is described in Section 6.3.1, and the consideration of alternative models is documented in Section 6.4.1. The screening of an alternative basis for the selection of ASHPLUME is also documented in Section 6.4.1 (see Table 6-2). Input parameter uncertainty is addressed in Section 4.1.2.

*(2) Parameter uncertainty accounts quantitatively for the uncertainty in parameter values derived from site data and the available literature (i.e., data precision) and the uncertainty introduced by model abstraction (i.e., data accuracy).*

Data precision is addressed in the mathematical description of the base case conceptual model (Section 6.5.1) and in the development of the input parameters (Section 6.5.2 and subsections). Data accuracy is addressed by evaluating uncertainties introduced by model abstraction. These uncertainties are explicitly addressed by the results of the model validation exercise (Sections 7.1, 7.2, and 7.3), which shows how well the ASHPLUME model outputs conform to evaluation criteria, including sensitivity of outputs to variations in input parameters (Section 7.2),

comparison of model ash thicknesses with observed thicknesses at analogue sites (Section 7.3), and conservation of mass (DOE 2003 [DIRS 166506]) (Section 7.3).

Uncertainties associated with changes in igneous processes are included in ASHPLUME analyses through the use of parameter distributions (Section 6.5.2). The bases for the selection of an appropriate distribution for each uncertain parameter are described in the report (Section 6.5.2). Parameter uncertainty is addressed in Section 4.1.2.

*(3) Where sufficient data do not exist, the definition of parameter values and associated uncertainty is based on appropriate use of expert elicitation conducted in accordance with NUREG-1563 (Kotra et al. 1996). If other approaches are used, the U.S. Department of Energy adequately justifies their use.*

Sufficient data exist to define the parameter values and associated conceptual models needed to model the atmospheric dispersal and deposition of tephra (Section 6.5.2). Expert elicitation has not been used in the definition of parameter values and associated conceptual models.

**Acceptance Criterion 4: Model Uncertainty is Characterized and Propagated Through the Model Abstraction**

*(1) Alternative modeling approaches to airborne transport of radionuclides are considered and are consistem with the available data and current scientific understandings, and the results and limitations are appropriately considered in the abstraction.*

The alternative models that were considered for modeling airborne transport of radionuclides are described in Section 6.4.1, including the screening of an alternative basis for the selection of ASHPLUME (see Table 6-2). The consistency of the ASHPLUME model with data and current scientific understanding is described in Sections 6.3.1 and 6.5.1. Sections 7.1 through 7.3 discuss validation of the model and show how the validation exercises have demonstrated the efficacy of the ASHPLUME model to represent observed variations in tephra deposit thicknesses at analogue sites. The validation work shows that the model is internally consistent and produces numerical convergence in simulations. Limitations of the ASHPLUME model are discussed in Section 1.3.

*(2) Uncertainties in abstracted models are adequately defined and documented, and effects of these uncertainties are assessed in the total system performance assessment.*

Uncertainties associated with ASHPLUME model outputs are described in Section 8.3, and input parameters and parameter uncertainties are described in Section 4.1.2. Section 7.2 describes the sensitivity analyses that were done to evaluate the response of the ASHPLUME model over the entire range of model input parameter values. The results show that the model is sensitive to variations in eruptive power, wind speed, wind direction, and eruption duration. TSPA sensitivity to parameter variations is beyond the scope of this report.

*(3) Consideration of conceptual model uncertainty is consistent with available site characterization data, laboratory experiments, field measurements, natural analog information, and process-level modeling studies; and the treatment of conceptual model uncertainty does not result in an under representation of the risk estimate.*

The basis of the ASHPLUME conceptual model is described in Section 6.3.1, and the mathematical description of the base-case conceptual model is provided in Section 6.5.1. Uncertainties in the model outputs are described in Section 8.3, and conservatisms included to assure that model outputs to the TSPA do not result in an under representation of risk are described as part of the conceptual model (Section 6.5.2 and subsections).

The alternative models that were considered for modeling airborne transport of radionuclides are described in Section 6.4.1 and are summarized in Section 6.4.3. The screening of an alternative basis for the selection of ASHPLUME is also documented in Section 6.4.1 (see Table 6-2). The consistency of the ASHPLUME model with data and current scientific understanding is described in Sections 6.3.1 and 6.5.1. Sections 7.1 through 7.3 discuss validation of the model and show how the validation exercises have demonstrated the efficacy of the ASHPLUME model to represent observed variations in tephra deposit thicknesses at analogue sites. The validation work shows that the model is internally consistent and produces numerical convergence in simulations. Limitations of the ASHPLUME model are discussed in Section 1.3.

**Acceptance Criterion 5: Model Abstraction Output is Supported by Objective Comparisons**

*(1) Models implemented in the airborne transport of radionuclides abstraction provide results consistent with output from detailed process-level models and/or empirical observations (laboratory and field testings and/or natural analogs).*

Section 6.2 lists the specific FEPs that are included in the ASHPLUME model. Section 6.3.1 provides a detailed description of the basis for the ASHPLUME conceptual model and the appropriateness of that model for the analysis of airborne transport of radionuclides. Section 6.5.1 provides a detailed description of the mathematical formulation of the base-case conceptual model and the consistency of that formulation with natural processes. Sections 7.1 through 7.3 of the model report discuss validation of the model and show how the validation exercises have shown the efficacy of the ASHPLUME model to represent observed variations in tephra deposit thicknesses at analogue sites. The validation work also shows that the model is internally consistent and produces numerical convergence in simulations.

*(2) Inconsistencies between abstracted models and comparative data are documented, explained, and quantified. The resulting uncertainty is accounted for in the model results.*

The model outputs are described in Section 8.2 and model output uncertainties are described in Section 8.3. Sections 7.1 through 7.3 discuss validation of the model and

show how the validation exercises have shown the efficacy of the ASHPLUME model to represent observed variations in tephra deposit thicknesses at analogue sites (Section 7.3). The validation work also shows that the model is internally consistent and produces numerical convergence in simulations.

## B6. NUREG 1804, REV 2, SECTION 2.2.1.3.13.3: INTEGRATED SUBISSUE: REDISTRIBUTION OF RADIONUCLIDES IN SOIL

The Yucca Mountain Review Plan (NUREG-1804, NRC 2003 [DIRS 163274]) associates the integrated subissue of redistribution of radionuclides in soil with the requirements listed in 10 CFR 63.114(a)-(c), (e)-(g), and 63.305 [DIRS 173273] as they relate to the redistribution of radionuclides in soil abstraction. NUREG-1804 (NRC 2003 [DIRS 163274], Section 2.2.1.3.13.3) describes the acceptance criteria that the NRC will use to evaluate the adequacy of information addressing the redistribution of radionuclides in soil in the license application. The following discussion provides a summary of how the information in this model report addresses those criteria that are associated with the development and use of the ash redistribution conceptual model.

**Acceptance Criterion 1: System Description and Model Integration Are Adequate**

*(1) Total system performance assessment adequately incorporates important features, physical phenomena and couplings between different models, and uses consistent and appropriate assumptions throughout the abstraction of redistribution of radionuclides in the soil abstraction process.*

Information in this model report describes the conceptual model for ash redistribution, the validity of the model, and providing model outputs for use in the TSPA-LA. Features, events, and processes included in the model are described in Section 6.2 and discussed in more detail in Table 6-1. The basis of the ash redistribution model is described in Section 6.3.2. The ash redistribution conceptual model is described in Section 6.6, and the two outcomes used to bound ash redistribution in the Yucca Mountain area are described in Sections 6.6.6 and 6.6.7. A general description of the tephra dilution process is provided in Section 6.6.3, and rates of surficial processes are described in Section 6.6.4. Assumptions associated with the use of the model are described in Sections 5.1.3 through 5.1.9, and results of the ash redistribution model are described in Section 6.7.2 and Table 6-5. Model report outputs are described in Section 8.2. Output uncertainties associated with the ash redistribution model are described in Section 8.3.

It is beyond the scope of this report to document the use of model outputs and abstractions in the TSPA-LA.

*(2) The total system performance assessment model abstraction identified and describes aspects of redistribution of radionuclides in soil that are important to repository performance, including the technical bases for these descriptions. For example, the abstraction should include modeling of the deposition of contaminated material in the soil and the determination of the depth distribution of the deposited radionuclides.*

Output from the ASHPLUME model provides estimates of the primary amount of contaminated ash in terms of concentration of waste per unit area ($g/cm^2$) (Table 6-4). The ash redistribution model abstraction is described in Section 6.7.2, and assumptions used in the model are documented in Sections 5.1.3 though 5.1.9.

*(3) Relevant site features, events, and processes have been appropriately modeled in the abstraction of redistribution of radionuclides, from surface processes, and sufficient technical bases are provided.*

Site FEPs included in the model are described in Section 6.2. The technical bases for the included FEPs are described in detail in Table 6-1.

*(4) Guidance in NUREG-1297 and NUREG-1298 (Altman et al. 1988; Altman et al. 1988), or other acceptable approaches for peer reviews is followed.*

NUREG-1297 describes the generic technical position with respect to the use of peer reviews on high-level waste repository programs. The use of independent peer reviews of the ash redistribution conceptual model is described in Section 7.4.2. These reviews were done in accordance with the Project procedure, *Peer Review* (AP-2.12Q), and are found in Appendix G. NUREG-1298 describes the generic technical position with respect to qualification of existing data. External sources have provided unqualified data that have been used as direct input to this document. The inputs from these sources are qualified for intended use within the document using the criteria found in LP-SIII.10Q-BSC, *Models*. These criteria represent a subset of the methods and attributes required for qualification of data per LP-SIII.2Q-BSC, *Qualification of Unqualified Data*. These methods and attributes are based on those that are presented in NUREG-1298, which are meant to provide "the level of confidence in the data ... commensurate with their intended use."

**Acceptance Criterion 2: Data Are Sufficient for Model Justification**

*(1) Behavioral, hydrological, and geochemical values used in the license application are adequately justified (e.g., irrigation and precipitation rates, erosion rates, radionuclide solubility values, etc.). Adequate descriptions of how the data were used, interpreted, and appropriately synthesized into the parameters are provided.*

Data sources that provided inputs for the development of parameters used in the ash redistribution conceptual model are identified in Section 4.1.1. The appropriateness of the data is also discussed. A general description of tephra redistribution processes is provided in Sections 6.3.2 and 6.6.3. Rates of surficial processes that are needed to support model development and use are documented in Section 6.6.4, and the $^{137}Cs$ data, used to identify a time stratigraphic marker in the surficial deposits and provide a

proxy for determining the soil depths that fine particles and associated radionuclides from waste could penetrate, are described in Section 6.6.4. Analogue studies to support the ash redistribution conceptual model are described in Section 7.3, and the results of an independent review of the ash redistribution model are described in Section 7.4.2 (see Appendix G for the reviews). Model output uncertainties associated with the ash redistribution conceptual model are described in Section 8.3. Outputs from the ash redistribution conceptual model are described in Section 6.7.2, and 8.2, and listed in Table 6-5. Guidelines for using the outputs in the TSPA model are also provided in Section 6.7.2.

*(2) Sufficient data (e.g., field laboratory, and natural analog data) are available to adequately define relevant parameters and conceptual models necessary for developing the abstraction of redistribution of radionuclides in soil in the total system performance assessment.*

Data sources that provide inputs for the development of parameters used in the ash redistribution conceptual model are identified in Section 4.1.1. The appropriateness of the data is also discussed. Rates of surficial processes that are needed to support model development and use are documented in Section 6.6.4, and the $^{137}Cs$ data that form a time stratigraphic marker in the surficial deposits and provide a proxy for determining the soil depths that fine particles and associated radionuclides from waste could penetrate are described in Section 6.6.4. Table 6-5 lists the TSPA factors that are provided by the ash redistribution conceptual model. Guidelines for using the outputs in the TSPA model are provided in Section 6.7.2.

**Acceptance Criterion 3: Data Uncertainty Is Characterized and Propagated Through the Model Abstraction**

*(1) Models use parameter values, assumed ranges, probability distributions, and bounding assumptions that are technically defensible, reasonably account for uncertainties and variabilities, do not result in an under-representation of the risk estimate, and are consistent with the characteristics of the reasonably maximally exposed individual in 10 CFR Part 63.*

Inputs for the ash redistribution conceptual model and the appropriateness of the inputs for use in the model are described in Section 4.1.1. Assumptions are described in Sections 5.1.3 through 5.1.9. Analogue studies undertaken to ensure the model appropriately considers sedimentary processes that affect tephra sheets are described in Section 7.3. Uncertainties in the model outputs are described in Section 8.3, and conservatisms included to assure that model outputs to the TSPA do not result in an under representation of risk are described as part of the conceptual model in Sections 6.3.2 and 6.6.2. However, the representation of risk is a TSPA function that is beyond the scope of this report. The method to incorporate conservatism is development of two model outcomes that bound the mechanisms of ash redistribution in the Yucca Mountain area. These outcomes are described in Sections 6.6.6 and 6.6.7, respectively.

The development and use of the ash redistribution conceptual model is not dependent on consideration of the characteristics of the reasonably maximally exposed individual. Characteristics of the RMEI are provided in *Characteristics of the Receptor for the Biosphere Model* (BSC 2005 [DIRS 172827]), which defines values for biosphere model parameters that are related to the dietary, lifestyle, and dosimetric characteristics of the receptor. Agricultural and environmental input parameters for the biosphere model are described in the report, *Agricultural and Environmental Input Parameters for the Biosphere Model* (BSC 2004 [DIRS 169673], Section 6).

(2) *The technical bases for the parameter values and ranges in the TSPA abstraction are consistent with data from the Yucca Mountain region (e.g., Amargosa Valley survey, Cannon Center for Survey Research 1997), studies of surface processes in the Fortymile Wash drainage basin, applicable laboratory testings, or other valid sources of data. For example, soil types, crop types, plow depths, and irrigation rates should be consistent with current farming practices, and data on the airborne particulate concentration should be based on the resuspension of appropriate material in a climate and level of disturbance similar to that which is expected to be found at the location of the reasonably maximally exposed individual during the compliance time period.*

The ash redistribution conceptual model is based on erosion-rate data, soil-profile data, and surficial-processes information collected in the Yucca Mountain area, including sample locations in Fortymile Wash and surrounding the Lathrop Wells cone. Figure 6-3 is an illustration of the conceptual model based on information from Fortymile Wash that shows redistribution of tephra toward a RMEI. Sample locations and study areas are shown in Figures 6-1 and 7-3. Figure 6-4 is an example of a $^{137}Cs$ profile in Fortymile Wash that illustrates the effects of erosion. Rates of surficial processes in Fortymile Wash are described in Section 6.6.4, and the cesium study on the Fortymile Wash alluvial fan is described in Section 6.6.4.

The development and use of the ash redistribution conceptual model is not dependent on consideration of the characteristics of the RMEI. Characteristics of the RMEI are provided in *Characteristics of the Receptor for the Biosphere Model* (BSC 2005 [DIRS 172827]), which defines values for biosphere model parameters that are related to the dietary, lifestyle, and dosimetric characteristics of the receptor. Agricultural and environmental input parameters for the biosphere model are described in the report, *Agricultural and Environmental Input Parameters for the Biosphere Model* (BSC 2004 [DIRS 169673]).

*(3) Uncertainty is adequately represented in parameters for conceptual models, process models, and alternative conceptual models considered in developing the total system performance assessment abstraction of redistribution of radionuclides in soil, either through sensitivity analyses, conservative limits, or bounding values supported by data, as necessary. Correlations between input values are appropriately established in the total system performance assessment.*

Model outputs that provide inputs (factors) for the TSPA are described in Table 6-5. As can be seen from Table 6-5, uncertainties in soil redistribution factors are provided as distributions for use in the TSPA. The ash redistribution conceptual model is described in Sections 6.3.1 and 6.6.3. Uncertainties in the model outputs are described in Section 8.3, and conservatisms included to assure that model outputs to the TSPA do not result in an under representation of risk are described as part of the conceptual model in Sections 6.3.2 and 6.6.2. However, the representation of risk is a TSPA function that is beyond the scope of this report. The method to incorporate conservatism is development of two model outcomes that bound the mechanisms of ash redistribution in the Yucca Mountain area. These outcomes are described in Sections 6.6.6 and 6.6.7, respectively. A general description of tephra redistribution processes is provided in Section 6.6.3, and effects of processes such as erosion and eolian inflation on $^{137}$Cs values are described in Section 6.6.4.

Section 1.3 discusses the limitations of the ash redistribution conceptual model.

*(4) Parameters or models that most influence repository performance based on the performance measure and time period of compliance, specified in 10 CFR Part 63, are identified.*

Section 8.2 notes that five factors related to the ash redistribution conceptual model are important to repository performance. These factors are described in Section 6.7.2 and are listed in Table 6-5. Guidance is also provided in Section 6.7.2 for using the factors in the TSPA model to best represent the factors given in this report.

**Acceptance Criterion 4: Model Uncertainty is Characterized and Propagated Through the Model Abstraction**

*(1) Alternative modeling approaches of features, events, and processes are considered and are consistent with available data, and current scientific understanding, and the results and limitations are appropriately considered in the abstraction.*

Consideration of an alternative conceptual model for ash redistribution is described in Section 6.4.2. Features, events, and processes included in the ash redistribution conceptual model are described in Section 6.2, and Table 6-1 provides details about the disposition of FEP 1.2.04.07.0C, Ash Redistribution Via Soil and Sediment Transport. A general description of tephra redistribution processes is provided in Section 6.6.3. Rates of surficial processes that are needed to support model development and use are documented in Section 6.6.4, and the $^{137}$Cs data used to identify a time stratigraphic marker in the surficial deposits and provide a proxy for determining the soil depths that fine particles and associated radionuclides from waste

could penetrate, are described in Section 6.6.4. Descriptions of how the data are used are provided in Section 6.7.2. Analogue studies to support the ash redistribution conceptual model are described in Section 7.3, and the results of an independent review of this model are described in Section 7.4.2. Uncertainties associated with the ash redistribution conceptual model outputs are described in Section 8.3. Model limitations are described in Section 1.3.

(2) *Sufficient evidence is provided that alternative conceptual models of features, events, and processes have been considered; that the preferred models (if any) are consistent with available data (e.g., field, laboratory, and natural analog) and current scientific understanding; and that the effect on total system performance assessment of uncertainties from these alternative conceptual models has been evaluated.*

The ash redistribution conceptual model is new, but consideration of alternative conceptual models for ash redistribution is discussed in Section 6.4.2. Development of the ash redistribution conceptual model is based on analogue data from sites at and near Yucca Mountain (Sections 6.3.2, 6.6.4, and 6.6.5). Features, events, and processes included in the ash redistribution conceptual model are described in Section 6.2, and Table 6-1 provides details about the disposition of **FEP** 1.2.04.07.0C, Ash Redistribution Via Soil and Sediment Transport. A general description of tephra redistribution processes is provided in Section 6.6.3.

Rates of surficial processes that are needed to support model development and use are documented in Section 6.6.4, and the $^{137}Cs$ data used to identify a time stratigraphic marker in the surficial deposits and provide a proxy for determining the soil depths that fine particles and associated radionuclides from waste could penetrate are described in Section 6.6.4. Descriptions of how the data are used are provided in Section 6.7.2. Analogue studies to support the ash redistribution conceptual model are described in Section 7.3. Uncertainties associated with the ash redistribution conceptual model outputs are described in Section 8.3. Model limitations are described in Section 1.3.

(3) *Consideration of conceptual model uncertainty is consistent with available site characterization data, laboratory experiments, field measurements, natural analog information and process-level modeling studies; and the treatment of conceptual model uncertainty does not result in an under-representation of the risk estimate.*

Inputs for the ash redistribution conceptual model and the appropriateness of the inputs for use in the model are described in Section 4.1.1. Assumptions are described in Sections 5.1.3 through 5.1.9. Analogue studies undertaken in the Yucca Mountain area to ensure the model appropriately considers sedimentary processes that affect tephra sheets are described in Section 7.3. Uncertainties in the model outputs are described in Section 8.3, and conservatisms included to assure that model outputs to the TSPA do not result in an under representation of risk are described as part of the conceptual model in Sections 6.3.2 and 6.6.2.

**Acceptance Criterion 5: Model Abstraction Output Is Supported by Objective Comparisons**

*(1) Models implemented in the abstraction provide results consistent with output from detailed process-level models and/or empirical observations (e.g., laboratory testing, field measurements, and/or natural analogs).*

Inputs for the ash redistribution conceptual model and the appropriateness of the inputs for use in the model are described in Section 4.1.1. Assumptions are described in Sections 5.1.3 through 5.1.9. Analogue studies undertaken in the Yucca Mountain area to ensure the model appropriately considers sedimentary processes that affect tephra sheets are described in Section 7.3.Model outputs are described in Section 8.2, and uncertainties associated with the model outputs are described in Section 8.3.

INTENTIONALLY LEFT BLANK

# APPENDIX C

# SENSITIVITY STUDIES

# APPENDIX C
# SENSITIVITY STUDIES

Sensitivity analyses were performed both to ensure that the ASHPLUME model operated over the parameter ranges selected and to demonstrate that there were not limitations in model validity due to numerical constraints (Keating 2005 [DIRS 173850], pp. 96 to 107). The sensitivity analyses were performed by varying the value of the following input parameters: eruptive power, mean ash particle diameter, ash particle diameter standard deviation, column diffusion constant (beta), initial rise velocity, wind speed, wind direction, eruption duration, and waste incorporation ratio. The range for each of these parameters is provided in Table 8-2. Values were chosen for the sensitivity analyses based on scientific judgment to evaluate the entire range of each parameter, and values for non-varying parameters were set at base-case values (Table C-12).

Additional sensitivity analyses were performed to evaluate the effect of the alternative waste particle size distribution developed in Appendix J and the effect of additional waste mass available due to lateral magma breakout scenarios.

Sensitivity analyses results are presented in this appendix in the form of tables and graphs that display the varying parameter values and calculated values for ash and fuel deposition ($g/cm^2$) at the RMEI location. These analyses were originally documented in Keating (2005 [DIRS 173850], pp. 96 to 107) and Keating (2005 [DIRS 174988], pp. 8 to 17) and the work has been brought forward and presented in this Appendix.

Figure C-1 shows the sensitivity of ash and fuel concentration to eruptive power. As power increases, the ash deposition 18 km downwind increases linearly as would be expected because of increased mass flux according to Equation 6-7b. The fuel concentration also increases because the increased eruptive column height resulting from the increased power of eruption encounters higher wind speeds to transport the ash-fuel mixture farther downwind toward the 18 km receptor location.

Figure C-2 shows the sensitivity of ash and fuel concentration to mean ash particle diameter and Figure C-3 shows sensitivity to mean ash particle diameter standard deviation. Those two figures show little sensitivity of ash concentration to these two parameters. However, fuel concentration increases by more than a factor of two over the parameter ranges. The cause of the dip in the ash curve in Figure C-3 is undetermined; however, it does not occur in the fuel concentration, which is what affects dose.

Figure C-4 shows the sensitivity of ash and fuel concentration to the column diffusion constant (Beta). Both ash and fuel concentration monotonically decrease as Beta increases, however the change is less than 10 percent. The Beta parameter, in effect, is related to the buoyancy of particles in the eruptive column and determines how high most particles will travel before exiting the column (see Section 6.5.3.2).

Figure C-5 shows the sensitivity of ash and fuel concentration to the initial rise velocity. The figure shows that ash and fuel concentration are not very sensitive to this parameter at values less

than about 1,000 cm/s. Above that value, ash and fuel concentrations at 18 km increase significantly.

Figure C-6 shows the sensitivity of ash and fuel concentration to wind speed. In general, as wind speed increases, the concentration at 18 km downwind would be expected to increase. Figure C-6 shows the expected response. Figure C-7 shows the sensitivity to wind direction of ash and fuel concentration at 18 km due south. This figure shows the expected response of maximum concentration when the wind is blowing directly towards the receptor and minimum concentration when wind is blowing directly away from the receptor.

Figure C-8 shows the sensitivity of ash and fuel concentration to the eruption duration. Ash concentration increases linearly with eruption duration because of the linear relationship between eruption volume and duration (Equation 6-7c). The fuel concentration in terms of $g/cm^2$ deposited on the surface remains constant because the mass of fuel available for transport was held constant.

Figure C-9 shows the sensitivity of ash and fuel concentration to waste incorporation ratio. Ash concentration is unaffected because this parameter only affects the amount of fuel carried with the ash and not the calculation of ash itself. Fuel concentrations vary by a factor of 3 across the range analyzed, following the decreasing capacity for fuel/ash particle attachment with increasing values of waste incorporation ratio (Section 6.5.1).

Figure C-10 shows the sensitivity of ash and fuel concentration to waste mass available for transport, related to the number of waste packages hit by the development of an eruptive conduit. The median value of waste packages hit, 5 (DTN: MO0504MWDNUMWP.001 [DIRS 173521]), results in a waste concentration of $2.8\times10^{-6}$ $g/cm^2$ at the RMEI location. Waste concentrations at the RMEI location increase by a factor of 8 as the number of waste packages increases to 40, the 95th percentile value from (DTN: MO0504MWDNUMWP.001 [DIRS 173521]). An increase to 120 waste packages, representing the evacuation of an entire drift, results in a 24-fold increase in waste concentration at the RMEI location. The ash concentration remains constant because the variation in number of waste packages hit does not affect the calculation of ash concentration.

Figure C-11 shows the sensitivity of ash and fuel concentration to waste particle size. The concentration of fuel calculated at the RMEI location decreases by 14 percent from the base case particle size distribution (min=0.0001, mode=0.0030, max=0.0500cm) to the alternative waste particle size distribution developed in Appendix J (0.0001, 0.0013, 0.2000 cm). The ash concentration remains constant because the variation in waste particle size parameters does not affect the calculation of ash concentration.

Table C-1. Sensitivity of Calculated Ash and Fuel Concentration to Eruptive Power

| Power (W) | Calculated Ash Deposition ($g/cm^2$) | Calculated Fuel Deposition ($g/cm^2$) |
|---|---|---|
| 6.17E+08 | 3.33E-02 | 4.57E-06 |
| 1.52E+09 | 8.59E-02 | 6.74E-06 |
| 3.73E+09 | 2.22E-01 | 7.26E-06 |
| 9.18E+09 | 5.75E-01 | 7.81E-06 |
| 2.26E+10 | 1.49E+00 | 8.41E-06 |
| 5.55E+10 | 3.89E+00 | 9.11E-06 |
| 1.37E+11 | 1.02E+01 | 9.89E-06 |
| 3.36E+11 | 2.68E+01 | 1.08E-05 |
| 8.26E+11 | 7.14E+01 | 1.19E-05 |
| 2.03E+12 | 1.89E+02 | 1.31E-05 |
| 5.00E+12 | 5.07E+02 | 1.44E-05 |

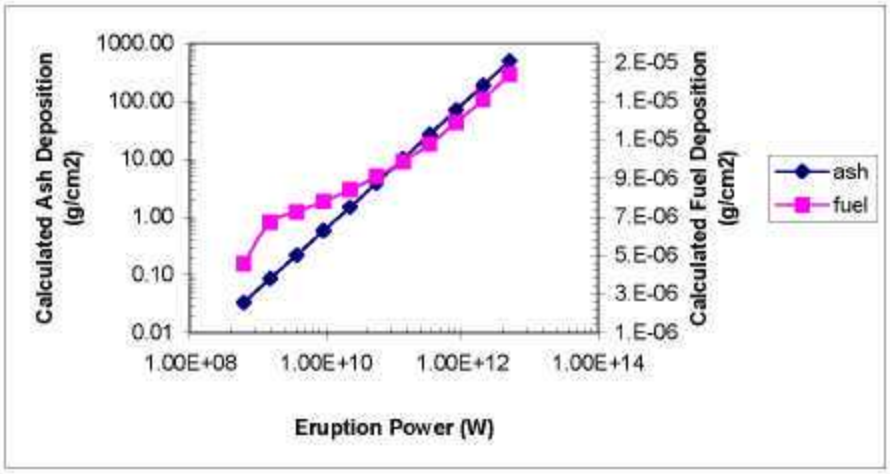


Figure C-1. Sensitivity of Calculated Ash and Fuel Concentration to Eruptive Power

Table C-2. Sensitivity of Calculated Ash and Fuel Concentration to Mean Ash Particle Diameter

| Mean Ash Particle Diameter (cm) | Calculated Ash Deposition ($g/cm^2$) | Calculated Fuel Deposition ($g/cm^2$) |
|---|---|---|
| 0.00100 | 3.32E+00 | 2.58E-06 |
| 0.00158 | 3.54E+00 | 3.03E-06 |
| 0.00251 | 3.72E+00 | 3.53E-06 |
| 0.00398 | 3.88E+00 | 4.11E-06 |
| 0.00631 | 3.95E+00 | 4.74E-06 |
| 0.01000 | 3.97E+00 | 5.47E-06 |
| 0.01585 | 3.93E+00 | 6.27E-06 |
| 0.02512 | 3.83E+00 | 7.16E-06 |
| 0.03981 | 3.68E+00 | 8.18E-06 |
| 0.06310 | 3.47E+00 | 9.27E-06 |
| 0.10000 | 3.24E+00 | 1.05E-05 |

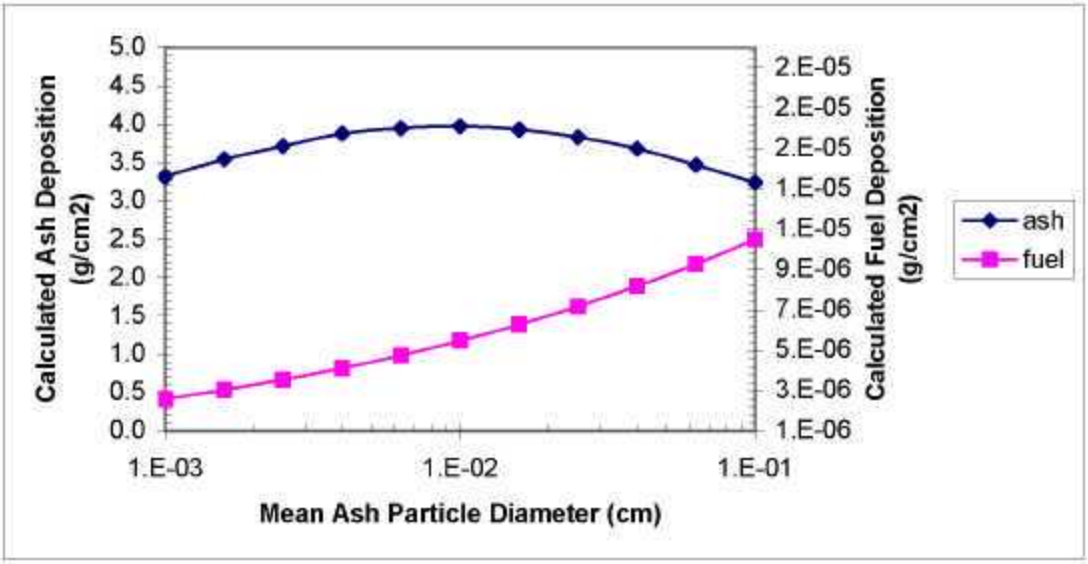


Figure C-2. Sensitivity of Calculated Ash and Fuel Concentration to Mean Ash Particle Diameter

Table C-3. Sensitivity of Calculated Ash and Fuel Concentration to Ash Particle Diameter Standard Deviation

| Ash Particle Diameter Standard Deviation (log (cm)) | Calculated Ash Deposition ($g/cm^2$) | Calculated Fuel Deposition ($g/cm^2$) |
|---|---|---|
| –1.9 | 3.08E+00 | 6.31E–06 |
| –1.84 | 3.15E+00 | 6.70E–06 |
| –1.78 | 3.24E+00 | 7.18E–06 |
| –1.72 | 3.01E+00 | 7.71E–06 |
| –1.66 | 3.43E+00 | 8.33E–06 |
| –1.6 | 3.52E+00 | 9.03E–06 |
| –1.54 | 3.62E+00 | 9.85E–06 |
| –1.48 | 3.73E+00 | 1.09E–05 |
| –1.42 | 3.83E+00 | 1.20E–05 |
| –1.36 | 3.96E+00 | 1.35E–05 |
| –1.3 | 4.06E+00 | 1.52E–05 |

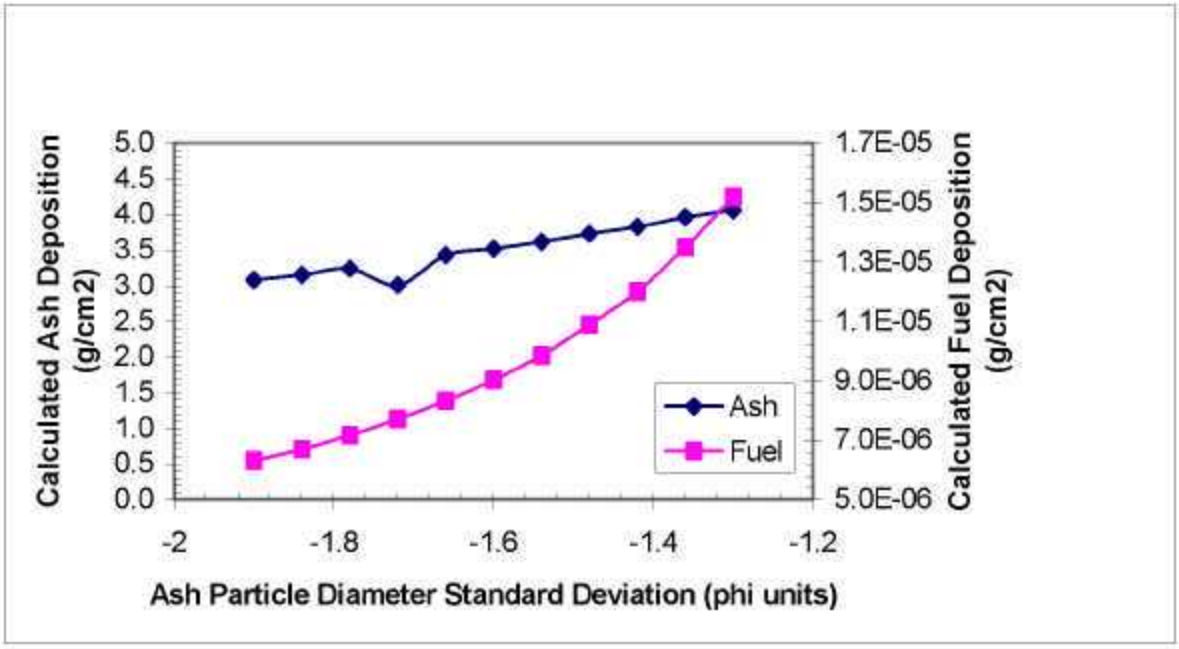


Figure C-3. Sensitivity of Calculated Ash and Fuel Concentration to Ash Particle Diameter Standard Deviation

Table C-4. Sensitivity of Calculated Ash and Fuel Concentration to Column Diffusion Constant (Beta)

| Column Diffusion Constant (Beta) | Calculated Ash Deposition ($g/cm^2$) | Calculated Fuel Deposition ($g/cm^2$) |
|---|---|---|
| 0.0100 | 3.90E+00 | 9.69E-06 |
| 0.0148 | 3.89E+00 | 9.67E-06 |
| 0.0219 | 3.87E+00 | 9.64E-06 |
| 0.0323 | 3.84E+00 | 9.60E-06 |
| 0.0478 | 3.81E+00 | 9.56E-06 |
| 0.0707 | 3.77E+00 | 9.49E-06 |
| 0.1046 | 3.72E+00 | 9.40E-06 |
| 0.1546 | 3.66E+00 | 9.29E-06 |
| 0.2287 | 3.58E+00 | 9.15E-06 |
| 0.3381 | 3.49E+00 | 8.98E-06 |
| 0.5000 | 3.39E+00 | 8.79E-06 |

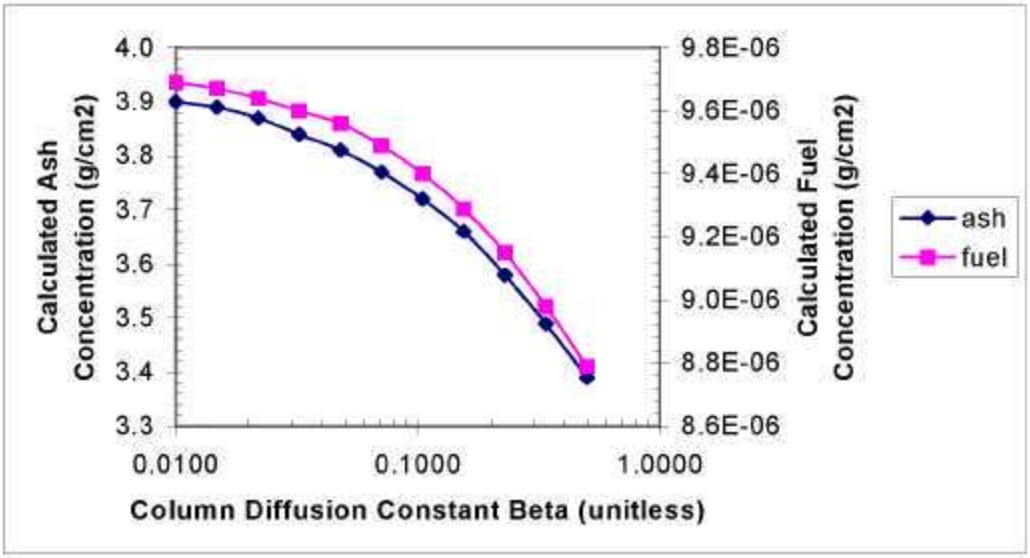


Figure C-4. Sensitivity of Calculated Ash and Fuel Concentration to Column Diffusion Constant (Beta)

Table C-5. Sensitivity of Calculated Ash and Fuel Concentration to Initial Rise Velocity

| Initial Rise Velocity (cm/s) | Calculated Ash Deposition ($g/cm^2$) | Calculated Fuel Deposition ($g/cm^2$) |
|---|---|---|
| 1 | 3.90E+00 | 9.69E-06 |
| 3 | 3.85E+00 | 9.62E-06 |
| 7 | 3.78E+00 | 9.51E-06 |
| 17 | 3.66E+00 | 9.29E-06 |
| 43 | 3.46E+00 | 8.91E-06 |
| 110 | 3.22E+00 | 8.44E-06 |
| 280 | 3.07E+00 | 8.22E-06 |
| 717 | 3.28E+00 | 8.95E-06 |
| 1,834 | 3.98E+00 | 1.10E-05 |
| 4,691 | 4.68E+00 | 1.31E-05 |
| 12,000 | 5.07E+00 | 1.43E-05 |

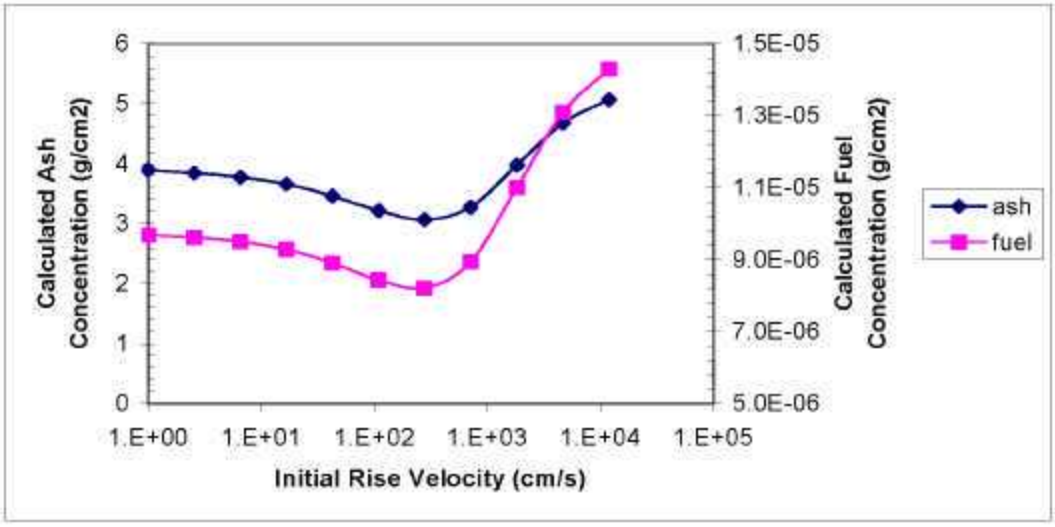


Figure C-5. Sensitivity of Calculated Ash and Fuel Concentration to Initial Rise Velocity

Table C-6. Sensitivity of Calculated Ash and Fuel Concentration to Wind Speed

| Wind Speed (cm/s) | Calculated Ash Deposition ($g/cm^2$) | Calculated Fuel Deposition ($g/cm^2$) |
|---|---|---|
| 0 | 2.67E-01 | 6.20E-07 |
| 566 | 4.26E+00 | 1.10E-05 |
| 1,132 | 1.28E+01 | 3.51E-05 |
| 1,698 | 2.43E+01 | 6.92E-05 |
| 2,264 | 3.20E+01 | 9.47E-05 |
| 2,830 | 5.32E+01 | 1.56E-04 |
| 3,396 | 7.83E+01 | 2.27E-04 |
| 3,962 | 8.56E+01 | 2.54E-04 |
| 4,528 | 1.00E+02 | 2.99E-04 |
| 5,094 | 1.16E+02 | 3.45E-04 |
| 5,660 | 1.34E+02 | 4.08E-04 |

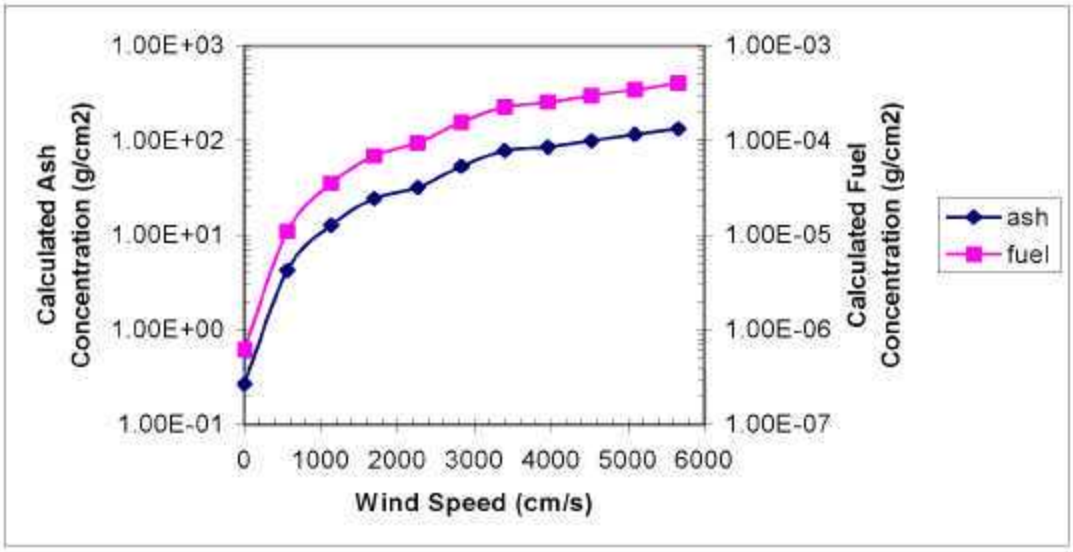


Figure C-6. Sensitivity of Calculated Ash and Fuel Concentration to Wind Speed

Table C-7. Sensitivity of Calculated Ash and Fuel Concentration to Wind Direction

| Wind Direction (degrees) | Calculated Ash Deposition ($g/cm^2$) | Calculated Fuel Deposition ($g/cm^2$) |
|---|---|---|
| –150 | 4.41E–02 | 1.06E–07 |
| –117 | 9.75E–01 | 2.48E–06 |
| –84 | 3.29E+00 | 8.42E–06 |
| –51 | 3.16E–01 | 7.93E–07 |
| –18 | 1.85E–02 | 4.26E–08 |
| 15 | 4.49E–03 | 9.43E–09 |
| 48 | 2.40E–03 | 4.78E–09 |
| 81 | 1.90E–03 | 3.72E–09 |
| 114 | 2.03E–03 | 4.00E–09 |
| 147 | 3.00E–03 | 6.08E–09 |
| 180 | 7.41E–03 | 1.61E–08 |

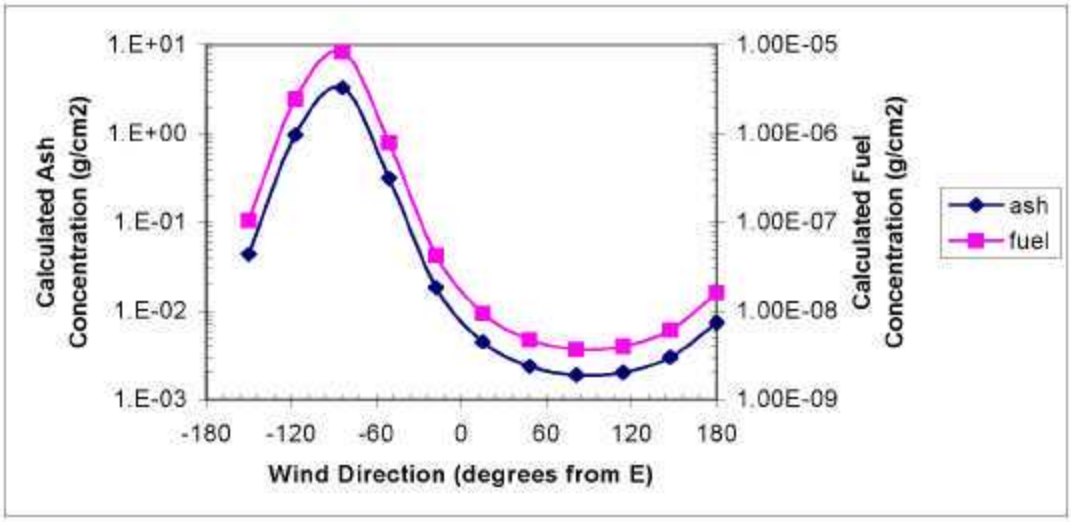


Figure C-7. Sensitivity of Calculated Ash and Fuel Concentration to Wind Direction

Table C-8. Sensitivity of Calculated Ash and Fuel Concentration to Eruption Duration

| Eruption Duration (s) | Calculated Ash Deposition ($g/cm^2$) | Calculated Fuel Deposition ($g/cm^2$) |
|---|---|---|
| 8.64E+04 | 1.18E-01 | 9.03E-06 |
| 1.33E+05 | 1.81E-01 | 9.03E-06 |
| 2.05E+05 | 2.79E-01 | 9.03E-06 |
| 3.16E+05 | 4.30E-01 | 9.03E-06 |
| 4.86E+05 | 6.61E-01 | 9.03E-06 |
| 7.48E+05 | 1.02E+00 | 9.03E-06 |
| 1.15E+06 | 1.56E+00 | 9.03E-06 |
| 1.77E+06 | 2.41E+00 | 9.03E-06 |
| 2.73E+06 | 3.71E+00 | 9.03E-06 |
| 4.21E+06 | 5.73E+00 | 9.03E-06 |
| 6.48E+06 | 8.81E+00 | 9.03E-06 |

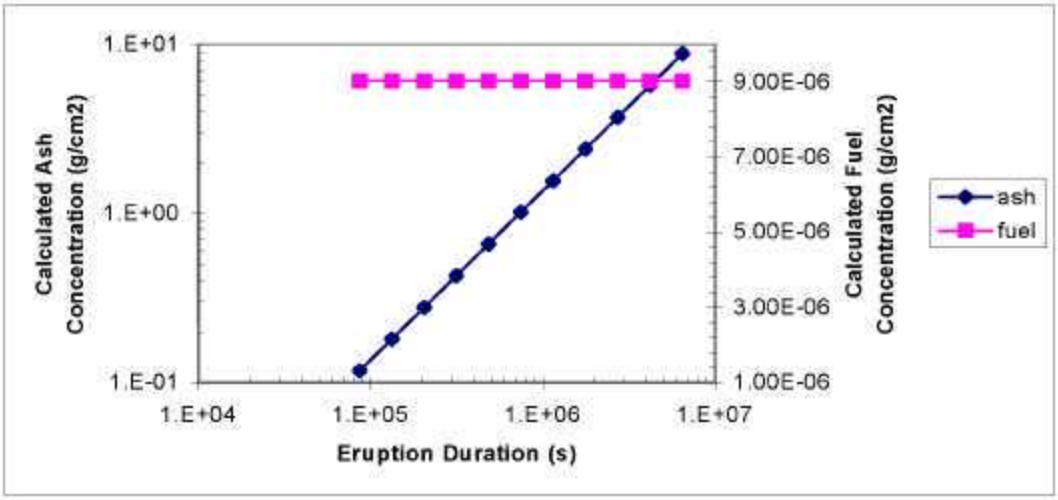


Figure C-8. Sensitivity of Calculated Ash and Fuel Concentration to Eruption Duration

Table C-9. Sensitivity of Calculated Ash and Fuel Concentration to Waste Incorporation Ratio

| Waste Incorporation Ratio | Calculated Ash Deposition ($g/cm^2$) | Calculated Fuel Deposition ($g/cm^2$) |
|---|---|---|
| 0.1 | 3.52E+00 | 2.23E-06 |
| 0.2 | 3.52E+00 | 2.13E-06 |
| 0.3 | 3.52E+00 | 2.01E-06 |
| 0.4 | 3.52E+00 | 1.87E-06 |
| 0.5 | 3.52E+00 | 1.72E-06 |
| 0.6 | 3.52E+00 | 1.55E-06 |
| 0.7 | 3.52E+00 | 1.37E-06 |
| 0.8 | 3.52E+00 | 1.19E-06 |
| 0.9 | 3.52E+00 | 1.01E-06 |
| 1.0 | 3.52E+00 | 8.41E-07 |

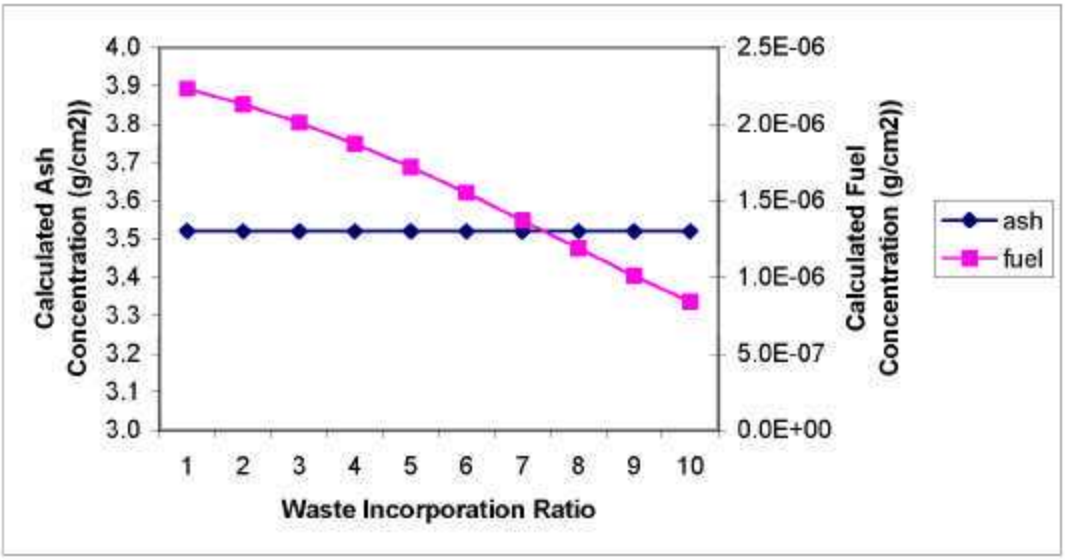


Figure C-9. Sensitivity of Calculated Ash and Fuel Concentration to Waste Incorporation Ratio

Table C-10. Sensitivity of Calculated Ash and Fuel Concentration to Waste Mass Available for Transport

| Waste Mass Available (g) | Calculated Ash Deposition ($g/cm^2$) | Calculated Fuel Deposition ($g/cm^2$) |
|---|---|---|
| 4.01E+07[a] | 1.13 | 2.80E-06 |
| 3.20E+08[b] | 1.13 | 2.24E-05 |
| 9.60E+08[c] | 1.13 | 6.74E-05 |

NOTES: [a] Median (5) waste packages hit (Section 7.1) (DTN: MO0504MWDNUMWP.001 [DIRS 173521])

[b] 95th percentile (40) waste packages hit (DTN: MO0504MWDNUMWP.001 [DIRS 173521])

[c] Entire drift evacuated, 120 waste packages: Planned total number of waste packages (11,184) (BSC 2005 [DIRS 173501], Table 13) divided by total number of active drifts (96) (BSC 2004 [DIRS 168370], Figure 2) equals 117, the average number of waste packages per drift; this value was rounded to 120 for the purposes of this analysis.

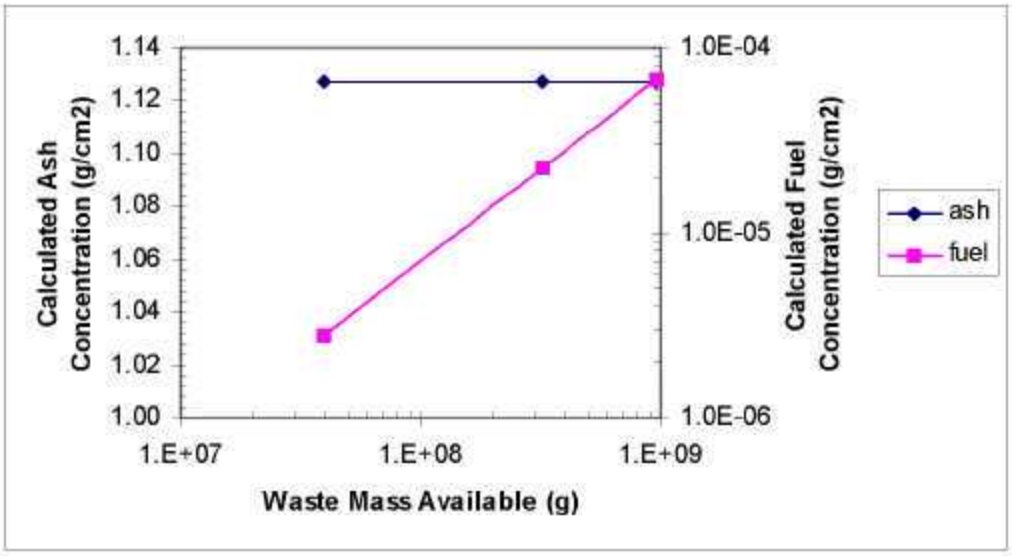


Figure C-10. Sensitivity of Calculated Ash and Fuel Concentration to Waste Mass Available for Transport

Table C-11. Sensitivity of Calculated Ash and Fuel Concentration to Waste Particle Size

| Run # | Waste Particle Size (cm) fdmin, fdmean, fdmax | Calculated Ash Deposition ($g/cm^2$) | Calculated Fuel Deposition ($g/cm^2$) |
|---|---|---|---|
| 1 | 0.0001, 0.0010 0.0050[1] | 1.13 | 8.67E-07 |
| 2 | 0.0001, 0.0016, 0.05[2] | 1.13 | 5.82E-07 |
| 3 | 0.0001, 0.0013, 0.2[3] | 1.13 | 5.00E-07 |

NOTES: [1] Fine-grained waste: minimum 1 micron, maximum 50 micron; this run provides context for extremely fine-grained waste, below the size range used for the base case.

[2] Base-case (Table 8-2): minimum 1 micron, mode 16 micron, maximum 500 micron.

[3] Alternative waste particle distribution (Appendix J): minimum 1 micron, mode 13 micron, maximum 2,000 micron (0.2 cm).

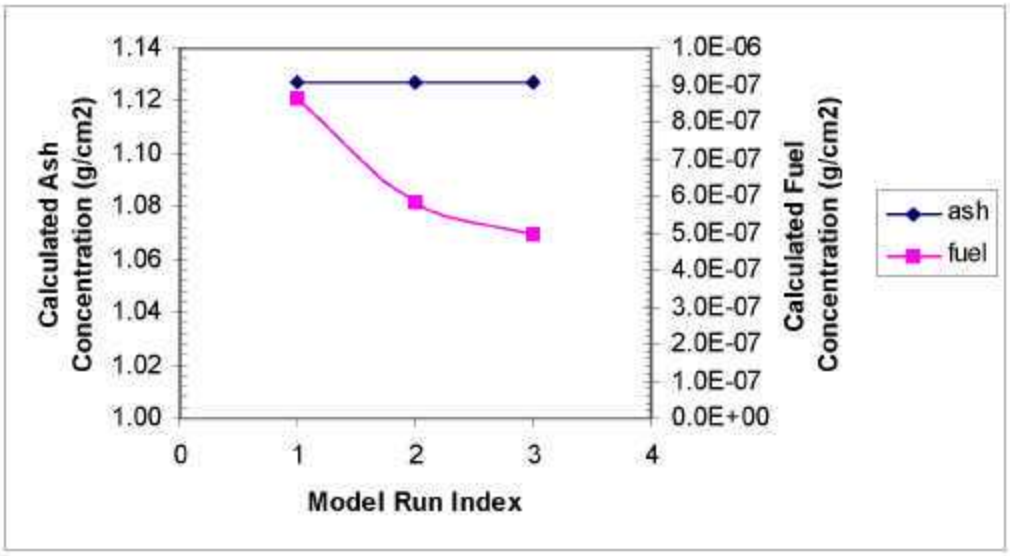


Figure C-11. Sensitivity of Calculated Ash and Fuel Concentration to Waste Particle Size

## Table C-12. Input Parameter Values for ASHPLUME Sensitivity Studies

| | Base Case (Total Range) | Base Case (50th %ile or Representative) | Sensitivity Analysis | | | | | | | | | | |
|---|---|---|---|---|---|---|---|---|---|---|---|---|---|
| | | | Power | dmean | dsigma | beta | Initial Rise Velocity | Wind Speed | Wind Direction | Eruption Duration | Waste Incorporation Ratio | Waste Mass Available | Waste Particle Size |
| Ashdenmin | 2 08 | 2 08 | 2 08 | 2 08 | 2 08 | 2 08 | 2 08 | 2 08 | 2 08 | 2 08 | 2 08 | 2 08 | 2 08 |
| ashdenmax | 1 04 | 1 04 | 1 04 | 1 04 | 1 04 | 1 04 | 1 04 | 1 04 | 1 04 | 1 04 | 1 04 | 1 04 | 1 04 |
| Ashrhollow | –3 | –3 | –3 | –3 | –3 | –3 | –3 | –3 | –3 | –3 | –3 | –3 | –3 |
| Ashrhohi | 0 | 0 | 0 | 0 | 0 | 0 | 0 | 0 | 0 | 0 | 0 | 0 | 0 |
| Fshape | 0 5 | 0 5 | 0 5 | 0 5 | 0 5 | 0 5 | 0 5 | 0 5 | 0 5 | 0 5 | 0 5 | 0 5 | 0 5 |
| Beta | 0 01-0 5 | 0 3 | 0 3 | 0 3 | 0 3 | 0 01-0 5 | 0 3 | 0 3 | 0 3 | 0 3 | 0 3 | 0 3 | 0 3 |
| particle (dmean) | 0 001-0 01-0 1 | 0 0572 | 0 0572 | 0 001 - 0 1 | 0 0572 | 0 0572 | 0 0572 | 0 0572 | 0 0572 | 0 0572 | 0 0572 | 0 0572 | 0 0572 |
| Dsigma (log (cm)) | (–1 9)–(–1 3) | –1 6 | –1 6 | –1 6 | (–1 9)–(–1 3) | –1 6 | –1 6 | –1 6 | –1 6 | –1 6 | 1 6 | 1 6 | 1 6 |
| Min waste particle size (fdmin) (cm) | 0 0001 | 0 0001 | 0 0001 | 0 0001 | 0 0001 | 0 0001 | 0 0001 | 0 0001 | 0 0001 | 0 0001 | 0 0001 | 0 0001 | 0 0001 |
| Mode waste particle size (fdmean) (cm) | 0 0016 | 0 0016 | 0 0016 | 0 0016 | 0 0016 | 0 0016 | 0 0016 | 0 0016 | 0 0016 | 0 0016 | 0 0016 | 0 0016 | 0 0010, 0 0016, 0 0013 |
| Max waste particle size (fdmax) (cm) | 0 05 | 0 05 | 0 05 | 0 05 | 0 05 | 0 05 | 0 05 | 0 05 | 0 05 | 0 05 | 0 05 | 0 05 | 0 0050, 0 0500, 0 2000 |
| wind dir (degrees) | –180–+180 | –90 | –90 | –90 | –90 | –90 | –90 | –90 | –180–+180 | –90 | –90 | –90 | –90 |
| wind speed (cm/s) | 0–5660 | 500 | 500 | 500 | 500 | 500 | 500 | 0–5660 | 500 | 500 | 500 | 500 | 500 |
| initial rise velocity (cm/s) | 1 0E+00–1 2E+04 | 3 30E+01 | 3 30E+01 | 3 30E+01 | 3 30E+01 | 3 30E+01 | 1 0E+00–1 2E+04 | 3 30E+01 | 3 30E+01 | 3 30E+01 | 3 30E+01 | 10 | 10 |
| power (W) | 6 17E+08–5E+12 | 5 06E+10 | 6 17E+08 –5E+12 | 5 06E+10 | 5 06E+10 | 5 06E+10 | 5 06E+10 | 5 06E+10 | 5 06E+10 | 5 06E+10 | 5 06E+10 | 4 00E+09 | 4 00E+09 |
| duration (s) | 8 64E+04–6 48E+06 | 2 59E+06 | 2 59E+06 | 2 59E+06 | 2 59E+06 | 2 59E+06 | 2 59E+06 | 2 59E+06 | 2 59E+06 | 8 64E+04 - 6 48E+06 | 2 59E+06 | 1 05E+07 | 1 05E+07 |
| mass of waste (g) | 1 13E+08 | 1 13E+08 | 1 13E+08 | 1 13E+08 | 1 13E+08 | 1 13E+08 | 1 13E+08 | 1 13E+08 | 1 13E+08 | 1 13E+08 | 1 13E+08 | 4 01E+07–9 8E+08 | 1 13E+08 |
| Waste incorporation ratio | 0 1–0 1 | 0 3 | 0 3 | 0 3 | 0 3 | 0 3 | 0 3 | 0 3 | 0 3 | 0 3 | 0 1–1 0 | 0 3 | 0 3 |

NOTE The analyzed range in wind speed spans the total range of observed values and is held fixed at the average wind speed for the 2 to 3 km altitude bin for evaluating ranges of the other parameters. The analyzed range in wind direction spans the total range of observed values and is held constant blowing due south (–90°) for evaluations of other parameters. The sensitivity analysis for waste incorporation ratio was performed for REV 01 of this report and uses dsigma = +1 6, consistent with revisions to the dsigma parameter values described in Section 6 5 2 5

# APPENDIX D

# DESERT ROCK WIND DATA ANALYSES

# APPENDIX D
# DESERT ROCK WIND DATA ANALYSES

A need exists to develop parameter distributions for atmospheric data inputs to the TSPA model according to LP-SV.1Q-BSC, *Control of the Electronic Management of Information*. Statistical analyses, including CDFs and probability distribution functions (PDFs) were performed on a qualified data set to develop these parameter distributions. The parameter distributions developed from these data account for uncertainty in the observed data. The parameters under consideration are wind speed and wind direction. Both the data and the methods used to develop these parameter distributions are also contained in the associated output DTN: MO0408SPADRWSD.002.

The wind data presented in this Appendix have been revised to address errors detected in the data reported in REV 00 of this Model Report (in Attachment III). These errors resulted from an incomplete download of the wind dataset from NOAA. The revised analysis presented in this Appendix is based on a complete data download from NOAA and increases wind speeds by approximately a factor of two compared to the earlier, erroneous analysis.

The first step in analyzing Desert Rock wind data involved importing a usable data file into Microsoft Access, *desertrock.zip* (NOAA 2004 [DIRS 171035]) provided through an FTP site (ftp.ncdc.noaa.gov) by Scott Stephens of the National Climatic Data Center in Asheville, North Carolina, on August 3, 2004. A total of 1,619,404 data lines were imported.

Column headers followed by blank lines were present within the data file received. As such, deletion of 48,321 header and blank rows was completed. Following, one wind speed column data value with a ".0" in the cell that had an associated direction reading was deleted. Then, three data lines having a wind speed reading without an associated direction were deleted. Next, a search for "999.9" and "999" (i.e., the designators for blank data fields) was completed for the wind speed and direction columns, respectively. In all, there were 124,253 lines of data deleted as a result of the blank field data search, for a total of 1,446,826 data lines left for analysis.

## Height Groupings

At the repository site, the crest of Yucca Mountain is approximately 4,905 ft (1,495 m) above sea level (CRWMS M&O 2000 [DIRS 153246], Figure 3.2-10; DTN: MO0103COV01031.000 [DIRS 155271], boring SD-6). As such, heights in meters above mean sea level in the data file were sorted by height in meters above Yucca Mountain. This was accomplished by setting the query field under the height column to the text shown in Table D-1. This process was repeated for each height interval, from 0 to 13 km, resulting in thirteen tables used for further data analyses as described later in this appendix.

The resulting datasets were saved as tables containing four columns including: height in meters (HEIGHT MTR), wind speed in meters per second (WNDSP MS), direction in degrees (DIR), and the id number (ID) assigned to each line by Access. These tables were then exported from Microsoft Access to Microsoft Excel for further analyses of wind direction and speed. Prior to being imported into Excel, all fields were changed from text to number format in the table design view. Table D-2 provides the format of the data tables used for the CDF and PDF analyses.

For the 1 to 2, 2 to 3, and 3 to 4 data groupings, the number of data lines exceeded the number able to be stored (65,536) per worksheet in Excel. As such, lines up to 65,536 were exported automatically by Access while the remaining lines were copied and pasted manually into an additional worksheet. Therefore, the CDFs and PDFs for these groupings were done separately for each worksheet then combined at the end.

Table D-1. Height Grouping Query Results

| Query Name (Number of Data Lines Resulting) | Query Field Contents Under Height Column |
|---|---|
| 0 to 1 (64,002) | >=" 1495" And <" 2495" |
| 1 to 2 (72,498) | >=" 2495" And <" 3495" |
| 2 to 3 (82,192) | >=" 3495" And <" 4495" |
| 3 to 4 (70,748) | >=" 4495" And <" 5495" |
| 4 to 5 (65,494) | >=" 5495" And <" 6495" |
| 5 to 6 (62,169) | >=" 6495" And <" 7495" |
| 6 to 7 (57,505) | >=" 7495" And <" 8495" |
| 7 to 8 (51,434) | >=" 8495" And <" 9495" |
| 8 to 9 (47,373) | >=" 9495" And <" 10495" |
| 9 to 10 (49,869) | >=" 10495" And <" 11495" |
| 10 to 11 (53,635) | >=" 11495" And <" 12495" |
| 11 to 12 (56,917) | >=" 12495" And <" 13495" |
| 12 to 13 (51,774) | >=" 13495" And <" 14495" |

Table D-2. Example of Table Exported from Access to Excel

| 0 to 1 Table | | | |
|---|---|---|---|
| HEIGHT MTR | WINDSP MS | DIR | ID |
| 1927 | 16 | 192 | 8 |

NOTES HEIGHT MTR = height in meters, WINDSP MD = wind speed in meters per second, DIR = direction in degrees, ID = ID number

## Wind Direction

The wind directions given in the raw data were in compass degrees *from* the indicated direction and needed to be converted to Ashplume degrees *toward* the indicated direction. For each of the heights indicated above, data were initially grouped into bins using the histogram function under the data analysis selection under the tools menu in Excel. Degree bins were entered manually into column E of the spreadsheet. After choosing tools, data analyses, and then histograms, a popup menu appeared and requested choices regarding input and output options. For the input, the wind direction data were entered (column C in the spreadsheet) in the input range cell like the following for the 0- to 1-km data table, "$C$2:$C$64003." Column E (bin degrees) was then chosen as the input for the bin range and typed in as: "$E$2:$E$15" under the Histogram function. This process was repeated for each of the remaining height groupings.

Table D-3 provides the histogram function analysis output.

Bins 0, 14, and 360 were combined to represent the 345- to 15-degree interval on the compass. The remaining bins represent the degree intervals as indicated in Table D-4.

Table D-3. 0 to 1 Histogram Function Output

| Bin (in Compass Degrees) | Frequency |
|---|---|
| 0 | 125 |
| 14 | 1,931 |
| 44 | 5,411 |
| 74 | 5,225 |
| 104 | 3,596 |
| 134 | 2,411 |
| 164 | 2,363 |
| 194 | 8,336 |
| 224 | 18,290 |
| 254 | 6,633 |
| 284 | 2,910 |
| 314 | 2,407 |
| 344 | 2,670 |
| 360 | 1,694 |

Output DTN MO0408SPADRWSD.002

Table D-4. Bins Converted to Compass Degree Intervals

| Compass Degree Intervals | Representative Bins |
|---|---|
| 345 to 15 | 0, 14, and 360 |
| 15 to 45 | 44 |
| 45 to 75 | 74 |
| 75 to 105 | 104 |
| 105 to 135 | 134 |
| 135 to 165 | 164 |
| 165 to 195 | 194 |
| 195 to 225 | 224 |
| 225 to 255 | 254 |
| 255 to 285 | 284 |
| 285 to 315 | 314 |
| 15 to 345 | 344 |

NOTE This table summarizes the histogram bins used to represent compass degree intervals

Converting compass degrees to Ashplume degrees is depicted by Figure D-1. Ashplume degrees (Figure D-1, Ashplume degrees are around the perimeter, compass degrees are inside) *toward* the indicated direction were determined by selecting the Ashplume direction exactly opposite of the indicated compass-degree interval and recording the midpoint of the degree interval (Table D-5).

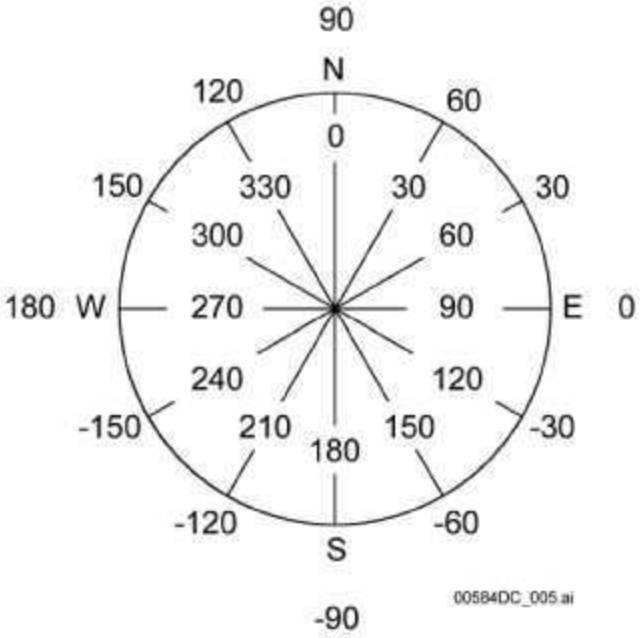


Figure D-1. Compass (Inside Numbers) and Ashplume (Outside Numbers) Degree Comparison

Table D-5. Compass Degrees from Direction Converted to Ashplume Degrees toward Direction

| Compass Degrees | Ashplume Degrees |
|---|---|
| 165 to 195 | 90 (North) |
| 195 to 225 | 60 |
| 225 to 255 | 30 |
| 255 to 285 | 0 (East) |
| 285 to 315 | –30 |
| 315 to 345 | –60 |
| 345 to 15 | –90 (South) |
| 15 to 45 | –120 |
| 45 to 75 | –150 |
| 75 to 105 | 180 (West) |
| 105 to 135 | 150 |
| 135 to 165 | 120 |

NOTE: This table summarizes the conversion of compass direction to Ashplume direction using the relationship depicted in Figure D-1.

Table D-6. Example PDF Results

| | A | B | C | D* | D |
|---|---|---|---|---|---|
| 1 | Compass Degrees | ASHPLUME degrees | Count/ Frequency | PDF | PDF |
| 2 | 165 to 195 | 90 (North) | 8,336 | =C2/(sumC2 C13) | 0 1303 |
| 3 | 195 to 225 | 60 | 18,290 | =C3/(sumC2 C13) | 0 2858 |
| 4 | 225 to 255 | 30 | 6,633 | =C4/(sumC2 C13) | 0 1036 |
| 5 | 255 to 285 | 0 (East) | 2,910 | =C5/(sumC2 C13) | 0 0455 |
| 6 | 285 to 315 | –30 | 2,407 | =C6/(sumC2 C13) | 0 0376 |
| 7 | 315 to 345 | –60 | 2,670 | =C7/(sumC2 C13) | 0 0417 |
| 8 | 345 to 15 | –90 (South) | 3,750 | =C8/(sumC2 C13) | 0 0586 |
| 9 | 15 to 45 | –120 | 5,411 | =C9/(sumC2 C13) | 0 0845 |
| 10 | 45 to 75 | –150 | 5,225 | =C10/(sumC2 C13) | 0 0816 |
| 11 | 75 to 105 | 180 (West) | 3,596 | =C11/(sumC2 C13) | 0 0562 |
| 12 | 105 to 135 | 150 | 2,411 | =C12/(sumC2 C13) | 0 0377 |
| 13 | 135 to 165 | 120 | 2,363 | =C13/(sumC2 C13) | 0 0369 |

NOTES This spreadsheet excerpt illustrates the method used to create wind direction PDFs for the 0 to 1 km interval

* = visible cell calculation

Next, a PDF was completed using Microsoft Excel for each data grouping. This was performed by taking the sample count for each interval and dividing by the total number of samples for that particular height interval. The ASHPLUME degrees and count were then plotted against one another using the radar-type graph under the chart function to produce a "wind rose" diagram like Figure D-2.

Specifically, Table D-6 was constructed for the 0 to 1 km interval in Excel. For final insertion into the TSPA model, four decimal places were used for the PDF values, and adjustments (+/- 0.0001) were made to ensure the sum of the distribution equaled exactly 1. ASHPLUME Degrees were arranged sequentially, and the "Frequency" and "Compass Degrees" columns were deleted as shown in output DTN: MO0408SPADRWSD.002.

Under the insert pull-down menu, chart was selected, radar was selected, and then the last example of radar graphs was chosen. Following, Columns B and C were plotted against each other to form the Figure D-2 for the 0 to 1 km interval. Tables for all 13 ntervals are displayed later in this appendix (Tables D-23 through D-35). For TSPA, these tables were formatted to contain only the PDF value and ASHPLUME degrees columns organized in ascending order (output DTN: MO0408SPADRWSD.002).

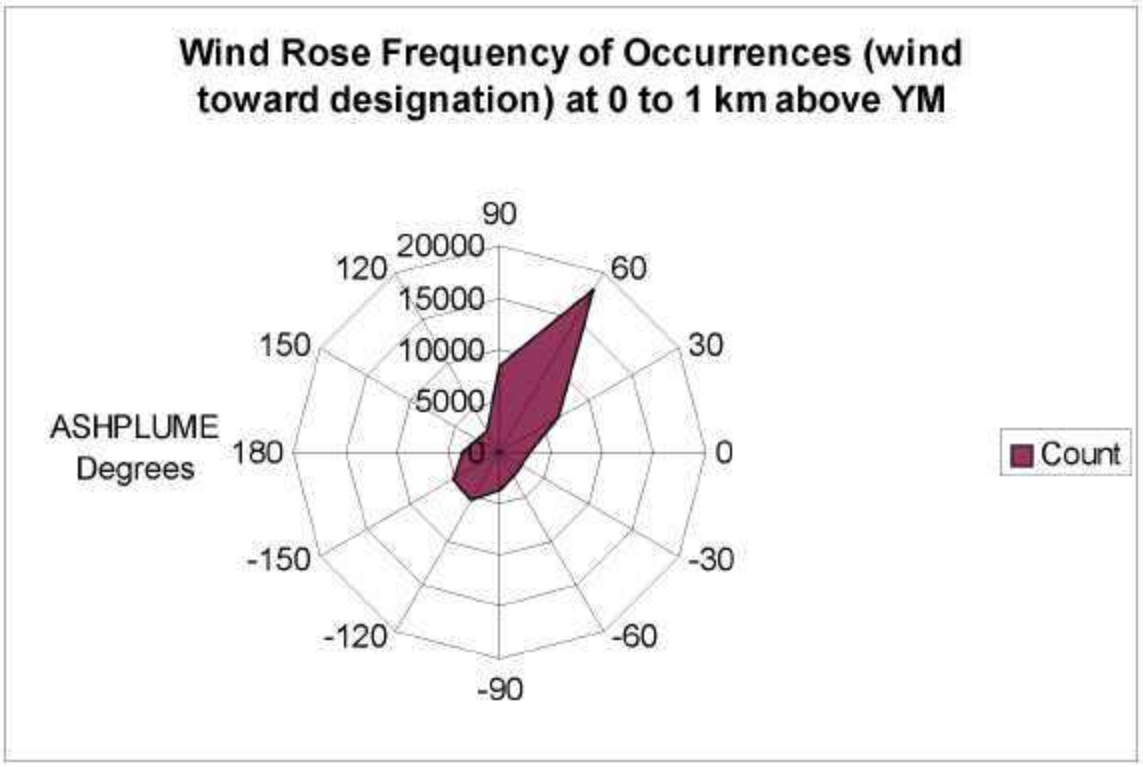


Output DTN: MO0408SPADRWSD.002.

NOTE: This figure illustrates the method used in presenting information graphically using a radar-type graph. This figure is the same as Figure D-3, which lists the source of information (NOAA 2004 [DIRS 171035]) and the data output.

Figure D-2. Wind Rose Diagram for 0 to 1 km above Yucca Mountain

### Wind Speed

A CDF was calculated for each height grouping also using the Histogram function under the data analysis menu in Microsoft Excel. The wind speed column from table "0_to_1_Table" was copied and pasted into column A of a new worksheet, named "0 to 1 windspeed." Following, the wind speeds in meters per second were converted to centimeters per second in column B by multiplying each cell by 100. Table D-7 below shows the conversion. After choosing tools, data analysis, and then histogram, a popup menu appeared and asked for input and output options. For the input, the wind-speed data were entered in the input range cell, "$B$2:$B$64003," for the 0- to 1-km example. Wind-speed bin intervals consisting of 100 cm/s each, up to the highest wind speed recorded (14,100 cm/s) for all applicable heights (0 to 13 km), were then pasted to each Excel table in Column C (Table D-7). This column was then chosen as the input for the bin range cell and typed in as: "$C$2:$C$143" under the Histogram function.

Table D-7. Format of Tables Used to Calculate Wind Speed CDFs

| A | B* | B | C |
|---|---|---|---|
| WNDSP MS | WNDSP CONV | WNDSP CMS | BINS CMS |
| 16 | = A2 x 100 | 1,600 | 0 |
| 15 | = A3 x100 | 1,500 | 100 |
| 9 | = A4 x100 | 900 | 200 |
| 7 | = A5 x100 | 700 | 300 |
| 8 | = A6 x100 | 800 | 400 |
| 7 | = A7 x100 | 700 | 500 |
| 8 | = A8 x100 | 800 | 600 |
| 7 | = A9 x100 | 700 | 700 |
| 6 | = A10 x100 | 600 | 800 |
| 6 | = A11 x100 | 600 | 900 |
| 1 | = A12 x100 | 100 | 1,000 |
| 3 | = A13 x100 | 300 | 1,100 |
| 2 | = A14 x100 | 200 | 1,200 |
| 3 | = A15 x100 | 300 | 1,300 |
| 2 | = A16 x100 | 200 | 1,400 |
| 1 | = A17 x100 | 100 | 1,500 |
| 2 | = A18 x100 | 200 | 1,600 |
| 4 | = A19 x100 | 400 | 1,700 |
| 4 | = A20 x100 | 400 | 1,800 |
| 3 | = A21 x100 | 300 | 1,900 |
| 3 | = A22 x100 | 300 | 2,000 |
| 9 | = A23 x100 | 900 | 2,100 |
| 13 | = A24 x100 | 1,300 | 2,200 |

NOTES This spreadsheet excerpt illustrates the method used to bin the wind speed data

* = visible cell calculation

Additionally, the cumulative percentage (converted to decimal in example Table D-8 below by simply formatting the cell) and chart output boxes in the output menu were selected, which resulted in a table similar to Table D-8.

Table D-8. 0 to 1 km CDF Table

| Bin (cm/s) | Frequency | CDF |
|---|---|---|
| 0 | 125 | 0 00195 |
| 100 | 2624 | 0 04295 |
| 200 | 3,326 | 0 09492 |
| 300 | 6,156 | 0 19110 |
| 400 | 8,571 | 0 32502 |
| 500 | 6,873 | 0 43241 |
| 600 | 4,840 | 0 50803 |
| 700 | 6,045 | 0 60248 |
| 800 | 5,301 | 0 68531 |
| 900 | 4,661 | 0 75813 |
| 1,000 | 3,916 | 0 81932 |
| 1,100 | 2,907 | 0 86474 |
| 1,200 | 2,252 | 0 89993 |
| 1,300 | 1,743 | 0 92716 |
| 1,400 | 1,271 | 0 94702 |
| 1,500 | 908 | 0 96120 |
| 1,600 | 695 | 0 97206 |
| 1,700 | 480 | 0 97956 |
| 1,800 | 382 | 0 98553 |
| 1,900 | 259 | 0 98958 |
| 2,000 | 135 | 0 99169 |
| 2,100 | 193 | 0 99470 |
| 2,200 | 121 | 0 99659 |
| 2,300 | 71 | 0 99770 |
| 2,400 | 48 | 0 99845 |
| 2,500 | 32 | 0 99895 |
| 2,600 | 22 | 0 99930 |
| 2,700 | 16 | 0 99955 |
| 2,800 | 12 | 0 99973 |
| 2,900 | 8 | 0 99986 |
| 3,000 | 5 | 0 99994 |
| 3,100 | 0 | 0 99994 |
| 3,200 | 1 | 0 99995 |
| 3,300 | 0 | 0 99995 |
| 3,400 | 0 | 0 99995 |
| 3,500 | 0 | 0 99995 |
| 3,600 | 0 | 0 99995 |
| 3,700 | 0 | 0 99995 |
| 3,800 | 1 | 0 99997 |
| 3,900 | 0 | 0 99997 |
| 4,000 | 0 | 0 99997 |

Table D-8. to 1 km CDF Table (Continued)

| Bin (cm/s) | Frequency | CDF |
|---|---|---|
| 4,100 | 0 | 0 99997 |
| 4,200 | 0 | 0 99997 |
| 4,300 | 0 | 0 99997 |
| 4,400 | 0 | 0 99997 |
| 4,500 | 1 | 0 99998 |
| 4,600 | 0 | 0 99998 |
| 4,700 | 1 | 1 00000 |
| 4,800 | 0 | 1 00000 |
| 4,900 | 0 | 1 00000 |
| 5,000 | 0 | 1 00000 |
| 5,100 | 0 | 1 00000 |
| 5,200 | 0 | 1 00000 |
| 5,300 | 0 | 1 00000 |
| 5,400 | 0 | 1 00000 |
| 5,500 | 0 | 1 00000 |
| 5,600 | 0 | 1 00000 |
| 5,700 | 0 | 1 00000 |
| 5,800 | 0 | 1 00000 |
| 5,900 | 0 | 1 00000 |
| 6,000 | 0 | 1 00000 |
| 6,100 | 0 | 1 00000 |
| 6,200 | 0 | 1 00000 |
| 6,300 | 0 | 1 00000 |
| 6,400 | 0 | 1 00000 |
| 6,500 | 0 | 1 00000 |
| 6,600 | 0 | 1 00000 |
| 6,700 | 0 | 1 00000 |
| 6,800 | 0 | 1 00000 |
| 6,900 | 0 | 1 00000 |
| 7,000 | 0 | 1 00000 |
| 7,100 | 0 | 1 00000 |
| 7,200 | 0 | 1 00000 |
| 7,300 | 0 | 1 00000 |
| 7,400 | 0 | 1 00000 |
| 7,500 | 0 | 1 00000 |
| 7,600 | 0 | 1 00000 |
| 7,700 | 0 | 1 00000 |
| 7,800 | 0 | 1 00000 |
| 7,900 | 0 | 1 00000 |
| 8,000 | 0 | 1 00000 |
| 8,100 | 0 | 1 00000 |
| 8,200 | 0 | 1 00000 |

Table D-8. to 1 km CDF Table (Continued)

| Bin (cm/s) | Frequency | CDF |
|---|---|---|
| 8,300 | 0 | 1.00000 |
| 8,400 | 0 | 1.00000 |
| 8,500 | 0 | 1.00000 |
| 8,600 | 0 | 1.00000 |
| 8,700 | 0 | 1.00000 |
| 8,800 | 0 | 1.00000 |
| 8,900 | 0 | 1.00000 |
| 9,000 | 0 | 1.00000 |
| 9,100 | 0 | 1.00000 |
| 9,200 | 0 | 1.00000 |
| 9,300 | 0 | 1.00000 |
| 9,400 | 0 | 1.00000 |
| 9,500 | 0 | 1.00000 |
| 9,600 | 0 | 1.00000 |
| 9,700 | 0 | 1.00000 |
| 9,800 | 0 | 1.00000 |
| 9,900 | 0 | 1.00000 |
| 10,000 | 0 | 1.00000 |
| 10,100 | 0 | 1.00000 |
| 10,200 | 0 | 1.00000 |
| 10,300 | 0 | 1.00000 |
| 10,400 | 0 | 1.00000 |
| 10,500 | 0 | 1.00000 |
| 10,600 | 0 | 1.00000 |
| 10,800 | 0 | 1.00000 |
| 10,900 | 0 | 1.00000 |
| 11,000 | 0 | 1.00000 |
| 11,100 | 0 | 1.00000 |
| 11,200 | 0 | 1.00000 |
| 11,300 | 0 | 1.00000 |
| 11,400 | 0 | 1.00000 |
| 11,500 | 0 | 1.00000 |
| 11,600 | 0 | 1.00000 |
| 11,700 | 0 | 1.00000 |
| 11,800 | 0 | 1.00000 |
| 11,900 | 0 | 1.00000 |
| 12,000 | 0 | 1.00000 |
| 12,100 | 0 | 1.00000 |
| 12,200 | 0 | 1.00000 |
| 12,300 | 0 | 1.00000 |
| 12,400 | 0 | 1.00000 |
| 12,500 | 0 | 1.00000 |

Table D-8. to 1 km CDF Table (Continued)

| Bin (cm/s) | Frequency | CDF |
|---|---|---|
| 12,600 | 0 | 1.00000 |
| 12,700 | 0 | 1.00000 |
| 12,800 | 0 | 1.00000 |
| 12,900 | 0 | 1.00000 |
| 13,000 | 0 | 1.00000 |
| 13,100 | 0 | 1.00000 |
| 13,200 | 0 | 1.00000 |
| 13,300 | 0 | 1.00000 |
| 13,400 | 0 | 1.00000 |
| 13,500 | 0 | 1.00000 |
| 13,600 | 0 | 1.00000 |
| 13,700 | 0 | 1.00000 |
| 13,800 | 0 | 1.00000 |
| 13,900 | 0 | 1.00000 |
| 14,000 | 0 | 1.00000 |
| 14,100 | 0 | 1.00000 |

Output DTN: MO0408SPADRWSD.002

This same procedure was followed for the remaining 12 tables (1 to 2 km, 2 to 3 km, 3 to 4 km, 4 to 5 km, 5 to 6 km, 6 to 7 km, 7 to 8 km, 8 to 9 km, 9 to 10 km, 10 to 11 km, 11 to 12 km, and 12 to 13 km).

For correct insertion into the TSPA model, the formatting of these tables was modified further. Specifically, all bins without samples (Frequency = 0) were deleted from the tables, the "Frequency" column was deleted, and only 5 decimal places were used for the CDF values. Additionally, the TSPA model requires the first bin CDF value to equal zero. As such, the zero wind speed bin was replaced with 1E-30 to account for data having a wind speed of zero, and the first bin was added which equaled zero. The wind speed CDF tables formatted for TSPA are inserted below (Tables D-10 through D-22). Table D-9 is the result of the minimum, maximum, and average wind speeds (in cm/s) calculated for each height interval in Access and then imported into one table in Excel. Tables D-23 through D-35 are the wind direction PDF tables.

Table D-9. Wind Speed Minimum, Maximum, and Average

| Height (km) | Minimum (cm/s) | Maximum (cm/s) | Average (cm/s) |
|---|---|---|---|
| 0 to 1 | 0 | 4,670 | 668 |
| 1 to 2 | 0 | 4,480 | 817 |
| 2 to 3 | 0 | 5,000 | 1,007 |
| 3 to 4 | 0 | 6,400 | 1,215 |
| 4 to 5 | 0 | 10,500 | 1,486 |
| 5 to 6 | 0 | 14,100 | 1,695 |
| 6 to 7 | 0 | 10,300 | 1,949 |
| 7 to 8 | 0 | 11,000 | 2,160 |
| 8 to 9 | 0 | 8,700 | 2,294 |
| 9 to 10 | 0 | 8,640 | 2,416 |
| 10 to 11 | 0 | 8,900 | 2,437 |
| 11 to 12 | 0 | 9,900 | 2,311 |
| 12 to 13 | 0 | 7,300 | 2,064 |

Output DTN MO0408SPADRWSD.002

Table D-10. 0 to 1 km CDF

| CDF | Bin (cm/s) |
|---|---|
| 0.00000 | 0 |
| 0.00195 | 1.00E-30 |
| 0.04295 | 100 |
| 0.09492 | 200 |
| 0.19110 | 300 |
| 0.32502 | 400 |
| 0.43241 | 500 |
| 0.50803 | 600 |
| 0.60248 | 700 |
| 0.68531 | 800 |
| 0.75813 | 900 |
| 0.81932 | 1,000 |
| 0.86474 | 1,100 |
| 0.89993 | 1,200 |
| 0.92716 | 1,300 |
| 0.94702 | 1,400 |
| 0.96120 | 1,500 |
| 0.97206 | 1,600 |
| 0.97956 | 1,700 |
| 0.98553 | 1,800 |
| 0.98958 | 1,900 |
| 0.99169 | 2,000 |

Table D-10. 0 to 1 km CDF (Continued)

| CDF | Bin (cm/s) |
|---|---|
| 0.99470 | 2,100 |
| 0.99659 | 2,200 |
| 0.99770 | 2,300 |
| 0.99845 | 2,400 |
| 0.99895 | 2,500 |
| 0.99930 | 2,600 |
| 0.99955 | 2,700 |
| 0.99973 | 2,800 |
| 0.99986 | 2,900 |
| 0.99994 | 3,000 |
| 0.99995 | 3,200 |
| 0.99997 | 3,800 |
| 0.99998 | 4,500 |
| 1.00000 | 4,700 |

Output DTN: MO0408SPADRWSD.002

Table D-11. 1 to 2 km CDF

| CDF | Bin (cm/s) |
|---|---|
| 0.00000 | 0 |
| 0.00110 | 1.00E-30 |
| 0.02928 | 100 |
| 0.06453 | 200 |
| 0.13111 | 300 |
| 0.23150 | 400 |
| 0.32544 | 500 |
| 0.39702 | 600 |
| 0.48348 | 700 |
| 0.56574 | 800 |
| 0.63869 | 900 |
| 0.70420 | 1,000 |
| 0.76024 | 1,100 |
| 0.80820 | 1,200 |
| 0.84620 | 1,300 |
| 0.88023 | 1,400 |
| 0.90612 | 1,500 |
| 0.92720 | 1,600 |
| 0.94547 | 1,700 |
| 0.95992 | 1,800 |
| 0.96983 | 1,900 |

Table D-11. 1 to 2 km CDF (Continued)

| CDF | Bin (cm/s) |
|---|---|
| 0.97528 | 2,000 |
| 0.98196 | 2,100 |
| 0.98708 | 2,200 |
| 0.99105 | 2,300 |
| 0.99379 | 2,400 |
| 0.99546 | 2,500 |
| 0.99669 | 2,600 |
| 0.99757 | 2,700 |
| 0.99832 | 2,800 |
| 0.99899 | 2,900 |
| 0.99937 | 3,000 |
| 0.99970 | 3,100 |
| 0.99982 | 3,200 |
| 0.99989 | 3,300 |
| 0.99996 | 3,400 |
| 0.99997 | 3,500 |
| 0.99999 | 3,700 |
| 1.00000 | 4,500 |

Output DTN: MO0408SPADRWSD.002

Table D-12. 2 to 3 km CDF

| CDF | Bin (cm/s) |
|---|---|
| 0.00000 | 0 |
| 0.00072 | 1.00E-30 |
| 0.01802 | 100 |
| 0.04272 | 200 |
| 0.08866 | 300 |
| 0.15890 | 400 |
| 0.22871 | 500 |
| 0.29000 | 600 |
| 0.36961 | 700 |
| 0.44771 | 800 |
| 0.52039 | 900 |
| 0.58798 | 1,000 |
| 0.64808 | 1,100 |
| 0.70021 | 1,200 |
| 0.74401 | 1,300 |
| 0.78398 | 1,400 |
| 0.81856 | 1,500 |

Table D-12. 2 to 3 km CDF (Continued)

| CDF | Bin (cm/s) |
|---|---|
| 0.84619 | 1,600 |
| 0.87071 | 1,700 |
| 0.89252 | 1,800 |
| 0.91219 | 1,900 |
| 0.92311 | 2,000 |
| 0.93829 | 2,100 |
| 0.95045 | 2,200 |
| 0.96087 | 2,300 |
| 0.96923 | 2,400 |
| 0.97591 | 2,500 |
| 0.98103 | 2,600 |
| 0.98463 | 2,700 |
| 0.98813 | 2,800 |
| 0.99088 | 2,900 |
| 0.99308 | 3,000 |
| 0.99517 | 3,100 |
| 0.99647 | 3,200 |
| 0.99759 | 3,300 |
| 0.99838 | 3,400 |
| 0.99883 | 3,500 |
| 0.99923 | 3,600 |
| 0.99951 | 3,700 |
| 0.99960 | 3,800 |
| 0.99968 | 3,900 |
| 0.99981 | 4,000 |
| 0.99987 | 4,100 |
| 0.99990 | 4,300 |
| 0.99995 | 4,400 |
| 0.99996 | 4,700 |
| 0.99999 | 4,800 |
| 1.00000 | 5,000 |

Output DTN: MO0408SPADRWSD.002

Table D-13. 3 to 4 km CDF

| CDF | Bin (cm/s) |
|---|---|
| 0.00000 | 0 |
| 0.00031 | 1.00E-30 |
| 0.01214 | 100 |
| 0.02960 | 200 |
| 0.06417 | 300 |
| 0.12112 | 400 |
| 0.17309 | 500 |
| 0.21907 | 600 |
| 0.28050 | 700 |
| 0.34572 | 800 |
| 0.41196 | 900 |
| 0.47477 | 1,000 |
| 0.53414 | 1,100 |
| 0.58985 | 1,200 |
| 0.63913 | 1,300 |
| 0.68183 | 1,400 |
| 0.71943 | 1,500 |
| 0.75362 | 1,600 |
| 0.78268 | 1,700 |
| 0.81033 | 1,800 |
| 0.83488 | 1,900 |
| 0.84985 | 2,000 |
| 0.87099 | 2,100 |
| 0.88892 | 2,200 |
| 0.90439 | 2,300 |
| 0.91888 | 2,400 |
| 0.93221 | 2,500 |
| 0.94343 | 2,600 |
| 0.95215 | 2,700 |
| 0.95943 | 2,800 |
| 0.96643 | 2,900 |
| 0.97232 | 3,000 |
| 0.97686 | 3,100 |
| 0.98103 | 3,200 |
| 0.98476 | 3,300 |
| 0.98759 | 3,400 |
| 0.98991 | 3,500 |
| 0.99208 | 3,600 |
| 0.99363 | 3,700 |

Table D-13. 3 to 4 km CDF (Continued)

| CDF | Bin (cm/s) |
|---|---|
| 0 99430 | 3,800 |
| 0 99542 | 3,900 |
| 0 99644 | 4,000 |
| 0 99734 | 4,100 |
| 0 99799 | 4,200 |
| 0 99842 | 4,300 |
| 0 99869 | 4,400 |
| 0 99888 | 4,500 |
| 0 99911 | 4,600 |
| 0 99935 | 4,700 |
| 0 99946 | 4,800 |
| 0 99960 | 4,900 |
| 0 99969 | 5,000 |
| 0 99979 | 5,100 |
| 0 99983 | 5,200 |
| 0 99987 | 5,300 |
| 0 99989 | 5,400 |
| 0 99990 | 5,500 |
| 0 99992 | 5,600 |
| 0 99993 | 5,700 |
| 0 99997 | 6,300 |
| 1 00000 | 6,400 |

Output DTN: MO0408SPADRWSD.002

Table D-14. 4 to 5 km CDF

| CDF | Bin (cm/s) |
|---|---|
| 0 00000 | 0 |
| 0 00026 | 1 00E-30 |
| 0 00864 | 100 |
| 0 02063 | 200 |
| 0 04692 | 300 |
| 0 08757 | 400 |
| 0 13023 | 500 |
| 0 16377 | 600 |
| 0 21110 | 700 |
| 0 26015 | 800 |
| 0 31218 | 900 |
| 0 36145 | 1,000 |
| 0 41169 | 1,100 |
| 0 46132 | 1,200 |
| 0 50883 | 1,300 |
| 0 55370 | 1,400 |
| 0 59263 | 1,500 |
| 0 62879 | 1,600 |
| 0 66191 | 1,700 |
| 0 69538 | 1,800 |
| 0 72596 | 1,900 |
| 0 74547 | 2,000 |
| 0 77370 | 2,100 |
| 0 79871 | 2,200 |
| 0 82075 | 2,300 |
| 0 84081 | 2,400 |
| 0 85904 | 2,500 |
| 0 87581 | 2,600 |
| 0 89146 | 2,700 |
| 0 90697 | 2,800 |
| 0 92016 | 2,900 |
| 0 93152 | 3,000 |
| 0 94102 | 3,100 |
| 0 94928 | 3,200 |
| 0 95607 | 3,300 |
| 0 96224 | 3,400 |
| 0 96797 | 3,500 |
| 0 97326 | 3,600 |
| 0 97696 | 3,700 |

Table D-14. 4 to 5 km CDF (Continued)

| CDF | Bin (cm/s) |
|---|---|
| 0 97923 | 3,800 |
| 0 98232 | 3,900 |
| 0 98499 | 4,000 |
| 0 98719 | 4,100 |
| 0 98913 | 4,200 |
| 0 99113 | 4,300 |
| 0 99282 | 4,400 |
| 0 99400 | 4,500 |
| 0 99519 | 4,600 |
| 0 99592 | 4,700 |
| 0 99670 | 4,800 |
| 0 99740 | 4,900 |
| 0 99776 | 5,000 |
| 0 99809 | 5,100 |
| 0 99832 | 5,200 |
| 0 99852 | 5,300 |
| 0 99882 | 5,400 |
| 0 99905 | 5,500 |
| 0 99918 | 5,600 |
| 0 99931 | 5,700 |
| 0 99942 | 5,800 |
| 0 99947 | 5,900 |
| 0 99951 | 6,000 |
| 0 99959 | 6,100 |
| 0 99969 | 6,200 |
| 0 99973 | 6,300 |
| 0 99974 | 6,400 |
| 0 99977 | 6,500 |
| 0 99979 | 6,600 |
| 0 99980 | 6,700 |
| 0 99982 | 7,000 |
| 0 99986 | 7,100 |
| 0 99992 | 7,200 |
| 0 99994 | 7,400 |
| 0 99995 | 7,500 |
| 0 99997 | 7,700 |
| 0 99998 | 8,500 |
| 1 00000 | 10,500 |

Output DTN MO0408SPADRWSD 002

Table D-15. 5 to 6 km CDF

| CDF | Bin (cm/s) |
|---|---|
| 0.00000 | 0 |
| 0.00032 | 1.00E-30 |
| 0.00668 | 100 |
| 0.01592 | 200 |
| 0.03474 | 300 |
| 0.06735 | 400 |
| 0.10101 | 500 |
| 0.13029 | 600 |
| 0.17049 | 700 |
| 0.20962 | 800 |
| 0.25323 | 900 |
| 0.29679 | 1,000 |
| 0.34035 | 1,100 |
| 0.38173 | 1,200 |
| 0.42336 | 1,300 |
| 0.46592 | 1,400 |
| 0.50623 | 1,500 |
| 0.54363 | 1,600 |
| 0.57879 | 1,700 |
| 0.61318 | 1,800 |
| 0.64714 | 1,900 |
| 0.66844 | 2,000 |
| 0.69956 | 2,100 |
| 0.72755 | 2,200 |
| 0.75391 | 2,300 |
| 0.77801 | 2,400 |
| 0.80003 | 2,500 |
| 0.82009 | 2,600 |
| 0.83867 | 2,700 |
| 0.85654 | 2,800 |
| 0.87201 | 2,900 |
| 0.88641 | 3,000 |
| 0.89852 | 3,100 |
| 0.91127 | 3,200 |
| 0.92163 | 3,300 |
| 0.93079 | 3,400 |
| 0.93920 | 3,500 |
| 0.94713 | 3,600 |
| 0.95488 | 3,700 |

Table D-15. 5 to 6 km CDF (Continued)

| CDF | Bin (cm/s) |
|---|---|
| 0 95877 | 3,800 |
| 0 96400 | 3,900 |
| 0 96894 | 4,000 |
| 0 97322 | 4,100 |
| 0 97706 | 4,200 |
| 0 98073 | 4,300 |
| 0 98343 | 4,400 |
| 0 98599 | 4,500 |
| 0 98827 | 4,600 |
| 0 99004 | 4,700 |
| 0 99164 | 4,800 |
| 0 99295 | 4,900 |
| 0 99416 | 5,000 |
| 0 99530 | 5,100 |
| 0 99616 | 5,200 |
| 0 99680 | 5,300 |
| 0 99725 | 5,400 |
| 0 99781 | 5,500 |
| 0 99791 | 5,600 |
| 0 99833 | 5,700 |
| 0 99878 | 5,800 |
| 0 99912 | 5,900 |
| 0 99936 | 6,000 |
| 0 99952 | 6,100 |
| 0 99958 | 6,200 |
| 0 99965 | 6,300 |
| 0 99969 | 6,400 |
| 0 99971 | 6,500 |
| 0 99973 | 6,800 |
| 0 99977 | 6,900 |
| 0 99982 | 7,100 |
| 0 99984 | 7,300 |
| 0 99987 | 7,400 |
| 0 99989 | 7,500 |
| 0 99992 | 7,800 |
| 0 99994 | 8,000 |
| 0 99995 | 8,200 |
| 0 99997 | 8,400 |
| 0 99998 | 10,700 |
| 1 00000 | 14,100 |

Output DTN MO0408SPADRWSD 002

Table D-16. 6 to 7 km CDF

| CDF | Bin (cm/s) |
|---|---|
| 0 00000 | 0 |
| 0 00023 | 1 00E-30 |
| 0 00478 | 100 |
| 0 01097 | 200 |
| 0 02393 | 300 |
| 0 04697 | 400 |
| 0 07062 | 500 |
| 0 09192 | 600 |
| 0 12373 | 700 |
| 0 15653 | 800 |
| 0 19172 | 900 |
| 0 22840 | 1,000 |
| 0 26559 | 1,100 |
| 0 30387 | 1,200 |
| 0 34115 | 1,300 |
| 0 38007 | 1,400 |
| 0 41815 | 1,500 |
| 0 45419 | 1,600 |
| 0 48723 | 1,700 |
| 0 52293 | 1,800 |
| 0 55764 | 1,900 |
| 0 57847 | 2,000 |
| 0 61010 | 2,100 |
| 0 64097 | 2,200 |
| 0 66989 | 2,300 |
| 0 69584 | 2,400 |
| 0 72037 | 2,500 |
| 0 74352 | 2,600 |
| 0 76503 | 2,700 |
| 0 78781 | 2,800 |

Table D-16. 6 to 7 km CDF (Continued)

| CDF | Bin (cm/s) |
|---|---|
| 0.80750 | 2,900 |
| 0.82567 | 3,000 |
| 0.84194 | 3,100 |
| 0.85747 | 3,200 |
| 0.87147 | 3,300 |
| 0.88413 | 3,400 |
| 0.89676 | 3,500 |
| 0.90849 | 3,600 |
| 0.91903 | 3,700 |
| 0.92526 | 3,800 |
| 0.93453 | 3,900 |
| 0.94244 | 4,000 |
| 0.94980 | 4,100 |
| 0.95663 | 4,200 |
| 0.96292 | 4,300 |
| 0.96844 | 4,400 |
| 0.97339 | 4,500 |
| 0.97652 | 4,600 |
| 0.97990 | 4,700 |
| 0.98256 | 4,800 |
| 0.98484 | 4,900 |
| 0.98744 | 5,000 |
| 0.98943 | 5,100 |
| 0.99134 | 5,200 |
| 0.99264 | 5,300 |
| 0.99383 | 5,400 |
| 0.99464 | 5,500 |
| 0.99544 | 5,600 |
| 0.99631 | 5,700 |
| 0.99711 | 5,800 |
| 0.99774 | 5,900 |
| 0.99824 | 6,000 |
| 0.99866 | 6,100 |
| 0.99894 | 6,200 |
| 0.99906 | 6,300 |
| 0.99939 | 6,400 |
| 0.99957 | 6,500 |
| 0.99970 | 6,600 |
| 0.99974 | 6,700 |
| 0.99977 | 6,800 |
| 0.99979 | 6,900 |
| 0.99983 | 7,000 |

Table D-16. 6 to 7 km CDF (Continued)

| CDF | Bin (cm/s) |
|---|---|
| 0.99984 | 7,300 |
| 0.99988 | 7,500 |
| 0.99990 | 7,700 |
| 0.99991 | 7,900 |
| 0.99993 | 8,200 |
| 0.99995 | 8,400 |
| 0.99997 | 8,600 |
| 0.99998 | 9,000 |
| 1.00000 | 10,300 |

Output DTN: MO0408SPADRWSD.002

Table D-17. 7 to 8 km CDF

| CDF | Bin (cm/s) |
|---|---|
| 0.00000 | 0 |
| 0.00019 | 1.00E-30 |
| 0.00325 | 100 |
| 0.00764 | 200 |
| 0.01684 | 300 |
| 0.03393 | 400 |
| 0.05211 | 500 |
| 0.06801 | 600 |
| 0.09231 | 700 |
| 0.11870 | 800 |
| 0.14712 | 900 |
| 0.17990 | 1,000 |
| 0.21268 | 1,100 |
| 0.24845 | 1,200 |
| 0.28145 | 1,300 |
| 0.31668 | 1,400 |
| 0.35111 | 1,500 |
| 0.38383 | 1,600 |
| 0.41778 | 1,700 |
| 0.45221 | 1,800 |
| 0.48596 | 1,900 |
| 0.50636 | 2,000 |
| 0.53783 | 2,100 |
| 0.56735 | 2,200 |

Table D-17. 7 to 8 km CDF (Continued)

| CDF | Bin (cm/s) |
|---|---|
| 0.59727 | 2,300 |
| 0.62570 | 2,400 |
| 0.65299 | 2,500 |
| 0.67893 | 2,600 |
| 0.70453 | 2,700 |
| 0.72711 | 2,800 |
| 0.74863 | 2,900 |
| 0.76994 | 3,000 |
| 0.79026 | 3,100 |
| 0.80849 | 3,200 |
| 0.82504 | 3,300 |
| 0.84063 | 3,400 |
| 0.85523 | 3,500 |
| 0.86972 | 3,600 |
| 0.88471 | 3,700 |
| 0.89188 | 3,800 |
| 0.90386 | 3,900 |
| 0.91568 | 4,000 |
| 0.92694 | 4,100 |
| 0.93658 | 4,200 |
| 0.94513 | 4,300 |
| 0.95260 | 4,400 |
| 0.95884 | 4,500 |
| 0.96388 | 4,600 |
| 0.96874 | 4,700 |
| 0.97327 | 4,800 |
| 0.97694 | 4,900 |
| 0.97994 | 5,000 |
| 0.98270 | 5,100 |
| 0.98538 | 5,200 |
| 0.98765 | 5,300 |
| 0.98979 | 5,400 |
| 0.99178 | 5,500 |
| 0.99273 | 5,600 |
| 0.99403 | 5,700 |
| 0.99483 | 5,800 |
| 0.99551 | 5,900 |
| 0.99625 | 6,000 |
| 0.99704 | 6,100 |
| 0.99745 | 6,200 |
| 0.99804 | 6,300 |
| 0.99850 | 6,400 |

Table D-17. 7 to 8 km CDF (Continued)

| CDF | Bin (cm/s) |
|---|---|
| 0 99887 | 6,500 |
| 0 99907 | 6,600 |
| 0 99926 | 6,700 |
| 0 99938 | 6,800 |
| 0 99951 | 6,900 |
| 0 99967 | 7,000 |
| 0 99973 | 7,100 |
| 0 99975 | 7,200 |
| 0 99981 | 7,500 |
| 0 99983 | 7,600 |
| 0 99984 | 7,700 |
| 0 99986 | 8,200 |
| 0 99988 | 8,500 |
| 0 99990 | 8,700 |
| 0 99992 | 9,100 |
| 0 99994 | 9,600 |
| 0 99996 | 10,000 |
| 0 99998 | 10,700 |
| 1 00000 | 11,000 |

Output DTN MO0408SPADRWSD 002

Table D-18. 8 to 9 km CDF

| CDF | Bin (cm/s) |
|---|---|
| 0 00000 | 0 |
| 0 00006 | 1 00E-30 |
| 0 00264 | 100 |
| 0 00538 | 200 |
| 0 01250 | 300 |
| 0 02531 | 400 |
| 0 03943 | 500 |
| 0 05271 | 600 |
| 0 07314 | 700 |
| 0 09434 | 800 |
| 0 12032 | 900 |
| 0 14648 | 1,000 |
| 0 17371 | 1,100 |

Table D-18. 8 to 9 km CDF (Continued)

| CDF | Bin (cm/s) |
|---|---|
| 0.20415 | 1,200 |
| 0.23410 | 1,300 |
| 0.26547 | 1,400 |
| 0.29842 | 1,500 |
| 0.33141 | 1,600 |
| 0.36487 | 1,700 |
| 0.39987 | 1,800 |
| 0.43679 | 1,900 |
| 0.45726 | 2,000 |
| 0.48747 | 2,100 |
| 0.51827 | 2,200 |
| 0.54909 | 2,300 |
| 0.57856 | 2,400 |
| 0.60765 | 2,500 |
| 0.63551 | 2,600 |
| 0.66306 | 2,700 |
| 0.68917 | 2,800 |
| 0.71591 | 2,900 |
| 0.73886 | 3,000 |
| 0.76280 | 3,100 |
| 0.78384 | 3,200 |
| 0.80388 | 3,300 |
| 0.82222 | 3,400 |
| 0.83928 | 3,500 |
| 0.85602 | 3,600 |
| 0.87073 | 3,700 |
| 0.87788 | 3,800 |
| 0.89055 | 3,900 |
| 0.90210 | 4,000 |
| 0.91385 | 4,100 |
| 0.92432 | 4,200 |
| 0.93365 | 4,300 |
| 0.94246 | 4,400 |
| 0.94970 | 4,500 |
| 0.95652 | 4,600 |
| 0.96194 | 4,700 |
| 0.96692 | 4,800 |
| 0.97121 | 4,900 |
| 0.97537 | 5,000 |
| 0.97936 | 5,100 |
| 0.98250 | 5,200 |
| 0.98571 | 5,300 |

Table D-18. 8 to 9 km CDF (Continued)

| CDF | Bin (cm/s) |
|---|---|
| 0.98820 | 5,400 |
| 0.99029 | 5,500 |
| 0.99105 | 5,600 |
| 0.99227 | 5,700 |
| 0.99350 | 5,800 |
| 0.99449 | 5,900 |
| 0.99521 | 6,000 |
| 0.99599 | 6,100 |
| 0.99658 | 6,200 |
| 0.99704 | 6,300 |
| 0.99755 | 6,400 |
| 0.99804 | 6,500 |
| 0.99856 | 6,600 |
| 0.99884 | 6,700 |
| 0.99916 | 6,800 |
| 0.99941 | 6,900 |
| 0.99956 | 7,000 |
| 0.99960 | 7,100 |
| 0.99966 | 7,200 |
| 0.99977 | 7,300 |
| 0.99979 | 7,400 |
| 0.99983 | 7,600 |
| 0.99987 | 7,700 |
| 0.99989 | 7,900 |
| 0.99992 | 8,100 |
| 0.99996 | 8,300 |
| 0.99998 | 8,500 |
| 1.00000 | 8,700 |

Output DTN: MO0408SPADRWSD.002

Table D-19. 9 to 10 km CDF

| CDF | Bin (cm/s) |
|---|---|
| 0.00000 | 0 |
| 0.00004 | 1.00E-30 |
| 0.00180 | 100 |
| 0.00445 | 200 |
| 0.00952 | 300 |
| 0.01927 | 400 |
| 0.02956 | 500 |
| 0.03962 | 600 |
| 0.05446 | 700 |
| 0.07231 | 800 |
| 0.09328 | 900 |
| 0.11484 | 1,000 |
| 0.13732 | 1,100 |
| 0.16225 | 1,200 |
| 0.18801 | 1,300 |
| 0.21603 | 1,400 |
| 0.24536 | 1,500 |
| 0.27693 | 1,600 |
| 0.30875 | 1,700 |
| 0.34212 | 1,800 |
| 0.37424 | 1,900 |
| 0.39463 | 2,.000 |
| 0.42945 | 2,100 |
| 0.46195 | 2,200 |
| 0.49434 | 2,300 |
| 0.52716 | 2,400 |
| 0.55842 | 2,500 |
| 0.58968 | 2,600 |
| 0.62069 | 2,700 |
| 0.65137 | 2,800 |
| 0.68058 | 2,900 |
| 0.70856 | 3,000 |
| 0.73597 | 3,100 |
| 0.76105 | 3,200 |
| 0.78450 | 3,300 |
| 0.80645 | 3,400 |
| 0.82616 | 3,500 |
| 0.84511 | 3,600 |
| 0.86324 | 3,700 |
| 0.87307 | 3,800 |
| 0.88726 | 3,900 |

Table D-19. 9 to 10 km CDF (Continued)

| CDF | Bin (cm/s) |
|---|---|
| 0.90138 | 4,000 |
| 0.91452 | 4,100 |
| 0.92675 | 4,200 |
| 0.93730 | 4,300 |
| 0.94586 | 4,400 |
| 0.95348 | 4,500 |
| 0.95996 | 4,600 |
| 0.96557 | 4,700 |
| 0.97102 | 4,800 |
| 0.97524 | 4,900 |
| 0.97830 | 5,000 |
| 0.98135 | 5,100 |
| 0.98370 | 5,200 |
| 0.98606 | 5,300 |
| 0.98817 | 5,400 |
| 0.99005 | 5,500 |
| 0.99092 | 5,600 |
| 0.99234 | 5,700 |
| 0.99358 | 5,800 |
| 0.99445 | 5,900 |
| 0.99521 | 6,000 |
| 0.99593 | 6,100 |
| 0.99643 | 6,200 |
| 0.99683 | 6,300 |
| 0.99713 | 6,400 |
| 0.99737 | 6,500 |
| 0.99765 | 6,600 |
| 0.99785 | 6,700 |
| 0.99803 | 6,800 |
| 0.99834 | 6,900 |
| 0.99858 | 7,000 |
| 0.99892 | 7,100 |
| 0.99926 | 7,200 |
| 0.99938 | 7,300 |
| 0.99952 | 7,400 |
| 0.99962 | 7,500 |
| 0.99970 | 7,600 |
| 0.99972 | 7,700 |
| 0.99974 | 7,800 |
| 0.99976 | 8,000 |
| 0.99984 | 8,100 |
| 0.99988 | 8,200 |

Table D-19. 9 to 10 km CDF (Continued)

| CDF | Bin (cm/s) |
|---|---|
| 0 99992 | 8,300 |
| 0 99996 | 8,500 |
| 0 99998 | 8,600 |
| 1 00000 | 8,700 |

Output DTN: MO0408SPADRWSD 002

Table D-20. 10 to 11 km CDF

| CDF | Bin (cm/s) |
|---|---|
| 0 00000 | 0 |
| 0 00002 | 1 00E-30 |
| 0 00119 | 100 |
| 0 00289 | 200 |
| 0 00736 | 300 |
| 0 01644 | 400 |
| 0 02470 | 500 |
| 0 03280 | 600 |
| 0 04581 | 700 |
| 0 06011 | 800 |
| 0 07581 | 900 |
| 0 09393 | 1,000 |
| 0 11502 | 1,100 |
| 0 13769 | 1,200 |
| 0 16032 | 1,300 |
| 0 18656 | 1,400 |
| 0 21464 | 1,500 |
| 0 24477 | 1,600 |
| 0 27641 | 1,700 |
| 0 30862 | 1,800 |
| 0 34336 | 1,900 |
| 0 36461 | 2,000 |
| 0 40188 | 2,100 |
| 0 43969 | 2,200 |
| 0 47603 | 2,300 |
| 0 51243 | 2,400 |
| 0 54951 | 2,500 |
| 0 58542 | 2,600 |
| 0 61831 | 2,700 |
| 0 65159 | 2,800 |

Table D-20. 10 to 11 km CDF (Continued)

| CDF | Bin (cm/s) |
|---|---|
| 0.68205 | 2,900 |
| 0.71259 | 3,000 |
| 0.74149 | 3,100 |
| 0.76924 | 3,200 |
| 0.79491 | 3,300 |
| 0.81779 | 3,400 |
| 0.84016 | 3,500 |
| 0.86050 | 3,600 |
| 0.87959 | 3,700 |
| 0.88931 | 3,800 |
| 0.90407 | 3,900 |
| 0.91783 | 4,000 |
| 0.92919 | 4,100 |
| 0.93995 | 4,200 |
| 0.94925 | 4,300 |
| 0.95702 | 4,400 |
| 0.96374 | 4,500 |
| 0.96881 | 4,600 |
| 0.97382 | 4,700 |
| 0.97779 | 4,800 |
| 0.98154 | 4,900 |
| 0.98369 | 5,000 |
| 0.98605 | 5,100 |
| 0.98818 | 5,200 |
| 0.98984 | 5,300 |
| 0.99105 | 5,400 |
| 0.99228 | 5,500 |
| 0.99297 | 5,600 |
| 0.99394 | 5,700 |
| 0.99467 | 5,800 |
| 0.99556 | 5,900 |
| 0.99646 | 6,000 |
| 0.99702 | 6,100 |
| 0.99746 | 6,200 |
| 0.99767 | 6,300 |
| 0.99802 | 6,400 |
| 0.99821 | 6,500 |
| 0.99843 | 6,600 |
| 0.99866 | 6,700 |
| 0.99886 | 6,800 |
| 0.99897 | 6,900 |
| 0.99914 | 7,000 |

Table D-20. 10 to 11 km CDF (Continued)

| CDF | Bin (cm/s) |
|---|---|
| 0 99924 | 7,100 |
| 0 99937 | 7,200 |
| 0 99944 | 7,300 |
| 0 99957 | 7,400 |
| 0 99968 | 7,500 |
| 0 99974 | 7,600 |
| 0 99979 | 7,800 |
| 0 99987 | 7,900 |
| 0 99991 | 8,000 |
| 0 99996 | 8,100 |
| 0 99998 | 8,600 |
| 1 00000 | 8,900 |

Output DTN: MO0408SPADRWSD.002

Table D-21. 11 to 12 km CDF

| CDF | Bin (cm/s) |
|---|---|
| 0 00000 | 0 |
| 0 00009 | 1 00E-30 |
| 0 00095 | 100 |
| 0 00281 | 200 |
| 0 00706 | 300 |
| 0 01478 | 400 |
| 0 02393 | 500 |
| 0 03340 | 600 |
| 0 04535 | 700 |
| 0 06093 | 800 |
| 0 07847 | 900 |
| 0 09690 | 1,000 |
| 0 11842 | 1,100 |
| 0 14433 | 1,200 |
| 0 17128 | 1,300 |
| 0 19922 | 1,400 |
| 0 22953 | 1,500 |
| 0 26001 | 1,600 |
| 0 29236 | 1,700 |

Table D-21. 11 to 12 km CDF (Continued)

| CDF | Bin (cm/s) |
|---|---|
| 0.32732 | 1,800 |
| 0.36624 | 1,900 |
| 0.39180 | 2,000 |
| 0.43337 | 2,100 |
| 0.47364 | 2,200 |
| 0.51610 | 2,300 |
| 0.55620 | 2,400 |
| 0.59444 | 2,500 |
| 0.63324 | 2,600 |
| 0.67006 | 2,700 |
| 0.70482 | 2,800 |
| 0.74001 | 2,900 |
| 0.77084 | 3,000 |
| 0.79857 | 3,100 |
| 0.82478 | 3,200 |
| 0.84739 | 3,300 |
| 0.86718 | 3,400 |
| 0.88578 | 3,500 |
| 0.90194 | 3,600 |
| 0.91709 | 3,700 |
| 0.92559 | 3,800 |
| 0.93747 | 3,900 |
| 0.94698 | 4,000 |
| 0.95613 | 4,100 |
| 0.96381 | 4,200 |
| 0.96997 | 4,300 |
| 0.97526 | 4,400 |
| 0.97948 | 4,500 |
| 0.98352 | 4,600 |
| 0.98647 | 4,700 |
| 0.98865 | 4,800 |
| 0.99055 | 4,900 |
| 0.99208 | 5,000 |
| 0.99329 | 5,100 |
| 0.99452 | 5,200 |
| 0.99533 | 5,300 |
| 0.99584 | 5,400 |
| 0.99638 | 5,500 |
| 0.99684 | 5,600 |
| 0.99728 | 5,700 |
| 0.99766 | 5,800 |
| 0.99814 | 5,900 |

Table D-21. 11 to 12 km CDF (Continued)

| CDF | Bin (cm/s) |
|---|---|
| 0.99838 | 6,000 |
| 0.99859 | 6,100 |
| 0.99882 | 6,200 |
| 0.99909 | 6,300 |
| 0.99916 | 6,400 |
| 0.99924 | 6,500 |
| 0.99944 | 6,600 |
| 0.99954 | 6,700 |
| 0.99960 | 6,800 |
| 0.99965 | 6,900 |
| 0.99972 | 7,000 |
| 0.99975 | 7,200 |
| 0.99977 | 7,300 |
| 0.99979 | 7,400 |
| 0.99988 | 7,600 |
| 0.99989 | 7,900 |
| 0.99991 | 8,000 |
| 0.99993 | 8,100 |
| 0.99996 | 8,200 |
| 0.99998 | 8,800 |
| 1.00000 | 9,900 |

Output DTN: MO0408SPADRWSD.002

Table D-22. 12 to 13 km CDF

| CDF | Bin (cm/s) |
|---|---|
| 0.00000 | 0 |
| 0.00002 | 1.00E-30 |
| 0.00160 | 100 |
| 0.00338 | 200 |
| 0.00805 | 300 |
| 0.01771 | 400 |
| 0.02870 | 500 |
| 0.03909 | 600 |
| 0.05427 | 700 |
| 0.07260 | 800 |
| 0.09468 | 900 |

Table D-22. 12 to 13 km CDF (Continued)

| CDF | Bin (cm/s) |
|---|---|
| 0.12039 | 1,000 |
| 0.14801 | 1,100 |
| 0.17996 | 1,200 |
| 0.21327 | 1,300 |
| 0.24941 | 1,400 |
| 0.28655 | 1,500 |
| 0.32655 | 1,600 |
| 0.36599 | 1,700 |
| 0.41104 | 1,800 |
| 0.45807 | 1,900 |
| 0.48590 | 2,000 |
| 0.53199 | 2,100 |
| 0.57681 | 2,200 |
| 0.62132 | 2,300 |
| 0.66192 | 2,400 |
| 0.70207 | 2,500 |
| 0.73888 | 2,600 |
| 0.77352 | 2,700 |
| 0.80529 | 2,800 |
| 0.83277 | 2,900 |
| 0.85825 | 3,000 |
| 0.88089 | 3,100 |
| 0.90169 | 3,200 |
| 0.91942 | 3,300 |
| 0.93304 | 3,400 |
| 0.94464 | 3,500 |
| 0.95461 | 3,600 |
| 0.96357 | 3,700 |
| 0.96784 | 3,800 |
| 0.97412 | 3,900 |
| 0.97935 | 4,000 |
| 0.98337 | 4,100 |
| 0.98650 | 4,200 |
| 0.98920 | 4,300 |
| 0.99142 | 4,400 |
| 0.99307 | 4,500 |
| 0.99446 | 4,600 |
| 0.99556 | 4,700 |
| 0.99662 | 4,800 |
| 0.99728 | 4,900 |
| 0.99791 | 5,000 |
| 0.99830 | 5,100 |

Table D-22. 12 to 13 km CDF (Continued)

| CDF | Bin (cm/s) |
|---|---|
| 0 99867 | 5,200 |
| 0 99890 | 5,300 |
| 0 99909 | 5,400 |
| 0 99932 | 5,500 |
| 0 99934 | 5,600 |
| 0 99948 | 5,700 |
| 0 99959 | 5,800 |
| 0 99969 | 5,900 |
| 0 99971 | 6,000 |
| 0 99979 | 6,100 |
| 0 99986 | 6,200 |
| 0 99990 | 6,400 |
| 0 99992 | 6,500 |
| 0 99996 | 6,800 |
| 0 99998 | 6,900 |
| 1 00000 | 7,300 |

Output DTN MO0408SPADRWSD 002

Table D-23. 0 to 1 km PDF

| Compass Degrees | ASHPLUME Degrees | Count | PDF |
|---|---|---|---|
| 165 to 195 | 90 | 8,336 | 0 1303 |
| 195 to 225 | 60 | 18,290 | 0 2858 |
| 225 to 255 | 30 | 6,633 | 0 1036 |
| 255 to 285 | 0 | 2,910 | 0 0455 |
| 285 to 315 | –30 | 2,407 | 0 0376 |
| 315 to 345 | –60 | 2,670 | 0 0417 |
| 345 to 15 | –90 | 3,750 | 0 0586 |
| 15 to 45 | –120 | 5,411 | 0 0845 |
| 45 to 75 | –150 | 5,225 | 0 0816 |
| 75 to 105 | 180 | 3,596 | 0 0562 |
| 105 to 135 | 150 | 2,411 | 0 0377 |
| 135 to 165 | 120 | 2,363 | 0 0369 |
| | Totals | 64,002 | 1 0000 |

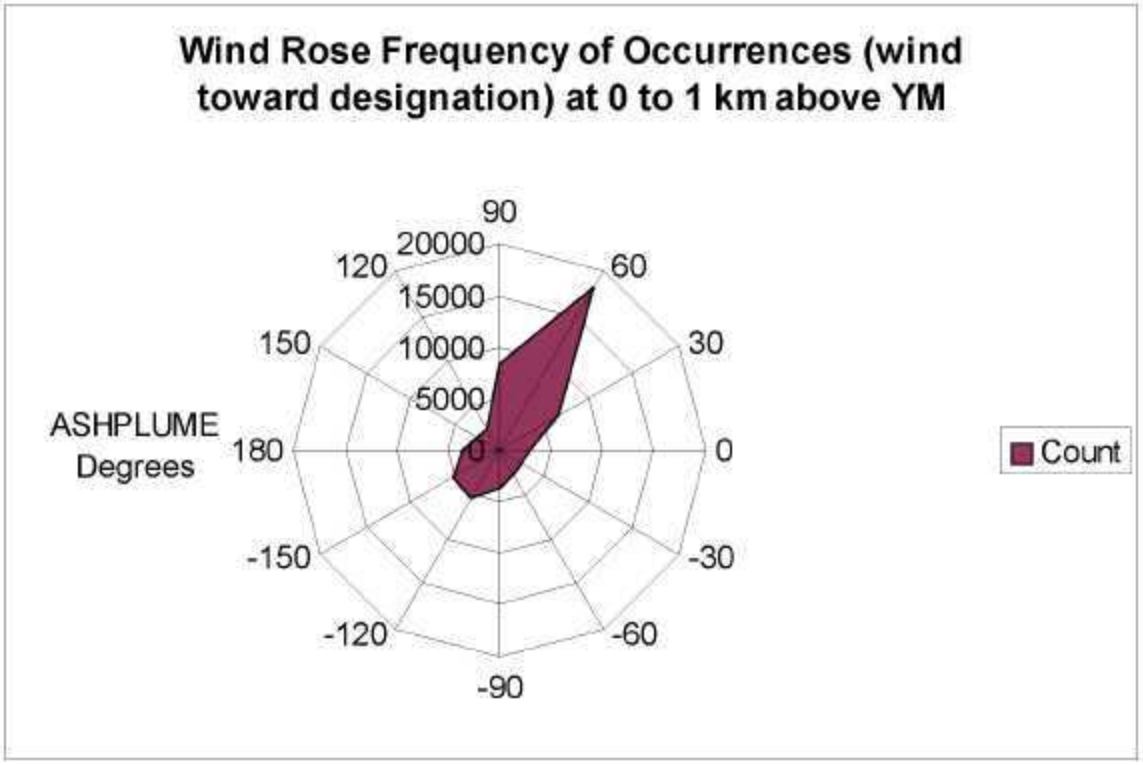


Output DTN: MO0408SPADRWSD.002.

Figure D-3. Wind Frequency of Occurrences at 0 to 1 km above Yucca Mountain

Table D-24. 1 to 2 km PDF

| Compass Degrees | ASHPLUME Degrees | Count | PDF |
|---|---|---|---|
| 165 to 195 | 90 | 9,213 | 0.1271 |
| 195 to 225 | 60 | 16,871 | 0.2327 |
| 225 to 255 | 30 | 9,220 | 0.1272 |
| 255 to 285 | 0 | 4,836 | 0.0667 |
| 285 to 315 | –30 | 4,869 | 0.0671 |
| 315 to 345 | –60 | 6,337 | 0.0874 |
| 345 to 15 | –90 | 6,299 | 0.0869 |
| 15 to 45 | –120 | 5,038 | 0.0695 |
| 45 to 75 | –150 | 2,871 | 0.0396 |
| 75 to 105 | 180 | 1,839 | 0.0254 |
| 105 to 135 | 150 | 1,908 | 0.0263 |
| 135 to 165 | 120 | 3,197 | 0.0441 |
| | Totals | 72,498 | 1.0000 |

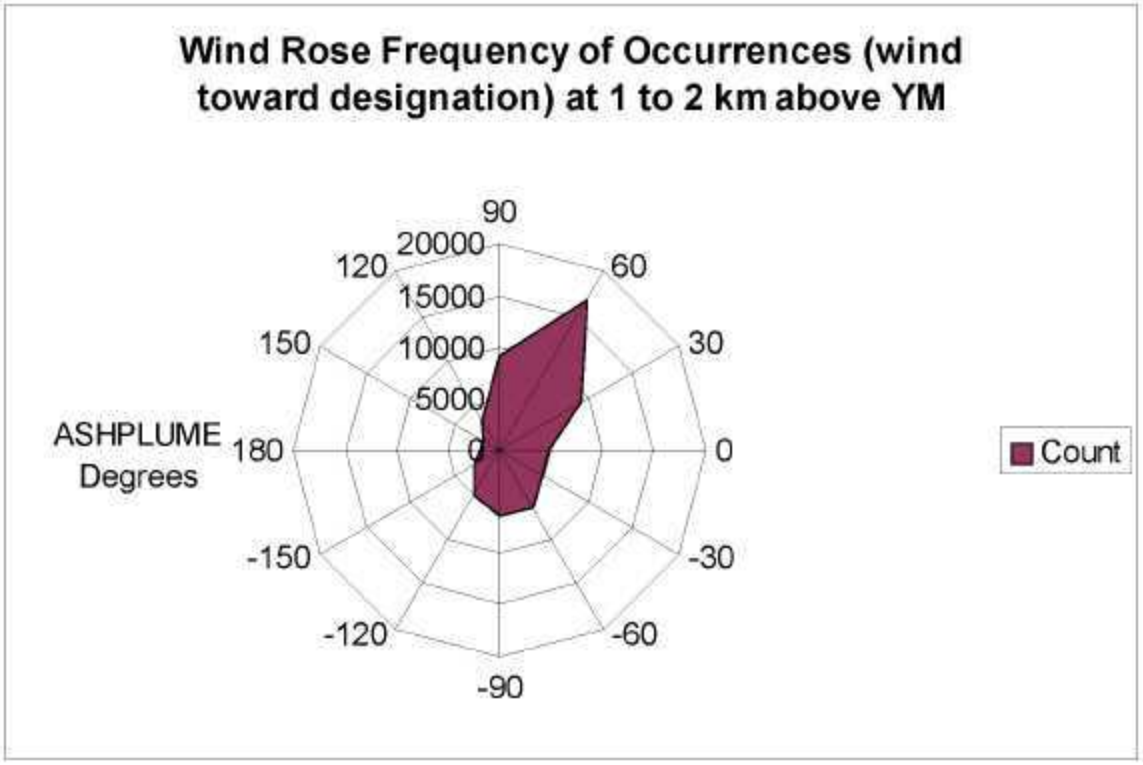


Output DTN: MO0408SPADRWSD.002.

Figure D-4. Wind Rose Frequency of Occurrences at 1 to 2 km above Yucca Mountain

Table D-25. 2 to 3 km PDF

| Compass Degrees | ASHPLUME Degrees | Count | PDF |
|---|---|---|---|
| 165 to 195 | 90 | 8,013 | 0.0975 |
| 195 to 225 | 60 | 12,663 | 0.1541 |
| 225 to 255 | 30 | 12,793 | 0.1557 |
| 255 to 285 | 0 | 9,373 | 0.1140 |
| 285 to 315 | –30 | 9,428 | 0.1147 |
| 315 to 345 | –60 | 9,049 | 0.1101 |
| 345 to 15 | –90 | 6,332 | 0.0770 |
| 15 to 45 | –120 | 3,696 | 0.0450 |
| 45 to 75 | –150 | 2,148 | 0.0261 |
| 75 to 105 | 180 | 1,811 | 0.0220 |
| 105 to 135 | 150 | 2,456 | 0.0299 |
| 135 to 165 | 120 | 4,430 | 0.0539 |
| | Totals | 82,192 | 1.0000 |

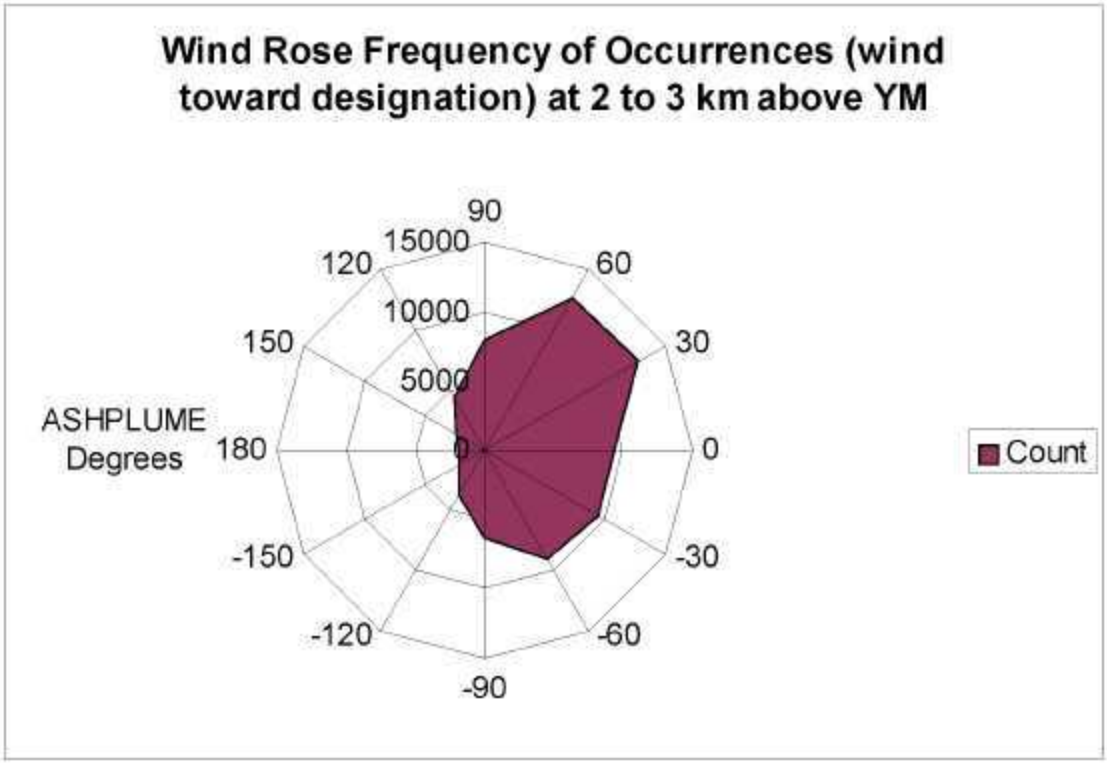


Output DTN: MO0408SPADRWSD.002.

Figure D-5. Wind Rose Frequency of Occurrences at 2 to 3 km above Yucca Mountain

Table D-26. 3 to 4 km PDF

| Compass Degrees | ASHPLUME Degrees | Count | PDF |
|---|---|---|---|
| 165 to 195 | 90 | 5,788 | 0.0818 |
| 195 to 225 | 60 | 9,821 | 0.1388 |
| 225 to 255 | 30 | 12,019 | 0.1699 |
| 255 to 285 | 0 | 11,030 | 0.1559 |
| 285 to 315 | –30 | 10,186 | 0.1440 |
| 315 to 345 | –60 | 7,486 | 0.1058 |
| 345 to 15 | –90 | 4,402 | 0.0622 |
| 15 to 45 | –120 | 2,497 | 0.0353 |
| 45 to 75 | –150 | 1,639 | 0.0232 |
| 75 to 105 | 180 | 1,407 | 0.0199 |
| 105 to 135 | 150 | 1,743 | 0.0246 |
| 135 to 165 | 120 | 2,730 | 0.0386 |
| | Totals | 70,748 | 1.0000 |

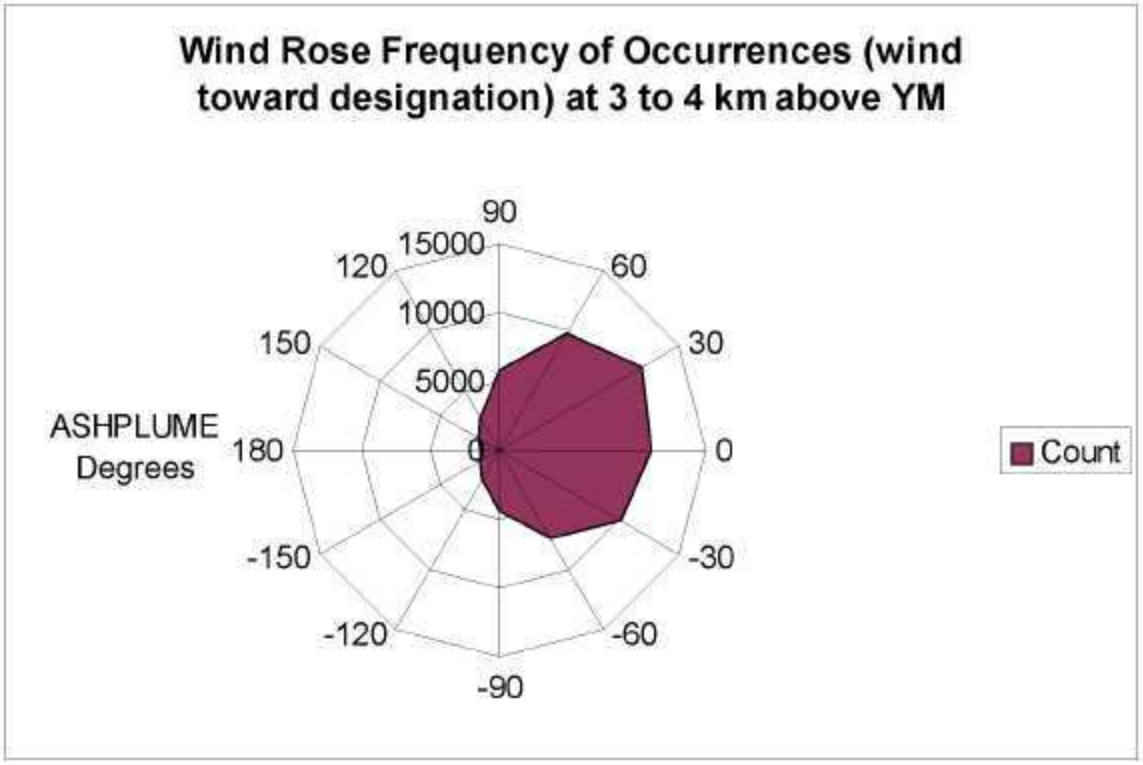


Output DTN: MO0408SPADRWSD.002.

Figure D-6. Wind Rose Frequency of Occurrences at 3 to 4 km above Yucca Mountain

Table D-27. 4 to 5 km PDF

| Compass Degrees | ASHPLUME Degrees | Count | PDF |
|---|---|---|---|
| 165 to 195 | 90 | 4,010 | 0.0612 |
| 195 to 225 | 60 | 8,761 | 0.1338 |
| 225 to 255 | 30 | 12,613 | 0.1926 |
| 255 to 285 | 0 | 12,291 | 0.1877 |
| 285 to 315 | –30 | 10,219 | 0.1560 |
| 315 to 345 | –60 | 6,696 | 0.1022 |
| 345 to 15 | –90 | 3,630 | 0.0554 |
| 15 to 45 | –120 | 2,051 | 0.0313 |
| 45 to 75 | –150 | 1,380 | 0.0211 |
| 75 to 105 | 180 | 1,014 | 0.0155 |
| 105 to 135 | 150 | 1,095 | 0.0167 |
| 135 to 165 | 120 | 1,734 | 0.0265 |
| | Totals | 65,494 | 1.0000 |

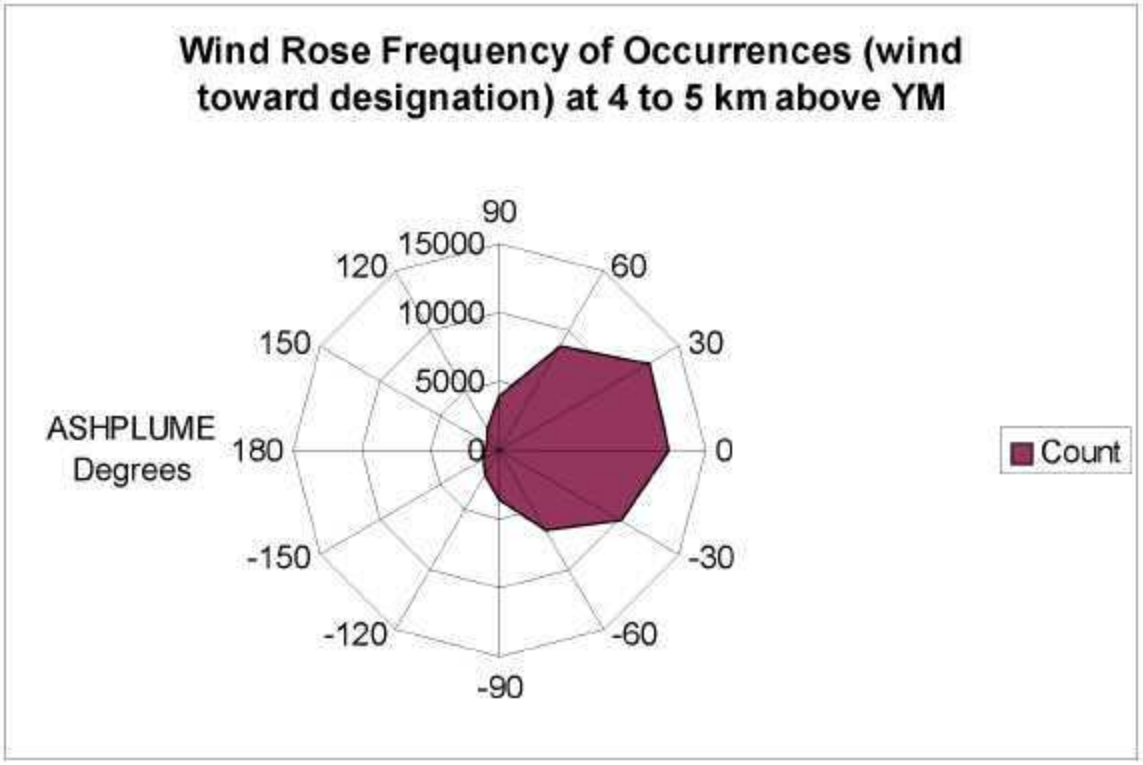


Output DTN: MO0408SPADRWSD.002.

Figure D-7. Wind Rose Frequency of Occurrences at 4 to 5 km above Yucca Mountain

Table D-28. 5 to 6 km PDF

| Compass Degrees | ASHPLUME Degrees | Count | PDF |
|---|---|---|---|
| 165 to 195 | 90 | 3,169 | 0.0509 |
| 195 to 225 | 60 | 8,423 | 0.1355 |
| 225 to 255 | 30 | 12,947 | 0.2083 |
| 255 to 285 | 0 | 12,401 | 0.1994 |
| 285 to 315 | –30 | 9,854 | 0.1585 |
| 315 to 345 | –60 | 6,098 | 0.0981 |
| 345 to 15 | –90 | 3,177 | 0.0511 |
| 15 to 45 | –120 | 1,807 | 0.0291 |
| 45 to 75 | –150 | 1,183 | 0.0190 |
| 75 to 105 | 180 | 838 | 0.0135 |
| 105 to 135 | 150 | 917 | 0.0148 |
| 135 to 165 | 120 | 1,355 | 0.0218 |
| | Totals | 62,169 | 1.0000 |

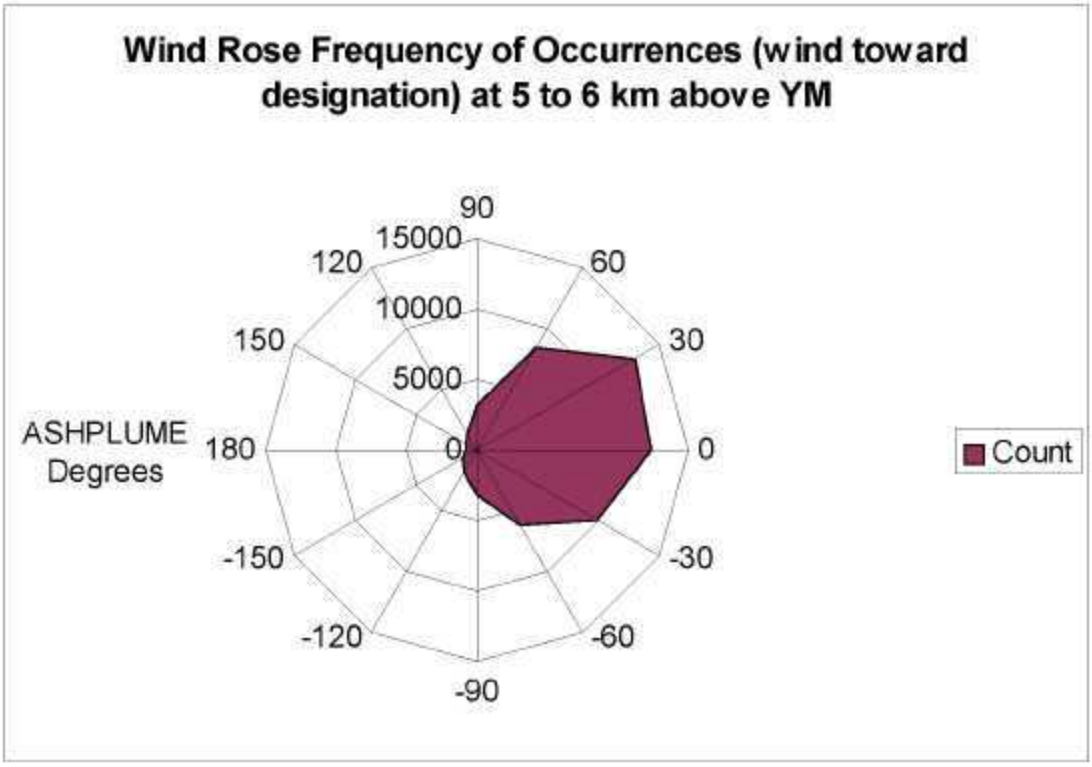


Output DTN: MO0408SPADRWSD.002.

Figure D-8. Wind Rose Frequency of Occurrences at 5 to 6 km above Yucca Mountain

Table D-29. 6 to 7 km PDF

| Compass Degrees | ASHPLUME Degrees | Count | PDF |
|---|---|---|---|
| 165 to 195 | 90 | 2,718 | 0.0473 |
| 195 to 225 | 60 | 7,349 | 0.1278 |
| 225 to 255 | 30 | 12,617 | 0.2194 |
| 255 to 285 | 0 | 11,934 | 0.2075 |
| 285 to 315 | –30 | 8,959 | 0.1558 |
| 315 to 345 | –60 | 5,696 | 0.0990 |
| 345 to 15 | –90 | 3,067 | 0.0533 |
| 15 to 45 | –120 | 1,750 | 0.0304 |
| 45 to 75 | –150 | 952 | 0.0166 |
| 75 to 105 | 180 | 703 | 0.0122 |
| 105 to 135 | 150 | 670 | 0.0117 |
| 135 to 165 | 120 | 1,090 | 0.0190 |
| | Totals | 57,505 | 1.0000 |

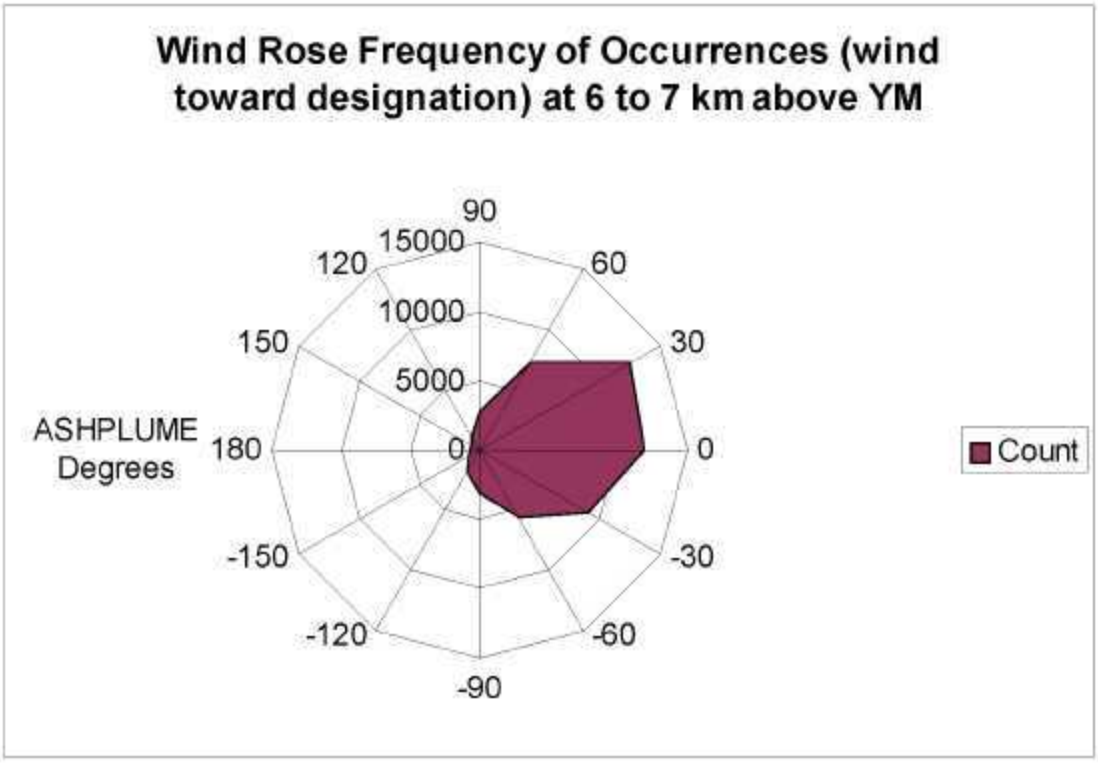


Output DTN: MO0408SPADRWSD.002.

Figure D-9. Wind Rose Frequency of Occurrences at 6 to 7 km above Yucca Mountain

Table D-30. 7 to 8 km PDF

| Compass Degrees | ASHPLUME Degrees | Count | PDF |
|---|---|---|---|
| 165 to 195 | 90 | 2,302 | 0.0448 |
| 195 to 225 | 60 | 6,333 | 0.1231 |
| 225 to 255 | 30 | 11,358 | 0.2208 |
| 255 to 285 | 0 | 11,152 | 0.2168 |
| 285 to 315 | –30 | 8,158 | 0.1586 |
| 315 to 345 | –60 | 5,123 | 0.0996 |
| 345 to 15 | –90 | 2,690 | 0.0523 |
| 15 to 45 | –120 | 1,523 | 0.0296 |
| 45 to 75 | –150 | 775 | 0.0151 |
| 75 to 105 | 180 | 518 | 0.0101 |
| 105 to 135 | 150 | 565 | 0.0110 |
| 135 to 165 | 120 | 937 | 0.0182 |
| | Totals | 51,434 | 1.0000 |

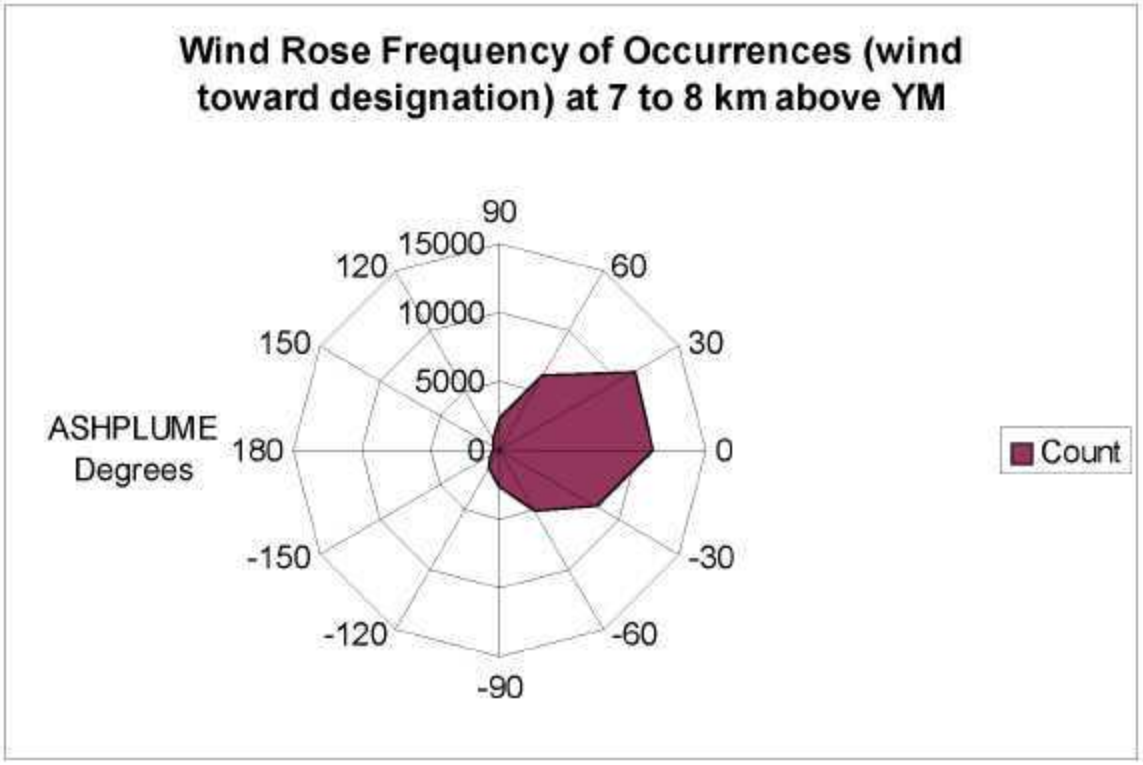


Output DTN: MO0408SPADRWSD.002.

Figure D-10. Wind Rose Frequency of Occurrences at 7 to 8 km above Yucca Mountain

Table D-31. 8 to 9 km PDF

| Compass Degrees | ASHPLUME Degrees | Count | PDF |
|---|---|---|---|
| 165 to 195 | 90 | 1,976 | 0.0417 |
| 195 to 225 | 60 | 5,646 | 0.1192 |
| 225 to 255 | 30 | 11,114 | 0.2346 |
| 255 to 285 | 0 | 10,783 | 0.2276 |
| 285 to 315 | –30 | 7,419 | 0.1566 |
| 315 to 345 | –60 | 4,503 | 0.0951 |
| 345 to 15 | –90 | 2,462 | 0.0520 |
| 15 to 45 | –120 | 1,254 | 0.0265 |
| 45 to 75 | –150 | 651 | 0.0137 |
| 75 to 105 | 180 | 428 | 0.0090 |
| 105 to 135 | 150 | 397 | 0.0084 |
| 135 to 165 | 120 | 740 | 0.0156 |
| | Totals | 47,373 | 1.0000 |

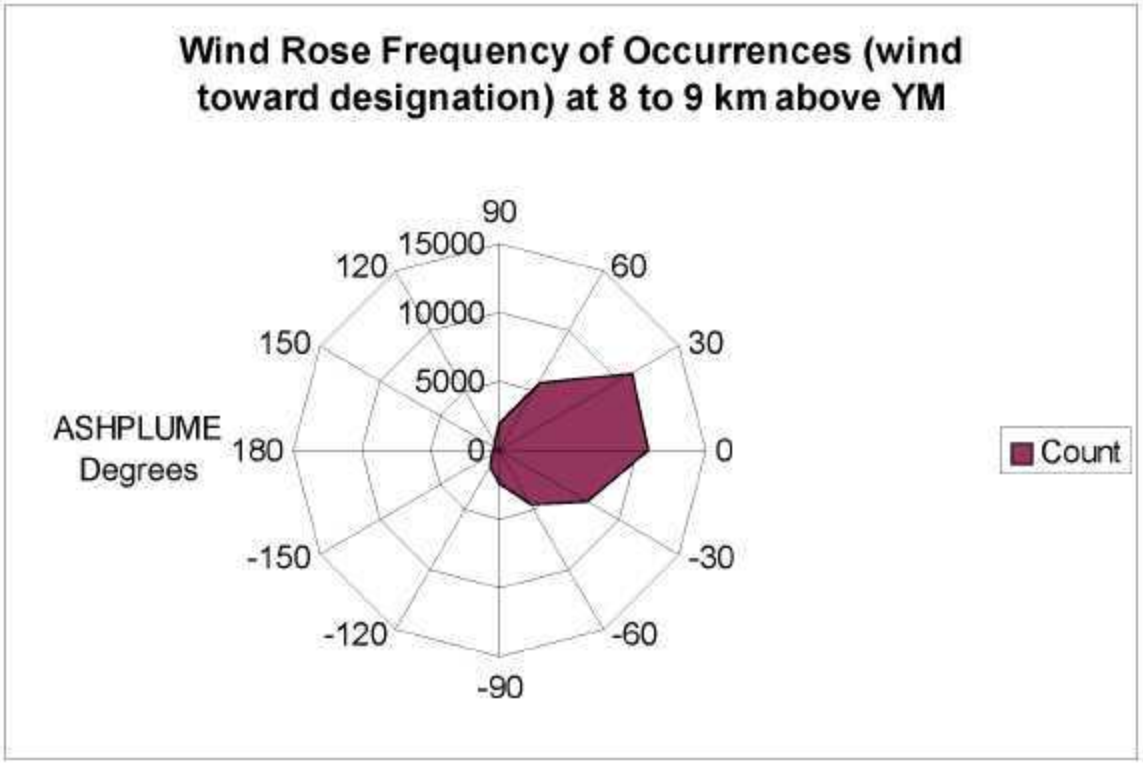


Output DTN: MO0408SPADRWSD.002.

Figure D-11. Wind Rose Frequency of Occurrences at 8 to 9 km above Yucca Mountain

Table D-32. 9 to 10 km PDF

| Compass Degrees | ASHPLUME Degrees | Count | PDF |
|---|---|---|---|
| 165 to 195 | 90 | 1,571 | 0.0315 |
| 195 to 225 | 60 | 5,534 | 0.1110 |
| 225 to 255 | 30 | 1,2081 | 0.2423 |
| 255 to 285 | 0 | 12,068 | 0.2420 |
| 285 to 315 | –30 | 8,405 | 0.1685 |
| 315 to 345 | –60 | 4,816 | 0.0966 |
| 345 to 15 | –90 | 2,356 | 0.0472 |
| 15 to 45 | –120 | 1,209 | 0.0242 |
| 45 to 75 | –150 | 566 | 0.0114 |
| 75 to 105 | 180 | 361 | 0.0072 |
| 105 to 135 | 150 | 349 | 0.0070 |
| 135 to 165 | 120 | 553 | 0.0111 |
| | Totals | 49,869 | 1.0000 |

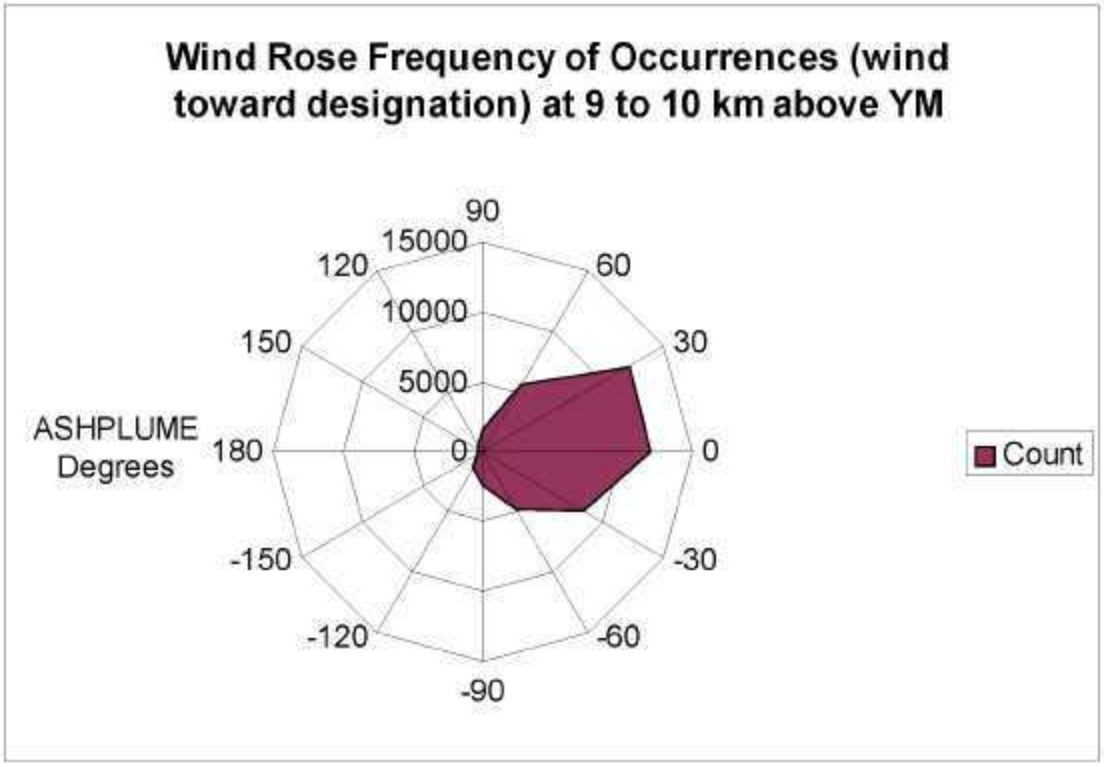


Output DTN: MO0408SPADRWSD.002.

Figure D-12. Wind Rose Frequency of Occurrences at 9 to 10 km above Yucca Mountain

Table D-33. 10 to 11 km PDF

| Compass Degrees | ASHPLUME Degrees | Count | PDF |
|---|---|---|---|
| 165 to 195 | 90 | 1,334 | 0.0249 |
| 195 to 225 | 60 | 5,272 | 0.0983 |
| 225 to 255 | 30 | 12,850 | 0.2396 |
| 255 to 285 | 0 | 14,714 | 0.2743 |
| 285 to 315 | –30 | 10,223 | 0.1906 |
| 315 to 345 | –60 | 4,782 | 0.0892 |
| 345 to 15 | –90 | 2,119 | 0.0395 |
| 15 to 45 | –120 | 943 | 0.0176 |
| 45 to 75 | –150 | 444 | 0.0083 |
| 75 to 105 | 180 | 238 | 0.0044 |
| 105 to 135 | 150 | 308 | 0.0057 |
| 135 to 165 | 120 | 408 | 0.0076 |
| | Totals | 53,635 | 1.0000 |

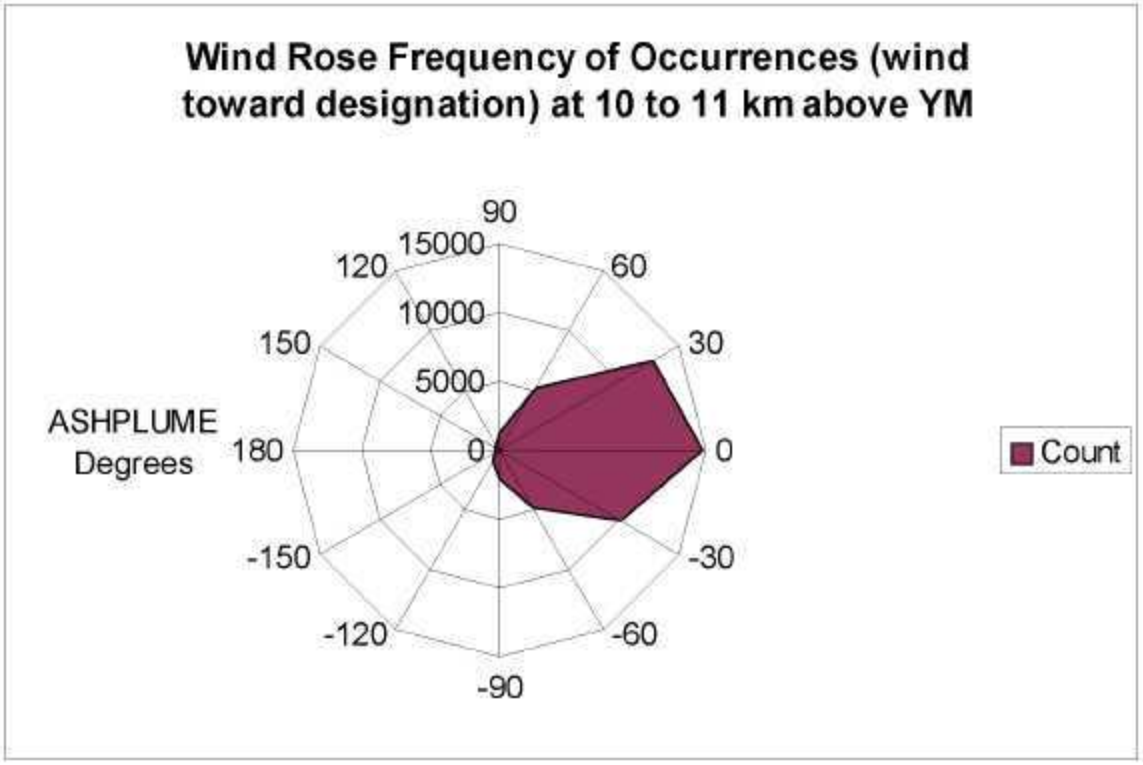


Output DTN: MO0408SPADRWSD.002.

Figure D-13. Wind Rose Frequency of Occurrences at 10 to 11 km above Yucca Mountain

Table D-34. 11 to 12 km PDF

| Compass Degrees | ASHPLUME Degrees | Count | PDF |
|---|---|---|---|
| 165 to 195 | 90 | 1,113 | 0.0196 |
| 195 to 225 | 60 | 4,989 | 0.0876 |
| 225 to 255 | 30 | 13,966 | 0.2454 |
| 255 to 285 | 0 | 17,353 | 0.3049 |
| 285 to 315 | –30 | 11,271 | 0.1980 |
| 315 to 345 | –60 | 4,564 | 0.0802 |
| 345 to 15 | –90 | 1,701 | 0.0299 |
| 15 to 45 | –120 | 821 | 0.0144 |
| 45 to 75 | –150 | 366 | 0.0064 |
| 75 to 105 | 180 | 192 | 0.0034 |
| 105 to 135 | 150 | 182 | 0.0032 |
| 135 to 165 | 120 | 399 | 0.0070 |
| | Totals | 56,917 | 1.0000 |

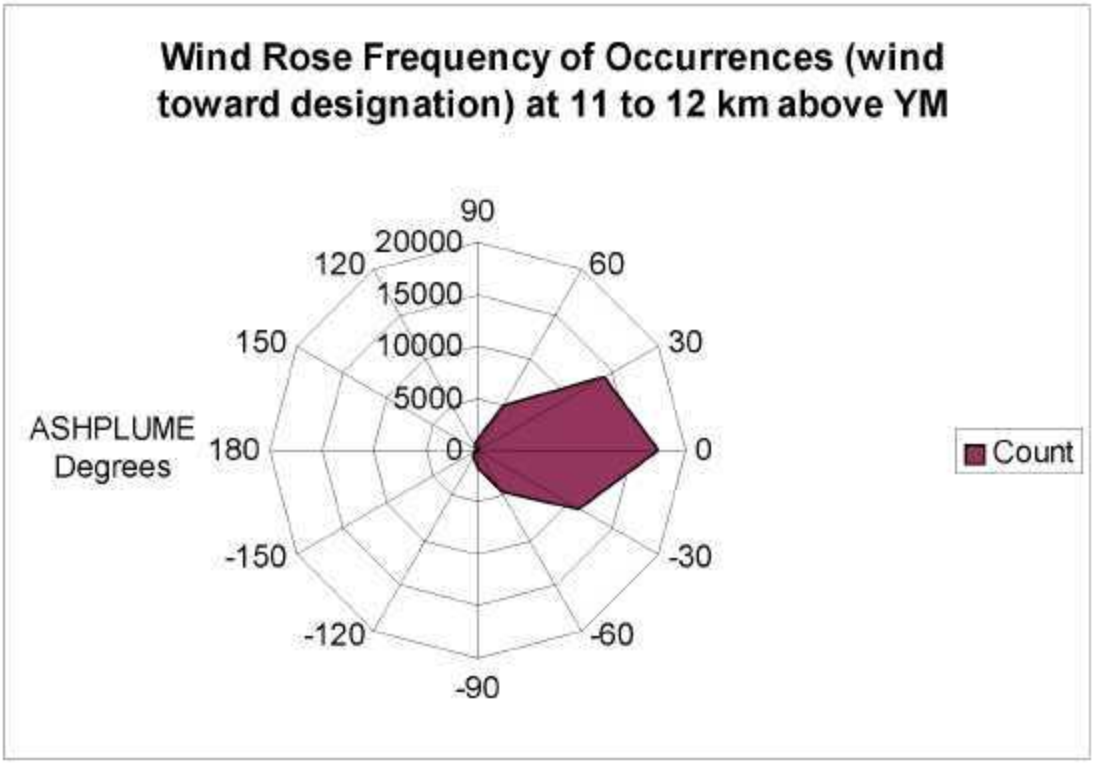


Output DTN: MO0408SPADRWSD.002.

Figure D-14. Wind Rose Frequency of Occurrences at 11 to 12 km above Yucca Mountain

Table D-35. 12 to 13 km PDF

| Compass Degrees | ASHPLUME Degrees | Count | PDF |
|---|---|---|---|
| 165 to 195 | 90 | 1,058 | 0.0205 |
| 195 to 225 | 60 | 4,236 | 0.0818 |
| 225 to 255 | 30 | 13,274 | 0.2564 |
| 255 to 285 | 0 | 1,6921 | 0.3268 |
| 285 to 315 | –30 | 10,050 | 0.1941 |
| 315 to 345 | –60 | 3,528 | 0.0681 |
| 345 to 15 | –90 | 1,262 | 0.0244 |
| 15 to 45 | –120 | 472 | 0.0091 |
| 45 to 75 | –150 | 276 | 0.0053 |
| 75 to 105 | 180 | 149 | 0.0029 |
| 105 to 135 | 150 | 191 | 0.0037 |
| 135 to 165 | 120 | 357 | 0.0069 |
| | Totals | 51,774 | 1.0000 |

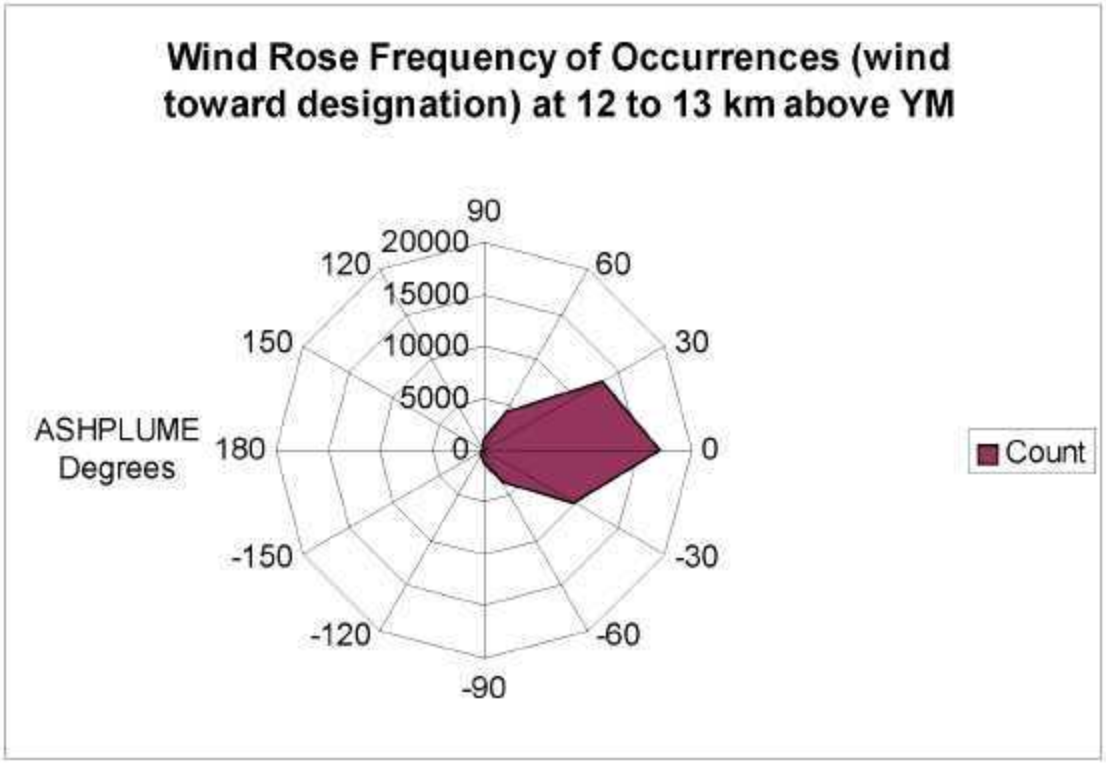


Output DTN: MO0408SPADRWSD.002.

Figure D-15. Wind Rose Frequency of Occurrences at 12 to 13 km above Yucca Mountain

# APPENDIX E
# INPUT VALUES FOR WASTE FORM CONCENTRATION AT THE RMEI LOCATION

# APPENDIX E
# INPUT VALUES FOR WASTE FORM CONCENTRATION AT THE RMEI LOCATION

The following tables contain the values of ASHPLUME parameters that were used to calculate the mean waste concentration at the RMEI location used in the ash redistribution model discussed in Section 6.7. Table E-1 contains the fixed (deterministic) values and Table E-2 contains the sampled (stochastic) values for each realization of the GoldSim/ASHPLUME simulation.

Table E-1. Fixed Input Values for ASHPLUME

| Input Parameters | | |
|---|---|---|
| Names Used in ASHPLUME Code[a] | Names Provided to TSPA[b] | Value[c] |
| xmin, xmax (km) | $X_{min}$, $X_{max}$ | 0, 0 |
| ymin, ymax (km) | $Y_{min}$, $Y_{max}$ | 0, -8 |
| numptsx | $N_x$ | 1 |
| numptsy | $N_y$ | 2 |
| ashdenmin | $\psi_p^{low}$ | 1 04 |
| ashdenmax | $\psi_p^{high}$ | 2 08 |
| ashrholow | $\rho_a^{low}$ | -3 |
| ashrhohi | $\rho_a^{high}$ | 0 |
| fshape | F | 0 5 |
| airden | $\psi_a$ | 0 001117 |
| airvis | $\eta_a$ | 0 0001758 |
| c | C | 400 0 |
| dmax | $d_{max}$ | 10 |
| acutoff | Ash Cutoff | 1e-10 |
| hmin | $H_{min}$ | 0 001 |
| fdmin, fdmean[e], fdmax | $\rho^f_{min}$, $\rho^f_{mode}$, $\rho^f_{max}$ | 0 0001, 0 0016, 0 05 |
| Rhocut | $\rho_c$ | 0 3 |
| mass of waste (g) | U | 4 01e7[d] |

Source Output DTN LA0408GK831811 001

NOTES [a] Variable names used in the ASHPLUME code

[b] Parameter names provided to TSPA (from Table 8-2) from the mathematical description in Section 6 5 1

[c] Values used in this modeling exercise, identical to those provided to TSPA in Table 8-2 Table 8-2 includes all but the last value in this table, which is a value developed in TSPA for each realization at run-time

[d] Mass of fuel available for entrainment derived from *Miscellaneous Waste-Form FEPs* (CRWMS M&O 2001 [DIRS 153938], p 49) 63,000 MTHM emplaced in 7,860 packages = 8 02E+06 g/package, assume 5 waste packages hit (median value from DTN MO0504MWDNUMWP 001 [DIRS 173521])

[e] Despite the name, "fdmean," this variable contains values of the *mode* of the waste particle size distribution

Table E-2. Realizations for Distributed Parameter Values

| Sampled Values | | | | | | | | | Calculated Values | | |
|---|---|---|---|---|---|---|---|---|---|---|---|
| Realization Number | Beta | Mean Ash Diameter (cm) | Ash Sigma | Wind Direction (Degrees) | Wind Speed (cm/s) | Eruptive Velocity (cm/s) | Event Power (W) | Event Duration (s) | Height (km) | Q | Volume ($km^3$) |
| 1 | 0 10855 | 0 018948 | 1 8939 | –90 | 1072 2 | 20 55 | 8 30E+11 | 8 89E+03 | 7 83E+00 | 1 13E+09 | 0 010 |
| 2 | 0 20335 | 0 003298 | 1 6046 | –90 | 3205 9 | 10 | 2 94E+12 | 1 40E+04 | 1 07E+01 | 4 01E+09 | 0 056 |
| 3 | 0 48714 | 0 03586 | 1 6411 | –90 | 2996 7 | 10 | 1 64E+12 | 18060 | 9 28E+00 | 2 23E+09 | 0 040 |
| 4 | 0 47457 | 0 005633 | 1 7244 | –90 | 2720 6 | 218 64 | 5 91E+11 | 1 96E+04 | 7 19E+00 | 8 05E+08 | 0 016 |
| 5 | 0 019063 | 0 003392 | 1 328 | –90 | 956 87 | 114 18 | 3 03E+10 | 6 55E+05 | 3 42E+00 | 4 13E+07 | 0 027 |
| 6 | 0 12575 | 0 001229 | 1 6709 | –90 | 823 49 | 26 855 | 4 16E+09 | 9 75E+05 | 2 08E+00 | 5 67E+06 | 0 006 |
| 7 | 0 40332 | 0 046453 | 1 7584 | –90 | 1716 6 | 39 758 | 1 18E+11 | 6 18E+04 | 4 80E+00 | 1 60E+08 | 0 010 |
| 8 | 0 34033 | 0 007207 | 1 578 | –90 | 620 56 | 62 124 | 1 30E+10 | 3 89E+05 | 2 77E+00 | 1 77E+07 | 0 007 |
| 9 | 0 14839 | 0 010347 | 1 5623 | –90 | 964 68 | 1201 5 | 1 66E+09 | 6 15E+06 | 1 65E+00 | 2 26E+06 | 0 014 |
| 10 | 0 49345 | 0 006209 | 1 4311 | –90 | 585 24 | 10006 | 1 08E+09 | 2 28E+07 | 1 49E+00 | 1 48E+06 | 0 034 |
| 11 | 0 39152 | 0 023954 | 1 7867 | –90 | 649 86 | 36 287 | 2 68E+11 | 2 75E+05 | 5 90E+00 | 3 65E+08 | 0 100 |
| 12 | 0 23733 | 0 004249 | 1 8278 | –90 | 1843 2 | 10 098 | 1 01E+12 | 6 86E+04 | 8 21E+00 | 1 37E+09 | 0 094 |
| 13 | 0 32695 | 0 002963 | 1 8567 | –90 | 1011 5 | 10 | 2 92E+11 | 1 86E+05 | 6 03E+00 | 3 98E+08 | 0 074 |
| 14 | 0 14144 | 0 001522 | 1 6183 | –90 | 1317 1 | 2722 | 1 89E+09 | 2 73E+06 | 1 71E+00 | 2 58E+06 | 0 007 |
| 15 | 0 32451 | 0 019181 | 1 8595 | –90 | 359 05 | 101 15 | 1 92E+10 | 8 41E+05 | 3 05E+00 | 2 62E+07 | 0 022 |
| 16 | 0 097629 | 0 022644 | 1 8126 | –90 | 2961 6 | 11039 | 9 59E+11 | 1 05E+04 | 8 12E+00 | 1 31E+09 | 0 014 |
| 17 | 0 061627 | 0 009993 | 1 513 | –90 | 2205 | 10 | 4 41E+11 | 1 27E+05 | 6 68E+00 | 6 01E+08 | 0 076 |
| 18 | 0 18016 | 0 018317 | 1 3848 | –90 | 926 73 | 18 434 | 3 88E+09 | 1 08E+06 | 2 05E+00 | 5 29E+06 | 0 006 |
| 19 | 0 11303 | 0 009411 | 1 7296 | –90 | 744 39 | 6362 5 | 3 67E+09 | 1 79E+07 | 2 02E+00 | 5 01E+06 | 0 090 |
| 20 | 0 16503 | 0 011044 | 1 5222 | –90 | 2802 7 | 11 982 | 2 40E+12 | 9449 2 | 1 02E+01 | 3 27E+09 | 0 031 |
| 21 | 0 24882 | 0 002086 | 1 6159 | –90 | 1503 9 | 10 | 3 60E+10 | 1 01E+06 | 3 57E+00 | 4 91E+07 | 0 049 |
| 22 | 0 4179 | 0 011312 | 1 8993 | –90 | 1383 3 | 8182 7 | 4 88E+10 | 2 16E+05 | 3 85E+00 | 6 65E+07 | 0 014 |
| 23 | 0 34529 | 0 030725 | 1 5963 | –90 | 1665 8 | 278 83 | 6 95E+09 | 1 12E+06 | 2 37E+00 | 9 47E+06 | 0 011 |

Table E-2. Realizations for Distributed Parameter Values (Continued)

| Sampled Values | | | | | | | | | Calculated Values | | |
|---|---|---|---|---|---|---|---|---|---|---|---|
| Realization Number | Beta | Mean Ash Diameter (cm) | Ash Sigma | Wind Direction (Degrees) | Wind Speed (cm/s) | Eruptive Velocity (cm/s) | Event Power (W) | Event Duration (s) | Height (km) | Q | Volume ($km^3$) |
| 24 | 0 057311 | 0 012236 | 1 5529 | –90 | 1577 3 | 33 608 | 1 05E+09 | 6 01E+06 | 1 48E+00 | 1 43E+06 | 0 009 |
| 25 | 0 4958 | 0 01719 | 1 4073 | –90 | 2695 6 | 1418 9 | 1 08E+12 | 11229 | 8 37E+00 | 1 48E+09 | 0 017 |
| 26 | 0 053379 | 0 005176 | 1 7736 | –90 | 733 56 | 891 07 | 3 35E+10 | 9 82E+05 | 3 51E+00 | 4 57E+07 | 0 045 |
| 27 | 0 39677 | 0 03559 | 1 4496 | –90 | 1774 1 | 3517 4 | 4 38E+11 | 2 97E+04 | 6 67E+00 | 5 96E+08 | 0 018 |
| 28 | 0 40069 | 0 013108 | 1 8177 | –90 | 1721 5 | 861 24 | 3 26E+09 | 4 25E+06 | 1 96E+00 | 4 45E+06 | 0 019 |
| 29 | 0 22168 | 0 016008 | 1 3598 | –90 | 918 64 | 6109 4 | 3 54E+11 | 3 62E+04 | 6 33E+00 | 4 83E+08 | 0 017 |
| 30 | 0 36982 | 0 008359 | 1 6889 | –90 | 661 35 | 10 | 2 06E+12 | 2 81E+03 | 9 82E+00 | 2 80E+09 | 0 008 |
| 31 | 0 040611 | 0 007032 | 1 34 | –90 | 2080 6 | 953 71 | 3 98E+12 | 2 21E+03 | 1 16E+01 | 5 42E+09 | 0 012 |
| 32 | 0 080302 | 0 006817 | 1 7857 | –90 | 1037 8 | 2330 2 | 2 47E+12 | 11491 | 1 03E+01 | 3 36E+09 | 0 039 |
| 33 | 0 20743 | 0 010202 | 1 4761 | –90 | 4734 2 | 10 | 1 93E+11 | 3 72E+05 | 5 43E+00 | 2 62E+08 | 0 098 |
| 34 | 0 020223 | 0 004745 | 1 5196 | –90 | 1278 6 | 98 09 | 6 96E+08 | 7 17E+07 | 1 33E+00 | 9 49E+05 | 0 068 |
| 35 | 0 29992 | 0 025372 | 1 3354 | –90 | 1168 2 | 171 97 | 4 38E+12 | 1 48E+03 | 1 19E+01 | 5 97E+09 | 0 009 |
| 36 | 0 45484 | 0 005445 | 1 4999 | –90 | 1060 1 | 10 | 6 39E+10 | 8 11E+05 | 4 12E+00 | 8 70E+07 | 0 071 |
| 37 | 0 010989 | 0 01088 | 1 6588 | –90 | 471 73 | 23 048 | 1 82E+09 | 2 10E+07 | 1 69E+00 | 2 48E+06 | 0 052 |
| 38 | 0 16747 | 0 00199 | 1 4541 | –90 | 1670 | 85 498 | 2 02E+12 | 2 73E+03 | 9 77E+00 | 2 75E+09 | 0 008 |
| 39 | 0 13409 | 0 063383 | 1 4968 | –90 | 1376 3 | 9120 1 | 6 64E+11 | 5 67E+04 | 7 40E+00 | 9 04E+08 | 0 051 |
| 40 | 0 46284 | 0 00165 | 1 7523 | –90 | 560 59 | 30 606 | 1 31E+09 | 6 92E+06 | 1 56E+00 | 1 79E+06 | 0 012 |
| 41 | 0 15246 | 0 005781 | 1 5842 | –90 | 606 16 | 10 | 1 60E+11 | 2 11E+05 | 5 18E+00 | 2 17E+08 | 0 046 |
| 42 | 0 41339 | 0 017692 | 1 8755 | v | 991 19 | 3718 9 | 1 05E+11 | 4 59E+04 | 4 67E+00 | 1 44E+08 | 0 007 |
| 43 | 0 11836 | 0 015189 | 1 7142 | –90 | 1619 9 | 80 014 | 1 37E+12 | 4994 7 | 8 86E+00 | 1 86E+09 | 0 009 |
| 44 | 0 25301 | 0 001606 | 1 6304 | –90 | 690 72 | 10 | 2 14E+09 | 7 68E+06 | 1 76E+00 | 2 92E+06 | 0 022 |
| 45 | 0 045761 | 0 002515 | 1 4227 | –90 | 677 59 | 8817 8 | 6 67E+08 | 3 12E+07 | 1 32E+00 | 9 09E+05 | 0 028 |
| 46 | 0 23332 | 0 038371 | 1 3446 | –90 | 2020 1 | 1949 9 | 4 44E+10 | 1 30E+06 | 3 76E+00 | 6 05E+07 | 0 079 |
| 47 | 0 43405 | 0 020972 | 1 7931 | –90 | 353 95 | 16 302 | 2 25E+09 | 1 36E+07 | 1 79E+00 | 3 06E+06 | 0 042 |

Table E-2. Realizations for Distributed Parameter Values (Continued)

| Sampled Values | | | | | | | | | Calculated Values | | |
|---|---|---|---|---|---|---|---|---|---|---|---|
| Realization Number | Beta | Mean Ash Diameter (cm) | Ash Sigma | Wind Direction (Degrees) | Wind Speed (cm/s) | Eruptive Velocity (cm/s) | Event Power (W) | Event Duration (s) | Height (km) | Q | Volume ($km^3$) |
| 48 | 0 35445 | 0 027366 | 1 7032 | –90 | 383 75 | 10 | 1 61E+10 | 1 67E+06 | 2 92E+00 | 2 20E+07 | 0 037 |
| 49 | 0 42556 | 0 016386 | 1 3722 | –90 | 806 47 | 10 | 6 03E+10 | 1 34E+05 | 4 06E+00 | 8 22E+07 | 0 011 |
| 50 | 0 17202 | 0 014384 | 1 5323 | –90 | 1703 3 | 4369 | 7 48E+11 | 42882 | 7 63E+00 | 1 02E+09 | 0 044 |
| 51 | 0 27116 | 0 043077 | 1 3679 | –90 | 1190 7 | 10 | 8 62E+09 | 5 21E+06 | 2 50E+00 | 1 17E+07 | 0 061 |
| 52 | 0 44325 | 0 006572 | 1 4686 | v | 887 76 | 52 072 | 7 12E+10 | 2 87E+05 | 4 24E+00 | 9 70E+07 | 0 028 |
| 53 | 0 028049 | 0 007309 | 1 4906 | –90 | 1118 6 | 10 | 2 72E+12 | 2277 8 | 1 05E+01 | 3 70E+09 | 0 008 |
| 54 | 0 031779 | 0 022379 | 1 7123 | –90 | 190 45 | 136 05 | 8 08E+09 | 1 78E+06 | 2 46E+00 | 1 10E+07 | 0 020 |
| 55 | 0 16036 | 0 032047 | 1 6966 | v | 307 78 | 10 | 9 87E+10 | 1 56E+05 | 4 60E+00 | 1 35E+08 | 0 021 |
| 56 | 0 30684 | 0 002662 | 1 5733 | –90 | 1445 | 121 4 | 1 32E+10 | 8 90E+05 | 2 78E+00 | 1 80E+07 | 0 016 |
| 57 | 0 43659 | 0 008017 | 1 8656 | –90 | 964 65 | 201 04 | 4 74E+09 | 1 60E+06 | 2 15E+00 | 6 47E+06 | 0 010 |
| 58 | 0 38654 | 0 004775 | 1 6479 | –90 | 569 57 | 1795 8 | 4 21E+10 | 2 24E+05 | 3 71E+00 | 5 73E+07 | 0 013 |
| 59 | 0 47669 | 0 006128 | 1 6765 | –90 | 652 97 | 2211 7 | 2 49E+09 | 1 11E+07 | 1 83E+00 | 3 39E+06 | 0 038 |
| 60 | 0 31493 | 0 013848 | 1 411 | v | 819 22 | 571 97 | 9 42E+10 | 1 96E+05 | 4 54E+00 | 1 28E+08 | 0 025 |
| 61 | 0 44932 | 0 009707 | 1 4602 | –90 | 625 38 | 475 9 | 5 60E+11 | 7 67E+03 | 7 09E+00 | 7 63E+08 | 0 006 |
| 62 | 0 30983 | 0 029505 | 1 8402 | –90 | 2068 7 | 418 54 | 7 63E+11 | 2 86E+04 | 7 66E+00 | 1 04E+09 | 0 030 |
| 63 | 0 29541 | 0 00637 | 1 7638 | –90 | 1267 1 | 24 881 | 2 12E+10 | 1 23E+06 | 3 13E+00 | 2 88E+07 | 0 035 |
| 64 | 0 23049 | 0 007643 | 1 382 | –90 | 612 94 | 66 365 | 7 61E+08 | 1 74E+07 | 1 36E+00 | 1 04E+06 | 0 018 |
| 65 | 0 36667 | 0 003942 | 1 5405 | –90 | 395 77 | 47 647 | 5 28E+10 | 2 76E+05 | 3 93E+00 | 7 19E+07 | 0 020 |
| 66 | 0 1047 | 0 005287 | 1 8093 | –90 | 2538 6 | 10 | 2 07E+11 | 46433 | 5 53E+00 | 2 82E+08 | 0 013 |
| 67 | 0 073021 | 0 008647 | 1 3173 | v | 1254 5 | 402 34 | 5 79E+09 | 1 31E+07 | 2 26E+00 | 7 88E+06 | 0 103 |
| 68 | 0 31901 | 0 01176 | 1 6933 | –90 | 2193 | 10 | 4 95E+11 | 88001 | 6 88E+00 | 6 75E+08 | 0 059 |
| 69 | 0 19196 | 0 032932 | 1 7357 | –90 | 3495 4 | 10 | 1 84E+12 | 1 38E+04 | 9 55E+00 | 2 50E+09 | 0 035 |
| 70 | 0 19945 | 0 050489 | 1 8797 | –90 | 995 2 | 154 76 | 1 45E+11 | 59774 | 5 06E+00 | 1 97E+08 | 0 012 |
| 71 | 0 037683 | 0 002338 | 1 5505 | –90 | 521 62 | 5450 7 | 2 88E+10 | 6 17E+05 | 3 38E+00 | 3 92E+07 | 0 024 |

Table E-2. Realizations for Distributed Parameter Values (Continued)

| Sampled Values | | | | | | | | | Calculated Values | | |
|---|---|---|---|---|---|---|---|---|---|---|---|
| Realization Number | Beta | Mean Ash Diameter (cm) | Ash Sigma | Wind Direction (Degrees) | Wind Speed (cm/s) | Eruptive Velocity (cm/s) | Event Power (W) | Event Duration (s) | Height (km) | Q | Volume ($km^3$) |
| 72 | 0 45702 | 0 002445 | 1 3526 | –90 | 230 81 | 44 731 | 5 35E+09 | 4 31E+06 | 2 22E+00 | 7 29E+06 | 0 031 |
| 73 | 0 185 | 0 008781 | 1 3975 | –90 | 2759 1 | 513 27 | 1 57E+10 | 2 91E+06 | 2 90E+00 | 2 14E+07 | 0 062 |
| 74 | 0 090665 | 0 011972 | 1 361 | –90 | 2047 5 | 10 | 7 83E+10 | 6 91E+05 | 4 34E+00 | 1 07E+08 | 0 074 |
| 75 | 0 26432 | 0 021554 | 1 839 | v | 870 42 | 11 429 | 2 53E+11 | 2 35E+04 | 5 82E+00 | 3 45E+08 | 0 008 |
| 76 | 0 21442 | 0 012546 | 1 5369 | –90 | 334 27 | 1362 9 | 8 53E+08 | 4 13E+07 | 1 40E+00 | 1 16E+06 | 0 048 |
| 77 | 0 33613 | 0 008167 | 1 6115 | –90 | 818 39 | 190 33 | 2 66E+09 | 1 51E+07 | 1 86E+00 | 3 62E+06 | 0 055 |
| 78 | 0 28486 | 0 015776 | 1 3015 | –90 | 1245 4 | 4080 9 | 3 03E+09 | 2 64E+07 | 1 92E+00 | 4 13E+06 | 0 109 |
| 79 | 0 12988 | 0 019728 | 1 3075 | –90 | 2786 7 | 626 73 | 3 17E+11 | 1 31E+05 | 6 15E+00 | 4 33E+08 | 0 057 |
| 80 | 0 075831 | 0 003778 | 1 4835 | –90 | 104 83 | 2513 | 9 61E+09 | 1 18E+06 | 2 57E+00 | 1 31E+07 | 0 015 |
| 81 | 0 28975 | 0 004592 | 1 4198 | –90 | 1666 4 | 6929 8 | 1 19E+12 | 7 07E+03 | 8 56E+00 | 1 62E+09 | 0 011 |
| 82 | 0 14403 | 0 01068 | 1 566 | –90 | 1665 3 | 1649 4 | 1 86E+10 | 2 53E+06 | 3 03E+00 | 2 53E+07 | 0 064 |
| 83 | 0 37684 | 0 002879 | 1 8479 | –90 | 2851 8 | 246 65 | 3 52E+12 | 1 75E+04 | 1 12E+01 | 4 79E+09 | 0 084 |
| 84 | 0 24032 | 0 008963 | 1 6635 | –90 | 1463 1 | 14 163 | 3 42E+12 | 1351 9 | 1 12E+01 | 4 66E+09 | 0 006 |
| 85 | 0 267 | 0 04095 | 1 6508 | –90 | 3886 8 | 10 | 1 48E+12 | 1 63E+04 | 9 04E+00 | 2 01E+09 | 0 033 |
| 86 | 0 42883 | 0 004346 | 1 7404 | –90 | 657 21 | 13 25 | 6 09E+09 | 5 15E+06 | 2 29E+00 | 8 29E+06 | 0 043 |
| 87 | 0 4825 | 0 009242 | 1 3194 | –90 | 1657 7 | 10 | 1 34E+11 | 1 12E+05 | 4 97E+00 | 1 83E+08 | 0 020 |
| 88 | 0 25842 | 0 007574 | 1 588 | –90 | 1654 3 | 10 | 1 20E+09 | 9 10E+06 | 1 52E+00 | 1 63E+06 | 0 015 |
| 89 | 0 36224 | 0 052305 | 1 6839 | –90 | 787 46 | 775 | 2 33E+11 | 2 91E+05 | 5 70E+00 | 3 18E+08 | 0 093 |
| 90 | 0 47001 | 0 012799 | 1 5064 | –90 | 1807 6 | 4746 | 2 39E+10 | 7 54E+05 | 3 22E+00 | 3 26E+07 | 0 025 |
| 91 | 0 36235 | 0 060861 | 1 8007 | –90 | 2723 5 | 700 97 | 3 75E+11 | 1 53E+04 | 6 42E+00 | 5 11E+08 | 0 008 |
| 92 | 0 21976 | 0 014724 | 1 4372 | –90 | 3381 4 | 17 184 | 2 55E+10 | 1 76E+05 | 3 28E+00 | 3 47E+07 | 0 006 |
| 93 | 0 066009 | 0 005064 | 1 4621 | –90 | 1039 7 | 10 | 7 15E+09 | 6 80E+06 | 2 38E+00 | 9 75E+06 | 0 066 |
| 94 | 0 19032 | 0 072279 | 1 8837 | –90 | 2180 2 | 1050 8 | 1 72E+11 | 1 14E+05 | 5 28E+00 | 2 34E+08 | 0 027 |
| 95 | 0 085915 | 0 025059 | 1 8287 | –90 | 246 21 | 10 | 1 03E+10 | 5 86E+06 | 2 61E+00 | 1 41E+07 | 0 083 |

Table E-2. Realizations for Distributed Parameter Values (Continued)

| Sampled Values | | | | | | | | | Calculated Values | | |
|---|---|---|---|---|---|---|---|---|---|---|---|
| Realization Number | Beta | Mean Ash Diameter (cm) | Ash Sigma | Wind Direction (Degrees) | Wind Speed (cm/s) | Eruptive Velocity (cm/s) | Event Power (W) | Event Duration (s) | Height (km) | Q | Volume ($km^3$) |
| 96 | 0 28279 | 0 027137 | 1 6251 | –90 | 1106 6 | 3193 9 | 1 14E+10 | 6 17E+05 | 2 68E+00 | 1 56E+07 | 0 010 |
| 97 | 0 27874 | 0 013535 | 1 7768 | –90 | 1267 8 | 68 764 | 4 85E+12 | 9 72E+02 | 1 22E+01 | 6 61E+09 | 0 006 |
| 98 | 0 40714 | 0 003095 | 1 4383 | –90 | 743 18 | 309 19 | 8 88E+08 | 6 04E+06 | 1 42E+00 | 1 21E+06 | 0 007 |
| 99 | 0 35277 | 0 004095 | 1 3929 | –90 | 1020 7 | 299 1 | 8 12E+10 | 7 80E+05 | 4 38E+00 | 1 11E+08 | 0 086 |
| 100 | 0 10117 | 0 003602 | 1 7491 | –90 | 616 56 | 370 56 | 1 42E+09 | 1 23E+07 | 1 59E+00 | 1 93E+06 | 0 024 |

Source Output DTN LA0408GK831811 001

# APPENDIX F

# INDEPENDENT TECHNICAL REVIEW OF MDL-MGR-GS-000002 REV 00B CONDUCTED BY DR. FRANK SPERA, UNIVERSITY OF CALIFORNIA, SANTA BARBARA

# APPENDIX F
# INDEPENDENT TECHNICAL REVIEW OF MDL-MGR-GS-000002 REV 00B

This appendix presents an independent technical review of Project document MDL-MGR-GS-000002 REV 00B conducted by F.J. Spera in the period 24 March-April 10, 2003. The structure of this review is based on six review criteria set out in "Exhibit D Amended Scope of Work: Independent Review for Model Validation." The review criteria are listed below as a series of questions. The analysis provided below addresses each of these issues.

1. Is the mathematical model (ASHPLUME) appropriate for representing the conceptual model, i.e., is this model appropriate for its intended use?

2. Are the inputs sufficient.

3. Were all reasonable alternative models identified and adequately treated? If not, what are they, what are their capabilities, and what are their limitations?

4. Are the assumptions appropriate for use in the model.

5. Do the outputs of the model represent the inputs, or are the limitations to the model such that the outputs are not representative of possible future states?

6. Are the outputs of the model a reasonable representation of what may be expected from a volcanic eruption at Yucca Mountain?

No computer codes were run during the course of this review. The review focuses on the conceptual and technical bases of Project work regarding the dispersal of volcanic ash using the computer code ASHPLUME. Results from ASHPLUME are used as input for the TSPA.

*Is the mathematical model (ASHPLUME) appropriate for representing the conceptual model, i.e., is this model appropriate for its intended use?*

**Introduction**–There are a number of ash dispersal mathematical models of differing sophistication. It is beyond the scope of this report to review the history of ash dispersal modeling. ASHPLUME traces its origin back to the model of Suzuki (1983). The Suzuki model applies to a steady eruption (constant eruptive mass flow rate, $\dot{M}$) from a circular cross-sectional vent. The fundamental factors governing the fallout distribution of volcanic tephra include the height of the steady state volcanic column (H), which is a function of the eruptive mass flow rate, $\dot{M}$, the total eruptive volume (V) and the spatial and temporal structure of the winds aloft during the eruptive event of duration $t_d$. The relationship between the total eruptive volume (V) and the volumetric eruptive rate ($\dot{V}$) for a steady eruption is simply $V=\dot{V}t_d$. Because the density of ash ($\rho_e$) is essentially constant, there is a simple relationship between the eruptive mass flow rate, $\dot{M}$, and the volumetric eruption rate $\dot{V}$. The relationship is $\dot{V}=\dot{M}/\rho_e$ where $\rho_e$ is the density of tephra particles at the vent. The size distribution of tephra also plays a role in ash dispersal. The distribution of ash particle size is relatively well-known based on

granulometric studies of tephra from Strombolian eruptions and varies between reasonably well-defined bounds.

**Plume Height (H), Mass Flow ($\dot{M}$), and Eruptive Volume(V)**

Volcanic plume height (H) scales with the eruptive mass flow rate, $\dot{M}$, according to:

$$H \propto \dot{M}^{1/4} \qquad \text{(Eq. 1)}$$

An example of a quantitative parameterization is the expression:

$$H = 0.24\dot{M}^{1/4} \qquad \text{(Eq. 2)}$$

with H measured in kilometers and the eruptive mass flow measured in kg/s. The scaling relation (1) comes from momentum-buoyancy plume theory and rests on a solid fluid dynamical footing. The determination of the constant in Equation 2 comes from an empirical calibration using data from a small number (~ 10-20) of volcanic eruptions for which column height is independently known. Its value may be uncertain by ± 20% due to unsteadiness of column height and the intrinsic difficulty of measuring column height during an eruption. Note that Equation 2 is strictly valid for steady eruptions where $\dot{M}$ (or $\dot{V}$) is constant. In fact, no volcanic eruption is truly steady. Variations in mass flow during eruptions give rise to time-varying column heights. For example, during the 1980 eruption at Mount Saint Helens, the mass flow (and hence column height) varied significantly in non-monotonic fashion during the ~ 10 hour Plinian phase of the eruption. Although the expected eruptive style at Yucca Mountain is Strombolian and not Plinian, eruptive unsteadiness is typical of all styles of eruption, even eruptive events dominated by lava flows. One way of incorporating unsteadiness into ash dispersal is to model a single eruption as a sequence of smaller eruptive phases each with its own characteristic parameters. In effect one could use the ASHPLUME steady state model serially to evaluate the effects of eruption unsteadiness at least to a first approximation. Whether or not this is important depends on the timescale associated with wind and magma discharge unsteadiness. For example, if the timescale for changes in wind direction are comparable to or shorter than eruptive duration ($t_d$) then unsteady winds could have a marked effect on the distribution of ash at the surface.

In the model used by the Project, critical input comes from two relations expressed as Equations (7a) and (7b) on p. 39 of MDL-MGR-GS-000002 REV 00B. The first is an assumed relationship between the eruptive volume of ash (V) and the duration of the eruption ($t_d$). This essentially defines the eruptive volume flow rate (and the eruptive mass flow rate) as a function of total eruptive volume (V). That is, Equation 7a may be recast as:

$$V/t_d = e^{-a} V^{1-b} \qquad \text{(Eq. 3)}$$

with a = 15.29 and b = 0.527 and the units of V in $km^3$ and $t_d$ in seconds. Because

$$\dot{V} = \dot{M}/\rho_e \qquad \text{(Eq. 4)}$$

it follows from the Project model that the eruptive mass flow rate is a function of eruptive volume:

$$\dot{M}=k\,\rho_e V^{1-b} \qquad \text{(Eq. 5)}$$

with $k = 229$, $V$ in km$^3$, $\rho_e$ in kg/m$^3$ and $\dot{M}$ in kg/s. On p. 44 of MDL-MGR-GS-000002 REV 00B the bounds on V are set between 0.004 km$^3$ and 0.08 km$^3$. This gives limits for $\dot{M}$ between $2.5\times10^4$ kg/s and $1.1\times10^5$ kg/s assuming an ash density of 1,500 kg/m$^3$. These values define bounds that vary by ~ one order of magnitude which seems somewhat on the small side of its potential range. Eruptive mass flow rates in the range $10^4$ kg/s to $10^6$ kg/s have been cited for Strombolian eruptions by some volcanologists (e.g., see Mastin 2002; Mastin and Ghiorso 2000; Mastin and Ghiorso 2001). *On what grounds can eruptions with mass flows ~ $10^6$ kg/s be excluded?*

According to Equation 7b on p. 39 of MDL-MGR-GS-000002 REV 00B, column heights corresponding to volumes of 0.004 km$^3$ and 0.08 km$^3$ are 2.2 km and 3.8 km, respectively. Again this is a rather small range and at the low to intermediate end for Strombolian eruptions. According to Equation 2, the aforementioned limits ($2.5\times10^4$ kg/s and $1.1\times10^5$ kg/s) for $\dot{M}$ correspond to column heights between 3 km and 4.3 km in good agreement with Project calculations.

The main point is that eruptive mass flow rates up to $10^6$ kg/s should not be excluded. At $\dot{M} = 10^6$ kg/s, a column height H = 7.6 km is predicted from Equation 2. Because the *a priori* assumption in Project ash dispersal calculations is the relationship between eruptive duration and eruptive volume, the range of corresponding eruptive mass flow rates is uniquely defined. It is the opinion of this reviewer that starting off by bounding eruptive mass flow rates ($\dot{M}$) rather than volume (V) might be advantageous partly because it is the correlation between $\dot{M}$ and H that has some fluid dynamical basis (i.e., unlike the V-$t_d$ correlation which is entirely empirical) and partly because the limits on $\dot{M}$ between ~ $10^4$ kg/ to $10^6$ kg/s encompass the range for normal Strombolian eruptions. Violent Strombolian eruption can attain even greater eruptive mass flow rates, up to $10^7$ kg/s. According to Equation 2, a violent Strombolian eruption with $\dot{M} = 10^7$ kg/s would generate a column height H = 13 km. It is not argued here that such a value is 'typical.' However, the range 2 to 4 km considered by the Project seems unduly restrictive. Should the Project wish to consider additional higher mass flow eruptions, it would not be difficult to perform the simulations using Project models.

**Structure and Variability of Winds Aloft**–In addition to plume column height, the structure of prevailing winds during an eruption is critical to determination of ash dispersal. In the most detailed model, one can imagine wind velocity (direction and magnitude) prescribed on a three-dimensional grid of specified spatial resolution. Because upper atmosphere winds are often different from low level winds, it is important to get a complete profile of wind versus height from the vent up to the top of the eruption column. The wind velocity (speed and direction) can also vary temporally. Indeed, the eruption used by the Project (see Section 7.4 Natural Analogue Study on p. 56 in MDL-MGR-GS-000002 REV 00B) to "ground test" ASHPLUME shows how variations in winds aloft *during* an eruption influence ash distribution. In the simplest ash dispersal model, the wind speed and direction is spatially constant (speed and

direction) with no temporal variability during the eruptive interval ($t_d$). ASHPLUME implements a simple model of constant wind speed and direction and uses the wind vector from a height equal to "upper elevations to which the ash plume reaches." Presumably this corresponds to the height of the eruption column (H) derived from the relationship between eruptive volume (V) and column height (H).

**Summary**–ASHPLUME is applicable to steady volcanic eruptions (constant mass flow, $\dot{M}$) characterized by eruption columns of fixed height (H). Although no volcanic eruption is truly steady, the state-of-the-art in volcanic plume modeling is not sufficiently advanced to consider eruptions with unsteady discharge. ASHPLUME can be used serially to approximately model discharge unsteadiness and/or variable winds.

Two critical factors affecting ash dispersal are the column height and structure of winds aloft. ASHPLUME uses an empirically calibrated correlation between eruptive volume (V) and column height, H. In fluid dynamical terms, the height of an eruption column (H) scales with the mass flow, $\dot{M}$ according to $H \sim \dot{M}^{1/4}$. The eruptive volume (V) as given in Equation 3 correlates to H provided the plume-generating eruption is steady (i.e., $\dot{M}$ is constant) and the density of ash is constant. Regarding the issue of the winds aloft, any single ASHPLUME realization of ash dispersal assumes a constant wind speed and direction. Clearly this is a gross approximation; the vertical structure of the winds will generally depend on height above the vent. On the other hand, predicting the structure of the winds aloft at some time in the future 10,000 years is not easily accomplished. The Monte Carlo method of drawing a constant wind velocity from a meteorologically-based distribution and performing many realizations and then sampled for TSPA purposes is sound.

The range of eruptive volumes leads to a range of eruptive mass flows that are in the low to intermediate range for Strombolian eruptions. Eruptive mass flow rates of $10^6$ kg/s cannot be precluded and should be computed.

***Are the Inputs Sufficient?***–discussion is keyed to numbered sections in MDL-MGR-GS-000002 REV 00B.

### 4.1.1 Data

The variation of volcanic ash size distributions for Strombolian eruptions based on granulometric studies of G.P.L. Walker and co-workers beginning in the early 1970's and continuing to the present today is well known. Although the precise distribution of particle size is unique to a given eruption, the variations are not large. Similarly, waste particle size distributions are adequately known for the purposes of the TSPA given other limitations of the ASHPLUME model.

### 4.1.2 Parameters and Parameter Uncertainty

The method of developing probability distributions for compatibility with MC methods used in the TSPA is a sound practice.

### 4.1.3 Other Model Inputs

Items in Table 4, p. 20 of MDL-MGR-GS-000002 REV 00B are needed to perform ASHPLUME simulations and are commented on here.

The mathematical model of Suzuki is the starting point. The Suzuki model was used by Jarzemba (1997) with an important correction (see Equation 2 in Jarzemba) in order to achieve mass conservation, a constraint that must be incorporated in any ash dispersal model. However, the paper by Jarzemba has at least two errors. The first is that Equation 1 in Jarzemba (1997) is missing a negative sign in front of the numerator in the exponential term. The second is that there is a missing factor of g in the third term in the denominator of Equation 3 in Jarzemba. I note that these errors have been corrected in the Project work; that is, Equation 2 and Equation 4 on p. 37 and p. 38 in MDL-MGR-GS-000002 REV 00B are correct unlike the analogous equations in Jarzemba (1997).

The physical properties used for air (viscosity and density) from Lide (1994) are adequate for the purposes of the TSPA.

***Are the Assumptions Justified?***–discussion is keyed to numbered sections in MDL-MGR-GS-000002 REV 00B.

**5.1.1**

The two-dimensional model may be sufficient for the purposes of the TSPA. It is hard to determine the level of confidence one should assign to ASHPLUME results without making a direct comparison between ASHPLUME and a three-dimensional code such as the one by G. Macedonio and co-workers (Armienti et al. 1988; Macedonia et al. 1988; 1990). Approximations are made in contracting a three-dimensional model to a two-dimensional model. The neglect of vertical diffusion is probably justified because vertical advection is many orders-of-magnitude larger than vertical diffusion. In the two-dimensional models one can increase the two-dimensional eddy diffusivity to roughly account for three-dimensional effects. The only way to evaluate the quality of the two-dimensional approximations is to carry out the full three-dimensional calculation and compare results. This reviewer has not made this comparison. Presumably, if the Project felt this was important, they could contact the Italian volcanologists mentioned and explore this possibility. Alternatively, the Project can generate two-dimensional ASHPLUME results and compare these to published three-dimensional forward models relevant to eruptions at Mount Vesuvius, Italy. My own guess is that for the purposes of the TSPA the two-dimensional model would suffice. Even with a sophisticated three-dimensional model, the lack of knowledge of the winds aloft at some time in the future 10,000 years may translate into a larger uncertainty in ash thickness at a specific location than that associated with a two-dimensional rather than three-dimensional model. But this is speculation on my part.

**5.1.2**

This is a very conservative assumption. Inspection of volcanological data suggests the ratio of lava to proximate tephra (cone-building deposits) to distal ash (the deposition that ASHPLUME and like models compute) is of order 1:1:<<1. That is, for the sort of eruption 'expected' at

Yucca Mountain, the distal ash will make up only a small portion of the total. Hence the assumption made by the Project, that the entire eruptive volume is processed through a Strombolian column, is conservative. For Lathrop Wells, if the entire eruptive volume of 0.06 $km^3$ is identified with the ash volume (it clearly is not!), then according to expressions used by the Project, the eruptive duration was ~ 11.5 days, the eruptive mass flow was $6\times10^4$ kg/s and the column height was H ~ 3.6 km.

**5.1.3**

Small ash particles cannot host large fuel waste particles. This seems to be a very reasonable assumption in no further need of documentation or explanation.

**5.2.1**

Even if one knew the future climate, predicting winds aloft and their variation in time and space is most difficult. The present winds aloft structure is as good as any other and is consistent with the level of approximation in ASHPLUME.

**5.2.2**

Waste is assumed to be unaltered spent commercial fuel. This is an adequate approximation given other uncertainties.

**5.2.3**

The Project adopts a relationship from Wilson and Head (1981) between vent exit radius ($r_e$) and eruptive velocity ($u_e$), as input for ASHPLUME. Neither the derivation of this relationship nor a discussion of the assumptions upon which it is based is given in MDL-MGR-GS-000002 REV 00B. It is noted here that this "correlation" is based on incompressible flow and assumes specific pressure gradients (based on a density differences between magma and host crust) and magma viscosities. *The conditions assumed to generate the values in Table 3 in Wilson and Head (1981) are not generally applicable to the highly compressible high-speed eruption of volatile-charged magma in the inertial regime.* Jarzemba (1997) also cites a relationship from Wilson and Head (1981) that provides a correlation amongst vent exit radius ($r_e$), mean density of ash particles ($\rho_p$) and eruption mass flow rate ($\dot{M}$) to determine the eruption velocity at the vent exit ($u_e$). It is important to insure that the Wilson and Head (WH) scaling relation does not implicitly or explicitly involve assumptions inconsistent with other assumed relations (e.g., Equation (7a) on p. 39 of MDL-MGR-GS-000002 REV 00B). In particular, the last few sentences of Section 5.2.3 on p. 26 of MDL-MGR-GS-000002 REV 00B are puzzling. *Results plotted on fig. 6a in WH (1981) pertain to specific exsolved magma water contents which are less than those expected for basaltic volcanism at Yucca Mountain (see Final Report of the Igneous Consequences Peer Review Panel, February 2003).*

From review of the documentation, it appears that the Project develops the input needed for ASHPLUME according to the following scheme. First, a value for the eruptive ash volume (V) is picked from a uniform distribution. Then using Equation 7a on p. 39 of MDL-MGR-GS-000002 REV 00B, the eruptive duration, $t_d$ is calculated (project literature calls this $T_d$; to

avoid confusion with the thermodynamic temperature used in some volcanic plume models, although not in ASHPLUME, use is made of the symbol $t_d$ here). Once $t_d$ and V are known, then Equation 7b on p. 39 of MDL-MGR-GS-000002 REV 00B is used to compute the column height, H. Once V and $t_d$ are known, $\dot{M}$ and M (eruptive mass) are easily computed given a density (based on particle size) of ash particles using $\dot{V}=\dot{M}/\rho_e$ and $V=M/\rho_e$, respectively. (Project uses symbol $\psi_p$ for particle density). Then the Project uses the Wilson and Head (WH) scaling relation (discussed above) amongst $r_e$, $\dot{M}$ and $\rho_e$ to obtain the vent exit radius, $r_e$ and finally, from the continuity expression $\dot{M}=\rho_e \pi r_e^2 u_e$, the eruption velocity at vent exit (labeled $W_0$ by Project and $u_e$ in this review).

*It seems, unless this reviewer is mistaken, that this procedure is redundant.* That is, once V and hence $t_d$ are determined, then indeed H is easily determined. However, implicit in the correlation between V and $t_d$ is the value of $\dot{M}$ and hence M, for an assumed ash density. It seems the vent exit velocity is uniquely determined once a value for $r_e$ is chosen using the expression $\dot{M}=\rho_e \pi r_e^2 u_e$. In other words, why does the Project resort to the use of the WH correlation, presumably identical to or a closely related to the one given as Equation 14 in Jarzemba (1997)?

First of all, it is not clear that Equations 7a and 7b on p. 39 of MDL-MGR-GS-000002 REV 00B are consistent with the WH relationship used by the Project. The density of the magmatic mixture depends on the pressure at the vent exit, which in turn depends on the volatile content. Do these considerations affect the $r_e$-$u_e$ scaling relationship assumed to obtain input parameters for ASHPLUME? *Secondly, and most importantly, it is not clear why the WH scaling correlation is needed at all.* Straightforward manipulation of Equation 7a on p. 39 of MDL-MGR-GS-000002 REV 00B gives:

$$\frac{V}{t_d} = e^{-a} V^{1-b} \qquad \text{(Eq. 6)}$$

where a and b are constants. Hence Equation 6 combined with continuity ($\dot{M}=\rho_e \pi r_e^2 u_e$) implies that

$$\pi r_e^2 u_e = e^{-a} V^{1-b} \qquad \text{(Eq. 7)}$$

From Equation 7 it appears that given V, a unique relationship between $r_e$ and $u_e$ exists. A selected value for $r_e$ completely determines $u_e$ without need for an additional WH correlation.

***Were all reasonable alternative models identified and adequately treated? If not, what are they, what are their capabilities, and what are their limitations?***

The short answer to this question is "No." The Project uses the ASHPLUME model. There has been no systematic comparison of results generated by ASHPLUME with other models. On p. 34 in MDL-MGR-GS-000002 REV 00B there is discussion of other models although no detailed comparisons have been made. The models briefly mentioned in MDL-MGR-GS-000002 REV 00B (Gaussian-Plume, PUFF and Gas-Thrust code) suffer limitations and

cannot generate the quantitative output needed for the TSPA without modification. A model not mentioned in MDL-MGR-GS-000002 REV 00B called VAFTAD (Hefter and Stunder 1993) has been found to accurately model the dispersion of volcanic ash in the atmosphere. That is, to predict the motion of airborne ash clouds. Unfortunately, VAFTAD like PUFF offers no prediction of ground-level ash accumulation and therefore unsuitable in its present form for TSPA purposes.

Fortunately, other volcanological ash dispersal models that provide quantitative results for ground-level ash accumulation exist and may be utilized by the Project to build confidence and discover the limitations of ASHPLUME. Perhaps the most cogent model is one developed by Hurst and co-workers (Hurst 1994) based on the earlier model of G. Macedonio and co-workers (Armienti et al. 1988; Macedonio et al. 1988, 1990). The code developed by the Italian group implements a three-dimensional particle diffusion model with allowance for wind direction and speed as a function of height. The original code was somewhat unwieldy requiring large three-dimensional arrays and long run times. Motivated by the need for an easy-to-implement Civil Defense tool, Hurst and co-workers developed a code called ASHFALL. This is a two-dimensional imensional code that accounts for variations in wind speed and direction as a function of altitude and time. Vertical diffusion of ash is neglected (as in ASHPLUME). The output of ASHFALL is the ash thickness at points on a rectangular grid centered on the vent. Details of the model can be found in the report and users guide entitled "ASHFALL-A Computer Program for estimating Volcanic Ash Fallout" by T. Hurst (1994). The characteristics and performance of ASHFALL are documented in the studies of Hurst and Turner (1999). A comparison of ASHFALL predictions with observed ash distributions of three ash-producing events from Ruapehu volcano in the North Island of New Zealand shows that actual ash thickness at any location are generally within a factor of two of that forecast by ASHFALL. The accuracy of the forecast wind direction is the main factor affecting quality of ASHFALL predicted tephra isopachs according to the study by Hurst and Turner (1999).

Finally, mention should be made of the Hybrid Particle and Concentration Transport Model (HYPACT) of Walko and Tremback (1985). HYPACT simulates the motion of atmospheric tracers under the influence of winds and turbulence. Its Lagrangian formulation enables representation of sources of any size and the maintenance of concentrated, narrow plumes until atmospheric dispersion dictates they should broaden. The Lagrangian particle plume can then be converted into a concentration field and advected using a Eulerian formulation. The Lagrangian particles are moved through space and time based on interpolated wind velocities plus a superimposed random motion scaled to the intensity of local turbulence. A spectrum of gravitational settling velocities related to particle size can be specified. The velocity field (all three components), the potential temperature and information regarding the scale of turbulence are necessary input for implementation of HYPACT. HYPACT is the most sophisticated model for following the trajectory of airborne particles known to this reviewer.

In the study of Turner and Hurst (2001) a comparison is made between HYPACT and ASHFALL using the Regional Atmospheric Modeling System (RAMS) for the winds aloft structure as input for both models (see Pielke et al. 1992 for details pertaining to RAMS). Comparison of the performance of RAMS/HYPACT with ASHFALL shows that RAMS/HYPACT provides more accurate spatial and temporal forecasts of ash transport. Although the HYPACT model is superior in reproducing the temporal and spatial movement of

the ash cloud, it is not suitable in its current form for quantifying the depth of ash. The code would need to be modified in order to determine the distribution of isopachs.

In summary, a detailed comparison should be made between ASHFALL and ASHPLUME. This can be done in two ways. First, one can select representative eruption and winds aloft parameters and compare predictions made by ASHPLUME and ASHFALL. Secondly, one can apply ASHPLUME to the 1995 and 1996 Mount Ruapehu, New Zealand eruptions. These have already been modeled using ASHFALL and results are readily available in the literature. Based on the results of such comparisons, one will be able to develop confidence in the results from ASHPLUME. Because the ASHFALL code is not freely available, Project geoscientists may want to work with Dr. Tony Hurst (T.Hurst@gns.cri.nz). Hurst is the developer of ASHFALL and may be available to run some models in coordination with Project geologists. ASHFALL unlike ASHPLUME can handle a time-varying vertical profile of wind speed and direction perhaps more appropriate to conditions during an eruption. It can also be used in the simpler ASHPLUME-like mode with constant wind speed and direction.

***Do the outputs of the model represent the inputs, or are the limitations to the model such that the outputs are not representative of possible future states?***

In general, the output of an ash dispersal model provides the type of information needed for the TSPA. The real issue is the quality of the forward model. Ash dispersal in all its complexity is a problem that has not been fully solved. However, for the purposes of the TSPA and given the state-of-the-art, a two-dimensional model such as ASHPLUME may suffice. However, further work should be accomplished to increase the confidence in ASHPLUME results. One way of doing this is to make a detailed comparison between ASHFALL and ASHPLUME. Another is to apply ASHPLUME to the 1995 and 1996 eruptions at Mount Ruapehu. Typically, these eruptions exhibit column heights H ~ 10 km consistent with eruptive mass flow $\dot{M} \sim 3\times10^6$ kg/s, eruptive volume V~ 0.08 $km^3$ and ~ 10-hr eruption duration. This is within the range of possibility for Strombolian eruptions at Yucca Mountain. Recall that Strombolian mass flows are generally in the range $10^4$-$10^6$ kg/s with very strong so-called 'violent' Strombolian eruptions having $\dot{M}$ up to ~ $10^7$ kg/s. The main need is to compare ASHPLUME results to results from another method. This task can probably be accomplished by 3-5 weeks or less if outside expertise (e.g., Dr. Tony Hurst for ASHFALL) contributes to the effort.

***Are the outputs of the model a reasonable representation of what may be expected from a volcanic eruption at Yucca Mountain?***–Tentatively the answer to this question is "probably yes." Comparison of ASHPLUME results with other codes would enable one to more definitively answer this question. *An explanation of the issue raised in section labeled 5.2.3 in this review should be provided to insure self-consistency is maintained in application of ASHPLUME.*

**Other Comments on MDL-MGR-GS-000002, REV 00B**–p. 41 reference to 'Suzuki et al.' should be to 'Jarzemba et al. (1997)'.

## REFERENCES CITED*

**NOTE**: These references were used at part of the technical review and are not reflected in the document input reference system as part of this AMR.

Armienti, P., Macedonio, G., and Pareschi, M.T. A numerical model for the distribution of tephra transport and deposition: applications to May 18, 1980 Mt. St. Helens eruption, *Jour. Geophys. Res.*, **93**, 6463-6476, 1988.

Hefter, J.L. and B.J. Stunder, Volcanic ash forecast and dispersion (VAFTAD) model, *Weather and Forecasting*, **8**, 533-541, 1993.

Hurst, T.W. and R.W. Turner, Performance of a program for volcanic ashfall forecasting, *N.Z. J. Geol. Geophys.*, **42**, 615-622, 1999.

Hurst, T.W., ASHFALL- a computer program for estimating volcanic ash fallout. Report and user guide. *Institute of Geological and Nuclear Sciences Science Report 94/23*. 22p., 1994.

Jarzemba, M.S., Stochastic radionuclide distributions after a basaltic eruption for Performance Assessments of Yucca Mountain, *Nucl. Tech.*, **118**, 132-142, 1997

Lide, D.R., ed. 1994. *CRC Handbook of Chemistry and Physics, A Ready-Reference Book of Chemical and Physical Data*. 75th Edition. Boca Raton, Florida: CRC Press. TIC: 102972.

Macedonio, G., Pareschi, M.T. and Santacroce, R., A numerical simulation of the plinian fall phase of 79 A.D. eruption of Vesuvius, *Jour. Geophys. Res*, **93**, 14817-14827, 1988.

Macedonio, G., Pareschi, M.T. and Santacroce, R., Renewal of explosive activity at Vesuvius: models for the expected tephra fallout, *Jour Volcanol. Geother. Res.*, **40**, 327-342, 1990.

Mastin, L.G., Insights into volcanic conduit flow from an open-source numerical model, *Geochem. Geophys. Geosys.*, *3*(7), 10.1029, 2002.

Mastin, L.G., and M.S. Ghiorso, *A Numerical Program for Steady-State Flow of Magma-Gas Mixtures Through Vertical Eruptive Conduits, U.S. Geological Survey*, Open-File Report 00-209, 2000.

Mastin, L.G., and M.S. Ghiorso, Adiabatic temperature changes of magma-gas mixtures during ascent and eruption, Contributions to *Mineralogy & Petrology*, **141**, 307-321, 2001.

Pielke, R.A., W.R. Cotton, C.J. Tremback, M.E. Nicholls, M.D. Moran, D.A. Wesley, T.J. Lee and J.H. Copeland, A comprehensive meteorological modeling system-RAMS, *Meteor. Atmos. Phys.*, **49**, 69-91, 1992.

Suzuki, T., A theoretical model for dispersion of tephra, *In*: Shimozuru, D. and I. Yokohama (*eds*) Arc volcanism: physics and tectonics, p. 95-113, 1983.

Turner, R and T.W. Hurst, Factors influencing volcanic ash dispersal from 1995 and 1996 eruptions of Mount Ruapehu, New Zealand, *J. Appl. Meteorol.*, **40**, 56-69, 2001.

Walko, R.L. and C.J. Tremback, HYPACT: The Hybrid Particle and Concentration Transport Model. User's guide, 13pp, 1995 [Available from ASTER Division, Mission Research Corporation, P.O. Box 466, Fort Collins, CO 80522]

Wilson, L. and J.W. Head, Ascent and eruption of basaltic magma on the Earth and Moon, *Jour. Geophys. Res.*, **86**, 2971-3001, 1981.

INTENTIONALLY LEFT BLANK

# APPENDIX G

# INDEPENDENT TECHNICAL REVIEW OF MDL-MGR-GS-000002, REV 00H ASH REDISTRIBUTION CONCEPTUAL MODEL

**Included In Appendix G Are The Following:**

## CRITERIA FOR TECHNICAL REVIEW OF THE ASH REDISTRIBUTION CONCEPTUAL MODEL

## INDEPENDENT TECHNICAL REVIEW: DR. DAVID BUESCH, U.S. GEOLOGICAL SURVEY

## INDEPENDENT TECHNICAL REVIEW: DR. DENNIS O'LEARY, U.S. GEOLOGICAL SURVEY

# APPENDIX G
# INDEPENDENT TECHNICAL REVIEW OF MDL-MGR-GS-000002, REV 00H ASH REDISTRIBUTION CONCEPTUAL MODEL

Model validation is the process used to establish confidence that the mathematical model (if applicable) and its underlying conceptual model adequately represent with sufficient accuracy the system process, or phenomenon, in question. Procedure AP-SIII.10Q, *Models*, which was the current procedure at the time of this independent technical review, identified a number of methods for validating models that range from simple documentation to peer review. For the ash redistribution conceptual model, REV 04 of the *Technical Work Plan: Igneous Activity Assessment for Disruptive Events* (BSC 2003 [DIRS 166289]), identified the post development method to achieve the desired level of model validation (Level II):

> "Technical review, planned in the applicable TWP, by reviewers independent of the development, checking, and interdisciplinary review of the model documentation (the Originator, Responsible Manager/Lead, Checker, QER, and interdisciplinary reviewers assigned to the model document/activity may not serve as an independent post-development model validation technical reviewer) (Section 5.4.1(c)(5))."

The TWP stated that the conceptual model, developed specifically for the Yucca Mountain Project, would be validated under AP-SIII.10Q to develop confidence in its intended use. The draft model report described the conceptual aspects of the ash redistribution conceptual model. The independent review focused on the unique application of this model on the Yucca Mountain Project. The intended use of the model is to describe erosion and dilution of contaminated ash as it may affect the RMEI after an eruption of a hypothetical volcanic event intersecting the repository for two end-member scenarios.

The criteria for this independent review were as follows:

1. Is the conceptual model reasonable and appropriate for its intended use?
2. For given inputs, are the outputs of the model reasonable?
3. Are limitations of field and analytical data as well as the conceptual model adequately described?
4. Are there other approaches that may enhance the confidence in use of this model?
5. Are there other alternative models that should be considered?

NOTE: References that appear here were used as part of the technical review and are not reflected in the document input reference system as part of this AMR.

Independent Technical Review
Dr. David Buesch, U.S. Geological Survey
November 13, 2003

**Independent Technical Review of the Ash Redistribution Conceptual Model**

The "Ash Redistribution Model" is a conceptual component of the "Atmospheric Dispersal and Deposition of Tephra from a Potential Volcanic Eruption at Yucca Mountain, Nevada" AMR. The document on which Dr. David Buesch (USGS) conducted the technical review has a Document Indicator (DI) of "MDL-MGR-GS-000002, REV 00H," and only those parts of the document related to the "Ash Redistribution Model" were reviewed. This part of the independent technical review lists responses to the review criteria and major comments and concerns regarding the data and conceptual model. Comments pertaining to logic flow of the text, presentation and consistency of text and figures, and text editing (or lack thereof) are as annotations on the manuscript.

The criteria for this independent review are as follows:

1. Is the conceptual model reasonable and appropriate for its intended use?

   The model lays out several detailed and "big picture" ideas that are based on some data, and in the end it provides some values for input into Total System Performance Analysis (TSPA) models. So, in that respect the model is appropriate for its intended use (i.e., TSPA gets some parameters). Having said that, the model is largely conceptual, so many of the components are not well developed and this diminishes the final intended use of the model (note the use of the word "diminishes", not "excludes").

2. For given inputs, are the outputs or the model reasonable?

   The current version of the model is mostly conceptual, but there are a few examples that are based on input data to develop values that are in turn generalized into values for TSPA models. One can follow (possibly even better with a little additional information and editing) the authors ideas for the detailed examples. So for these detailed examples, one can see the logic from input to reasonable output, even though the amount of data is probably less than what one might like to have in order to make solid and defendable arguments for model results.

3. Are limitations of the model adequately described?

   Most of the model manuscript is used to explain the conceptual model and present and develop supporting data and ideas, so there is very little explicit discussion on the limitations and uncertainty of the model and results. There are some limitations on the data directed toward the use by TSPA models.

4. Are there other validation approaches that may enhance the confidence in use of this model?

   The current model is mostly conceptual and is pretty sparse on data, so one technique for validation is to acquire additional data to test several of the hypotheses or components of the model. The current model focuses on dilution of ash (and waste) by mechanical erosion and mixing of the sediment during transportation and deposition, and it briefly discusses the possible mechanical process of infiltration into deposits. The data used to evaluate these processes are few and localized, but are used to extrapolate to "full model" conclusion. The authors have shown some interesting initiative using the radionuclide Cs-137 as a tracer (however, the appropriateness of this application must be better understood and described), and there are numerous possibilities of using other radionuclide and non-radionuclide tracers to quantify physical and chemical process. Collection of data that better quantify the processes of erosion, local storage, and flushing of the material through (or farther down) the system would greatly enhance these components of the model and thereby reduce (or at least quantify) uncertainty and enhance confidence. There are atmospheric wind velocity and direction data from numerous sites near Yucca Mountain and Fortymile Wash in addition to regional data, typically from 10 m above the ground surface (Fransioli and Ambros 1997). These wind data might be used in conjunction with the distributions of sediment types to determine (calculate) potential for erosion by eolian deflation processes that is part of the Cesium (Cs)-137 study, and that might occur at many locations affected by the potential tephra sheets in the model. Having said all this, one must acknowledge that quantifying wind- and water-related processes in a desert such as at Yucca Mountain is challenging because events are few and far between; therefore, collecting appropriate data and developing it into conceptual and numerical models will probably be one of the few avenues upon which rational discussion and evaluation can take place.

   *Fransioli, P.M., and Ambros, D.S., 1997, Regional and Local Wind Patterns Near Yucca Mountain: Civilian Radioactive Waste Management System Management & Operating Contractor, Las Vegas, NV, 200 p. November 20, B00000000-01717-5705-00081 REVISION 00, MOL.19980204.0319.*

5. Are there other alternative models that should be considered?

   There are many details on the physical processes that can be included and considered for other models. These processes include refinements to eolian, colluvial, fluvial, pedogenic, mechanical, and chemical processes that result in determining better (and hopefully more realistic) estimates of amounts of materials on the landscape and time during which processes are active. It is the interaction and sum of these processes that can emerge as a model and, which in turn, can be discussed and tested using numerical modeling techniques. The long and short answer to this question is that by focusing more on the diversity of physical processes, collecting appropriate data to evaluate these processes, and integrating them into full-basin and sub-basin models, then another "new" model will emerge, and that model is what should be considered for the redistribution of ash and waste.

In summary, the conceptual model and the semi-qualitative (semi-quantitative?) results can probably be used for the intended use as input into TSPA models. However, the model should probably be considered as a starting point upon which refinements and enhancements will result in a more rigorous and defendable model.

**Major comments and concerns**

There are five major comments and concerns regarding the "Ash Redistribution Model," and although individually none of the concerns result in invalidating the model, together the comments point out some of the gaps in the current model. [Note: the word is "gaps," not "invalidate."] Several of these comments and concerns can probably be initially addressed with additions to the existing document, but others might require additional work to more thoroughly document and substantiate components of the conceptual (and possibly future quantitative and numerical) model. As with many products for the Yucca Mountain Project (AMRs, etc.), there are numerous citations of other reports or data sources rather than providing and developing data with the report so a reader does not have to jump around from product to product.

1. Most of the supporting and component parts of the model focus on two small (scoping?) studies, and these studies are the basis for "scaling up" to the current conceptual model. The Lathrop Wells Cone "ash dilution" consists of nine samples along two transects that are 1 and 2.5 km long. Additionally, the drainage basin that includes Lathrop Wells Cone has an upstream drainage basin (relative to the tephra sheet) compared to the downsteam drainage area that is expressed as a ratio of 6:1. Several (pertinent) reasons are listed for why the Lathrop Wells data should not be directly developed as a simple scaling factor for the ash-dilution values; however, shortly after these statements are made, the Fortymile Wash drainage is expressed in the same type of ratio and a dilution distance is quoted. Observations at Sunset Crater, Arizona, are only briefly described in a scientific notebook; therefore, relations are of limited scope and detail. The Cesium Study for surficial processes consists of 51 samples in approximately a 12 $km^2$ area south of Highway 95 on the distributary fan of Fortymile Wash. Each of these studies has merit, especially because the Lathrop Wells Cone and the distributary fan of Fortymile Wash are near the typically cited "reasonably maximum exposed individual" (RMEI). However, using these studies as the sole basis for "scaling up" to complete ash redistribution model is, in my opinion, a stretch.

2. The Cesium Study for Surficial Processes in the Fortymile Wash alluvial fan is an interesting use of a radionuclide tracer; however, it is not clear that Cesium (Cs)-137 is an appropriate tracer for the mechanical and possibly chemical processes described or inferred. According to the U.S. Environmental Protection Agency (http://www.epa.gov/radiation/radionuclides/cesium.htm), Cesium (including Cs-137) is one of only three metals that is liquid at about 83°F and has a half-life of 30.17 years. These properties raise several issues that need to be addressed.

    a. Is Cs-137 transported to the site and deposit as atoms, complexed into molecules, or attached to (or entrained in) particles, and if with particles, then what size are these particles? The physical form of Cs-137 at the time of deposition (or

"shortly" thereafter) might influence the susceptibility to mechanical erosion or chemical reaction.

b. It is proposed that Cs-137 infiltration can be used as a general proxy for the depth to which fine particles (clay, silt, and ash or sand-sized grains) might transported into the soil. It seems that this proposal assumes mechanical infiltration; however, with a Cs-137 liquidus of about 83°F the potential of mechanical and chemical processes must be evaluated and explained.

c. With Cs-137 potentially being deposited during several periods in the 20 years from the mid-1940s to the mid-1960s and a half-life of about 30 years, how might these competing processes of accumulation and decay be manifest in the data? For example, material deposited in the mid-1940s (about 57 years ago) will have undergone almost 2 half-life cycles, so only about 27 percent of the original material is still in the system.

3. On the basis of model results of "ASHPLUME," establishment of two tephra sheets is a good use of end-member distributions where, relative to Yucca Mountain, one sheet is deposited south and the other sheet is deposited to the east. However, how and in what depth these two models are discussed differs greatly.

   a. A figure (or two) illustrating these two model distributions should be included early in the Ash Redistribution section of the in the report so the reader can visualize the distribution, thickness, and even gain size in the tephra sheets. Location of the RMEI should be included (as it is, partially, on Figure 5).

   b. The tephra sheet deposited to the south of Yucca Mountain would deposit ash on the RMEI area. Although the current model appears to emphasizes only eolian processes, this area contains numerous ridges and basins, including the one in which Lathrop Wells Cone is located, the Fortymile Wash alluvial fan, and both of these sites are described in detail for the fluvial redeposition of material. So, the emphasis on eolian processes in this model distribution under represents the fluvial processes in the area.

   c. The tephra sheet deposited to the east of Yucca Mountain would deposit ash across Jackass Flats and in the drainage basin between the Calico Hills and Shoshone Mountain that is drained by Topopah Wash. The current model focuses on the fluvial redistribution of ash along Fortymile Wash. However, after introduction of this model end member, it is rarely described except through inference of colluvial and fluvial processes, in which most of this discussion is associated with the Lathrop Well Cone and Fortymile Wash alluvial fan studies. The discussions on short-duration, intense thunderstorms and the more aerially extensive, long-duration storms are apparently provided in support of the sediment transport into and through Fortymile Wash, but these same storm conditions are applicable throughout the area, including for the south-directed tephra sheet.

d. The RMEI is typically identified in the area of the Lathrop Wells Cone and Fortymile Wash; however, if the 18-km distance from the proposed repository site is the fundamental criteria, then an arc can be drawn to the east-northeast to where it intersects the southwestern edge of Little Skull Mountain. This minor eastward continuation of the 18-km arc intersects Topopah Wash just north of where this wash transitions into a distributary fan similar to the Fortymile Wash fan. So, the east-directed end-member model should probably include redeposition from the drainage of Topopah Wash and Jackass Flats because most of the tephra sheet would be deposited across these areas. According to Christensen and Spahr (1980), significant parts of Jackass Flats would be affected in 100-year storms, and especially 500-year and maximum flood events. So, eroded ash from the Jackass Flats area and the drainage near Calico Hills might be a contributing source of material to the RMEI area.

*Christensen, R.C., and Spahr, N.E., 1980, Flood Potential of Topopah Wash and Tributaries, Eastern Part of Jackass Flats, Nevada Test Site, Southern Nevada: U.S. Geological Survey, Lakewood, CO, Open-File Report 80-963, 22 p. [TIC Catalog Number 203211]*

4. Erosion, transportation, and deposition of ash from different types of slopes (orientation and inclination) and substrates (Miocene, densely welded ignimbrite versus colluvial and old or young alluvial surfaces) can differ greatly, but these variations are not discussed. Here are two aspects of how these conditions and processes might be applied to the model.

   a. There are some minor discussions of material being eroded from steeper slopes and accumulating in the washes at the base of these slope (possibly during thunderstorms), and at later times (during long-duration regional storms) being flushed farther out into the fluvial system. These processes and times for each process to be active are challenging to quantify, especially in desert environments where there is sparse runoff data; however, estimates of thickness and rates of erosion are provided as "soil redistribution factors" for the TSPA model (Table 7-1). So, there are a few examples of attempts at quantifying amounts and processes, and there are many that have not been addressed.

   b. In the discussion on tephra deposits on the RMEI in northern Amargosa Valley (paragraph 2 on page 64) it is stated that because of the strong eolian action in this area, it is "highly unlikely a that tephra deposit ... would remain in place and/or undiluted for more than a few decades". There are other places in the text that complete (or near complete) removal of the tephra deposits is described as part of the model. It is hard to judge if complete (or near complete) removal of the ash in "a few decades" has positive or negative affects on the concentration of ash and waste materials, but it is not clear that these conditions are even appropriate. For example, consider the amount of ash deposited on the highly varied topography near Mount St. Helens, Washington, in 1980, and how much of this ash has been eroded off the slopes in the last 23 years. It is true that Mount St. Helens is in a different climate and environment. It is also true that there are no specific measurements that can be cited (just some oral communication estimates from

some of those who have worked extensively in the area), but estimates of the amount of eroded 1980 ash vary from about 10 to 20 percent, and this means that 80 to 90 percent of the primary deposit is still on the hillsides. Erosion of the ash is primarily by the formation of rills, and once the rills are established, there is very little lateral cutting to strip of the material that remains on the interfluve ridges. Coming back to the Yucca Mountain area, rills and interfluve ridges are pretty common on many types of slopes and substrates. All this means is that more of the primarily deposited ash might not be eroded in the short time frame inferred in the current model.

5. There is an assumption from the ASHPLUME model that "waste" is incorporated into the ash and the two form individual grains that are deposited to form the tephra sheets; however, this "mixed grain of ash and waste" might not be appropriate for the Ash Redistribution model. I understand that the "mixed grain of ash and waste" has been an assumption in ASHPLUME model for quite a while, and that this is not part of the tasked technical review. However, from a fragmentation process-base mechanistic point of view, I think formation of mingled and mixed grains it is difficult to do and it is very likely that the majority of waste and ash would be erupted as mostly individual particles (this complicates the calculations). If particles deposited in the tephra sheets are mostly individual grains of ash and waste, then each would have very different hydrodynamic and possibly chemical properties. These different properties would affect the erosion, transportation, deposition, and fractionation potential of the particles.

Finally, the intended use of the Ash Redistribution model is to provide some parameters to the TSPA, and that is what the (conceptual-semiqualitative-semiquantitative) model does. However, although the current model is a reasonable start, it only contains a few localized aspects of the physical processes that are likely to affect the redistribution of ash (and waste). Because processes that affect the redistribution of ash and waste operate at a wide variety of scales, a more integrated model is probably in order. For example, there are eolian and aqueous processes, localized processes of erosion on a slope, small drainage basin scales processes of erosion, transportation, and deposition, and full drainage basin scale processes of erosion, transportation, and deposition. Most of the basaltic eruptive (disruptive) processes, including the redistribution of ash and waste materials, are typically considered as postclosure events and there has not been a clear link between these issues and pre-closure issues such as potential flood events. The importance of fluvial and eolian processes described in the current model, and hopefully emphasized in this review, indicates that an integrated, full-basin model of potential flooding and sediment transport (including a few sub-basin models) would be important for evaluating both potential pre- and postclosure events. Such a quantitative model (or submodels) could provide a powerful tool in evaluating the redistribution of ash and waste material.

Independent Technical Review
Dr. Dennis O'Leary, U.S. Geological Survey
November 19, 2003

**Independent Technical Review of the Ash Redistribution Conceptual Model**

I reviewed sections 6.6: Ash Redistribution Conceptual Model, 6.7: Model Results, and 7: Model Validation, in Atmospheric Dispersal and Deposition of Tephra from a Potential Volcanic Eruption at Yucca Mountain, Nevada. I found no fatal flaws or other lapses. The constraints identified from field observations and from analytical data are considered in the report as fully relevant factors in the deposition and redistribution processes of tephra. The conceptual model is appropriate and the discussions and reasoning are presented in adequate detail to support the conclusions and inferences in these sections. Application of ASHPLUME is well reasoned and is appropriate for its intended use. The outputs of the model are reasonable with respect to the given inputs; the outputs adequately explain the distribution of tephra as a basis for analyzing its fate by erosion, fluvial and eolian transport, as described in the text. The limitations of the model are adequately described. I do not know of other validation approaches that may enhance the confidence in the use of the model, and I do not know of other alternative models that should be considered.

The following comments are suggestions pertaining to technical details in the interest of providing a more complete presentation.

1. To give an accurate impression of the distribution of tephra outfall, it should not be described as a sheet; it is actually an attenuated apron deposit continuous with the cone itself, distinguished mainly by the variation in particle size with distance from the vent. The scenarios implicitly assume a tephra dispersion profile based on size-related weight distribution I think more should be said about the presumed waste particle distribution within the single eruption tephra deposit. Namely, will the waste content distribution mimic the tephra particle size distribution or is there a particle size waste adherence limit, as implied in Sec. 6.5.1? I suspect the nature of the waste particle distribution within the tephra distribution might have some bearing on the erosional dispersion of contaminated tephra by wind or water over time. Is windborn volcanic dust, then, ever a hazard?

2. Note that a single flood event in Fortymile Wash (and there have been a couple of bank-to-bank flows within the time I have been on the project) will distribute tephra from A to D (Fig. 2) instantaneously (i.e., within a day). The time lapse will be insignificant in this case but the tephra concentration downstream will probably be as shown in Fig 2. Note also that the amount of tephra contributed to bedload from the slopes of Yucca Mountain may be trivial if the flood event is a result of cloudburst/snowmelt from the Timber Mountain part of the drainage basin. It would seem that Timber Mountain weather would be a much bigger contributor to runoff in the channel than the relatively infrequent Yucca Mountain-wide flank storms. Therefore, the amount of contaminated waste fed to Fortymile Wash may be metered by local storms and fed to a channel that is repeatedly cleared of tephra. It may be

correct to think of relatively small slugs of contaminated tephra fed to the channel on an infrequent basis but sluiced down to Amargosa Valley in large, relatively frequent homogenizing flood events. If this is true, it would tend to decrease the rate of tephra delivery to RMEI. Fig 5 (p. 76) would be more useful if you could show on it the inferred area of a tephra deposit that would form from a violent strombolian eruption through the repository. Just a glance at Red and Black and Lathrop Wells Cones suggests that a tephra deposit(s) would occupy a small part of the Fortymile Wash drainage basin and that the tributary systems that dominate its delivery to Fortymile Wash would be Yucca, Midway, and Dune Washes. Has any study been done to estimate the sediment contribution these tributaries made to Fortymile Wash in late Pleistocene -Holocene? I recommend you adjust fig. 5 to show the entire Fortymile Wash watershed to the north at Timber Mountain; this will make clear the enormous potential diluting effect available from upstream.

Fig. 2 shows the concentration of tephra in the channel decreasing as a non-linear concave decay curve, notably at A. Is there a basis for this? I would assume a linear decrease incrementally stepped down to the right, each step representing a flood/erosion event (the slope could reflect tributary input of tephra, so I guess the curve would flatten with time as the tephra source becomes depleted or otherwise stabilized upslope). Is there a basis for having the concentrations at B, C, and D build to a maximum concentration and then begin to decrease? Since each subsequent flood through A brings down an increasingly diluted tephra load, shouldn't there be a net decrease in tephra at B and C after the first flood event (B and C also suffer erosion during each flood so I don't expect much of an incremental increase in tephra at those points.) D is harder to understand because it is more clearly an aggrading environment that C and B. The text says that the plots in fig. 2 are purely conceptual; perhaps some simple flume experiments would help support this concept.

3. Page 73 presents data on a tephra transport and redeposition study. It would be helpful to know the tephra grain size with distance from head of input. The text mentions ash and microscopic analysis, which suggests a fine sand size. How does the ash size in channel samples compare to tephra size at the presumed source (margin of intact tephra deposit)? Has there been appreciable size sorting by stream/erosion transport? Some estimates should be given to the size distribution and agglomeration of fragmented waste to the overall tephra distribution. I suspect that waste particle sizes will form a leptokurtic subpopulation of large particles, and more important, be discriminated by high density. If so, this suggests that contaminated tephra or waste particles will be relatively large and form a distribution of placer deposits and perhaps be strung out as lag deposits within Fortymile Wash rather than being uniformly fed to Amargosa Valley with a light fraction of sediment. Seems to me some large-scale flume experiments are in order. Or were such already performed by you? Another factor that probably should be mentioned is bedload transport abrasion. Most clasts of stream-bed basalt look fairly well-rounded. Has any work been done on rounding with transport distance and mixing? My guess is that the vesicular tephra are susceptible to comminution during stream transport. Does grain fining by abrasion have an effect on your waste travel calculations? I suspect it is insignificant, but we probably should give the impression of having thought of every contingency. Note that this point is

relevant to statements in Sec 6.7.2.4. On p. 88 (Sec. 6.7.2.4) there is a good discussion of ash removal with time. There is mention of "residual contamination that may have leached into the underlying sediments." This statement implies that there can be significant dissolution of ash during its time in the stream bed, allowing adhered waste particles to either dissolve and precipitate in the substrate, or migrate downward as very fine particles released from the dissolved ash host grains. Should the solubility of ash be discussed here? Is it a significant factor in the migration of waste?

4. I disagree that sediment mixing occurs at higher rates on steeper hillslopes (p. 70) and that drainage channels that form and flow across newly deposited tephra have well-mixed sediment loads after small transport distances (last sentence, first ¶, p. 70). Unless these streams cut into pre-tephra substrate, no mixing with other sediment types occurs. Drainage on steeper slopes is restricted to relatively narrow rill or gully incisions, and if the slopes are well-graded to the axial channels, upper slope tephra contributions should progressively diminish with time. Higher order channels gather a larger volume of more compositionally heterogeneous sediment, hence mixing is increased with channel size on lower slopes.

5. Sec. 6.7.2.3 p. 87 informs that "a layer of contaminated ash . . . appears immediately following eruption . . ." This contradicts the redistribution scenario presented in Sec. 6.6.1.2. You might want to make some appropriate qualification to mitigate this apparent discrepancy.

6. 7.3.1 Why did you use Cerro Negro as an analog instead of Paricutin? I would have chosen Paricutin because of: 1. its monogenetic eruption behavior is more analogous to the Yucca Mountain volcanoes, 2. It would be a worst-case scenario compared to Yucca Mountain eruptions, 3. the time since eruption ceased is sufficient to give some indication of how ash is being redistributed from a pristine state by erosion in an arid climate comparable to that of the Yucca Mountain area. In light of F. Spera's comment in Sec. 7.4 I would add Paricutin to your analogs.

# APPENDIX H

# AN ESTIMATE OF FUEL-PARTICLE SIZES FOR PHYSICALLY DEGRADED SPENT FUEL FOLLOWING A DISRUPTIVE VOLCANIC EVENT THROUGH THE REPOSITORY

**CONDUCTED BY**

**DR. R.J. FINCH, ARGONNE NATIONAL LABORATORY**

# APPENDIX H
# AN ESTIMATE OF FUEL-PARTICLE SIZES FOR PHYSICALLY DEGRADED SPENT FUEL FOLLOWING A DISRUPTIVE VOLCANIC EVENT THROUGH THE REPOSITORY[1]

### Input To "Waste Particle Diameter In Magmatic Environment" (PA-WP-99383.R)

## H1. INTRODUCTION

This document addresses estimates of particle-size distributions for spent nuclear fuel exposed to a potential disruptive magmatic event through the proposed repository at Yucca Mountain, Nevada. As stated in the AP-3.14Q input request, "Waste Particle Diameter in Magmatic Environment" (PA-WP-99383.R ), the probability distribution for fuel particles should consider mechanical and chemical degradation of the fuel at the time of the disruptive event. A disruptive event may occur at any time while the degradation of fuel due to oxidation and/or aqueous corrosion is expected to increase over time. However, the estimated extent of fuel degradation that will have occurred at the time of the event is not addressed here.

The following discussion is based largely on laboratory examinations of commercial spent nuclear fuels performed at Argonne National Laboratory but conducted for purposes outside the realm of understanding particle size. The aim of the sample preparation, from which much of the discussed information was obtained, was to disaggregate spent-fuel fragments in order to maximize the fuel's surface area before using it in "accelerated" aqueous-corrosion tests. There is no statistical information available for the distribution of particle sizes caused by the disaggregation and grinding of spent $UO_2$ fuels in the laboratory. There is a similar paucity of data for oxidized and corroded fuels. Particle-size estimates reported here, as well as estimates for mean sizes and ranges, are based on a combination of data obtained from intentional crushing and grinding of "unaltered" spent fuel, as well as this author's experience with handling and examining spent commercial fuel in various states of degradation. These observations are augmented by citations to selected open-literature reports on the physical condition of spent commercial fuel, as well as naturally occurring $UO_2$ (the later being considered a useful natural analogue for severely corroded spent commercial fuel). It is emphasized that no formal statistical treatment was performed to justify the mean sizes and ranges reported here.

The following discussion concerns commercial spent $UO_2$-based fuels.

## H2. FUEL DEGRADATION

Three states of fuel degradation can be defined: (1) unaltered fuel (i.e., uncorroded and unoxidized); (2) dry-air oxidized fuel; and (3) aqueous-corroded fuel. Particle sizes are estimated for each below.

[1] This work was completed in 1999 by Dr. R.J. Finch, Argonne National Laboratory. This text was updated by R.J. Finch for REV 01 of this model report in May through August 2004. Reference citations were clarified in REV 02.

## H2.1 UNALTERED FUEL (UNCORRODED AND UNOXIDIZED)

Unaltered spent fuel shows a range of physical characteristics that depend largely on fission-gas release and possibly burnup; however, there is no clear understanding of the relationship between such parameters and the relative ease with which fuel may fragment under stress or the grain sizes that might result from fragmentation. Fission-gas release appears to be a crucial parameter affecting fuel microstructure, including grain growth (Guenther et al. 1988a and 1988b), a characteristic that could strongly impact the distribution of fuel-particle sizes from a fuel following exposure to a disruptive volcanic event.

When crushing spent $UO_2$ fuel during the preparation of samples for aqueous-corrosion studies on fuel being conducted at Argonne National Laboratory (ANL), it was found that reducing the particle sizes of a fuel of moderate burnup [approved testing material (ATM) 103: ~ 30 MW-d/kg-U] was readily achieved by using a two-step crushing and grinding process. Fuel fragments that had been removed from the cladding (with fragment sizes of several millimeters across) were initially crushed by using a stainless-steel impact tool, followed by sieving the resulting pieces through two stacked sieves with nominal openings of 0.015 cm and 0.0045 cm (i.e., 200 and 325 mesh, respectively). The largest size fraction (> 0.015 cm) was then placed into a stainless-steel-ball mill [an ANL-designed and built vibratory roller mill cylinder] and ground for a total of 31 minutes. After each grinding step, the fuel was emptied from the ball mill into the stack of three sieves, with the largest size fraction (> 0.015 cm) being returned to the ball mill for re-grinding (Finch 1999, ANL scientific notebook #1547, page 9). The distribution of particles sizes obtained after crushing and milling was approximately bimodal, with numerous large (>0.015 cm diameter) fragments and material less than 0.0045 cm, which subsequent SEM examination revealed to be approximately single fuel grains (approximately 0.020 mm diameter). A relatively small number (~11 percent) of fuel particles were between ~ 0.0045 cm and 0.015 cm in diameter. No attempt was made to estimate the relative distribution of these three particle sizes during the initial grinding; however, following the sample preparation procedure, in which the largest fragments (>0.0075 cm) were crushed and milled a second time, the final distribution of particle sizes obtained after preparation for the ANL tests given in Table H-1 was achieved.

A second grinding was performed as part of the same sample preparation for additional tests at ANL (Finch 1999). The procedure followed was similar to that followed for the first grinding described above; however, the fuel was ground in the ball mill for a total of 55 minutes, nearly twice as long as for Trial 1. Also, masses were determined for only two size fractions following the second grinding procedure: that fraction with particles less than 0.0045 cm, which was 76 percent of the total mass, and that with particles larger than 0.0045 cm, which was 24 percent of the total mass. The distribution for this second grinding differs slightly from, but is nevertheless consistent with, that reported after the first grinding. That is, most of the crushed and ground fuel was reduced to less than 0.0045 cm grain sizes (76 percent), much of which consisted of single fuel grains (Finch 1999, ANL scientific notebook #1547, page 20).

Table H-1. Final Distribution of Fuel Particle Sizes After All Grinding Cycles (ANL Tests)

| Size Fraction (Particle Diameter) | Mass (Gram) | Relative Amount* |
|---|---|---|
| <0 0045 cm (ave ~0 0020 cm) (mostly single fuel grains) | 2 3252 | 81 percent |
| 0 0045 to 0 015 cm | 0 3063 | 11 percent |
| >0 015 cm | 0 2520 | 9 percent |

Source DTN LL001104412241 019

NOTE * Total relative amounts may exceed 100 percent due to rounding

Several powders of spent $UO_2$ fuels were prepared for flow-through dissolution studies conducted at Pacific Northwest National Laboratory (PNNL) by crushing and grinding de-clad segments, and the results are reported by Gray and Wilson (1995), who reproduce SEM micrographs of the prepared powders. Gray and Wilson (1995) do not discuss what fraction of the crushed fuel had a size fraction exceeding that used in the flow-through studies, and it is assumed here that the distribution is similar to that given in Table H-1. The most important factor illustrated by Gray and Wilson (1995), in terms of understanding the potential distribution of particle sizes produced during a disruptive volcanic event, is that not all fuels prepared by them show identical particle size distributions. Several fuels display very small particles—on the order of 0.001 cm or less. Although SEM examinations of the ANL fuel grains revealed relatively few particles of ATM103 fuel with sizes less than single grains, the PNNL results from a wider variety of fuel types necessitates shifting the potential distribution of grain sizes to smaller particle sizes than that estimated from the ATM103 results alone. We consider here that 0.0001 cm diameter particles represent a reasonable lower limit on particle sizes for all unaltered fuels exposed to a disruptive volcanic event.

## H2.2 DRY-AIR OXIDIZED FUEL

Spent $UO_2$ fuel that has been oxidized in the absence of moisture may form a series of oxides, with concomitant degradation of the integrity of the fuel meat (i.e., the $UO_2$ pellets only, but not the cladding, stainless steel spacers, and other components that make up a complete fuel bundle). Oxidation up to a stoichiometry of $UO_{2.4}$ leads to volume reduction of the $UO_2$ matrix. This can open grain boundaries and may result in the disaggregation of the fuel into single fuel grains (Einziger et al. 1992). Further oxidation to $U_3O_8$ and related oxides results in a large volume expansion and potentially extreme degradation of the fuel into a powder with particle sizes less than one micrometer in diameter. SEM examination of spent fuel oxidized to approximately $U_3O_8$ indicates particle sizes of approximately 2.5 μm (0.0025 cm dia.) with lower limits of approximately 0.5 μm (0.00005 cm dia.) (Gray and Wilson 1995), with larger particles ranging up to approximately 50 μm diameter (0.005 cm) (Table 2). An estimate of the larger limit on the range of particle sizes is more difficult to make with much certainty. Based on qualitative observations of ATM103 fuel following preparation for the ANL corrosion studies, an upper limit of 0.05 cm diameter is chosen (Table 2).

## H2.3 AQUEOUS-CORRODED FUEL

SEM examinations of corroded spent fuel following interaction with simulated groundwater at 90°C are reported by Finch et al. (1999). The grain sizes of uranium(VI) alteration products on

corroded fuel commonly reach 0.01 cm (Finch et al. 1999); however, based on our understanding of the physical properties of uranium(VI) compounds, these phases are similar to gypsum or calcite in terms of hardness and fracture toughness. Therefore, a powerful eruptive event will probably fragment nearly all of the larger crystals of secondary U phases, which is why a smaller upper limit of 0.001 cm diameter is chosen for the range of particle sizes for aqueous-corroded fuel (Table 2). The lower value for the particle-size range is based on the SEM examinations reported in Finch et al. (1999), who demonstrate the extremely fine-grained nature of many alteration products, with crystal dimensions as small as 0.5 μm or less (≤0.00005 cm).

## H2.4 SUGGESTED PARTICLE SIZE RANGES

Based on the foregoing data, cited sources and experience of the author, a professional judgment of suggested particle-size ranges and average values for particle sizes (based on light-water-reactor fuels) for modeling disaggregation effects such as from a volcanic eruption through the repository are listed in Table 2. No firm statistical foundation underlies the averages or ranges listed in Table 2; however, based on observation experience with fuels and literature sources, the listed averages are considered reasonable. Limiting values for the ranges are perhaps less-well constrained, but a reasonable estimate is that 80 to 90 percent of the fuel particles will fall within the ranges reported in Table 2.

Table 2. Estimated Fuel-Particle Sizes

| Degradation State | Mean (cm dia.) | Range (cm dia.) |
|---|---|---|
| Unaltered fuel | 0 0020 | 0 0001 to 0 050 |
| Oxidized in dry air | 0 00025 | 0 00005 to 0 0005 |
| Corroded fuel | 0 0002 | 0 00005 to 0 001 |

Sizes indicate particle diameters. Size estimates based on sources cited in the text and the experience of the author.

Based on our current level of understanding, it seems reasonable to treat both categories of altered fuel (dry-air oxidized and aqueous corroded) as identical, since their estimated particle sizes are not very different from each other. The altered fuel is substantially more friable than (most) unaltered fuel, with size distributions that may be skewed to quite small sizes.

## H2.5 OTHER TYPES OF SPENT FUEL

In addition to commercial spent nuclear fuel (CSNF), which constitutes the vast majority of the fuel inventory destined for permanent disposal, there are additional fuel types that may exhibit physical properties that are quite distinct from those of CSNF. These "other" spent fuels include those from research reactors, military-use reactors, and other sources. They are highly variable in their physical characteristics, and include materials from metals to carbides, and may be in a variety of forms, from ingots to granules. No attempt is made here to estimate potential particle sizes for this broad category of fuel types. Furthermore, there are too few data currently available on the physical properties of these fuels following physical and/or chemical degradation that may occur in the repository following their disposal.

### H2.6 DEFENSE HIGH-LEVEL WASTE (DHLW) GLASS

Whereas DHLW glass will constitute a large volume fraction of the total volume of waste in the repository, it is not the major contributor to total activity. DHLW glass is probably best treated in a manner similar to the Tuff rock, which also consists of a large volume of glass. Similarly, an intrusive, rapidly cooling magma is likely going to be glassy as well.

## H3. REFERENCES

NOTE: These references were used as part of the technical report and are not reflected in the document input reference system as part of this AMR.

Einziger, R.E.; Thomas, L.E.; Buchanan, H.C.; and Stout, R.B. 1992. "Oxidation of Spent Fuel in Air at 175 to 195°C." Journal of Nuclear Materials, 190, 53-60.

Finch R.J. 1999. "Petri-dish Tests. Spent Fuel." ANL-CMT Scientific Notebook 1547. (Argonne National Laboratory).

Finch, R.J.; Buck, E.C.; Finn, P.A.; and Bates, J.K. 1999. "Oxidative Corrosion of Spent Fuel in Vapor and Dripping Groundwater at 90°C." *Materials Research Society Symposium Proceedings*, 556, 431-438.

Gray W.J.; and Wilson, C.N. 1995. "Spent Fuel Dissolution Studies FY1 1991 to 1994." PNL-10540 (Pacific Northwest National Laboratory, Richland, WA).

Guenther et al. 1988a. "Characterization of spent fuel approved testing material - ATM-103." PNL-5109-103 (Pacific Northwest National Laboratory, Richland, WA).

Guenther et al. 1988b. "Characterization of spent fuel approved testing material - ATM-106." PNL-5109-106 (Pacific Northwest National Laboratory, Richland, WA).

LL001104412241.019. An Estimate of the Fuel-Particle Sizes for Physically Degraded Spent Fuel Following a Disruptive Volcanic Event Through the Repository. Submittal date: 11/29/2000.

INTENTIONALLY LEFT BLANK

# APPENDIX I

# ALTERNATIVE MODEL FOR ASH REDISTRIBUTION

# APPENDIX I
# ALTERNATIVE MODEL FOR ASH REDISTRIBUTION

## II. PURPOSE

This alternative numerical model for ash and fuel redistribution is presented as an enhancement to the existing ash redistribution conceptual model in the main body of this model report. The purpose is to describe a basis for calculation of near-surface and at-depth fuel (waste) concentrations through time in soil near the RMEI location. The reason for the enhanced numerical model is to provide a more complete representation of the redistribution mechanisms involved, and to eliminate the mass balance conservatism of the existing simplified ash redistribution conceptual model. This alternative model is still under development and is not yet ready for use within TSPA.

### II.1 SCOPE

This alternative redistribution model uses a spatially-distributed Geographic Information System (GIS) framework to calculate the ash and fuel transported to the RMEI location from the upper Fortymile Wash watershed by hillslope and fluvial processes. This redistributed ash and fuel is combined with the primary ash and fuel (if any) that was deposited directly on the RMEI location. The model eliminates the need to distinguish between the two bounding cases described in Sections 5.1.3 and 6.3.2. By explicitly modeling the primary ash fall and redistribution processes, the model directly computes the ash and fuel transported to the RMEI location under any wind conditions.

The alternative redistribution model further considers the fate of ash and fuel delivered to the RMEI location, distinguishing between channels and recent (< 10 kyr) depositional surfaces (i.e., "channels"), and older (> 10 kyr) interchannel divide surfaces on the RMEI location. Ash and fuel delivered from the upper Fortymile Wash watershed are deposited only in channels. This treatment assumes that areas of the RMEI location that have not been subject to fluvial erosion or deposition (i.e., interchannel divides by definition) over the last approximately 10 kyr will not be subject to fluvial acitivity within the next 10 kyr. The model also distinguishes between channels and divides for the purposes of modeling the redistribution of fuel within the soil profile. Vertical redistribution within the profile is modeled as a diffusion process within a soil layer of finite depth. The lower boundary of the soil layer represents the presence of impermeable calcic soil horizons. Channels and divides in the model are characterized by different values for radionuclide diffusivity and permeable soil thickness. The alternative redistribution model outputs data for the surface and depth-averaged fuel concentration on channels and divides at the RMEI location through time following an eruption.

## I1.2 MODEL LIMITATIONS

Because of uncertainties, incomplete data and avoidance of mathematical complexity that does not provide value commensurate with the model purpose, limitations are recognized in the capabilities of the alternative redistribution model. The recognized limitations include:

- The alternative model does not include representation for eolian erosion or deposition.
- The long-term geologic dynamics of fan interchannel divide and channel interactions are not represented.

# I2. QUALITY ASSURANCE

See Section 2.

# I3. USE OF SOFTWARE

## I3.1 SOFTWARE TRACKED BY CONFIGURATION MANAGEMENT

None.

## I3.2 EXEMPT SOFTWARE

Commercial, off-the-shelf software used in support of this alternative model is listed in Table I-1. This software is exempt from the requirements of LP-SI.11Q-BSC, *Software Management*.

Table I-1. Exempt Software

| Software Name and Version (V) | Description | Computer and Platform Identification |
|---|---|---|
| Microsoft Excel, 2000 | The commercial software, Microsoft Excel 2000, was used for plotting graphs and statistical calculations. Only built-in standard functions in this software were used | PC, Windows 2000/NT |

# I4. INPUTS

## I4.1 DATA, PARAMETERS AND OTHER MODEL INPUTS

### I4.1.1 ASHPLUME Output Grids of Ash and Fuel Concentration

The alternative model accepts grids of ash and fuel concentration in g/cm$^2$ from ASHPLUME. The input grids are assumed to be in polar coordinates (i.e., a function of radius r and azimuth $\theta$), with radial increments starting from an initial radius $\Delta r$ and increasing geometrically (with a factor equal to rfactor) to a maximum of $N_r$ radial samples (e.g., 200 m, 400 m, 800 m... 51.2 km, if $\Delta r$ = 200 m, rfactor = 2.0, and $N_r$ = 8). The azimuthal resolution of the grids is also input (e.g., $\Delta\theta = 10°$, for a total of 36 samples at each radius).

### I4.1.2 ASHPLUME Output Points of Ash and Fuel Concentration at the RMEI Location

The alternative model accepts values for the ash and fuel concentration computed by ASHPLUME at the RMEI location approximately 18 km south of the repository.

### I4.1.3 DEM and Watershed Boundary Grid

The model accepts a 30-meter-resolution USGS DEM that covers the Fortymile Wash drainage basin down to the latitude of the Fortymile Wash fan apex. This grid also includes information on the boundary of the Fortymile Wash drainage basin: all grid pixels within the Fortymile Wash watershed have values equal to the DEM elevation, all pixels outside the drainage basin have a value equal to –9999.0.

### I4.1.4 Values for the Model Physical Parameters

Model parameters include the critical slope "S," drainage density "X," scour depth "H," RMEI fan area "A", fraction of RMEI fan area comprised of channels "F," the permeable soil depth in channels "$L_c$," the permeable soil depth on divides "$L_d$," the vertical diffusivity of radionuclides in channels "$D_c$," and the vertical diffusivity of radionuclides on divides, "$D_d$," and the biosphere depth "B."

Table I-2 lists these and other parameter inputs to the alternative redistribution model, their data types, units, range of values accepted, and their range of values typical in physically-realistic model runs.

Table I-2. Input Parameters to the Alternative Ash Redistribution Model

| Parameter | Type | Units | Acceptable Range | Typical Value/Range |
|---|---|---|---|---|
| ashdepositionRMEI | float | $g/cm^2$ | 0 – ∞ | $10^{-3}$ – $10^{1}$ |
| fueldepositionRMEI | float | $g/cm^2$ | 0 – ∞ | $10^{-9}$ – $10^{5}$ |
| criticalslope, S | float | | 0 – ∞ | 0 25 – 0 4 |
| drainagedensityupperbasin, X | float | $km^{-1}$ | 0 – ∞ | 1 0 – 10 0 |
| scourdepth, H | float | cm | 0 – ∞ | 50 0 – 200 0 |
| RMEIarea, A | float | $km^2$ | 0 – ∞ | 30 0 |
| Fractionchannel, F | float | | 0 – 1 | 0 1 – 0 4 |
| Ldivide, $L_d$ | float | cm | 0 – ∞ | 80 0 – 120 0 |
| Lchannel, $L_c$ | float | cm | 0 – ∞ | 200 0 |
| Ddivide, $D_d$ | float | $cm^2/yr$ | 0 – ∞ | 0 01 – 0 05 |
| Dchannel, $D_c$ | float | $cm^2/yr$ | 0 – ∞ | 0 05 – 0 2 |
| ashdensity, $\rho$ | float | $g/cm^3$ | 0 – ∞ | 1 0 |
| deltar, $\Delta r$ | float | m | 0 – ∞ | 100 0 |
| deltatheta, $\Delta\theta$ | float | degrees | 0 1 – 360 | 5 0 – 15 0 |
| rfactor | float | | 1 – ∞ | 1 5 – 2 0 |
| lattice_size_r | integer | | 1 – ∞ | 10 – 15 |

Table I-2. Input Parameters to the Alternative Ash Redistribution Model (Continued)

| Parameter | Type | Units | Acceptable Range | Typical Value/Range |
|---|---|---|---|---|
| timestep, $\Delta t$ | float | yr | 0.1 – ∞ | 10.0 |
| simulationlength, T | float | yr | 0.1 – ∞ | 10,000.0 |
| delta_DEM, $\Delta x$ | integer | m | 30, 60, 90 (any multiple of 30) | 30 |
| Bdepth, B | float | cm | 0 – ∞ | 10.0 – 30.0 |
| oflag | integer | | 0 or 1 | 0 or 1 |

## I4.2 CRITERIA

See Section 4.2.

# I5. ASSUMPTIONS

## I5.1. MODEL ASSUMPTIONS

### I5.1.1 Future Climate

**Assumption**–The climate through much of the regulatory period will be similar to today's climate and, even with a projected increase in annual precipitation, will have relatively little impact on the Fortymile Wash alluvial fan.

**Rationale**–See Future Climate Analysis (BSC 2004 [DIRS 170002]). If climate changes to a wetter period the pluvial period is projected to have about 1-1/2 to 2 times the current annual precipitation. However this is seen to require no adjusted use of current data since the expected effects would include more vegetation and this will result in less ash being derived from the hillslopes. It should also be noted that, while total precipitation in pluvial climate would be greater, increased peak discharges or storm intensities would not be expected. The precipitation increase would come primarily in the form of more frequent rainfall events.

**Where Used**–Sections I6.4.1.2 and I6.4.2.6. Basis for using a constant radionuclide diffusivity to describe dispersion in the soil column.

### I5.1.2 Stability of Distributary Channels and Neglect of Fluvial Erosion and Deposition on Interchannel Divides in the RMEI Location

**Assumption**–The model assumes that distributary channels in the RMEI location are stable and do not migrate. Therefore, the areal fraction of channels and interchannel divides does not change with time.

**Rational**–Alluvial fans are dynamic landforms that can evolve topographically over both long and short time scales. A distinction can be made, however, between the evolution of alluvial fans over time scales of millions of years and the evolution of "entrenched" or "segmented" alluvial fans over shorter time scales. In tectonically-active areas and over time scales of millions of years, alluvial fans aggrade by sedimentation in channels and by channel shifting (avulsion). Over these long time scales, alluvial fans are best considered to be subject to

redeposition across the entire fan area. The Quaternary period, however, has caused cycles of channel aggradation and incision on alluvial fans in the western Unites States (Bull 1991 [DIRS 102040], pp. 114-121). As a result of these cycles, fluvial activity on many alluvial fans is confined to a small fraction of the piedmont area near the modern channels. Older terraces are commonly preserved from previous episodes of aggradation and incision, but these terraces are no longer subject to fluvial activity, even during extreme events based on evidence of pavement development and other geomorphic development (Bull 1991 [DIRS 102040], pp. 52-55). Surficial characteristics observed in the field, including well-developed desert pavement and varnish, provide evidence for the stability of channels and the lack of significant, soil-disruptive flood events on interchannel divides. Harrington (2003 [DIRS 164775]) observed well-developed desert pavements and varnish on interchannel divide materials near the RMEI location, indicating that most of these interchannel divide surfaces are Pleistocene in age and have not been subject to significant flooding for at least 10,000 years. As a result, they may be considered to be stable for performance assessment purposes.

**Where Used**–Sections I6.4.1.1 and I6.4.2.5. Basis for the stability of the areal ratio F over time.

### I5.1.3 Discounting Eolian Redistribution to the RMEI Location

**Assumption**–The model assumes that eolian transport to the RMEI location can be neglected compared with fluvial transport processes.

**Rationale**–Fluvial transport is considered to be the dominant redistribution process for ash and fuel from the upper Fortymile Wash for two reasons. First, the prevailing wind is away from the RMEI location and towards the drainage basin, so eolian transport is most likely to redistribute ash into the drainage basin (i.e., away from the RMEI location). Second, fluvial transport processes in a tributary drainage system have the effect of focusing material onto the RMEI location, while eolian processes act to disperse ash by repeated episodes of entrainment, turbulent dispersion in the atmosphere, and redeposition.

**Where Used**–Sections I6.4.1 and I6.4.2.5

## I5.2 PARAMETER ASSUMPTIONS

There are no parameter assumptions associated with the alternative ash redistribution model.

# I6. MODEL DISCUSSION

The potential consequences of an igneous event intersecting the repository (BSC 2004 [DIRS 169989]) require consideration of both the eruption and deposition of pyroclastic material and the redistribution of that pyroclastic material after initial deposition. Section 6 (main text) presents the objectives, technical bases, and application of the two models that represent the eruption, deposition, and redistribution of volcanic ash. This Appendix I section presents an alternative model for redistribution of the ash and the contained fuel.

## I6.1 MODELING OBJECTIVES

The overall objective of the alternative ash redistribution model is to represent the processes and the associated potential consequences related to redistribution of contaminated ash to and at the RMEI location.

The consequences of a volcanic eruption include consideration of the potential for increased waste concentration at the location of the RMEI from the transport of contaminated ash through sedimentary processes. This potential consequence is described in Section I6.4 as a specific disruptive events FEP (FEP 1.2.04.07.0C).

The objective of the alternative ash redistribution model is to numerically represent the range of conditions that allow for the transport of fuel-contaminated volcanic ash to the location of the RMEI by sedimentary processes. The alternative ash redistribution model also addresses the temporal near-surface and at-depth concentrations of fuel in soil conditions at the location of the RMEI.

## I6.2 BASIS OF ALTERNATIVE REDISTRIBUTION MODEL

The basis of the alternative ash redistribution model is presented conceptually in Section I1.1 above. The alternative ash redistribution model would provide simulated waste concentrations for output grid locations that could be combined with BDCFs to estimate dose to the RMEI.

## I6.3 CONSIDERATION OF OTHER ALTERNATIVE REDISTRIBUTION MODELS

Apart from the ash redistribution conceptual model described in Section 6.6, this alternative model is unique.

## I6.4 DESCRIPTION OF THE ALTERNATIVE REDISTRIBUTION MODEL

This section describes the concepts of the proposed alternative ash redistribution model (Section I6.4.1) and the numerical aspects (Section I6.4.2). As noted in Section I6.1 above, this discussion addresses the disruptive events FEP 1.2.04.07.0C (Ash redistribution via soil and sediment transport).

### I6.4.1 Primary Redistribution to RMEI Location Following an Eruption

The alternative ash redistribution model divides the Fortymile Wash drainage basin into two areas, the upper basin and the fan. The upper basin includes the repository location, and most of the area that would receive primary ash fall if an eruption were to intersect the repository. The RMEI location is considered to be on the Fortymile Wash fan, south of the fan apex. The upper basin and the fan are divided at the fan apex.

The alternative model calculates the mass and concentration of fuel transported from the upper basin to the RMEI location by hillslope and fluvial processes. This is accomplished within the alternative model using a spatially-distributed, GIS analysis of the upper basin. The software assumes that primary ash fall is mobilized and transported to the RMEI location if it falls on steep slopes or on active channels. The model performs a GIS analysis of the slopes and

contributing areas (a proxy for channel flow) for the entire basin using the input DEM. These values are then compared to critical slope and drainage density values on a pixel-by-pixel basis to integrate the total mass of mobilized ash and waste that could be delivered to the RMEI location.

Before the mobilized ash and fuel are deposited at the RMEI location, they are transported through the alluvial channel system where they are mixed with uncontaminated channel sediments. This mixing leads to ash dilution (Section 7.3.2). Mixing occurs during flood events as sediment and ash are entrained from the bed, mixed by turbulent flow, and redeposited on the bed. The depth to which ash and channel sediment are mixed is the scour depth. The dilution factor (i.e., the fraction of channel sediment composed of ash) can be calculated by dividing the effective thickness of mobilized ash in channels of the upper basin (i.e., the thickness of ash if it were spread uniformly over the total area of alluvial channels within and downstream from the primary ash fall zone) by the scour depth. To calculate the effective thickness of ash, the dilution zone is mapped and its total area is computed. The dilution zone is defined as the area of alluvial channels within the primary ash fall zone and downstream of it to the fan apex. The ratio of the effective ash thickness and scour depth is the fraction of channel-bed material composed of ash when the redistributed ash and fuel reach the RMEI location.

#### I6.4.1.1 Distinction Between Channels and Interchannel Divides in the RMEI Area

At the RMEI location, the alternative model segregates the fan into channels and interchannel divides. In the natural system, the fan is composed of a complex suite of "terraces" that result from episodes of aggradation, incision, and lateral channel migration. Soil-geomorphic mapping provides the basis to group these terraces into two types: terraces, or interchannel divides, that have not been subject to fluvial erosion and deposition for approximately the last 10 ka or longer (Pleistocene-age terraces), and channels that have been subject to erosion and deposition over the last 10 ka (including both active channels and Holocene-age terraces that may be reoccupied over the time scale of the repository). Preliminary analysis indicates that channels comprise 18 percent of the RMEI area, while interchannel divides comprise 82 percent (Harrington 2003 [DIRS 164775]).

On interchannel divides, fuel is considered to be deposited only from primary fallout. This fallout is initially concentrated at the surface. This assumption is consistent with the definition of interchannel divides as surfaces that have not been subject to fluvial erosion or deposition over the time scale of the repository (10 kyr). In channels, the initial fuel concentration includes the primary fallout as well as the fuel redistributed from the upper basin. Both of these components will be mixed with channel sediments by fluvial scour and redeposition.

The mass of fuel redistributed from upstream is assumed to be deposited in the RMEI area without any transport downstream to the Amargosa River. As such, the RMEI area is considered an ideal "trap," or depozone, for ash redistributed from upstream. This is a conservative approximation to the natural system, in which some of the ash transported from upstream may be transported past the RMEI area into the Amargosa River, but it is difficult to quantify how much. The alternative redistribution model does not treat the RMEI location using a spatially-distributed model. Instead, the complex suite of channels and divides is represented as one hypothetical divide (with area equal to (1-F)A, where F is the fraction of the RMEI area

comprised of channels and A is the total area of the RMEI location including divides and channels) and one hypothetical channel (with area FA), with their respective areas equivalent to the total areas of all divides and all channels within the mapped area of the RMEI location (Figure 1).

#### I6.4.1.2 Redistribution in the Soil Column at the RMEI Location

The alternative model considers the redistribution of radionuclides within the soil as a diffusion process. Redistribution occurs primarily through suspension and redeposition of fine particles by infiltration, and physical mixing of soil particles by freeze-thaw cycles and bioturbation. Confidence building in the use of the diffusion equation for radionuclide redistribution is described in Section I7. A single value of diffusivity is applied to fuel, representing all radionuclides. Support for this approximation comes from Anspaugh et al. (2002 [DIRS 169793]), who noted that measurements indicate that different radionuclide species are dispersed in the soil column at similar rates (Anspaugh et al. 2002 [DIRS 169793]). Diffusion is assumed to occur within a finite thickness corresponding to the distance from the surface to impermeable soil horizons at depth (with different thickness for the divide and channel). Soils in arid environments develop a petrocalcic horizon by solution and reprecipitation of calcium carbonate over time scales of tens to hundreds of thousands of years (Machette 1985 [DIRS 104660]). Deposition of calcium carbonate at depth in the soil decreases permeability locally until an impermeable layer forms.

The diffusivity values vary between the divide and channel. Diffusion within the channel is likely to occur faster because of the higher permeability of channel-bed sediments (which increases the rate of fine-particle transport by suspension and redeposition) and the additional physical mixing of sediments that can occur by scour during extreme flood flows.

### I6.4.2 Mathematical Description of the Alternative Ash Redistribution Model

Figure I-1 is a flow chart to aid in understanding the alternative redistribution model.

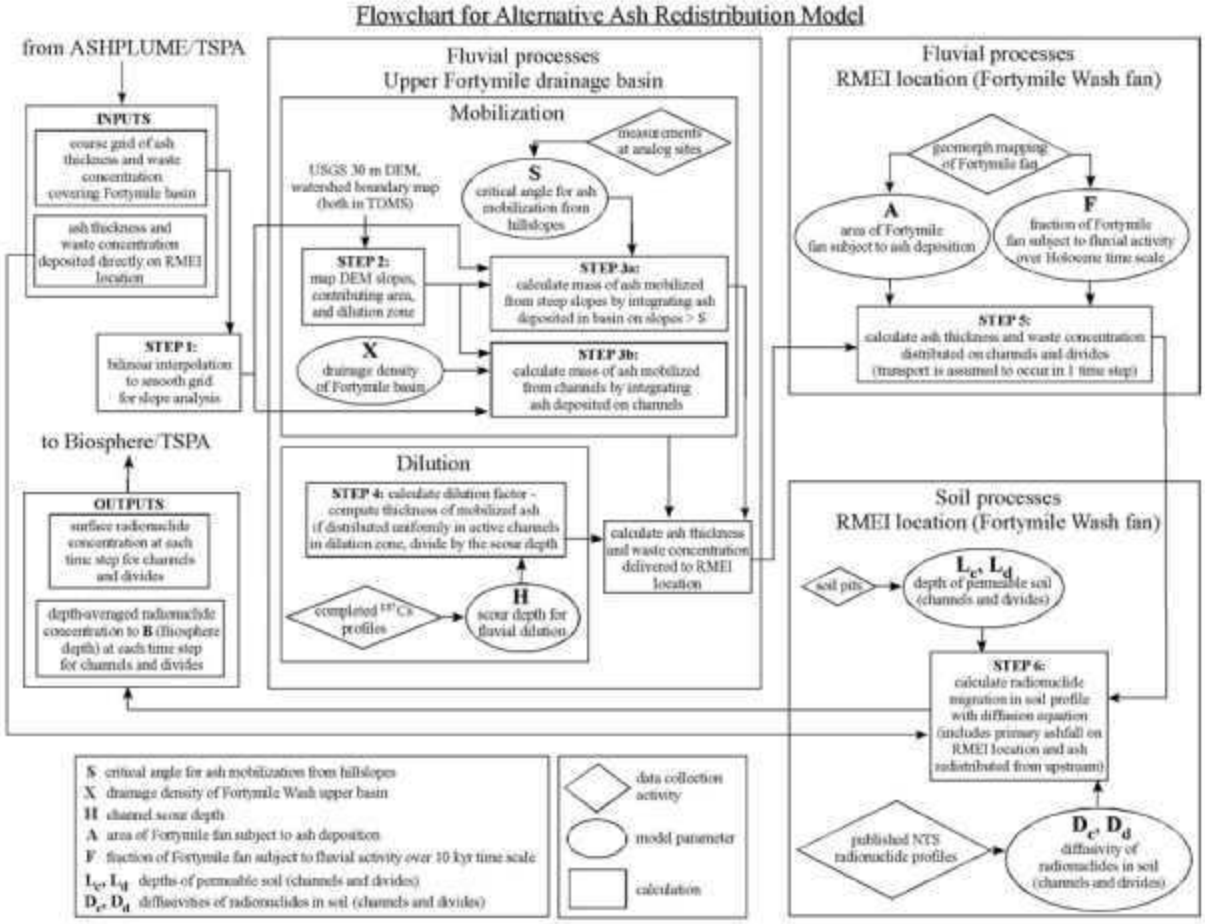


Figure I-1. Flow Chart for Alternative Ash Redistribution Model

### I6.4.2.1 Definition of Model Variables

| | |
|---|---|
| z | depth in the soil profile below the surface |
| t | time following the eruption |
| $C_{d0}$ | initial radionuclide concentration in the soil profile on interchannel divides |
| $C_{c0}$ | initial radionuclide concentration in the soil profile in channels |
| $C_d$ | radionuclide concentration in the soil profile on interchannel divides (includes temporal effects of diffusion) |
| $C_c$ | radionuclide concentration in the soil profile in channels |
| ashdepositionRMEI | primary ash fallout ($g/cm^2$) on the RMEI location |
| fueldepositionRMEI | primary fuel fallout ($g/cm^2$) on the RMEI location |

| | |
|---|---|
| $d_{dw}$ | ash thickness on RMEI interchannel divides |
| $d_{cw}$ | ash thickness in channels of the RMEI location |
| S | The critical angle for ash mobilization from hillslopes |
| X | The average drainage density in the Fortymile Wash drainage basin |
| H | The depth of scour in active alluvial channels for calculating fluvial dilution/mixing |
| A | The area of the Fortymile Wash alluvial fan subject to redistributed ash deposition |
| F | The fraction of the area of the Fortymile Wash alluvial fan subject to fluvial activity (channels) over a 10 kyr time scale |
| $L_c$ | The depth of permeable soil in channels at the RMEI location |
| $L_d$ | The depth of permeable soil on interchannel divides at the RMEI location |
| $D_c$ | The diffusivity of radionuclides in channels at the RMEI location |
| $D_d$ | The diffusivity of radionuclides on interchannel divides at the RMEI location |
| $\rho$ | The ash settled density |
| $\Delta r$ | The radial resolution of the input ASHPLUME grids |
| $\Delta\theta$ | The azimuthal resolution of the input ASHPLUME grids |
| rfactor | The radial multiplicative factor for the input ASPLUME grids. Radial coordinates within the ASHPLUME input grids are not linear, but increase geometrically with rfactor. For example, if rfactor = 2.0, each radial sample is greater than the last by a factor of 2.0 |
| $N_r$ | The number of radial samples of the ASHPLUME grids |
| $\Delta t$ | The output time step in years |
| T | The model duration in years |
| $\Delta x$ | The spatial resolution of the Geographic Information System (GIS) analysis within the alternative model |

| | |
|---|---|
| **B** | The biosphere depth; The model outputs the depth-averaged radionuclide concentration between the surface and depth **B**, which represents a critical depth in the Biosphere Model (e.g., tillage depth). |
| totalash | The total mass of ash deposited in the upper basin of Fortymile Wash |
| totalfuel | The total mass of fuel deposited in the upper basin of Fortymile Wash |
| mobilizedash | The total mass of ash mobilized from steep slopes and active channels in the upper basin of Fortymile Wash |
| mobilizedfuel | The total mass of fuel mobilized from steep slopes and active channels in the upper basin of Fortymile Wash |
| dilutionarea | The total area of all active channels within the primary ash fall zone and downstream of that zone to the fan apex |
| effectiveashthickness | The thickness of ash that results if the mobilized ash is spread uniformly over the dilution area (dilutionarea) |
| dilutionfactor | The fraction of channel sediment composed of ash (by volume) at the RMEI location |
| ashthicknessRMEI | The thickness of ash deposited directly on the RMEI location by primary ash fall |
| fuelinitsurfacedivide | The initial surface concentration of fuel on interchannel divides at the RMEI location (distributed through a surface layer of thickness equal to ashthicknessRMEI) |
| fuelinitdepthBdivide | The initial depth-averaged concentration of fuel on interchannel divides at the RMEI location (averaged from z = 0 to z = B) |
| fueldepthchannels | The thickness of contaminated channel sediments at the RMEI location |
| fuelinitsurfacechannel | The initial surface concentration of fuel in the channels at the RMEI location (distributed through a layer of thickness equal to fueldepthchannels) |
| fuelinitdepthBchannel | The initial depth-averaged concentration of fuel in the channels at the RMEI location (averaged from z = 0 to z = B) |

### I6.4.2.2 Initial Conditions

The initial conditions for the alternative ash redistribution model correspond directly with the input data. These are:

- Grids of ash and fuel concentration ($g/cm^2$) computed by ASHPLUME. The grids are assumed to be in circular coordinates (i.e., a function of radius r and azimuth $\theta$), with radial increments increasing in powers of 2 (e.g., 200 m, 400 m, 800 m, ...). The azimuthal resolution of the grids is input (e.g., $\Delta\theta = 10°$, for a total of 36 samples at each radius). Also, the initial radius and the number of radial samples is given (e.g., 200 m and 9 samples, resulting in a range of radii from 200 m to 51.2 km).

- Values for the ash and fuel concentration at the RMEI location approximately 18 km south of the repository computed by ASHPLUME.

- A 30-meter-resolution DEM that covers the Fortymile Wash drainage basin down to the latitude of the Fortymile Wash fan apex. This grid also includes information on the drainage-basin boundaries. Each pixel within the drainage basin has a value equal to the DEM elevation. Each pixel outside the drainage basin has a value of –9999.0.

- Values for model parameters, including the critical slope "S," drainage density "X," scour depth "H," RMEI fan area "A", fraction of RMEI fan area comprised of channels "F," the permeable soil depth in channels "$L_c$," the permeable soil depth on divides "$L_d$," the vertical diffusivity of radionuclides in channels "$D_c$," and the vertical diffusivity of radionuclides on divides, "$D_d$," and the biosphere depth "B."

### I6.4.2.3 Calculation of Fluvial Transport of Ash from Upper Watershed

The alternative redistribution model uses input grids of ash and fuel concentration computed by ASHPLUME. ASHPLUME grids are computed at a relatively coarse resolution, while the model software performs the grid analysis at the much finer resolution of the DEM (e.g., 30 m). For this reason, it is necessary to interpolate the ASHPLUME results to the same scale as the DEM. To do this, a bilinear interpolation procedure is used. Bilinear interpolation assumes that the ash and fuel concentrations vary linearly between ASHPLUME samples in both grid axes. The bilinear interpolation formula for the concentration C at a point (x,y), given concentration values at $C_{i,j}$, $C_{i+1,j}$, $C_{i,j+1}$, and $C_{i+1,j+1}$ at neighboring grid point locations $(x_i,y_j)$, $(x_{i+1},y_j)$, $(x_i,y_{j+1})$, $(x_{i+1},y_{j+1})$, respectively, is given by (Press et al. 1992 [DIRS 174134], p. 123) as:

$$C(x,y) = (1-u)(1-v)C_{i,j} + u(1-v)C_{i+1,j} + uvC_{i+1,j+1} + (1-u)vC_{i,j+1}, \qquad \text{(Eq. I.1)}$$

where

$$u = \frac{x - x_i}{x_{i+1} - x_i}, \quad v = \frac{y - y_j}{y_{j+1} - y_j} \qquad \text{(Eq. I.2)}$$

Alternative interpolation schemes are available (e.g., bicubic interpolation), but these methods can lead to errors when interpolating functions with steep gradients. Bilinear interpolation is the most robust interpolation method for two-dimensional functions.

Following the bilinear interpolation procedure, the grid is rectified to the DEM. This is done by transforming the grid so that the origin (center) of the interpolated grid (the vent location, which is placed at the center of the emplacement drift area) corresponds to the repository location in the DEM.

The alternative redistribution model performs a set of digital map analyses on the input DEM. These analyses include mapping the DEM slope, contributing area, and dilution area for the drainage basin. The DEM slope is used to determine the mass of ash mobilized from steep hillslopes throughout the drainage basin. In the model, the locations of steep hillslopes are determined by mapping the slope throughout the drainage basin and comparing each value to a critical value "S" (in dimensionless units, or m/m). All of the ash that falls on pixels with slopes greater than or equal to S is assumed to be mobilized into the channels by mass wasting, overland flow, and/or rilling.

Mathematically, the slope is defined as:

$$|\nabla h| = \sqrt{\left(\frac{\partial h}{\partial x}\right)^2 + \left(\frac{\partial h}{\partial y}\right)^2} \qquad \text{(Eq. I.3)}$$

The model implements Equation 3.3 using centered derivatives:

$$|\nabla h| = \sqrt{\left(\frac{h_{i+1} - h_{i-1}}{2\Delta x}\right)^2 + \left(\frac{h_{j+1} - h_{j-1}}{2\Delta x}\right)^2} \qquad \text{(Eq. I.4)}$$

Equation I.4 assumes that the DEM pixel resolution is the same in the x and y directions ($\Delta y = \Delta y$). Other techniques are available for computing the DEM slope. For example, the slope can be computed as the rise-over-run between each pixel and its neighboring pixel along the direction of steepest-descent. Equation I.4 was chosen for the alternative redistribution model because it has been found to be the most accurate method based on comparisons with synthetic grids using mathematical functions (Jones 1998 [DIRS 174197]).

This approach is a standard means of identifying potentially unstable slopes. An example of this approach is described by Pareschi et al. (2002 [DIRS 171394]). Illustrations of the mapping results, applied to assessment of drainage basin hazard potential, are shown in Figures I-2 and I-3 (Pareschi et al. 2002 [DIRS 171394], Figures 7 and 8). These figures are meant to illustrate the operations that the alternative redistribution model will perform.

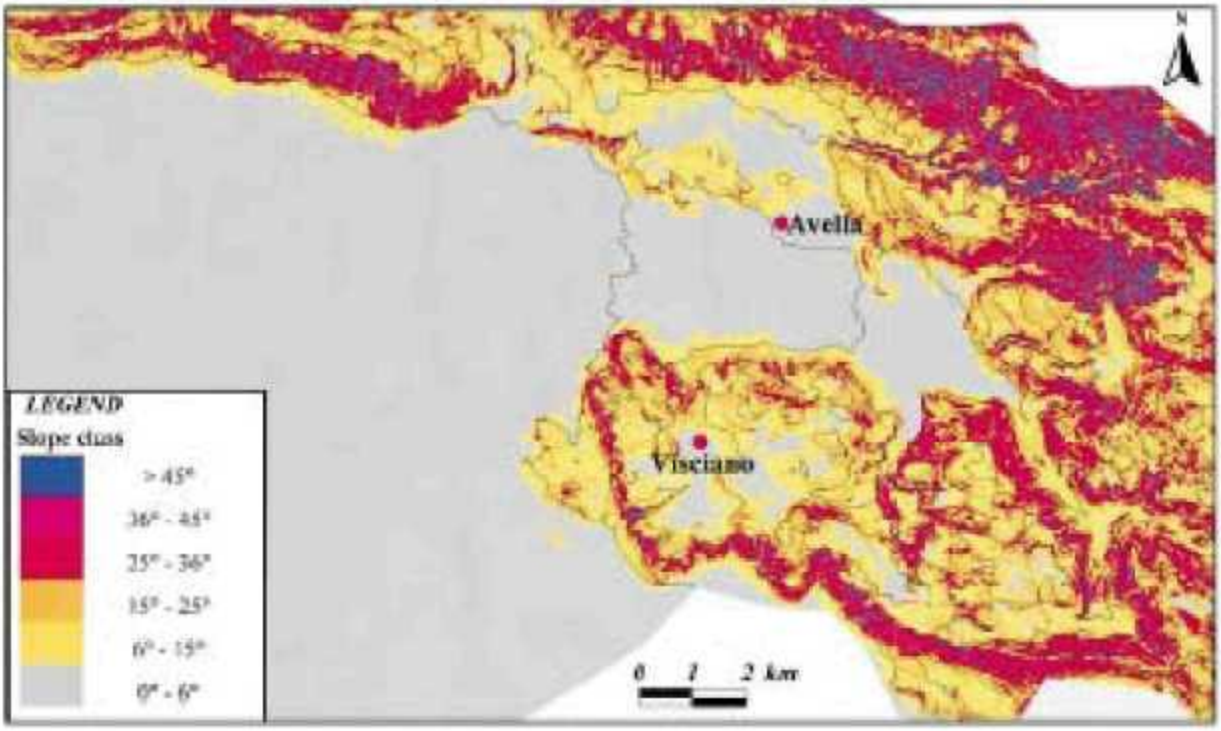


Source: Pareschi et al. 2002 [DIRS 171394], Figure 7.

NOTE: The slope map is derived directly from the DEM.

Figure I-2. Illustration of Drainage Basin Slope Mapping Derived from DEM Dataset

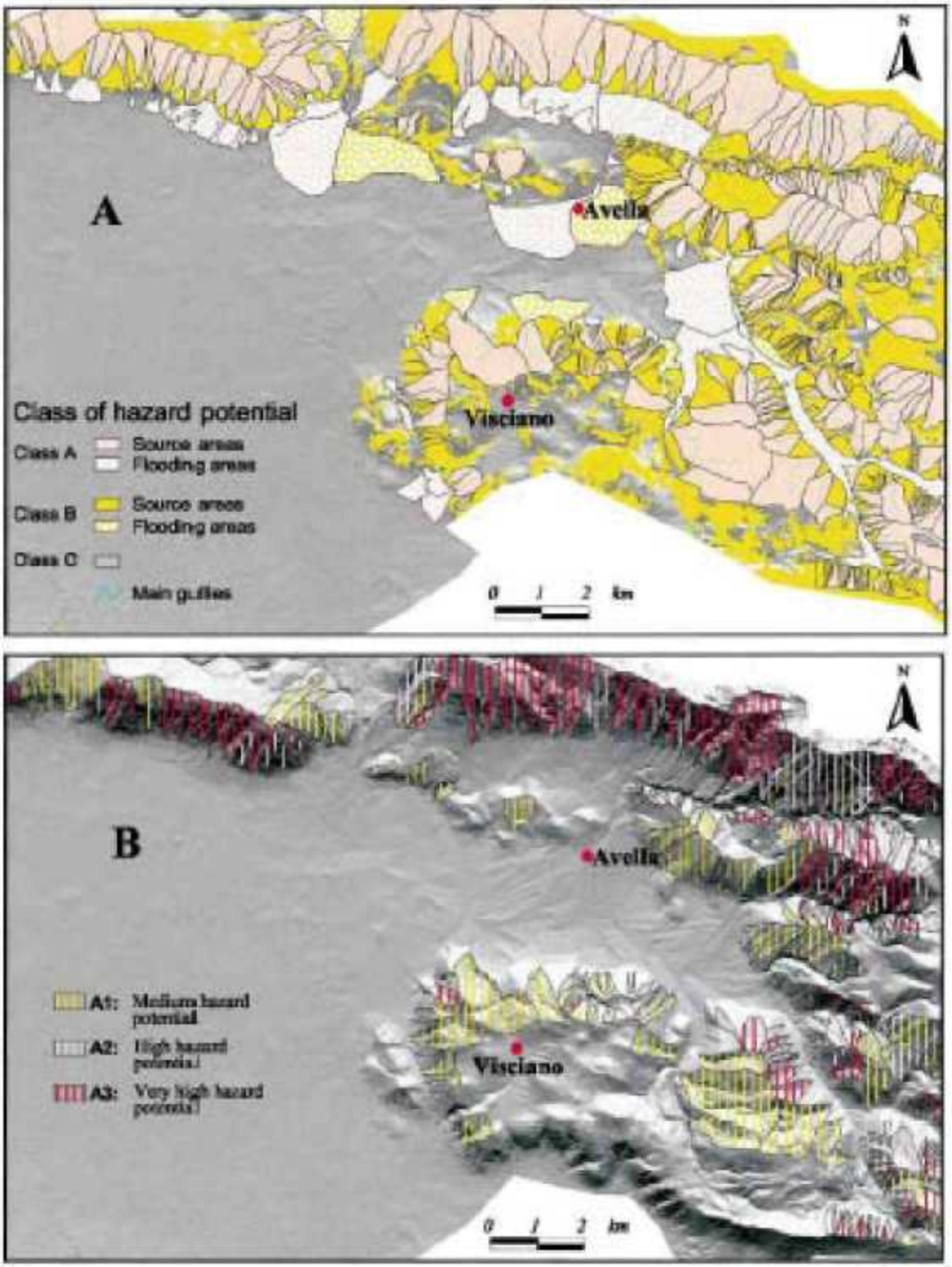


Source: Pareschi et al. 2002 [DIRS 171394], Figure 8.

Figure I-3. Illustrated Hazard Assessment Use of Drainage Basin Slope Mapping Derived from DEM Dataset

The contributing area is used to determine the mass of ash mobilized from active channels throughout the drainage basin. In the alternative model, the locations of active channels are determined by mapping the contributing area into each point of the drainage basin and comparing those values to the critical value of $1/X^2$, where "X" is the drainage density ($km^{-1}$). This criterion is consistent with the fact that channels in nature occur when runoff or contributing area is greater than a threshold value. Flows above this threshold are sufficient to entrain bed material and maintain an incised channel despite the tendency of hillslope processes to fill channel heads. The simplest method for computing the contributing area on a grid is to assume that all of the flow entering a pixel is routed along the direction of steepest descent. This method enforces a tributary drainage structure even in areas with distributary flow. As such, the steepest-descent method performs poorly in wide channels and low-relief areas. The alternative redistribution model uses an different method developed by Freeman (1991 [DIRS 174195]) called "bifurcation routing." In this method, all incoming flow to a pixel is partitioned between each of the downslope pixels, weighted by slope. In an area with multiple downslope pixels with equal slopes, contributing area is split evenly in each downslope direction. To use this method, each DEM pixel is first assigned a contributing area equal to $\Delta x^2$ (i.e., the local area represented by the pixel). Contributing area values are then routed as "flow" through the basin from highest to lowest elevation, following the same paths that runoff would take to the basin outlet. To move from highest to lowest elevation, the alternative redistribution model creates an index list that ranks the DEM pixels from highest to lowest. This ranked list is computed efficiently within the alternative model software using the Quicksort algorithm (Press et al. 1992 [DIRS 174134], pp. 338-340).

Following the construction of the index list, the alternative model begins the bifurcation-routing algorithm by calculating the contributing area at the highest pixel in the DEM. This pixel has no upstream tributaries, so its contributing area is equal to its initial value (i.e., $\Delta x^2$). This contributing area is then routed downslope by partitioning it between each of its eight neighbors on the grid (including diagonals), weighted by slope. Each of these eight neighbors receives some flow from the highest pixel, which is added to their initial values. The alternative model then proceeds to the next lowest pixel, routing contributing area from the highest to lowest pixels in the DEM. By moving through the grid in this order, the method ensures that all of the contributing area has been accumulated before routing the values downslope, because all incoming flow must come from higher elevations. The primary importance of bifurcation routing for the alternative model is that it provides an accurate method for mapping the entire channel area in a DEM, even if channels vary in width in a complex manner. The steepest-descent method would force all flow into the lowest point in the channel. As such, the steepest-descent method can provide an accurate measure of channel length, but channel width cannot be determined. In the bifurcation-routing method, flow expands to accommodate the entire channel between opposite banks. This difference is important for enabling the alternative model to integrate all of the ash that falls on active channels, and for calculating the dilution area. Pelletier (2004 [DIRS 174135]) compared results of steepest-descent and bifurcation routing applied to 30-m USGS DEMs (Figure I-4).

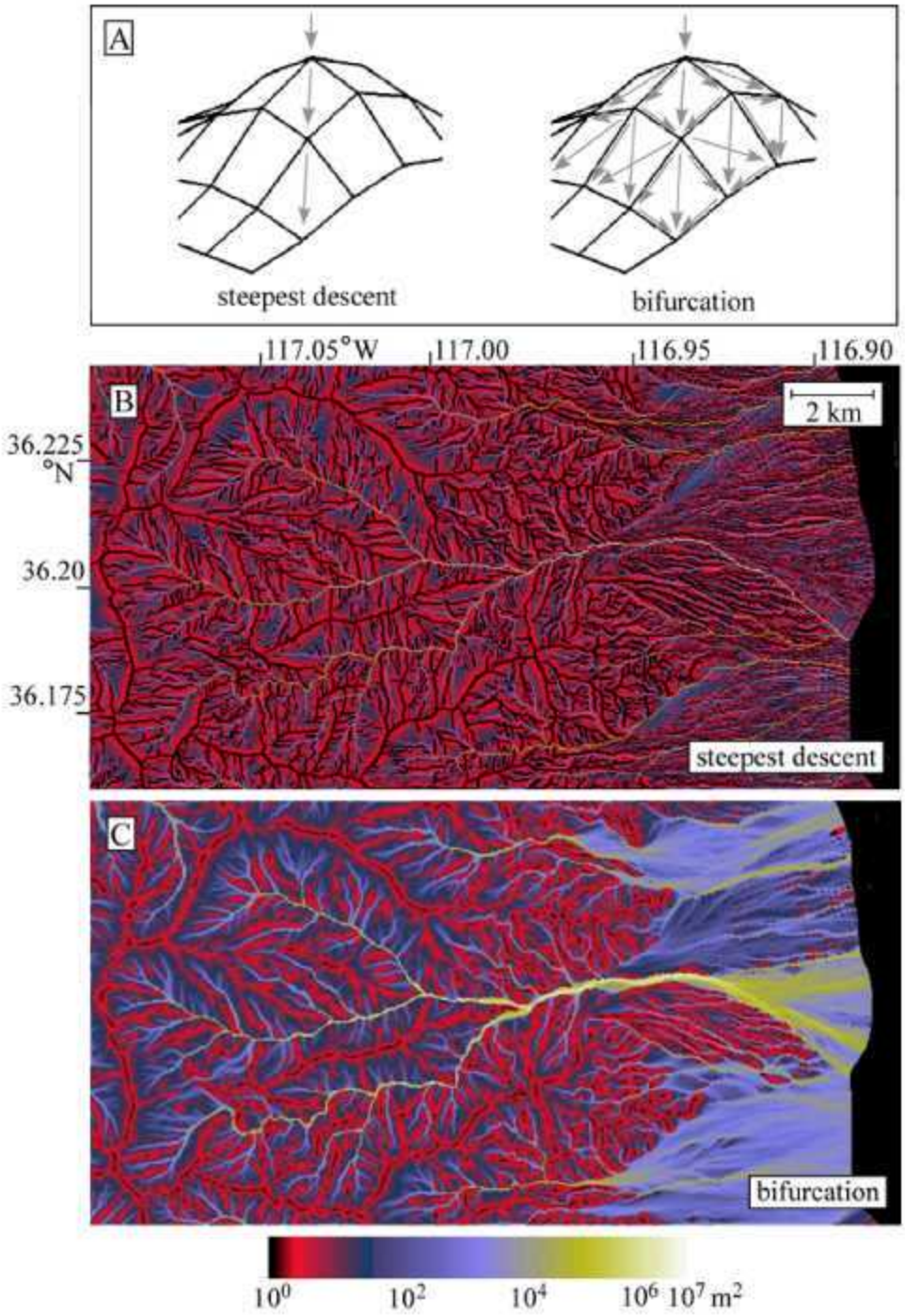


Source: Pelletier 2004 [DIRS 174135], Figure 1.

Figure I-4. Comparison of Steepest-Descent and Bifurcation Flow-Routing Algorithms on the Same 30-m USGS DEM (Hanaupah Canyon, Death Valley, California)

The total mass of mobilized ash and fuel are computed by comparing the slope and contributing area of each pixel to threshold values. If the pixel slope is greater than or equal to S, or the contributing area is greater than or equal to $1/X^2$, then the ash and fuel deposited on that pixel is added to the total amount of mobilized ash and fuel.

### I6.4.2.4 Calculation of Fluvial Dilution

The dilution area and the scour depth are used to determine the volume of sediment mixed with ash. The scour depth represents the thickness of channel-bed sediment that is entrained, mixed by turbulence, and redeposited during a sequence of floods. The effect of this process is to uniformly mix the ash with sediment, thereby diluting the ash. The dilution factor represents the fraction of ash within the channel-bed sediment when the ash and sediment reach the RMEI location. In order to compute the dilution factor, the alternative model first computes the total mass of ash mobilized from steep slopes and active channels (in kg). That mass is divided by the ash density (in $g/cm^3$) and the dilution area (in $m^2$) to determine an effective ash thickness. This value is the thickness of ash that would occur if the mobilized ash were spread out uniformly in all of the active channels within and downstream of the zone of primary ash fall. The dilution factor is then computed by comparing the average ash thickness with the scour depth. If the ash thickness is equal to or greater than the scour depth, no dilution will occur and the dilution factor is equal to one. If the ash thickness is less than the scour depth, the dilution factor is the ratio of the ash thickness to the scour depth, a value between 0 and 1. This type of mass-conservative dilution-mixing model is widely used in modeling the downstream dilution of trace metals in stream sediments (Hawkes 1976 [DIRS 174136], Helgen and Moore 1996 [DIRS 174138]).

Calculating the dilution factor requires the calculation of dilution area first. The dilution area is defined as the total area of all active channels within the zone of primary ash fall and all areas downstream from that zone to the fan apex. The zone of primary ash fall is defined as all areas with an ash thickness equal to or greater than 1 percent of the maximum ash thickness deposited in the upper basin. The dilution area is computed using a similar algorithm to the one that the alternative model uses to compute contributing area. First, the channels within the zone of primary ash fall are identified by setting the value of a dilution zone mask grid equal to one. All other pixels in the basin are given a value of zero. The bifurcation routing algorithm is then used to route the mask values downstream. This has the effect of making all pixels downstream equal to some non-zero value. The dilution zone is then considered to be all the pixels with a nonzero value for the dilution mask (the specific number is unimportant). The alternative model computes the total area of the dilution zone to determine the dilution area (in $km^2$).

Mathematically, the effective ash thickness is given by:

$$\text{effectiveashthickness} = \text{ashmobilized} * \Delta x^2 / (\rho * \text{dilutionarea}) \qquad \text{(Eq. I.5)}$$

where the dilution area is calculated by summing the total area of all non-zero pixels within the dilution mask. The dilution factor is then calculated as

$$\begin{aligned} &\text{dilutionfactor} = 1 && \text{if } H <= \text{effectiveashthickness} \\ &\text{dilutionfactor} = \text{effectiveashthickness}/H && \text{if } H > \text{effectiveashthickness} \end{aligned} \qquad \text{(Eq. I.6)}$$

### I6.4.2.5 Transfer of Ash and Fuel from Upper Watershed to RMEI Location

This step represents the transfer of fuel from the upper basin to the RMEI location within the alternative model. On divides, the thickness and concentration of fuel is determined solely from the primary ash fall deposited directly on the RMEI location. This is consistent with the

assumption that divides are not subject to fluvial activity (erosion and deposition) over the 10 kyr time scale of the repository. Soil-geomorphic mapping is being performed to calculate the fraction of the RMEI location area that is subject to fluvial activity over a 10 kyr time scale. As part of this work, divides are defined to be surfaces that have no evidence of fluvial erosion or deposition over time scales of at least 10 kyr (i.e., they are Pleistocene in age based on soil development and other age indicators). Surficial characteristics observed in the field, including well-developed desert pavement and varnish, provide evidence for the relative stability of channels and the lack of significant, soil-disruptive flood events on interchannel divides. Harrington (2003 [DIRS 164775]), for example, observed well-developed desert pavements and varnish on interchannel divides at the RMEI location, indicating that most of these interchannel divide surfaces are Pleistocene in age and have not been subject to significant flooding for at least 10,000 years.

The concentration of fuel on interchannel divides at the RMEI location is a direct input from ASHPLUME. The thickness of the ash layer is determined by dividing the ash concentration ($g/cm^2$) by the ash density ($g/cm^3$) to obtain an ash thickness in cm. Mathematically, the ash thickness on divides at the RMEI location is given by ashdepositionRMEI/$\rho$. This thickness is used to calculate the initial surface and depth-averaged fuel concentrations on divides. Mathematically, these are given by:

$$\text{fuelinitialsurfacedivide} = \text{fueldepositionRMEI}/\text{ashthicknessRMEI} \quad \text{(Eq. I.7)}$$

$$\text{fuelinitialdepthBdivide} = \text{fueldepositionRMEI}/B \quad \text{(Eq. I.8)}$$

In channels, the mass of fuel is the sum of the primary fallout and the fuel transported from the upper basin by fluvial processes. The alternative model assumes that the entire mass of fuel is deposited within the RMEI location. The entire fan area is bounded by the fan apex (upstream) and the Amargosa River (downstream). The RMEI location includes the upper and middle portions of the fan only. This portion of the fan was chosen because it is the portion of the fan with the greatest fraction of channels. This is the portion of the fan where flow is partitioned between many active threads of flow. This partitioning lowers flow velocity in these reaches, encouraging deposition. Field mapping has shown that the lower fan is composed primarily of divide surfaces. At least some of the ash that is transported to the RMEI location will move through the fan into the Amargosa River. However, the alternative model assumes that all of the fuel is deposited at the RMEI location. In other words, the upper and middle fan is the depozone for redistributed ash, and that depozone stores 100 percent of the redistributed fuel.

In the upper basin, masses of ash and fuel are distributed within a volume of channel bed material. As that material is transported to the RMEI location, the alternative redistribution model keeps the mass and concentration the same. To do so, the thickness of channel-bed material through which the ash and fuel are dispersed changes between the upper basin and RMEI location. In the upper basin, the ash and fuel are distributed uniformly from the surface to the scour depth. The thickness of contaminated sediments at the RMEI location is calculated by the alternative model to be the scour depth multiplied by the ratio of the upper basin dilution area to the area of channels at the RMEI location (FA). The total mass of fuel in channels of the RMEI location is equal to the total mass of ash mobilized from the upper basin and the mass deposited as primary ash fall. This total mass is assumed to be dispersed uniformly within the

thickness of contaminated sediments, providing a value for the initial concentration of ash in channels of the RMEI location.

Mathematically:

$$\text{fueldepthchannels} = \text{ashmobilized}*\text{dilutionfactor}/\rho \quad \text{(Eq. I.9)}$$

$$\text{fuelinitialsurfacechannels} = (\text{fueldepositionRMEI} + \text{fuelmobilized}/A)/\text{depthfuelchannels} \quad \text{(Eq. I.10)}$$

$$\text{fuelinitialdepthBchannels} = \begin{cases} \text{fuelinitsurfacechannel}*H/B & \text{if } B < H \\ \text{fuelinitsurfacechannel} & \text{if } B >= H \end{cases} \quad \text{(Eq. I.11)}$$

#### I6.4.2.6 Redistribution in the Soil Column

The alternative model considers the redistribution of radionuclides within the soil to be a diffusion process. Diffusion of radionuclides occurs within a finite depth range representing the permeable soil. Divide surfaces accumulate pedogenic calcium carbonate and clay at depth, decreasing the soil permeability over time. Pleistocene-age surfaces can be considered to be impermeable compared with channel sands. Field work is being performed to measure the permeable soil thickness on divide surfaces. The measured values will be used to prescribe a range of values for $L_d$. Soil horizons do not form in channel sediments because they are continually reworked by floods. The permeable soil thickness is greater in channels than on divides, but it may be limited by the occurrence of paleosols at depth. Field work is being performed to establish a minimum permeable depth in channels. That minimum permeable depth or range of depths will be used for the value of $L_c$ in the alternative model.

The equation describing the evolution of the fuel concentration C by diffusive processes is given by the solution to the diffusion equation in a finite layer from z = 0 to z = $L_d$ with no-flux boundary conditions (Carslaw and Jaeger 1959 [DIRS 100968], Section 3.4).

$$C(z,t) = C_0 d_w \left( \frac{1}{L_d} + \sum_{n=1}^{\infty} \frac{2}{L} \cos\left( \frac{n\pi z}{L_d} \right) e^{-n^2 \pi^2 D t / L^2} \right), \quad \text{(Eq. I.12)}$$

where $C_0$ is the initial concentration within a layer of thickness $d_w$ at the surface. Figure I-5 illustrates the behavior of the model for $D_d$ = 0.1 cm$^2$/yr and $L_d$ = 100 cm. Within the first few decades to several hundred years, the dispersion process dominates. After t = 10,000 yr, the fuel is almost completely mixed within the permeable soil column, and the profile approaches a uniform fuel concentration equal to:

$$C(z,\infty) = \frac{C_0 d_w}{L_d} \quad \text{(Eq. I.13)}$$

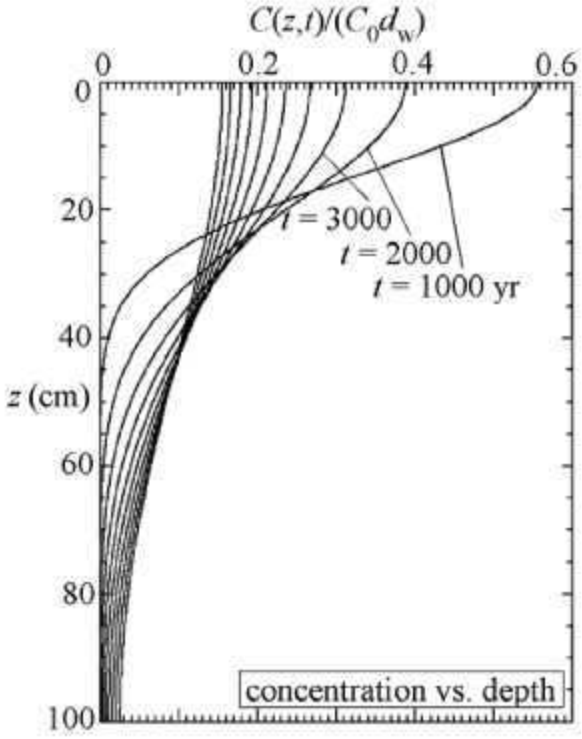


Source: Harrington 2004 [DIRS 171907], pp. 82-94.

Figure I-5. Plots of Concentration (Normalized to Initial Concentration) vs. Depth for a Range of Values of Time ($t$) Model Parameters are $L$ = 100 cm and $D$ = 0.1 cm$^2$/yr.

The alternative redistribution model produces four output time series: 1) the surface radionuclide concentration on divide surfaces at the RMEI location, 2) the surface radionuclide concentration in channels at the RMEI location, 3) the depth-average radionuclide concentration on divide surfaces at the RMEI location, and 4) the depth-average radionuclide concentration in channels at the RMEI location. The surface concentration is required for use in calculating the dose corresponding to inhalation pathways in the Biosphere Model within TSPA. The depth-averaged concentration is used within the Biosphere Model to calculate the dose from processes that depend on bulk concentrations (e.g., tillage, plant respiration). The alternative model accepts an input "biosphere depth" B and computes the average concentration from the surface to that depth for each time step.

The surface concentration on divides is calculated using Equation I.12, evaluated at z = 0:

$$C_d(0,t) = C_{d0} d_{dw} \left( \frac{1}{L_d} + \sum_{n=1}^{\infty} \frac{2}{L_d} e^{-n^2 \pi^2 D_d t / L_d^2} \right), \qquad \text{(Eq. I.14)}$$

where $C_{d0}$ is the initial surface concentration on divides (fuelinitsurfacedivide), $d_{dw}$ is the ash thickness on divides (ashthicknessRMEI), and t is time ($\Delta t$ times the time step number).

The equation for the surface concentration in channels is identical in form to Equation I.14 but with divide parameters replaced by channel parameters:

$$C_c(0,t) = C_{c0} d_{cw} \left( \frac{1}{L_c} + \sum_{n=1}^{\infty} \frac{2}{L_c} e^{-n^2 \pi^2 D_c t / L_c^2} \right), \qquad \text{(Eq. I.15)}$$

where $C_{c0}$ is the initial surface concentration in channels (fuelinitsurfacechannels), $d_{cw}$ is the ash thickness in channels (fueldepthchannels).

The depth-averaged concentration on divides and in channels is calculated by integrating Equation I.12 from $z = 0$ to $z = B$ and dividing by B. On divides the depth-averaged concentration is:

$$\frac{1}{B}\int_0^B C_d(z,t)dz = \frac{C_{d0} d_{dw}}{L_d} + \frac{L_d}{B}\sum_{n=1}^{\infty}\frac{1}{n}\sin\left(\frac{n\pi B}{L_d}\right) e^{-n^2\pi^2 D_d t / L_d^2} = \qquad \text{(Eq. I.16)}$$

In channels the depth-averaged concentration is:

$$\frac{1}{B}\int_0^B C_c(z,t)dz = \frac{C_{c0} d_{cw}}{L_c} + \frac{L_c}{B}\sum_{n=1}^{\infty}\frac{1}{n}\sin\left(\frac{n\pi B}{L_c}\right) e^{-n^2\pi^2 D_c t / L_c^2} \qquad \text{(Eq. I.17)}$$

## I6.5 MODEL RESULTS

This section summarizes the model results for ash redistribution for use in the TSPA model.

The proposed output parameters of the alternative ash redistribution model for use in TSPA are summarized in Table I-3 in terms of the two main geomorphic features at the RMEI location (interchannel divides and distributary channels). The format of Table I-3 is parallel to that of Table 6-5, which describes the abstraction of the existing conceptual ash redistribution model.

## I7. MODEL VALIDATION

Should this alternative mathematical diffusion model be used in the future, it must be validated for its intended use. In this section we consider validation of the soil redistribution component only. Validation should proceed by correlating observed radionuclide concentrations in soils from several appropriate analogue sites with predictions by the alternative ash redistribution model. The objective of the validation tests would be to assess how well the diffusion model predicts the concentration-depth profiles of radionuclides. Selection and/or assessment of compared $D$ values would require consideration for differences in climate and soil type. Data identified as available for use in this analysis include $^{137}Cs$ data from the Ukraine after the Chernobyl accident (Likhtarev et al. 2002 [DIRS 169810]), and $^{137}Cs$ data from a field experiment in the UK (Gale et al. 1964 [DIRS 169807]). Other considerations for suitable sites would include a search for natural radionuclide tracer analogues involving alluvial sedimentation and climate appropriate to that of the Yucca Mountain region.

Table I-3. Results of Ash Redistribution Model for TSPA

| AREAL WEIGHT | Interchannel Divide (1-F) | Distributary Channels F |
|---|---|---|
| | Initial condition<br>Ash and fuel concentration ($g/cm^2$) at the RMEI location approximately 18 km south of repository calculated by ASHPLUME in the TSPA model<br><br>Temporal Values at the RMEI<br>Numerical expressions will be provided for calculation of,<br>a) Near-surface fuel concentration in soil column<br>b) Depth-averaged fuel concentration (from surface to specified depth B) in soil column | Initial condition<br>Ash and fuel concentration ($g/cm^2$) at the RMEI location approximately 18 km south of repository calculated by ASHPLUME in the TSPA model<br><br>Ash and fuel concentrations for the region surrounding the repository calculated by ASHPLUME on a polar-coordinate grid<br>Model will calculate the mass of ash and fuel mobilized from Fortymile Wash watershed by fluvial processes, including dilution<br><br>Temporal Values at the RMEI<br>Numerical expressions will be provided for calculation of,<br>a) Near-surface fuel concentration in soil column<br>b) Depth-averaged fuel concentration (from surface to specified depth B) in soil column |

## 18. CONCLUSIONS

**Summary Of Modeling Activity**–The mathematical model of this appendix is presented as an alternative to the conceptual model for tephra redistribution described in this model report. The model explicitly includes redistribution within the soil column and erosion and deposition within and out of the RMEI location. Fluvial erosion and deposition within channels in the RMEI location is not considered explicitly, but is implicitly included by enhanced mixing in the soil column of channel environments. Redistribution in the soil column is governed by the diffusion equation.

# I9. SUPPLEMENTARY SUPPORTING DATA

## I9.1 DESCRIPTION OF REDISTRIBUTION OF RADIONUCLIDES IN SOIL CRITERIA

The health physics community has studied the processes of radionuclide migration into soils since the advent of the atomic age, mostly from the point of view of resuspension of radionuclides for airborne transport and potential human dose. It was recognized early that one of the factors controlling the concentration of radionuclides available for resuspension is its "weathering," in which the radionuclides becomes less erodible (Anspaugh et al. 1975 [DIRS 151548], p. 576). This weathering process includes mixing with surface soil and vertical migration into the soil (Anspaugh et al. 2002 [DIRS 169793], p. 677). From the body of work summarized in Anspaugh et al. (2002 [DIRS 169793], p. 677) and others where noted, the following are general statements that reflect the state of knowledge about radionuclide migration into soil:

- Radionuclides deposited in soil immediately experience a surface-roughness process that is equivalent to shielding by a 1-mm layer of soil.
- Radionuclides move to an average depth of about 1 cm within one month.
- Within a year radionuclides move to a depth of 3 cm and slowly move to greater depths.
- Results for $^{129}I$, $^{137}Cs$, $^{239}Pu$, and $^{240}Pu$ studies after the Chernobyl accident indicate that all of these radionuclides move into the soil at the same rate and that their distributions in the soil were essentially identical. Anspaugh et al. (2002 [DIRS 169793]) conclude that the process of radionuclide migration into soil is essentially a physical, rather than chemical process, and although data are limited on other radionuclides, the $^{235}U$ data from the Nevada Test Site (Gilbert and Eberhardt 1976 [DIRS 169808]) seem to follow similar migration rates.
- Local climate and soil conditions may result in significant differences in radionuclide migration rates.
- Vertical migration of radionuclides in montmorillonite and illite-bearing soils (like those at the Nevada Test Site) is due to freeze/thaw and wet/dry cycles that granulate the soil by aggregation and dispersion, enhancing the mechanical movement and downward migration of high-density particles. Migration of radionuclides in solution in infiltrating water is considered less important (Romney et al. 1970 [DIRS 169811], pp. 488-489).

Radionuclide concentrations measured in the field are bulk measurements. Rather than measure point concentrations, the concentration within different depth intervals is usually measured (BSC 2004 [DIRS 169980], Table 6-8). For the purposes of extracting model parameters from observed data, it is most accurate to represent measured data cumulatively as the fraction of total concentration to a given depth. To compare the diffusion-model predictions to this normalized cumulative curve, it is necessary to integrate the solution to the diffusion equation in a

semi-infinite column with a no-flux boundary condition at the surface and a fuel mass of $C_0 d_w$ input at $z = 0$ at $t_1 = 0$ (Carslaw and Jaeger 1959 [DIRS 100968], Chapter 14.2, Eq. (1)):

$$\frac{C(z,t_1)}{C_0 d_w} = \frac{1}{\sqrt{\pi D t_1}} e^{-z^2/4Dt_1}, \quad \text{(Eq. I-18)}$$

to give

$$\int_0^z \frac{C(\zeta,t_1)}{C_0 d_w} d\zeta = \text{erf}\left(\frac{z}{\sqrt{4Dt_1}}\right), \quad \text{(Eq. I-19)}$$

where "erf" is the error function and $\zeta$ is an integration variable for depth. Equations I-18 and I-19 approximate the permeable soil layer as semi-infinite. This is an accurate approximation, even in a soil with a petrocalcic horizon at depth, because radionuclides do not penetrate far into the soil over time scales of several decades (the maximum time scale for man-made radionuclides). As such, near-surface concentrations are not affected by the presence of an impermeable barrier at 10 cm depth. It should also be noted that radioactive decay need not be considered explicitly in this analysis because decay does not affect the spatial distribution of radionuclide concentration for a normalized cumulative curve.

$^{137}$Cs distributions (DTN: LA0308CH831811.002 [DIRS 164853]) were used to calibrate values of the radionuclide diffusivity $D$. To calculate $D$, the fraction of total activity at 3 cm was first computed by dividing the activity from 0-3 cm by the total activity from 0-6 cm (column 2 in Table I-4). Equation I-19 was then used to infer the value of the error function argument, equal to $z/\sqrt{4Dt_1}$, corresponding to the fraction of activity at 3 cm after 50 yr of diffusion following nuclear testing (column 3 in Table I-4). A table of calculated error function values was used for this purpose. This value was then used to solve for $D$ (column 4 in Table I-4).

Table I-4. Calibration Values for $D$

| Sample ID | Fraction at 3 cm= erf(3 cm/(4$D$ 50 yr)$^{1/2}$) | 3 cm/(4$D$ 50 yr)$^{1/2}$ | $D$ (cm$^2$/yr) |
|---|---|---|---|
| Cs-071702-A | 0 8274 | 0 965 | 0 0468 |
| Cs-071702-B | 0 5387 | 0 521 | 0 165 |
| Cs-071702-C | 0 8100 | 0 929 | 0 052 |
| Cs-071702-E | 0 7644 | 0 839 | 0 063 |
| Cs-071702-G | 0 9593 | 1 448 | 0 021 |
| Cs-071802-H | 0 9695 | 1 530 | 0 019 |
| Cs-071802-I | 0 9614 | 1 463 | 0 021 |
| Cs-071802-J | 0 6387 | 0 643 | 0 108 |
| Cs-071802-K | 0 9558 | 1 423 | 0 022 |
| Cs-071802-N | 0 9082 | 1 192 | 0 031 |
| Cs-071802-P | 0 9428 | 1 345 | 0 024 |
| Cs-071802-Q | 0 9951 | 1 990 | 0 011 |
| Cs-071802-R | 0 9578 | 1 437 | 0 021 |

Table I-4. Calibration Values for $D$ (Continued)

| Sample ID | Fraction at 3 cm = erf(3 cm/(4$D$ 50 yr)$^{1/2}$) | 3 cm/(4$D$ 50 yr)$^{1/2}$ | $D$ (cm$^2$/yr) |
|---|---|---|---|
| Cs-071802-S | 0 8807 | 1 101 | 0 037 |
| Cs-071802-U | 0 5488 | 0 533 | 0 158 |
| Cs-071802-V | 0 9938 | 1 938 | 0 012 |
| Cs-071802-W | 0 7185 | 0 762 | 0 077 |
| Cs-071802-X | 0 8771 | 1 092 | 0 037 |
| Cs-071802-Y | 0 6616 | 0 684 | 0 096 |
| Cs-071802-Z | 0 7547 | 0 822 | 0 066 |
| Cs-071802-AA | 0 9450 | 1 359 | 0 024 |
| Cs-071802-BB | 0 7943 | 0 895 | 0 056 |

Corroboration of the calibrated values for $D$ was obtained by analyzing $^{239}$Pu and $^{235}$U radionuclide profiles in soils at the Nevada Test Site (Anspaugh et al. 1975 [DIRS 151548]; Gilbert and Eberhardt 1976 [DIRS 169808]; Romney et al. 1970 [DIRS 169811]). These measurements expand the list of radionuclides analyzed, and also increase the range of time scales to those as small as 1.3 years.

The Nevada Test Site is considered the best available analogue for the RMEI location. Datasets for the concentration of $^{239}$Pu and $^{235}$U were measured by Romney et al. (1970 [DIRS 169811]) and Anspaugh et al. (1975 [DIRS 151548]), and concentrations of $^{235}$U were measured by Gilbert and Eberhardt (1976 [DIRS 169808]) at the Nevada Test Site. In all of these literature sources, the concentration is measured in three or more depth intervals. Only the first depth interval and the total activity were used, however, to reduce the analysis to the error function value at a single point (analogous to the calibration data in Table I-4). Proposed work includes a more complete analysis, including nonlinear curve fitting of Equation I-14 to the complete measured profiles.

**Romney et al. (1970) Data**–Romney et al. (1970 [DIRS 169811], Table I-1) provided three profiles measured over two different time scales: 1.3 years and 10.8 years. The inferred $D$ values are comparable despite the order-of-magnitude difference in time scale. This provided confidence that the diffusion model was accurately reproducing the temporal evolution of the migration process.

Table I-5. Inferred $D$ Values from Romney et al. ( 1970)

| Radionuclide, t | Fraction at 3 cm = erf(3 cm/(4$Dt$)$^{1/2}$) | 3 cm/(4$Dt$)$^{1/2}$ | $D$ (cm$^2$/yr) |
|---|---|---|---|
| $^{239}$Pu, 1 3 yr | 0 9231 | 1 251 | 1 105 |
| $^{239}$Pu, 10 8 yr | 0 8007 | 0 908 | 0 252 |
| $^{239}$Pu, 10 8 yr | 0 7151 | 0 757 | 0 363 |

**Anspaugh et al. (1975) Data**–Anspaugh et al. (1975 [DIRS 151548]) measured one profile in detail approximately 20 years after nuclear testing. The best-fit $D$ value is 0.01 cm$^2$/year, or

more than an order-of-magnitude less than the values obtained for Romney et al. (1970 [DIRS 169811]) for the same radionuclide.

Table I-6. Inferred *D* Values from Anspaugh et al. (1975)

| Radionuclide, t | fraction at 0.5 cm= erf(0.5 cm/(4*Dt*)$^{1/2}$) | 0.5 cm/(4*Dt*)$^{1/2}$ | *D* (cm$^2$/yr) |
|---|---|---|---|
| $^{239}$Pu, 20 yr | 0.6009 | 0.596 | 0.0088 |

**Gilbert and Eberhardt (1976) Data**–Gilbert and Eberhadt (1976 [DIRS 169808], Table 8, site A, area 11) also measured one profile in detail. The best-fit *D* value is 0.060 cm$^2$/year. The inferred *D* values from Anspaugh et al. (1975 [DIRS 151548]) and Gilbert and Eberhardt (1976 [DIRS 169808]) using $^{239}$Pu and $^{235}$U are comparable to the calibration values obtained using the $^{137}$Cs profiles (DTN: LA0308CH831811.002 [DIRS 164853]).

Table I-7. Inferred *D* Values from Gilbert and Eberhardt (1976)

| Radionuclide, t | fraction at 2.5 cm= erf(2.5 cm/(4*Dt*)$^{1/2}$) | 2.5 cm/(4*Dt*)$^{1/2}$ | *D* (cm$^2$/yr) |
|---|---|---|---|
| $^{235}$U, 20 yr | 0.8920 | 1.138 | 0.060 |

These results indicate that *D* values do not differ systematically between radionuclides, indicating that different radionuclide species become mixed within the soil profile at comparable rates. This result is consistent with the conclusions of Anspaugh et al. (2002 [DIRS 169793]). Individual profiles do show large variability, however, from a minimum of 0.008 cm$^2$/yr to a maximum of 1.1 cm$^2$/yr. Some of this variability could reflect geomorphic position (i.e., channels vs. interchannel divides). It is difficult to test this hypothesis, however, because only limited information on sample position is provided in these NTS reports.

INTENTIONALLY LEFT BLANK

# APPENDIX J

# ALTERNATIVE WASTE PARTICLE SIZE DISTRIBUTION AND ALTERNATIVE CONCEPTUAL MODEL OF MAGMA-WASTE INTERACTION

# APPENDIX J
# ALTERNATIVE WASTE PARTICLE SIZE DISTRIBUTION AND ALTERNATIVE CONCEPTUAL MODEL OF MAGMA-WASTE INTERACTION

## J1. INTRODUCTION

The assumption rationale for the waste particle size distribution (Section 5.2.4) is presented based on criteria from a professional judgment by Argonne National Laboratory. That judgment was based on observations of disaggregation of fuel to near spent-fuel grain size by the effects of oxidation of the fuel form. The purpose of this alternative analysis is to determine if there is a more robust basis for the waste particle size criteria used in Section 5.2.4 that does not include unwarranted conservatism.

The work to date on ash-waste dispersal and deposition during an eruption through the repository has assumed that the waste in packages impacted by rising magma would be instantaneously available and simultaneously vented with ash in an eruption plume (Section 6.3.1). In short, the magma-waste interaction and rise through the conduit to the vent have been treated as a 'black box', and only a limited technical basis has been developed for the processes of waste incorporation into the magma and its eruptive products. The purpose of this analysis is to provide a more robust conceptual model for the incorporation of waste in magma, including accounting for the volume of waste-containing magma that is deposited in geologically stable landforms that will not contribute to dose during the postclosure period.

The results presented in this Appendix provide alternative assumption rationales and values for waste particle size, waste partitioning in magma, and waste incorporation in volcanic ash.

## J2. WASTE PARTICLE SIZE

### J2.1 METHOD

This alternative analysis of the assumption and rationale for defining the waste particle size criteria is based on literature review. One finding is that definition of spent particle size distribution in a manner directly applicable to the Ashplume model report has not been a common determination. Further, authors are not always explicit on the manner of particle sampling or size measurement, complicating equitable comparison.

### J2.2 POTENTIAL INFLUENCE ON WASTE PARTICLE SIZE

Two eruptive scenarios can be described, based on different potential effects on waste particle size and incorporation in the dispersed volcanic ash. These two scenarios are dependent on whether the rising magma flux is effusive or explosive at the point of interaction with the repository drifts. The pre-eruptive and eruptive stage steps and potential effects on the waste interaction are shown in Figure J-1.

In Scenario 1 of Figure J-1 shows that an effusive magma flux interaction with the failed waste packages could result in physical mixing of the waste particles within the molten magma. This interaction and physical incorporation might include some degree of waste-magma eutectic

formation. However, independent of this and of the degree to which the waste fragments are altered through the effects of oxidation, the considered potential overall effect is a distribution of the waste into the magma as a mixed mass fraction. The waste would then distribute, disperse and deposit as a mass fraction of the lava, scoria and tephra.

Scenario 2 is representative of the case currently modeled in Section 6. An explosive magma flux through the repository results in the disaggregation of waste to the assumed particle size distribution and incorporation with ash particles during the plume formation. The descriptions in **Figure J-1** and Section J3 revise this process to include mixing of the waste with the magma during transport through the conduit and subsequent distribution, dispersal, and deposition of the waste as a mass fraction of the lava, scoria, and tephra.

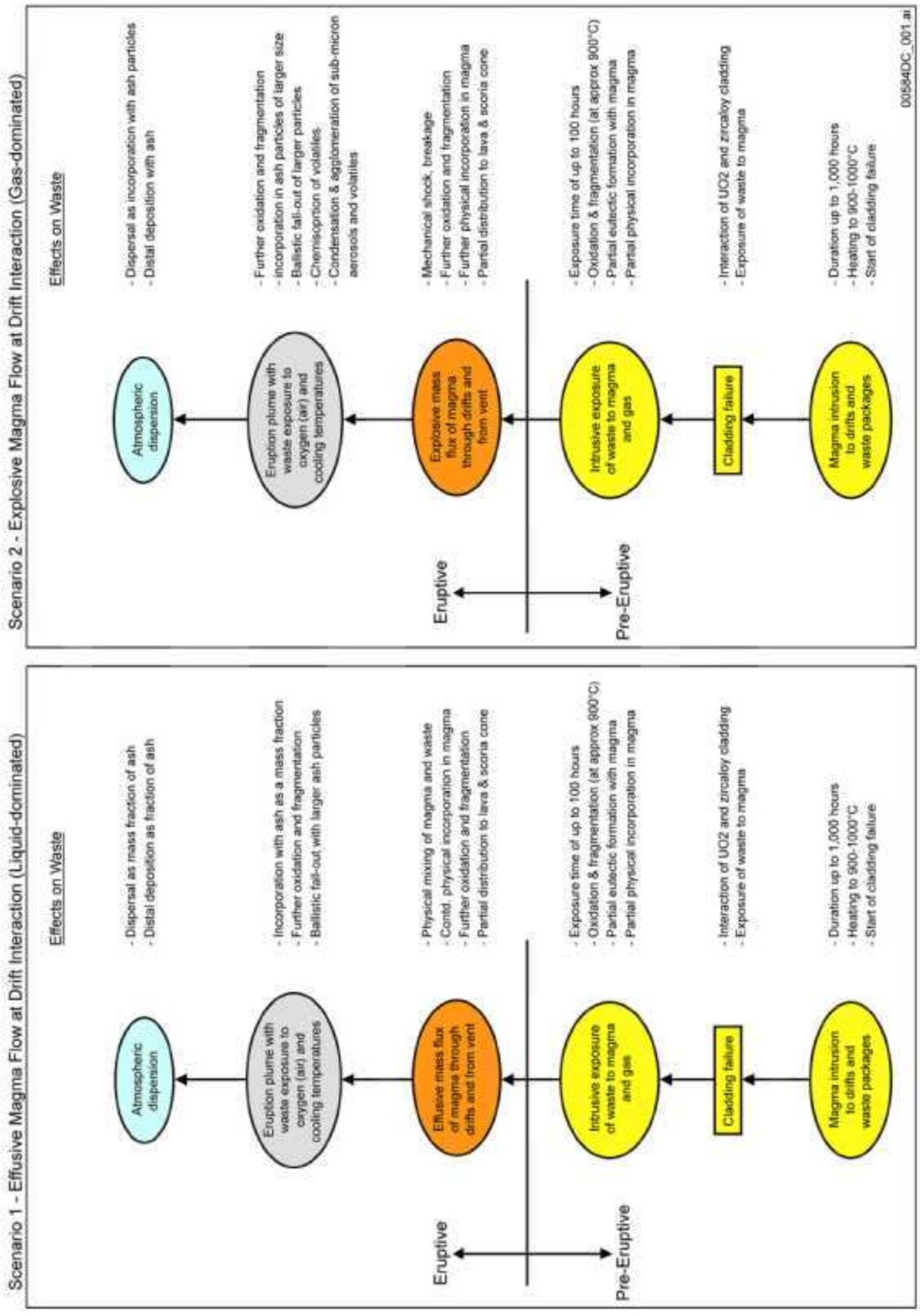


Figure J-1. Extrusive Event Sequence of Potential Influences on Waste and Waste Particle Size

## J2.3 SUMMARY OBSERVATIONS AND COMMENTS

From the literature survey, the following summary observations are made:

a) **Spent Fuel Characterization**–Extensive investigations have been conducted by Pacific Northwest Laboratory (PNL) for the DOE OCRWM Program to characterize spent fuel and the physico-chemical effects that can occur under long-term storage conditions. The investigations include inter- and intra-granular physical and chemical effects; however spent fuel particle size distribution is not noted to be addressed in a manner of direct applicability to the Ashplume AMR. Approved Testing Material (ATM) test report photomicrographs (Guenther, Blahnik, Jenquin, et al. 1991 [DIRS 109207]; Guenther, Blahnik, Campbell, et al. 1991 [DIRS 127061]) show significant fragmentation of irradiated fuel while the upper-end integral fuel particle size (in both dimensions) is visually gauged from some photomicrographs to be approximately equivalent to half pellet diameter, i.e., approximately 4.5 to 5 mm. Example fuel pellet fragmentation is shown in Figure J-2. The Fuel form pellet in this case was 9.56 mm dia. × 11.4 mm long.

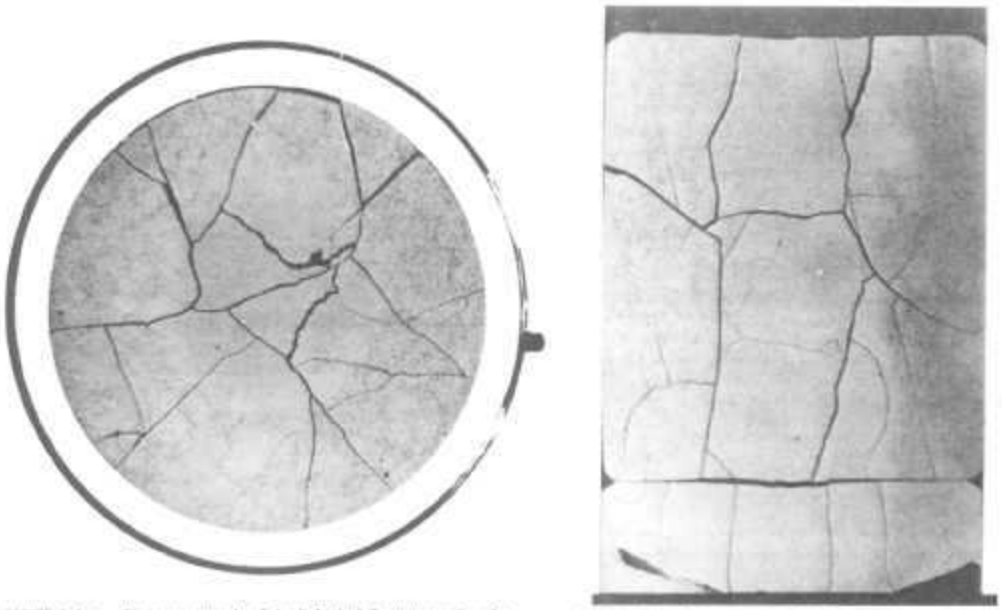

Source: Guenther, Blahnik, Campbell et al. 1991[DIRS 127061], Figures E.1.g and E.1.h.

Figure J-2. Photomicrographs Illustrating Spent Fuel Fragmentation

b) **Fuel Form**–The grain size for fuel form is proprietary to the source and application, with a typical assessment being that average grain size (RMS dia.) generally ranges from 7 to 12 μm, with good reproducibility around 9 μm (Guenther, Blahnik, Jenquin, et al. 1991 [DIRS 109207], p. 3.4). It is not consistently clear whether this relates to the attainable grain size through disaggregation processes (see below).

"Oxidation of Spent Fuel in Air at 175 to 195°C" (Einziger et al. 1992 [DIRS 101607] lists the grain size for the ATM fuels and a Turkey Point fuel as shown in Table J-1.

Table J-1. Spent Fuel Grain Size

| Spent Fuel | Grain Size, µm |
|---|---|
| ATM-103 | 18 5 |
| ATM-104 | 5–15 |
| ATM-105 | 11–15 |
| ATM-106 | 10–13 |
| Turkey Point | 20–30 |

Source Einziger et al 1992 [DIRS 101607], Table 2

c) **Oxidation of $UO_2$**–Extensive studies have investigated the oxidation effects on irradiated and non-irradiated $UO_2$ fuel (DOE 2003 [DIRS 166027], p. 19). Mostly these have been for temperature ranges up to about 400°C, presumably pertaining to spent fuel handling and storage. The chemistry of the uranium oxide system is complex because of the existence of hyperstochiometric oxides (DOE 2003 [DIRS 166027], p. 20). $U_3O_8$ is cited as being well known as the crystalline phase responsible for fuel swelling and disaggregation when oxidized (Dehaudt 2001 [DIRS 164019], p. 13). At lower temperatures, the progressive oxidation of $UO_2$ to the higher valence state involves an incubation time, which ranges from 23 to 80 minutes at 400°C and tends towards 0 at 500°C (Dehaudt 2001 [DIRS 164019]; Einziger et al. (1992 [DIRS 101607]) report that oxidation up to $UO_{2.4}$ leads to volume reduction of the $UO_2$ matrix, so opening grain boundaries that can result in disaggregation of fuel into single fuel grains. Further oxidation to $U_3O_8$ and related oxides results in a large volume expansion and potentially extreme degradation of the fuel into a powder with particle sizes less than one micrometer in diameter.

For high temperatures, (magma interaction is ~1,100°C), and somewhat countering the foregoing perspective, other work reports that above ~350°C, the intermediate $U_3O_7/U_4O_9$ is generally not observed in major quantities; instead, the bulk oxidation appears to proceed directly to $U_3O_8$. Above ~500°C the rate of $U_3O_8$ formation on sintered $UO_2$ pellets does not display Arrhenius behavior, but rather, it declines with increasing temperature. This behavior has been attributed to the increased plasticity of $U_3O_8$ above 500°C; thus the $U_3O_8$ formed does not readily spall from the $UO_2$ surface but instead forms a barrier to retard further oxidation. The particle size of $U_3O_8$ powder generated by air oxidation of $UO_2$ pellets increases with oxidation temperature, perhaps because of increasing $U_3O_8$ plasticity between 400 and 700°C. The major product of $UO_2$ oxidation remains $U_3O_8$ up to ~1,100°C, above which $U_3O_8$ decomposes to a series of oxides with slightly lower O:U ratios (McEachern and Taylor 1997 [DIRS 101726], Section 2.1).

d) **Mechanical Shock**–Sandia National Laboratories performed sub-scale and full-scale tests to evaluate the capability of high energy devices to breach spent fuel truck casks and disperse cask contents (Sandoval et al. 1993 [DIRS 156313]). This work is one of few that report particle size distribution for the outcome. The reported mass median particle diameter in this case is 210 µm. However, this test represents mechanical shock at ambient temperatures and may not be a most appropriate analogue for an

eruptive event in which fuel has been pre-heated to elevated temperature (resulting in plasticity) and shock forces from molten magma and gas.

e) **Chernobyl Accident as an Analogue**–There have been numerous international scientific studies on various aspects of the Chernobyl Nuclear Power Plant accident on April 26, 1986. The major coverage in those studies has been the radiological and health impacts.

The incident was not a volcanic event; however, there are some aspects that support the use as an analogue for an igneous event at Yucca Mountain. The initial phase included two explosions. This was followed by days of elevated thermal exposure in which it has been estimated that temperatures >1,900°C were reached in the core melt (Ushakov et al. 1997 [DIRS 174141]). In comparison to a volcanic event, the fuel dispersal was more as a discrete material without the proportionately massive volcanic ash component.

While there are numerous references to particulate and aerosol sizes in the reported work, only one reference was found with a quantification of particle size range in a form that might apply as an analogue for an extrusive event at Yucca Mountain. The referenced quantification listed in Mück et al. (2002 [DIRS 170378]) (Table J-2) was provided as the product of a personal communication with a Russian worker, but unfortunately without elaboration of the methodology for sampling or measurement. The quantification also lacks specificity of the numerical data basis though it has been considered reasonable to assume, for the purpose of data interpretation, that mass fraction representation was intended.

Table J-2. Fraction of Hot Particles of a Given Particle Size Depending on Distance from the Chernobyl Nuclear Power Plant

| Distance from ChNPP (km) | Fraction of Hot Particles with a Given Particle Size | | | |
|---|---|---|---|---|
| | 0–20µm | 20–50 µm | 50–100 µm | 100–200 µm |
| 4 | — | 12 5% | 75% | 12 5% |
| 10 | — | 65% | 35% | — |
| 20 | 8% | 87% | 5% | — |
| 37 | 40% | 60% | — | — |
| 55 | 65% | 35% | — | — |

Source Muck et al 2002 [DIRS 170378]

These data were extrapolated to obtain the maximum near-source waste particle size. The histogram-type data from the literature (Table J-2) were converted to cumulative size distributions (Table J-3) and transformed to a log-probability plot for log-normal distributions for the distal values. For analysis, the 10-km and 37-km data (which each had only two data points) were adjusted to reflect log-probability size distribution slopes similar to those of the other distal data. From the log-probability size distribution lines (Figure J-3), including the adjusted lines for 10-km and 37-km, intersect values are read and tabulated (Table J-4) to provide minimum, median (50 percent cumulative) and maximum particle diameters for each of the distal plot lines.

Table J-3. Transformation of Chernobyl Histogram Data to Cumulative Size Distributions

| Distance from CH NPP(km) | Cumluative Size Distribution of Hot Particles (mass %) | | | |
|---|---|---|---|---|
| | 20 µm | 50 µm | 100 µm | 200 µm |
| 4 | — | 12.5 | 87.5 | 100 |
| 10 | — | 65 | 100 | — |
| 20 | 8 | 95 | 100 | — |
| 37 | 40 | 100 | — | — |
| 55 | 65 | 100 | — | — |

Source: Developed DTN: MO0506SPACHERN.000.

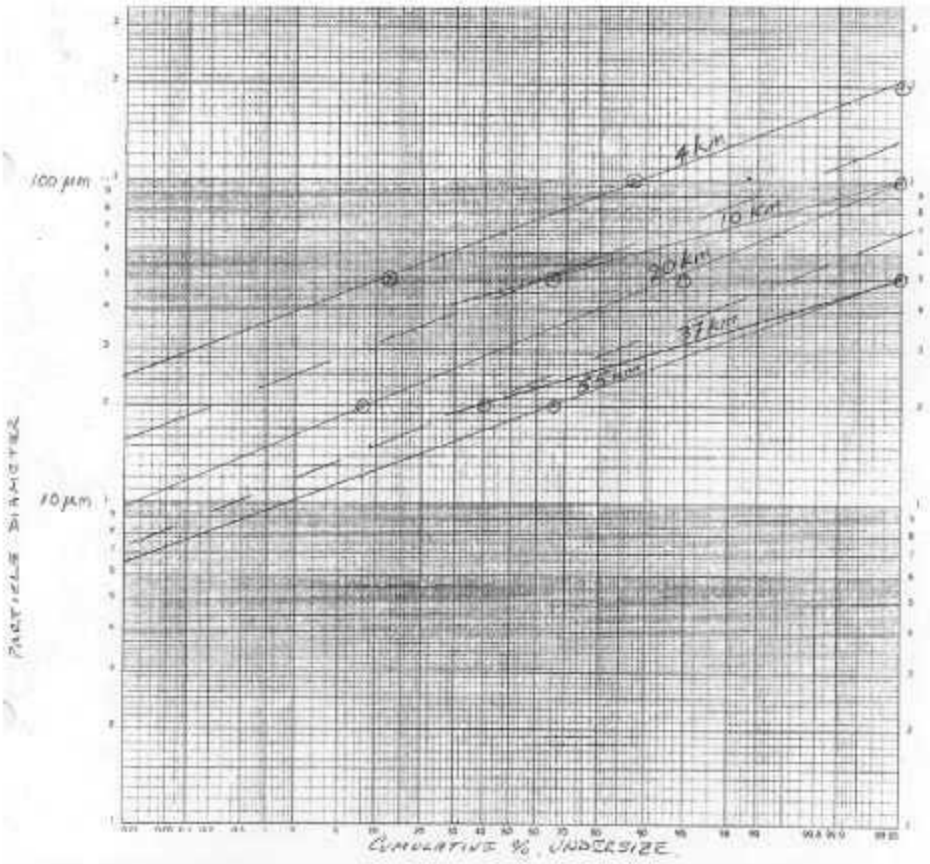


Source: Developed DTN: MO0506SPACHERN.000.

NOTE: Labels on trend lines refer to distance from the Chernobyl Power Plant. It is observed that the best-fit linear lines (solid) for the distal data sets have similar slopes, with the exception of the 10-km and 37-km data sets (dashed). Those two data sets have only two values; a mid size point and a top size point. Since the mid-size points are in somewhat interpolative positions relative to the other distal line plots, it is assumed that for the statistically weak representation, the top size sampling may be more suspect. With this assumption, hand drawn plot lines are made through the 10-km and 37-km mid size data such that the lines are approximate interpolations from the other distal plot lines.

Figure J-3. Plot of Chemobyl Hot Particle Cumulative Size Data

Table J-4. Estimated Chernobyl Hot Particle Size Statistics by Distance

| Distance (km) | Maximum Diameter (µm) | Median Diameter (µm) | Minimum Diameter (µm) |
|---|---|---|---|
| 4 | 210 | 70 | 25 |
| 10 | 140 | 45 | 15 |
| 20 | 100 | 31 | 10 |
| 37 | 70 | 22 | 7.2 |
| 55 | 50 | 18 | 6.5 |

Source: Developed DTN: MO0506SPACHERN.000.

A trend line of maximum particle size by distance was then generated in Excel 2003 and extrapolated to estimate the maximum size at the emission source (Figure J-4). The distal size data (Table J-4) were plotted using the standard charting functions of the Excel spreadsheet (Figure J-4). The best-fit trendline for the maximum particle size plot line in this Excel chart was produced by the standard Excel charting function "Add Trendline." A logarithmic type trendline was selected for this purpose. The logarithmic equation derived by Excel for the trendline was used to extrapolate for near source-term maximum hot particle diameters (Table J-5).

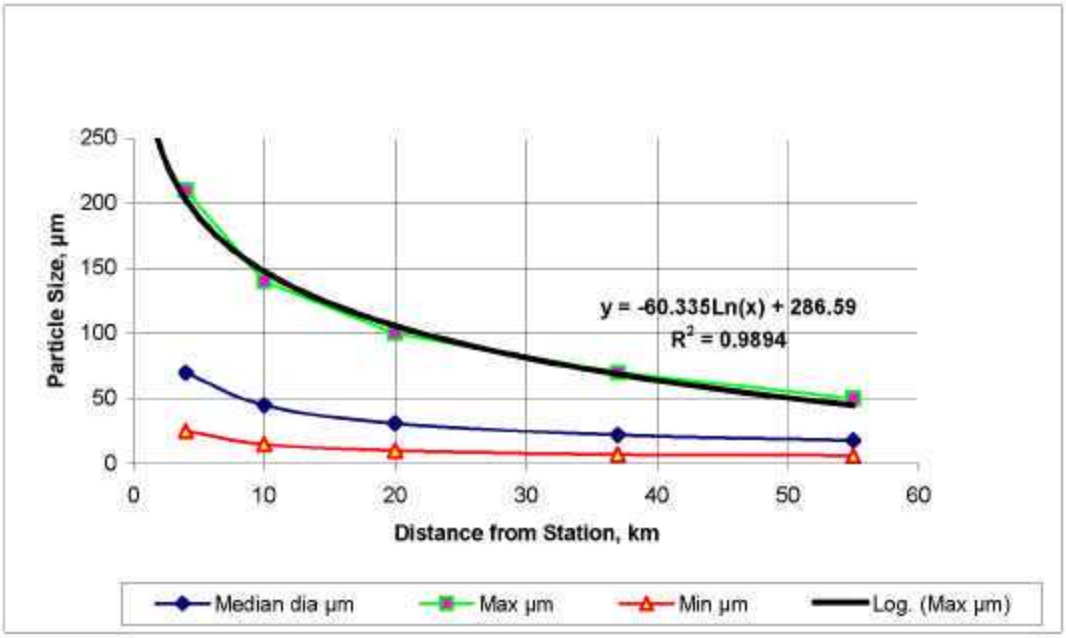


Source: Developed DTN: MO0506SPACHERN.000.

NOTE: Data are from Table J-4. Trend line for Y-intercept (Figure J-4) is approximately 1 mm maximum diameter. This extrapolation (to source) of maximum airborne particles may exclude larger particles that have behaved ballistically at short range and are therefore not represented in the distal field data.

Figure J-4. Extrapolation of Chernobyl Hot Particle Size by Distance

Table J-5. Best-Fit Estimate of Maximum Near-Source Chernobyl Hot Particle Size

| Distance (km) | Extrapolated Maximum Particle Diameter (µm) |
|---|---|
| 0.001 | 703 |
| 0.01 | 564 |
| 0.1 | 426 |
| 1 | 287 |
| 2 | 245 |
| 4 | 203 |

Source: Developed DTN: MO0506SPACHERN.000

NOTE: Based on equation for loganthmic trend line developed in Figure J-4)

The most highly contaminated area was the 30-km zone surrounding the Chernobyl reactor. The principal physico-chemical forms of the deposited radionuclides were dispersed fuel particles, condensation-generated particles, and mixed-type particles. The distribution in the nearby contaminated zone (<100 km) reflected the radionuclide composition of the fuel and differs from that in the far zone (>100 km to 2,000 km) (NEA 2002 [DIRS 174224], pp. 39 and 44).

Sub-micron size particulate emission is reported; however, it is also commented that since nuclei mode aerosol (c.a. 0.01 µm diameter) is inherently unstable with respect to growth mechanisms such as coagulation and condensation, there is a tendency for growth, leading to formation of accumulation mode particles (c.a. 0.1 up to 1 or 2 µm) (Harrison 1993 [DIRS 173851], Chapter 3).

In the concentrates of hot particles obtained (at distances 1-12 km) the Zr-U-containing particles accounted for 10 to 45 percent of the total amount of hot particles. The remaining part is represented by fuel particles with block morphology characteristic of irradiated fuel. The size of the examined particles (from 10 to 200 µm) and their distance from the 4th unit (power station accident source) allow the conclusion that the given particles were thrown out as a result of the explosions and, hence did not undergo possible changes connected with interaction with structural materials after the accident (Ushakov 1997 [DIRS 174141])

f) **EPRI Report**–The EPRI report (EPRI 2004 [DIRS 171915]) identifies two founding principles for the determination of waste particle size in an extrusive event. The first is the crushing and milling techniques by Argonne Laboratory in preparation for fuel dissolution experiments. This is the basis used in the assumption rationale in Section 5.2.4 and Appendix H. EPRI questions the relevance of this with respect to the disaggregation of fuel under an impact of magma.

The second source of information to which EPRI refers is from studies on the consequences of transportation accidents involving shipping casks and the used fuel inside. This is the basis that EPRI preferred and it selects a conservative (low energy/low fragmentation) energy density to determine a particle size distribution for

the volcanic scenarios. Based on this, the EPRI-recommended particle size distribution for the disaggregation of used fuel following impact of a rock projectile on the waste package is a log-normal distribution having a mass median particle size of 900 μm and a standard deviation of 19 μm.

## J2.4 REVISED WASTE PARTICLE SIZE

### J2.4.1 Discussion

It is convenient to present possible interpretations of waste particle size in a consistent manner to compare size distributions from different sources and to illustrate the significance of a selected recommendation. This is done in Figure J-3, in which some selected log-normal particle size distributions are plotted on a single log-probability graph. The following notes are in reference to the plotted size distribution lines.

Lines A, B and C represent size distributions provided by Argonne National Laboratory as professional judgments for suggested use in modeling fuel disaggregation effects from such as a volcanic eruption through the repository (Appendix H, p. H-4). No firm statistical foundation underlies the ranges; however, they are based on fuel observation experience and literature sources. The limiting values were less well constrained, but were estimated to apply to 80 to 90 percent of the fuel. The judgments were partly based on crushing and grinding of fuels in preparation for wet dissolution tests. The suggested size distribution for unaltered fuel has been used in the assumption rationale in Section 5.2.4.

Line D is derived from an analysis of the Chernobyl data tabulated in Table J-5. This estimated maximum was then applied (as a judgment) to the 99.9 percent probability to conceptually allow an end-member "tail" of larger ballistic size that would likely be omitted from the more distant field data. Drawing upon the observation (noted in Section J2.3f) that sub-micron particles have a tendency to grow (to 0.1 and up to 1 or 2 μm), the Line D is plotted with 0.1 mass percent at one μm in recognition of a 'tail" of sub-micron size.

Line E is a log-normal interpretation of distribution where the upper end-member represents a particle approximating a half fuel pellet diameter. This speculation is based on the possible ejection of some spent fuel in size fractions relatively unaffected by the magma. The half pellet diameter is based on some of the ATM test photomicrographs of the type shown in Figure J-2 (also see Guenther, Blahnik, Jenquin, et al. 1991 [DIRS 109207], Figure 8.3). The speculated scenario for survival of such pieces also includes the case of core-ends that have not been fully exposed to the magma or fuel pieces that have formed Zr(O)-$UO_2$ complexes and which then may not fragment in like manner to $UO_2$. The lower-end member for Line E is derived in the same manner as for Line D.

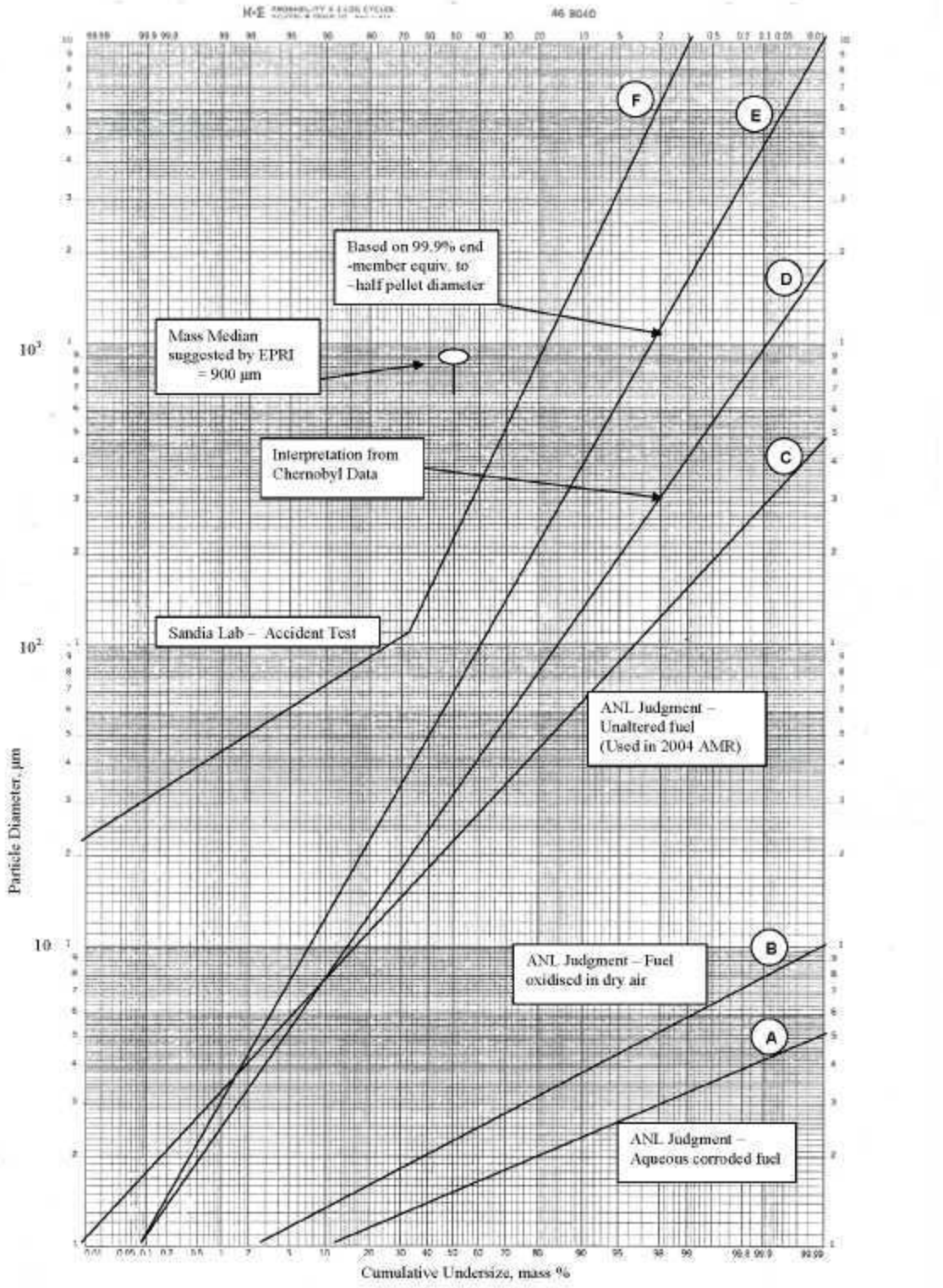


Figure J-5. Plot of Various Waste Particle Size Distributions, Single Log-Probability vs. Log Particle Diameter

Line F is reproduced from work reported by Sandoval et al. (1983 [DIRS 156313]). The full-scale test subjected a 25.45-tonne generic truck cask containing a section of a single surrogate PWR spent fuel assembly. The use of different instruments for capture and measuring applicable size ranges, plus a limitation of mass accountability (estimated error ± 10 percent), might explain the distribution slope change at around 100 μm, otherwise it might represent bimodality. The mass median Stokes diameter for the collected particle range is reported as 210 μm.

The accident test represents mechanical shock at ambient temperatures and is not necessarily an appropriate analogue for an eruptive event in which fuel has been pre-heated to elevated temperature (resulting in plasticity) and shock forces from molten magma and gas. However it is a useful comparative plot line since, with the relative exclusion of high temperature and time for oxidation-caused fragmentation, Line F might represent a reasonable upper limit of the range of possibilities considered for the igneous event.

### J2.4.2 Summary Regarding Waste Particle Size

For the purpose of the Ashpume AMR and ASHPLUME model, it would be reasonable to base the waste particle size distribution criteria on the Line D that is derived from Chernobyl data. For the ASHPLUME model purpose, it would also be considered reasonable to modify the minimum-end of the log-distribution such that the minimum particle diameter is one micrometer, but that the mass median particle diameter is based on the distribution as shown in Line D, which recognizes sub-micron sizes. This results in the following:

| | |
|---|---|
| **Minimum particle diameter** | **1 μm (0.0001 cm)** |
| **Maximum particle diameter** | **2000 μm (0.2 cm)** |
| **Mass median diameter** | **30 μm (0.0030 cm)** |

(See Section J4 for a recalculation of the mass median diameter to the necessary mode value for use in the ASHPLUME model.) These size criteria would be applied to either the effusive or explosive magma flux scenarios depicted in Figure J-1.

Some considerations in support of selecting the Chernobyl-derived data as a basis include:

- It is a full-scale analogue in which irradiated fuel was exposed to explosive forces, temperature and $UO_2$ oxidation. The dispersal may differ from an igneous case in which massive ash volumes are available for particle incorporation; however that does not invalidate the extrapolation of the Chernobyl distal particle depositions to estimate source term maximum particle size. On the other hand, rejection of Chernobyl data would require explanation.

- The log-normal size distribution derived from the Chernobyl data is not too dissimilar from that of the judgment-based sizing criteria provided by Argonne National Laboratory for unaltered fuel (as used in Section 5.2.4 and Appendix H) but which lacked specific supporting data.

The assumptions upon which Line E is based do not seem unreasonable but lack data support. Line E is more conservative than the log-normal size distribution from Chernobyl in that it

would provide a greater proportion of short-range deposition; however it would be tenuous to apply the more conservative interpretation without supporting data.

## J3. ALTERNATIVE CONCEPTUAL MODEL OF MAGMA-WASTE INTERACTION

The following conceptual model for the interaction of waste and magma accounts for the physical nature of the incorporation of waste into the magma in the repository drifts and for the volume of waste-containing magma that is deposited in various eruptive products. Rising magma intersects a repository drift at 300 m depth, impacting waste canisters as a conduit forms. The magma is a mixture of liquid and exsolving gas of various proportions, which produces an effusive (liquid-dominated) and/or pyroclastic (gas-dominated) flow. Over the course of 1,000 hours at 900-1,000°C, the impacted canisters fail, exposing the waste to the magma (BSC 2004 [DIRS 170028], Section 6.4.8; BSC 2005 [DIRS 173802], Section 3.3). The waste form has been degraded during reactor service and by exposure to the magmatic environment, and it consequently consists of particles in the size range 1 μm to 2 mm (reduced by fracturing from the original 9 × 11 mm pellet size, (Sections J2.3, J2.4.2)). Some portion of these waste particles is lifted out of the canisters by surrounding magma, suspended and well-mixed with the magma, carried to the surface through the conduit, and erupted at the vent. The eruption typically involves several phases, including Strombolian and violent Strombolian activity (cone building and tephra sheet deposition) and effusion of lava flows. The waste incorporated into the magma is therefore deposited in various eruptive products—scoria cone, lava flows, and tephra blanket—over the course of the eruption.

### J3.1 MAGMA PARTITIONING INTO ERUPTIVE PRODUCTS

The Ashplume model of the eruption column, ash dispersal, and deposition assumes that violent Strombolian activity dominates and considers only the portion of the eruption products that are transported aerially away from the vent (Section 5.1.1). This assumption conceptually excludes the volume of magma and waste incorporated into the scoria cone and lava flows. The input parameter values for the Ashplume model are based on estimates of eruptive style and volumes in the Yucca Mountain region, especially Lathrop Wells Cone (LWC), the youngest and best-preserved of the scoria cones in the region (BSC 2004 [DIRS 169980], Section 6.3.3). Analysis of LWC indicates that a significant proportion of the eruptive products resulted from Strombolian and violent Strombolian activity, contributing mass to the cone, lava flows, and tephra sheet (BSC 2004 [DIRS 169980], Section 6.3.3). However, the Ashplume model assumes that all waste mixed at depth with the magma enters the eruptive column and is deposited in the tephra sheet only.

Estimates of the relative proportions of magma deposited in various eruptive products are available from studies at LWC and at other sites described in the literature (Table J-6). At LWC, the tephra proportion (calculated by dense rock equivalent, DRE) is ~0.26, but comparison with other volcanoes in the Yucca Mountain region and worldwide reduces the mean proportion of magma deposited in the tephra sheet to approximately 0.20. Assigning more weight to the younger, better-documented analogues (e.g., Lathrop Wells, Tolbachik, Sunset Crater, Cerro Negro) supports a value of 0.3. With this in mind, the waste-containing magma in the conceptual model will erupt into scoria cone, lava flows, and tephra sheet in the mean

proportions listed in Table J-3, with only about one-third of the waste erupting in the tephra sheet. The remainder of the waste will be deposited with the magma in relatively resistant geologic features (scoria cone and lava flows) and will not be available to provide dose at the RMEI location during the 10,000-year regulatory period.

If the magma entering the repository drifts is not liquid-dominated, but instead has fragmented into a gas-dominated fluid containing silicate melt pyroclasts, partitioning of waste-containing magma into various eruptive products is still reasonable, given that multiple states of magma may exist in the conduit below the vent as a result of complex magma pathways, transient blockages, variations in magma flux and pressure, and annular flow. Field observations support this conceptual model, including simultaneous pyroclastic and effusive eruptions (e.g., Luhr and Simkin 1993 [DIRS 144310], p. 69).

## J3.2 WASTE INCORPORATION RATIO

This alternative to the conceptual model for magma-waste interaction would require a revision to the parameter values used in the ASHPLUME model. In the original formulation, Jarzemba (1997 [DIRS 100460], pp. 134-5) conceived of magma-waste mixing by the model

$$R(x, y) = X(x, y)\frac{A}{Q}, \qquad \text{(Eq. J-1)}$$

where

$R(x,y)$ = quantity of radioactivity per unit area accumulated at location (x,y) (Ci/cm$^2$)
$X(x,y)$ = mass of ash per unit area accumulated at location (x,y) (g/cm$^2$)
$A$ = total amount of radioactivity released
$Q$ = total mass of ash erupted.

This relationship simply multiplies the mass of ash deposited in a particular location by the ratio of total masses of waste and ash erupted. While this model does not account for the gravitational influence of the waste's relatively higher density on the transported particles, it is suitable for a homogeneous mix of waste in magma prior to fragmentation and eruption.

Table J-6. Proportional Volumes of Magma Partitioned into Eruptive Products at Basaltic Volcanoes

| Volcano | Observed Volume ($km^3$) | | | | Volume, DRE[6] ($km^3$) | | | | Proportion, DRE | | |
|---|---|---|---|---|---|---|---|---|---|---|---|
| | Cone | Lavas | Tephra Sheet | Total | Cone | Lavas | Tephra Sheet | Total DRE | Cone | Lavas | Tephra Sheet |
| Lathrop Wells[1] | 0 018 | 0 029 | 0 039 | 0 086 | 0 015 | 0 027 | 0 015 | 0 057 | 0 27 | 0 47 | **0.26** |
| Hidden Cone[2] | 0 019 | 0 009 | 0 038 | 0 066 | 0 016 | 0 008 | 0 015 | 0 039 | 0 41 | 0 21 | **0.37** |
| Little Black Peak[2] | 0 006 | 0 007 | 0 012 | 0 025 | 0 005 | 0 006 | 0 005 | 0 016 | 0 31 | 0 40 | **0.29** |
| SW Little Cone[2,3] | 0 002 | 0 022 | 0 004 | 0 028 | 0 002 | 0 020 | 0 002 | 0 024 | 0 07 | 0 86 | **0.07** |
| Red cone[2,4] | 0 005 | 0 089 | 0 005 | 0 099 | 0 004 | 0 082 | 0 002 | 0 088 | 0 05 | 0 93 | **0.02** |
| Black cone[2,4] | 0 011 | 0 065 | 0 011 | 0 087 | 0 009 | 0 060 | 0 004 | 0 074 | 0 13 | 0 82 | **0.06** |
| Cerro Negro 1971[5] | added to ash | 0 | 0 07 | 0 07 | n/c | 0 000 | 0 027 | 0 027 | n/c | 0 00 | n/c |
| Cerro Negro 1968[5] | added to ash | 0 003 | 0 017 | 0 02 | n/c | 0 003 | 0 007 | 0 009 | n/c | 0 30 | n/c |
| Tolbachik 1[2] | 0 093 | 0 025 | 0 122 | 0 24 | 0 079 | 0 023 | 0 047 | 0 149 | 0 53 | 0 16 | **0.32** |
| Tolbachik 2[2] | 0 098 | 0 242 | 0 099 | 0 439 | 0 083 | 0 223 | 0 038 | 0 344 | 0 24 | 0 65 | **0.11** |
| Sunset Crater[2] | 0 284 | 0 15 | 0 44 | 0 874 | 0 240 | 0 138 | 0 169 | 0 548 | 0 44 | 0 25 | **0.31** |
| Paricutin[2] | 0 069 | 0 7 | 0 41 | 1 179 | 0 058 | 0 646 | 0 158 | 0 862 | 0 07 | 0 75 | **0.18** |
| Hermaey[2] | 0 015 | 0 18 | 0 012 | 0 207 | 0 013 | 0 166 | 0 005 | 0 183 | 0 07 | 0 91 | **0.03** |
| Serra Gorda[2] | 0 03 | 0 015 | 0 042 | 0 087 | 0 025 | 0 014 | 0 016 | 0 055 | 0 46 | 0 25 | **0.29** |
| Cerro Negro 1850-1995[2] | 0 08 | 0 043 | 0 132 | 0 255 | 0 068 | 0 040 | 0 051 | 0 158 | 0 43 | 0 25 | **0.32** |
| | | | | | | | | **mean** | **0.27** | **0.48** | **0.20** |

NOTES [1] DTN LA0305DK831811 002 [DIRS 164678]

[2] NRC 1999 [DIRS 151592], Table 3

[3] Volume corrected for 50 percent erosion

[4] Volume corrected for 33 percent erosion

[5] Rose et al 1973 [DIRS 116087], Figure 2

[6] DRE volumes calculated based on density values used for Lathrop Wells DRE conversions fall = 1,000 kg/$m^3$, lavas = 2,400 kg/$m^3$, cone = 2,200 kg/$m^3$ (SN-LANL-SCI-286-V2 (Krier 2004 [DIRS 173810], p 55))

n/c = not calculated

The waste incorporation model included in the ASHPLUME V1.0 and V.2.0 codes is more sophisticated, involving a conceptual model of the combination of two particle streams. The particles of waste are "instantaneously" homogenized in ash particles, and the controlling parameter is related to the relative sizes of the waste and ash particle populations:

$$\rho_c = \log_{10}\left[\frac{d^a_{\min}}{d^f}\right] \qquad \text{(Eq. J-2)}$$

where

$\rho_c$ = waste incorporation ratio
$d^a_{\min}$ = minimum ash particle size needed for incorporation in cm
$d^f$ = fuel particle size in cm.

For a "typical" value of $\rho_c = 0.3$ (Jarzemba et al. 1997 [DIRS 100987], p. 2-6), waste particles can only be incorporated into ash particles twice their size.

The mass of waste deposited on the ground at a particular location is calculated in this model by the use of a fuel fraction term ($FF(\rho^a)$):

$$FF(\rho^a) = \frac{U}{Q} \bullet \int_{\rho=-\infty}^{\rho=\rho^a} \frac{m(\rho-\rho_c)}{1-F(\rho)}\, d\rho \qquad \text{(Eq. J-3)}$$

where

$Q$ = total mass of ash ejected in the event in g

$U$ = total mass of fuel ejected in the event in g

$m(\rho)$ = probability density function of mass of fuel as a function of fuel particle size

$\rho^a$ = $\log_{10}$ of the ash particle diameter in cm, and

$F(\rho^a)$ = cumulative distribution of $f(\rho^a)$, the distribution of ash mass as a function of ash particle size.

This model assumes that all fuel particles of a size smaller than ($\rho^a$-$\rho_c$) will be simultaneously incorporated into volcanic ash particles of size $\rho^a$ or larger. The combination of particles is carried out in the integrand by dividing the mass of waste in particles of size ($\rho$-$\rho_c$) by the mass of ash in particles less than ($\rho^a$-$\rho_c$). The fuel fraction is calculated by summing up all the incremental contributions of fuel mass to the volcanic ash mass from fuel sizes smaller than ($\rho^a$-$\rho_c$) (Jarzemba et al. 1997 [DIRS 100987], pp. 2-6). The density of the combined ash-waste particles is adjusted to account for the presence of the high-density waste. To determine the mass of fuel deposited at a particular location, the main model equation that calculates ash distribution (Equation 6-2) is multipled by this fuel fraction term and re-integrated by particle size and eruption column height (Section 6.5.1).

This mathematical model is appropriate for the conceptual model of two separate particle streams combining in the rising ash plume, but its application can be challenging in the conceptual model of magma interactions with waste in a repository drift. Returning to the effusive end-member of the magma-waste alternative conceptual model, the liquid magma flows into the drift, degrades the waste packages, releases the waste, and incorporates it as a suspension of waste particles in the silicate melt. These particles are assumed to be relatively inert; that is, no melting or dissolution of the particles occurs that would dissolve waste material into solution in the melt. Flow dynamics within the magma in the drift and conduit prior to eruption are assumed to produce a well-mixed (homogeneous) suspension of waste particles throughout the magma. At the vent, the magma erupts to produce various deposits, and the portion destined for the tephra blanket is fragmented and becomes entrained in the buoyant plume. Note that, in this scenario, the waste is already incorporated into the melt prior to fragmentation, and the mathematical formulation in Equation J-3 above using the waste incorporation ratio, $\rho_c$, does not pertain conceptually. However, this mathematical model can still be used by prescribing a relatively neutral value for $\rho_c$, which would simply allow the natural size distributions of tephra (produced in the fragmentation process) and waste particles (retained from the original release of waste from the waste packages) to prevail in the tephra-waste mixture. Thus the waste particles can be treated as refractory 'xenoliths' in the melt, which, upon magma fragmentation, will reappear in the tephra as mixed particles of waste and silicate melt (glass).

The appropriate 'neutral' value for $\rho_c$ is one that simply allows the combination of the original particle size distributions of waste and ash. In this case, a value of $\rho_c=0$ is used in Equation J-3 (that is, the ratio of particle sizes is 1:1, Equation J-2).

In the second scenario for magma-waste interaction in the drift, gas-dominated magma erupts explosively into the drift. In this case, the conceptual model of mixing particle streams seems more appropriate, but the path through the conduit to eventual eruption at the vent will arguably involve homogenization of the once-fragmented melt with other rising liquid-dominated magma, resulting in a well-mixed magma-waste suspension. The conceptual model of partitioning of the rising magma into various eruptive products also pertains in this case; simultaneous eruption of a violent Strombolian plume and passive effusion of lava flows has been documented in historic eruptions (e.g., Paricutin, February 24, 1943; Luhr and Simpkin 1993 [DIRS 144310], p. 69). The waste incorporation ratio should also be used in a neutral mode ($\rho_c=0$) here as well, since the partitioning of magma into eruptive products will have already reduced the eruptive mass of waste, and the turbulent rise of the (fragmented) magma-waste suspension in the conduit will allow the refractory waste particles to form composite tephra particles with the silicate melt according to a simple mixture of grain sizes, as described for the first scenario, above.

## J3.3 IMPACT FOR MAGMA PARTITIONING

The analyses described above result in the following observation with regard to executing the ASHPLUME code:

1) The value for the ASHPLUME parameter, "mass of waste available for transport, $U$," could be prescribed by reducing the mass in impacted waste packages by a 'magma partitioning factor' to account for waste erupted in magma that forms geologically stable features (scoria cone and lava flows). The mass of waste available from waste

packages impacted by the development of a volcanic conduit (calculated by the method described in BSC (2005 [DIRS 174066] would be multiplied by the magma partitioning factor of 0.3, the proportion of magma producing the tephra blanket. The resulting mass (g) would be provided as the input to "mass of waste available for transport, *U*" in ASHPLUME.

2) The value for the ASHPLUME parameter, 'waste incorporation ratio', $\rho_c$, could be revised to 0.0 in order to be consistent with the premixing of waste and magma before eruption. This value is consistent with the use of the magma partitioning factor (above) and would allow ash and waste particles to enter the modeled violent Strombolian plume according to their respective particle size distributions without additional limitations.

## J4. SUMMARY OF ALTERNATIVE ANALYSES

1. The values for ASHPLUME model input parameters in this alternative model are revised according to the following table.

Table J-7. Parameter Values Derived from Alternative Analyses

| ASHPLUME Parameter Name | Revised Value |
|---|---|
| Minimum waste particle size | 0 0001 cm (unchanged) |
| Maximum waste particle size | 0 2 cm |
| "Median" (mode) waste particle size | 0 0013 cm |
| Waste incorporation ratio | 0 0 |
| Magma partitioning factor | 0 3 |

Source Developed DTN MO0505WPSDISTR 001

The mass median diameter (0.0030 cm) provided in Section J2.4.2 must be converted to mode for use in the ASHPLUME parameter "median waste particle size" (Jarzemba et al. 1997 [DIRS 100987]); this is done according to $\mu = (a + b + c)/3$ where $\mu$ is the log of the mean value, a is the log of the minimum value, b is the log of the mode value, and c is the log of the maximum value (Evans et al. 1993 [DIRS 112115]). The mode calculated in this way is 0.0013 cm.

2. An additional parameter, "magma partitioning factor," is added in this alternative model. The waste mass in waste packages impacted by volcanic conduits (eruptive case) are multiplied by this factor to account for the proportion of the magma-waste mixture that enters the eruptive plume and is deposited in the tephra sheet.

The results of these alternative analyses and the sensitivity analyses included in Appendix C indicate that the alternative waste particle size and magma partitioning conceptual model would each decrease the waste concentration calculated at the RMEI location. The alternative waste particle size distribution alone provides a 14 percent decrease in waste concentration at the RMEI (Appendix C) compared to the base case distribution (Table 8-2). The alternative conceptual model regarding magma partitioning concludes that only about one-third of the waste would likely be entrained in the tephra sheet, with the remaining being incorporated in relatively

resistant geologic features (scoria cones and lava flows) that would be relatively stable on the landscape. The current TSPA-LA model assumes that all the waste is deposited in the tephra sheet. These assessments indicate that the values in Table 8-2 that are used by TSPA-LA are conservative with regard to the impact on the dose at the RMEI location during the 10,000-year regulatory period.

INTENTIONALLY LEFT BLANK